DISRUPTION OF SPATIO-TEMPORAL PROCESSING IN HUMAN VISION USING TRANSCRANIAL MAGNETIC STIMULATION

Laura Kate Stevens, MSc.

Thesis submitted to the University of Nottingham

for the degree of Doctor of Philosophy

JULY 2009

Abstract

Transcranial magnetic stimulation (TMS) is a non-invasive technique used to reversibly modulate the activity of cortical neurons using time-varying magnetic fields. Recently TMS has been used to demonstrate the functional necessity of human cortical areas to visual tasks. For example, it has been shown that delivering TMS over human visual area V5/MT selectively disrupts global motion perception. The temporal resolution of TMS is considered to be one of its main advantages as each pulse has a duration of less than 1 ms. Despite this impressive temporal resolution, however, the critical period(s) during which TMS of area V5/MT disrupts performance on motion-based tasks is still far from clear.

To resolve this issue, the influence of TMS on direction discrimination was measured for translational global motion stimuli and components of optic flow (rotational and radial global motion). The results of these experiments provide evidence that there are two critical periods during which delivery of TMS over V5/MT disrupts performance on global motion tasks: an *early* temporal window centred at 64 ms prior to and a *late* temporal window centred at 146 ms post global motion onset. Importantly, the *early* period cannot be explained by a TMS-induced muscular artefact. The onset of the *late* temporal window was contrast-dependent, consistent with longer neural activation latencies associated with lower contrasts. The theoretical relevance of the two epochs is discussed in relation to feedforward and

feedback pathways known to exist in the human visual system, and the first quantitative model of the effects of TMS on global motion processing is presented.

A second issue is that the precise mechanism behind TMS disruption of visual perception is largely unknown. For example, one view is that the "virtual lesion" paradigm reduces the effective signal strength, which can be likened to a reduction in perceived target visibility. Alternatively, other evidence suggests that TMS induces neural noise, thereby reducing the signal-to-noise ratio, which results in an overall increase in threshold.

TMS was delivered over the primary visual cortex (area V1) to determine whether its influence on orientation discrimination could be characterised as a reduction in the visual signal strength, or an increase in TMS-induced noise. It was found that TMS produced a uniform reduction in perceived stimulus visibility for all observers. In addition, an overall increase in threshold (JND) was also observed for some observers, but this effect disappeared when TMS intensity was reduced. Importantly, susceptibility to TMS, defined as an overall increase in JND, was not dependent on observers' phosphene thresholds. It is concluded that single-pulse TMS can both reduce signal strength (perceived visibility) and induce task-specific noise, but these effects are separable, dependent on TMS intensity and individual susceptibility.

Acknowledgements

My thanks go to Tim Ledgeway and Paul McGraw for their perseverance and excellent supervision. I would also like to acknowledge my colleagues in the Nottingham Visual Neuroscience group for their encouragement and many useful discussions. Thanks also go to the participants of my experiments, to whom I am greatly indebted.

I would also like to thank my parents and Mark for their continued support.

TABLE OF CONTENTS

Chapter 1: Literature review

1.1 The visual pathway

1.1.1 Anatomy of the visual pathway

1.1.1.1 Pre-cortical visual pathway

The first stage of visual processing is the conversion of light into an electrical signal by retinal photoreceptors. There are on average one hundred million photoreceptors on the posterior surface of the human eye (Curcio, Sloan, Kalina & Hendrickson, 1990), and these can be broadly divided into two receptor types – rods and cones. Rods respond well under dim light (scotopic conditions) [e.g. Nakatani, Tamura & Yau, 1991], whereas cones operate under relatively high light intensity (photopic conditions) [e.g. Schnapf, Nunn, Meister & Baylor, 1990]. The different sensitivities of these two types of receptor cover the full range of environmental light intensities (10^{10}). There are three varieties of cone each sensitive to a different part of the electromagnetic spectrum (e.g. Schnapf, Kraft & Baylor, 1987). Rods and cones do not produce action potentials, and instead respond to light with graded changes in membrane potential (e.g. Baylor & Fettiplace, 1976). Cones are heavily concentrated in the central region of the retina (the fovea), whereas rods are completely absent from the fovea but are more densely packed 12 deg to 15

deg in the periphery (e.g. Curcio et al., 1990). Photoreceptors are connected, via a network of intermediary cells, to retinal ganglion cells.

The axons of ganglion cells form the optic nerve, which leaves the eye through the anatomical blind spot and projects to the thalamus (Tasman, 1973). In higher mammals, prior to reaching the thalamus, the axons originating from the nasal half of the retina from each eye cross the midline to combine with those from the temporal half of the opposite eye; this is called decussation and occurs at the optic chiasm (Hoyt & Luis, 1963; Meissirel & Chalupa, 1994). The optic chiasm fibres form the left and right optic tracts, which contain axons from the ipsilateral half of the retina of each eye, and therefore carry a complete representation of the contralateral visual field.

The optic tracts project to three subcortical regions of the thalamus: the pretectum, the superior colliculus (SC) and the lateral geniculate nucleus (LGN). The pretectum is responsible for controlling pupillary reflexes (e.g. Papageorgiou, Wermund & Wilhelm, 2009), whereas the SC controls saccadic eye movements (e.g. Pierrot-Deseilligny, Rosa, Masmoudi, Rivaud & Gaymard, 1991). The SC also contains cells that respond selectively to the direction of visual motion (e.g. Horwitz & Newsome, 1999), which renders it possible that the SC is involved in pathways to extrastriate areas that bypass earlier visual cortical regions (this will be expanded upon later). Approximately 90 % of retinal ganglion axons terminate in the LGN (Perry & Cowey, 1984; Silveira & Perry, 1991).

Each LGN has 6 layers – three from the ipsilateral and three from the contralateral eye – and processes information from the contralateral visual field. Each LGN has two magno- (M) and four parvocellular (P) layers. Intracellular staining of ganglion cells projecting to feline (Bowling & Michael, 1980) and primate (Silveira & Perry, 1991) LGN shows little violations of layer boundaries. Between the M and P layers of the LGN there are also koniocellular (K) cells, although their properties remain largely unknown, primarily because they occur in thin laminae and exhibit heterogenous properties (e.g. Hendry & Reid, 2000).

1.1.1.2 Cortical visual pathway

The sub-cortical projection to primary visual cortex (area V1, or striate cortex) is strongly dominated by M and P pathways that are relayed by the M and P layers of the LGN, and little vision exists when both of these pathways are destroyed (e.g. Schiller, Logothetis & Charles, 1990). The outputs of cells in the M and P layers of the LGN are anatomically segregated in area V1; the axons of M cells terminate principally in layer 4Cα, whereas the axons of P cells terminate principally in layer 4Cβ (e.g. Fitzpatrick, Lund & Blasdel, 1985). Retrograde tracer studies have shown that projections from some K cells in the LGN terminate in layers 2 and 3 of area V1 (e.g. Hendry & Yoshioka, 1994), although evidence for direct konio input to 4Cβ and 4A (Yazar, Mavity-Hudson, Ding, Oztas & Casagrande, 2004) and extrastriate cortex (e.g. Sincich, Park, Wohlgemuth & Horton, 2004) has also been reported. According to the tripartite model of the visual system (Livingstone &

Hubel, 1984; Livingstone & Hubel, 1987; Livingstone & Hubel, 1988), area V1 transforms the three input streams from M, P and K cells into three output streams that project to area V2 (Figure 1.1).

However, complex intracortical circuitry within area V1 indicates that the three input streams do not remain segregated after the level of the geniculate input. For example, the glutamatergic spiny stellate cells in 4Cβ – with which P cells principally synapse – project not only to layers 2 and 3 but also 4Cα, 4A and 4B (e.g. Callaway & Wiser, 1996). This indicates that the signal from P cells is integrated with that from M and K cells, which terminate in layers 4Cα and 4A, respectively. Additionally, Callaway & Wiser (1996) reported that cells in 4Cα and 4Cβ project to layers 5 and 6, which in turn have reciprocal connections with layers 2 and 3, implying further mixing of geniculate channels.

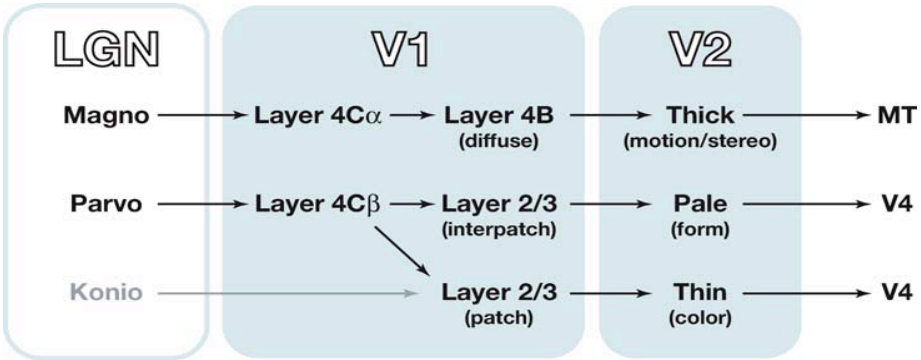

Figure 1.1. The tripartite model of the visual system. According to this model, area V1 transforms the three inputs from the LGN (from magno, parvo and konio cells) into three outputs that project to area V2 (that form motion/stereo, form and colour pathways). Taken from Sincich & Horton (2005), adapted from Livingstone & Hubel (1988) and Van Essen & Gallant (1994).

Livingstone & Hubel (1984, 1987, 1988) suggested that the three pathways are segregated in area V2, and separate pathways from V2 project to visual areas V4 and the middle temporal area MT[1] (Figure 1.1). The function of a visual area is traditionally derived from the set of visual features to which it is tuned. Area V4 is known as a colour or form area, as many cells show selectivity for particular wavelengths (e.g. Dubner & Zeki, 1971; Zeki, 1973; Zeki, 1980) or shapes (e.g. Desimone & Schein, 1987; Gallant, Connor, Rakshit, Lewis & Van Essen, 1996). Area V5/MT has been labelled a motion area as many cells respond selectively to aspects of motion such as direction or speed (e.g. Maunsell & Van Essen, 1983; Movshon, Adelson, Gizzi & Newsome, 1986; Maunsell & Newsome, 1987).

The selectivity of V4 and V5/MT neurons to specific properties of visual stimuli has come to symbolise the characteristics of what are considered to be two separate and distinct processing streams in the visual cortex (e.g. Ungerleider & Mishkin, 1982; Young, 1992). One pathway is thought to be important for encoding motion and spatial location, and projects dorsally to area V5/MT and then the parietal cortex. The second pathway is thought to be necessary for the perception of colour and shape, and projects ventrally to area V4 and then the temporal cortex (Figure 1.2). These anatomical locations in

[1] Neuroimaging studies have provided unequivocal evidence for a homologue of monkey MT in the human visual system, known as area V5 (e.g. Zeki, Watson, Lueck, Friston & Frackowiak, 1991; Watson, Myers, Frackowiak, Hajnal, Woods, Mazziotta & Shipp, 1993; Orban, Dupont, De Bruyn, Vogels, Vandenberghe, & Mortelmans, 1995; Tootal, Reppas, Kwong, Malach, Born, Brady, Rosen & Belliveau, 1995; Heeger, Boynton, Demb, Seideman & Newsome, 1999; Huk, Dougherty & Heeger, 2002) – hereafter referred to in both species as V5/MT.

the human brain, as determined by retinotopic mapping using functional magnetic resonance imaging (fMRI), are depicted in Figure 1.3. Ungerleider & Mishkin (1982) performed a series of lesion studies on primates and discovered that lesions of the temporal cortex impaired performance on an object discrimination task whereas lesions of the parietal cortex impaired performance on an object localisation task. The two pathways were consequently dubbed the dorsal/"where" and the ventral/"what" pathways (Ungerleider & Mishkin, 1982). Support for this distinction has come from single unit studies, and from observations of the perceptual consequences of damage to the pathways (e.g. Livingstone & Hubel, 1988; Zeki & Shipp, 1988; Merigan & Maunsell, 1993). However, as can be seen in Figure 1.4a, there many interconnections between primate cortical regions associated with each parallel processing stream. These connections typically allow the flow of information between cortical areas, suggesting that the streams are not as segregated as once thought (Felleman & Van Essen, 1991). Furthermore, in

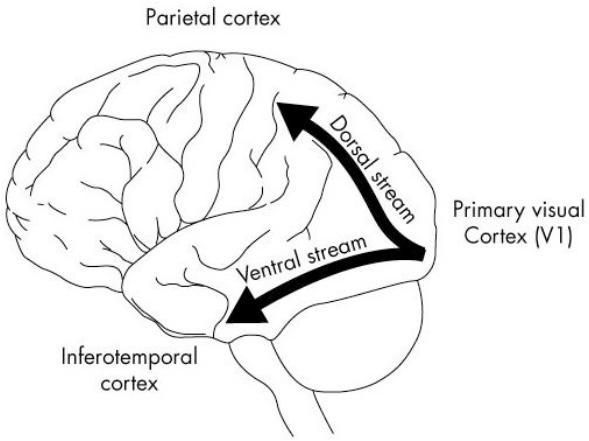

Figure 1.2. A schematic of the two processing streams in monkey cortex. The dorsal pathway projects to the parietal cortex, the ventral pathway projects to the inferotemporal cortex. Taken from Ungerleider & Mishkin (1982).

addition to connections between cortical areas in series (e.g. V1 projects to V2, which in turn projects to V3, etc.), there exist many direct connections between areas at the lowest and the highest levels of the hierarchy (for example, area V1 has direct connections with area V5/MT [Cragg, 1969; Zeki, 1969]). Ascending projections from 'lower' to 'higher' visual areas are known as feedforward connections. Most connections between areas are reciprocal, and the descending projections from higher to lower visual areas are known as feedback connections (Felleman & Van Essen, 1991). Cortical regions typically have numerous layers, and the layers from which the connections arise are indicative of whether they project to higher or lower cortical areas (Bullier, 2003). As can be seen in Figure 1.4b, there are by comparison far fewer anatomically demonstrated connections that have been shown in human cortex (Zilles & Clarke, 1997).

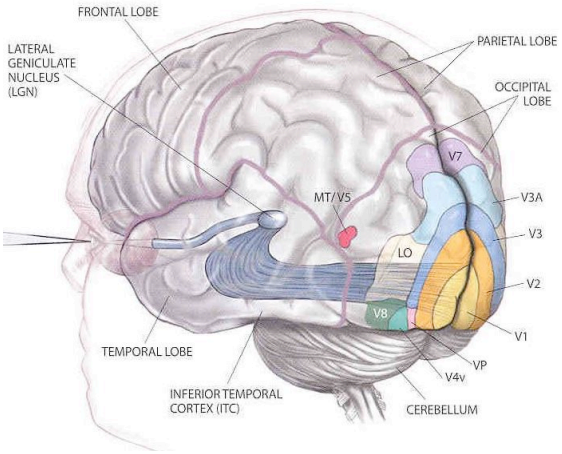

Figure 1.3. A schematic of visual areas in human occipital cortex. Area V1 receives visual input and begins the processing of colour, motion and shape. Cells in area V1 have the smallest receptive field size. Areas V2, V3 and VP continue processing, each level has progressively larger receptive fields; V3A is biased for perceiving motion; V4v, function unknown; MT/V5 detects motion; V7, function unknown; V8 processes colour; LO processes large scale objects. Taken from Logothetis (1999).

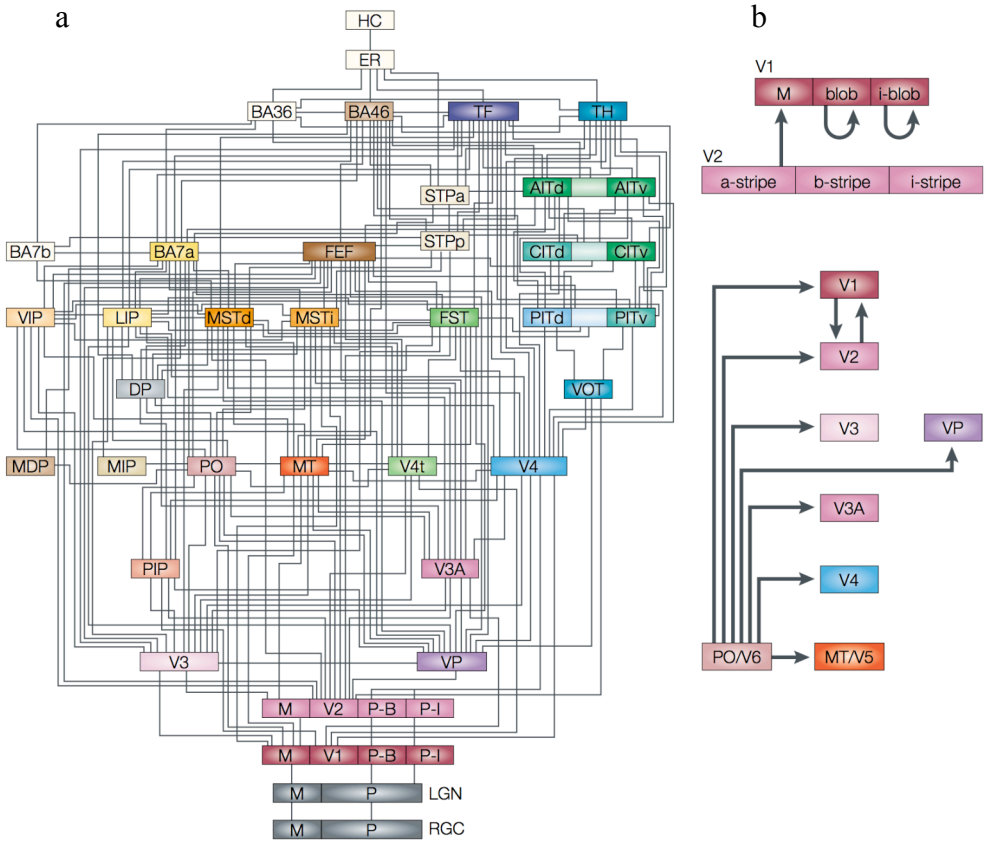

Figure 1.4. The anatomical hierarchy of visual areas and their interconnections in macaque and human. a) The anatomically demonstrated connections between visual areas in macaque cortex, adapted from Felleman & Van Essen (1991). Thirty-two visual cortical areas, as well as two subcortical levels and several non-visual areas are shown, connected by 187 anatomically demonstrated connections, most of which are reciprocal. b) The anatomically demonstrated connections between visual areas in human cortex, as proposed by Zilles & Clarke (1997). By comparison, there have been far fewer studies of the pattern of connections between human visual areas.

M, blob and i-blob are subdivisions of V1, and a-stripe, b-stripe and i-stripe are subdivisions of V2, all characterised using cytochrome oxidase staining. AIT, anterior inferotemporal cortex; BA, Brodmann area; CIT, central inferotemporal cortex; d, dorsal; DP, dorsal prelunate area; ER, entorhinal cortex; FEF, frontal eye fields; FST, floor of superior temporal cortex; HC, hippocampus; l, lateral; LGN, lateral geniculate nucleus; LIP, lateral intraparietal area; M, magnocellular regions; MDP, mediodorsal parietal area; MIP medial intraparietal area; MST, medial superior temporal area; MT, medial temporal area (V5); P, parvocellular regions; P-B, parvo-blob; P-I, parvo-interblob; PIP, posterior intraparietal area; PIT, posterior inferotemporal cortex; PO, parieto-occipital area (V6); RGC, retinal ganglion cells; STPa, anterior part of the superior temporal polysensory area; STPp, posterior part of the superior temporal polysensory area; TF, TH, temporal areas; v, ventral; VOT, visual occipitotemporal area; VP, ventroposterior visual area.

Note: Figure 1.4a (taken from Rees, Kreiman & Koch, 2002) contains a reproduction error from the original schematic by Felleman & Van Essen (1991): above is listed *MSTi*, where there should read *MSTl*.

1.1.2 Spatial processing

1.1.2.1 Pre-cortical spatial processing

Instead of signalling all light that activates the photoreceptors, most retinal ganglion cells principally signal differences in light intensity. This is made possible by the way photoreceptors are connected to ganglion cells: via bipolar cells (direct pathway) and via bipolar and horizontal cells (indirect pathway). Both pathways can have either an excitatory or an inhibitory influence on the firing rate of the ganglion cell, but they are always of opposite polarity. The receptive field of ganglion cells is roughly circular and is divided into two parts – a circular centre and an antagonistic surround – which may be 'on-centre' or 'off-centre' (Kuffler, 1953; Hubel & Wiesel, 1962; Enroth-Cugell & Jones, 1963). On-centre cells have the highest response when a circular spot of light falls only within the centre of the receptive field, as light on the surround inhibits the response. The most effective inhibitory stimulus for an on-centre ganglion cell would be a ring of light that falls on its entire inhibitory surround. Off-centre ganglion cells respond best when light falls in the surround but not the centre of the receptive field, and are inhibited by light at the centre. If uniform illumination fell on the entire receptive field of either type of cell, the response would be similar to that when no light is present at all. The fact that optimal firing rate does not occur with uniform illumination is due to lateral inhibition (Hartline, 1956). The result is that the perceived contrast at luminance borders is increased, which in turn enhances spatial resolution. This facilitation is a possible explanation for the increase in

perceived contrast at the luminance borders of Mach bands (Ratliff, 1965). For this reason, ganglion cells have been described as "edge detectors".

The receptive fields of cells in the LGN are very similar to those of ganglion cells, and have on- or off-centre concentric receptive fields of around 1 deg diameter (Hubel & Wiesel, 1962). The reason for the similarity is possibly due to the fact that LGN neurons receive input from only a few ganglion axons. Cells in the M layers receive input from parasol ganglion cells, and typically have: larger receptive fields, higher sensitivity to contrast, lower sensitivity to colour, and transient responses, whereas cells in the P layers receive input from midget ganglion cells, and typically have: smaller receptive fields, lower sensitivity to contrast, higher sensitivity to colour, and sustained responses (Shapley, Kaplan & Soodak, 1981).

1.1.2.2 Cortical spatial processing

As described earlier, cells in the LGN project to area V1. The organisation of neurons is such that neighbouring regions of the visual field stimulate neighbouring cortical neurons. This creates a retinotopic map – known as such because it is governed by retinal co-ordinates – which is pervasive in many visual cortical areas. Electrophysiological studies indicate that the receptive fields of V1 cells are different to those of LGN or ganglion cells. For example, whereas a spot of light could strongly activate pre-cortical neurons, cells in V1 are more strongly activated by an elongated bar. Three categories of V1 cell were identified by Hubel and Wiesel: simple, complex and hypercomplex

(Hubel, 1959; Hubel & Wiesel, 1959), although it has been more recently suggested that these fall on a continuum (Chance, Nelson & Abbott, 1998; Geisler & Albrecht, 2000; Mechlar & Ringach, 2002).

Simple cells – which are the dominant cell type in layer 4 of V1 (Gilbert, 1977) – have antagonistic receptive fields similar to those of LGN and ganglion cells, but the receptive fields are typically larger and elongated (rather than concentric) with adjacent on- and off-regions. Due to the elongated nature of typical simple cell receptive fields, the highest firing rate occurs when a bar of light falls only on a excitatory region of the receptive field (or a dark bar on an inhibitory region), that is, when the stimulus is of the cell's preferred orientation (Gilbert, 1977; Jones & Palmer, 1987). When the orientation of the stimulus departs from the preferred orientation of the cell, it excites less of the excitatory region(s) and more of the inhibitory region(s) of the receptive field, and firing rate decreases.

As only a small proportion of complex cells have a direct input from LGN neurons, it is typically assumed that the receptive fields of complex cells are mainly built from the inputs from groups of simple cells with similar axes of orientation preference and whose receptive fields are spatially offset from each other (Hubel & Wiesel, 1962). The receptive fields of complex cells are usually larger than those of simple cells, and rarely have clearly defined on- or off-regions. Therefore, although complex cells are orientation selective, the position of the stimulus within the receptive field is less critical than it is for simple cells. Also, the firing rate of simple cells can be predicted by summing

the responses to their excitatory and inhibitory receptive field regions, in a similar manner to ganglion and LGN neurons. Complex cells, however, have a non-linear response in that their output cannot be predicted by summing the responses to their excitatory and inhibitory receptive field regions (e.g. Skottun De Valois, Grosof, Movshon, Albrecht & Bonds, 1991). Hypercomplex cells show size-modulated responses, termed as "end-stopping" (Hubel & Wiesel, 1962).

In addition to orientation selectivity, a large number of cells in V1 are also selective for spatial frequency when tested with sinusoidal gratings (e.g. Maffei & Fiorentini, 1973; De Valois, Albrecht & Thorell, 1982; Movshon, Thompson & Tolhurst, 1978; Skottun, Bradley, Sclar, Ohzawa & Freeman, 1987). For example, individual simple and complex cells each respond over a discrete range of spatial frequencies. Bandwidths are commonly expressed as the full-width at half-height of the tuning curve for mean firing rate over a range of stimulus spatial frequencies (e.g. Skottun et al., 1987). Spatial frequency bandwidth varies with the cortical area, but the average bandwidth is typically ~ 1.5 octaves (e.g. Campbell et al., 1969; Cooper & Robson, 1968; Movshon et al., 1978; Robson et al., 1988).

The spatial organisation of V1 cells has been mapped in animals using electrophysiology and neural staining techniques (e.g. Hubel & Wiesel, 1968; Tootell, Silverman, Switkes & De Veloy, 1982; Yoshioka, Blasdel, Levitt & Lund, 1996). Each hemisphere shows distinct regions of neurons dominated by inputs from left and right retinae, known as ocular dominance columns, which

when stained are visible as stripes along the cortical surface. Small hypercolumns running perpendicular to the cortical surface consist of two layers (one from a left- and one from a right-ocular dominance column), each containing numerous orientation columns, which are made up of cells selective for a particular orientation. Each hypercolumn signals a specific location within the retinotopic map, and can signal every axis of orientation.

Hubel & Wiesel (1962) suggested a simple hierarchical model to explain orientation selectivity by proposing that elongated V1 receptive fields are constructed from convergent inputs from several concentric LGN cells whose receptive fields overlap along a particular orientation (Figure 1.5). When a stimulus is of the preferred orientation and falls on the excitatory regions of several LGN receptive fields, the resulting synaptic input brings the simple cell to threshold and an action potential is elicited. When a stimulus is of a non-preferred orientation, it cannot elicit an excitatory response in all the LGN neurons at the same time, so the simple cell does not reach threshold. When a stimulus of non-preferred orientation passes along the receptive field of the simple cell, the number of spikes elicited by each LGN cell will be equal to if stimulus was of optimum orientation, but they will be temporally separated (asynchronous), and therefore do not elicit an action potential in the simple cell (Ferster, 2004). The non-linearity of the spike threshold ensures a long-lasting low amplitude input from a non-optimal stimulus elicits no response, whereas a short duration high amplitude input from an optimal stimulus elicits a response.

Hubel & Wiesel's model of orientation tuning in V1 cells, and successors of this, are known as feedforward models, as information flows in one direction – from LGN neurons to simple cells, and then to complex cells. However, feedforward models cannot account for all properties of orientation tuning in simple cells. A different type of model has since been developed by a number of researchers to account for properties of orientation tuning that cannot be explained using a simple feedforward rule – and this class of model is known as a feedback model (Ben-Yishai, Bar-Or & Sompolinsky, 1995; Douglas, Koch, Mahowald, Martin & Suarez, 1995; Sommers, Nelson & Sur, 1995; Sompolinsky & Shapley, 1997; Sillito, Kemp, Milson & Berardi, 1980). The principles of feedback models of orientation tuning are as follows: information reverberates within an excitatory feedback loop between cells within a cortical column, and the responses of each cell are modified over time. The spatial distribution of inputs from LGN cells is not as crucial as the inhibitory lateral

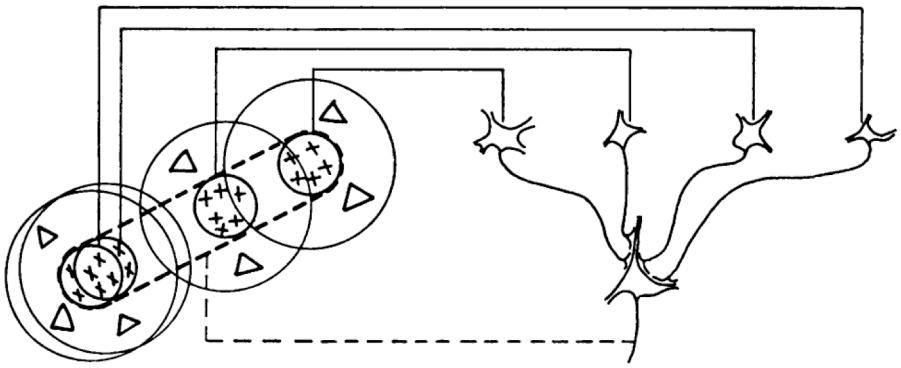

Figure 1.5. Model of the construction of a simple cell receptive field from the input from LGN neurons. The receptive fields of four on-centre LNG cells are shown on the left, projecting to one simple cell, shown on the right. The dashed outline in the receptive field diagram depicts the elongated on-centre region of the V1 cell. Taken from Hubel & Wiesel (1962).

connections between cells, and simple cells are not passive filters. Feedback models propose that neurons within a cortical column (that are all selective for the same orientation) excite one another and therefore amplify the signal from the LGN, but this amplification is prevented from spreading between columns by lateral inhibitory connections. A "winner-takes-all mechanism" is initiated whereby a column that is initially activated more strongly will suppress the weaker activation in other columns via inhibitory projections, and will itself be activated more strongly. Eventually the column that had stronger initial activation will be fully active, and other columns will be silent.

There is a great deal of support for the feedforward model of visual processing. The main premise of feedforward models is that the receptive field of a simple cell arises from the inputs of several LGN cells with overlapping receptive fields. Indeed, Reid & Alonso (1996) simultaneously recorded from neurons in the LGN and in V1 and found strong short-latency spike correlations only when the centre of the LGN receptive field overlapped a subregion of the same polarity in the simple cell. Subregions of simple cells therefore appear to arise as a result of direct LGN input, as postulated by Hubel & Wiesel (1962). Feedback models predict that orientation selectivity can only arise when the local cortical circuits are intact. However, when this prediction was tested by cooling the cortex so that most cortical cells and interneurons stopped firing, the orientation tuning of the residual responses was almost identical to when the cortex was intact, suggesting that the response originated primarily from inputs from the LGN (Ferster, Chung & Wheat, 1996). Another study interrupted local circuits by applying an electric current to the cortex that

evoked a 200 ms inhibition of nearly every cell within a 1 mm radius throughout the depth of the cortex (Chung & Ferster, 1998). Although no spikes were elicited by an optimally-oriented grating during the period of inhibition, intracellular recording revealed that the membrane potential was reduced by ~ 50 % in simple cells that had a direct input from the LGN, and the orientation selectivity of this response was not significantly different from when the cortical circuits were active. It therefore appears from the studies mentioned above that the cortical circuit does not appear to refine orientation selectivity beyond that of the LGN inputs.

It has also been demonstrated that the tuning width of simple cells (commonly expressed as the full-width at half-height of the tuning curve for mean firing rate over a range of stimulus orientations) can be predicted by the length and width of receptive field subregions (e.g. Jones & Palmer, 1987, Gardner, Anzai, Ohzawa & Freeman, 1999). According to the feedforward model, a longer and narrower receptive field subregion entails a greater sensitivity to small changes in stimulus orientation. Lampl, Anderson, Gillespre & Ferster (2001) mapped the receptive fields of simple cells using small spots of light and predicted orientation sensitivity using linear summation. Lampl et al. (2001) found that the width of the predicted tuning curve matched the measured curve of the majority of cells. Further evidence in support of a feedforward model of orientation tuning lies in the predictions the model makes about orientation selectivity during the early part of a response. For example, it is predicted that if all LGN input cells are excited at the same time, the simple cell should be well-tuned as soon as orientation tuning can be

measured. Conversely, the feedback model would predict that the orientation tuning width would narrow over the first part of the response, as the initial input from LGN cells is poorly tuned, and this is then sharpened by inhibitory connections from other cortical columns. When membrane potential is measured intracellularly, it has been found that at the earliest time that the responses can be measured above noise, the width of orientation tuning is identical to that observed at the peak of the response (Gillespie, Lampl, Anderson & Ferster, 2001). However, other evidence suggests that orientation selectivity of V1 neurons does in fact change over time (Dragoi, Sharma, Miller & Sur, 2002). Dragoi and colleagues reported that brief adaptation (400 ms) to an oriented grating impaired identification of nearby orientations by broadening orientation selectivity and changing the preferred orientation, and importantly, enhanced the identification of orthogonal orientations by sharpening neuronal selectivity. This implies that it is likely that feedback mechanisms play a role in orientation selectivity of V1 neurons, which refines selectivity beyond LGN inputs. In conclusion, the exact mechanism underlying orientation selectivity remains controversial.

Contrast invariance of orientation tuning refers to the phenomenon that orientation selectivity varies little with contrast, even though the amplitude of the response of a V1 cell increases approximately linearly over log contrast (e.g. Sclar & Freeman, 1982; Skottun, Bradley, Sclar, Ohzawa & Freeman, 1987). The feedforward model of orientation tuning, however, would predict broadening of tuning with increasing contrast, as the cell's membrane potential elicited by non-optimal orientations would increase with contrast and would

therefore be more likely to reach threshold at higher contrasts. The feedback model does not suffer from this shortcoming due to the nature of the "winner-takes-all" activity in the cortical column with the preferred orientation that most closely matches that of the stimulus, therefore the pattern of activity is relatively independent of contrast. With minor modifications however (such as feedforward inhibitions from other simple cells), the feedforward model is able to explain most of the orientation tuning properties of V1 cells (Ferster, 2004).

Numerous psychophysical studies have demonstrated orientation-selective mechanisms in the human visual system, primarily through the use of adaptation, masking and summation experiments. For example, in two classical adaptation studies by Blakemore & Campbell (1969a; 1969b), it was reported that adaptation to a high contrast grating reduces the amplitude of the occipital evoked potential to a subsequently presented grating, in addition to raising psychophysical contrast thresholds for subsequently presented gratings. Importantly, this contrast threshold elevation is limited to test stimuli of similar orientations to the adaptor. Orientation adaptation bandwidths can therefore be estimated psychophysically by plotting changes in sensitivity (e.g. contrast threshold) after adaptation, for a continuum of stimulus orientations or spatial frequencies. However, it must be noted that bandwidths measured psychophysically are an estimate of the combined output of a large neural population.

Behavioural estimates of orientation bandwidths also vary with psychophysical method used to measure them. For example, adaptation studies have suggested

bandwidth to be ~ 15 deg (e.g. Blakemore & Campbell, 1969a; Blakemore & Campbell, 1969b), masking studies suggest ~ 27 deg (e.g. Campbell & Kulikowski, 1966) and summation studies estimate bandwidth to be as narrow as 6 deg (e.g. Kulikowski, Abadi & King-Smith, 1973). Furthermore, orientation bandwidths depend on other stimulus factors such as spatial frequency (e.g. Anderson & Burr, 1985; Burr & Wijesundra, 1991).

The relationship between activation of individual neurons and perception remains a key challenge in sensory neuroscience. Taken to its fullest conclusion, the lower envelope principle states that a single neuron governs the behavioural threshold. For example, Geisler & Albrecht (1997) compared neural and psychophysical sensitivity for contrast and spatial frequency in the visual system in monkeys, where they employed signal detection theory to determine the minimum increment of contrast or spatial frequency that could be reliably signalled as different by V1 neurons. Geisler & Albrecht (1997) reported that the best V1 neurons closely matched psychophysical performance, consistent with the lower envelope principle for relating neural activity and behaviour. However, this model requires that the observer has knowledge about which neurons should be monitored, and assumes that observers can identify the group of neurons that deliver the best information for a particular task. A potential problem for cortical cells is that a similar response may be elicited in an individual cell by two different visual stimuli. For example, a cell might respond weakly to a low-contrast stimulus of optimum orientation, but have the same response to a high-contrast stimulus of non-optimal orientation. The theory of population coding is thought to

overcome the problem. By comparing the distribution of activation across a population of neurons that sample the same region of space, the overall firing rate will differ independently with changes in, for example, orientation and contrast. This ensures that a cell's firing rate is devoid of orientational ambiguity regardless of contrast (e.g. Lamme, 2004).

The presence of orientation-selective mechanisms in human (as well as animal) primary visual cortex is corroborated by high-resolution neuroimaging studies. Fang, Murray, Kersten & He (2005) reported that the magnitude of the fMRI signal evoked by a test stimulus was proportional to the difference in orientation of the test stimulus relative to an adapting stimulus, in accordance with psychophysical adaptation effects. Fang et al. also found that the magnitude of post-adaptation fMRI signal in area V1 was dependent on adaptation duration, in a similar manner to contrast threshold elevation (longer adaptation periods yielded a greater effect). The specificity of adaptation of V1 cells to first order (luminance-defined) and not second order (contrast-defined) oriented edges was shown in a subsequent fMRI experiment by Larsson, Landy & Heeger (2006).

Evidence that the human visual system is composed of spatial frequency sensitive mechanisms or channels was first provided by Campbell & Robson (1968). Campbell & Robson measured detection thresholds for sinusoidal gratings, as a function of spatial frequency, to create a contrast sensitivity function (CSF). Sensitivity, the reciprocal of detection threshold, varied across spatial frequencies, with peak sensitivity at or around 4 c/deg. As spatial

frequency departs from ~ 4 c/deg, higher contrast levels are necessary for detection (reflecting lower sensitivity); this 'window of visibility' is demonstrated in Figure 1.6. Human observers are typically unable to detect spatial frequencies lower than ~ 0.1 c/deg or higher than ~ 60 c/deg. Blakemore and Campbell (1969) adapted observers to stationary gratings and found that contrast thresholds were increased for subsequently presented test gratings whose spatial frequency was similar to that of the adaptor. When a channel is adapted, its sensitivity (and that of neighbouring channels) is temporarily depressed. Similar effects have also been reported by Pantle & Sekuler (1968). It has been suggested that the CSF reflects the tuning properties of many overlapping spatial frequency channels, each sensitive to a particular spatial frequency range.

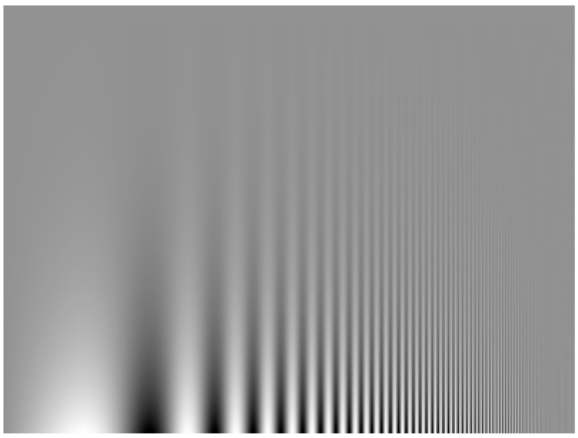

Figure 1.6. A spatial frequency ramp demonstrating how contrast sensitivity varies with spatial frequency. Contrast increases from the bottom to the top of the figure, and spatial frequency increases from the left to the right of the figure. (Taken from Campbell & Robson, 1968.)

1.1.3 Temporal processing

As discussed earlier in this chapter, retinal ganglion cells have specific spatial properties. Similarly, they also have specific temporal properties. All ganglion cells have a discrete region of space from which they are receptive to photons of light (their receptive field), in addition to a temporal limit to their receptivity, which is known as their critical duration (Hart Jr, 1992). If a sufficient number of photons fall on the receptive field within the critical duration, the cell will fire. This process is known as temporal summation. Whereas rod cells respond slowly in order that the effects of photons absorbed over a period of around 100 ms summate, the temporal integration for cones is ~ 15 ms, and they can resolve flicker up to 55 Hz. Rods cannot resolve flicker greater than around 12 Hz (e.g. Stewart, 1972).

Within the critical duration, perceived brightness of a stimulus varies with its luminance and duration. This relationship is known as Bloch's Law, and states that for a stimulus at detection threshold to remain detectable at half the duration, luminance would need to be doubled. When the stimulus exceeds the critical duration, however, perceived intensity is independent of duration and instead depends on luminance.

As discussed earlier, magno cells in the LGN have different properties to those of parvo cells. Magno cells are approximately ten times more sensitive to low spatial frequency gratings than parvo cells when the visual stimulus is flickered at a high rate (Kaplan & Shapley, 1982; Derrington & Lennie, 1984).

The behavioural effect of lesions in the magno and parvo layers of the primate LGN is consistent with this. After a parvo layer lesion but not after a magno layer lesion, contrast sensitivity to stationary gratings decreases. However, the reverse is true for low frequency flickering grating (Merigan, Byrne & Maunsell, 1991; Merigan, Katz & Maunsell, 1991).

Temporal resolution can be measured psychophysically by measuring the Critical Flicker Fusion frequency (CFF), which is the maximum temporal frequency at which a flickering light can be reliably discriminated from a non-flickering steady light. In optimal conditions, CFF can be as high as 65 Hz (65 on/off cycles per second), but is typically ~ 30 – 60 Hz (Hart Jr, 1992). In a seminal study by Kelly (1961), temporal contrast sensitivity function was measured by varying the luminance contrast amplitude at a range of temporal frequencies until flicker could reliably be detected. The traditional shape of the contrast sensitivity function only holds with stimuli of low temporal frequencies (e.g. Robson, 1966; van Nes, Koenderink, Nas & Bouman, 1967). At mid to high temporal frequencies, sensitivity to low spatial frequencies showed a marked increase, eradicating low spatial frequency attenuation. This was then later addressed using stabilised retinal images that allow precise control of temporal frequency (Kelly, 1984), where it was found that contrast sensitivity changes from a bandpass function at low temporal frequencies to a low-pass function as temporal frequency increases (that is, sensitivity is enhanced at lower spatial frequencies).

1.1.4 Spatio-temporal processing

Electrophysiological studies have shown that approximately 20 % of complex cells are directionally selective (Hubel & Wiesel, 1968) (Figure 1.7). As cells in area V1 have comparatively small receptive fields (on the order of 1 – 2 deg at the fovea) they detect only the local motion directions of an object's component parts. This results in ambiguous information regarding the direction of the object as is detailed in the well-known 'aperture problem'. This problem arises as V1 cells respond only to the proportion of motion orthogonal to the length of an edge (Marr & Hildreth, 1980) and so different parts of the object appear to move in different directions. As the output of any individual V1 neuron is ambiguous with regard to direction, information from many V1 cells must be subsequently combined (integrated or pooled) across

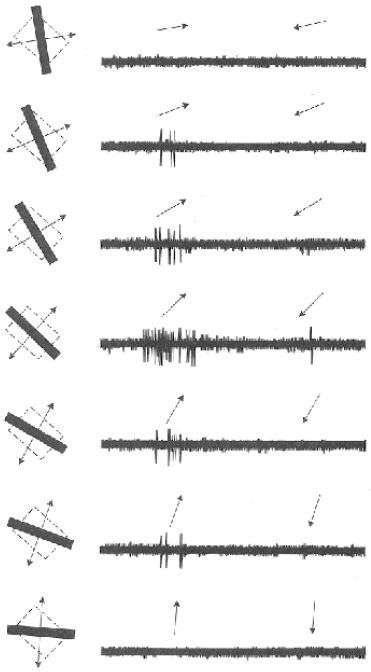

Figure 1.7. The responses of a complex cell in layer 4B of primary visual cortex of monkey. The responses of the cell (shown as the unfilled rectangle) to a bar (shown as the filled rectangle) presented at 7 different orientations, were measured in terms of spike rate (shown on the right) for motion in both directions perpendicular to the orientation of the bar. It can be seen that the preferred orientation for this cell is ~ 45 deg anticlockwise of vertical, and that the cell responds preferentially when the bar moves towards the upper right. When the bar moves to the lower left there is only a very small response. As the orientation of the bar departs from the preferred orientation, neural responses become weaker. When the orientation of the bar is ~ 45 deg different to the preferred orientation, there is little or no response. (Taken from Hubel and Wiesel, 1968.)

space and time to determine the overall (global) stimulus direction (Williams & Sekuler, 1984). It is known that neurons in V1 project to specialised "higher" visual cortical areas, such as areas V2, V3 and V5/MT, that in turn pool information from their earlier inputs allowing them to respond selectively to more complex features of a visual stimulus (e.g. Van Essen & Maunsell, 1983; DeYoe & Van Essen, 1988; Livingstone & Hubel, 1988; Zeki & Shipp, 1988). Livingstone & Hubel (1984) reported that complex cells in layer 4B are typically non-selective for colour, magno-dominated and direction-tuned. Directionally tuned complex cells have been demonstrated to project upstream from layer 4B to the 'motion centre', area V5/MT (Movshon & Newsome, 1996). Complex cells in layer 4B of V1 also project to areas V2 and V3 (Felleman & Van Essen, 1991) but it has been reported that different populations of cells project to each of these areas, and the proportion of directionally selective cells projecting to V2 and V3 is less clear (Sincich & Horton, 2003).

The integration of local motion signals, necessary to overcome the aperture problem, is thought to take place in area V5/MT where receptive fields are estimated to be up to tenfold larger in diameter than those of V1 neurons (Gattass & Gross, 1981; Albright & Desimone, 1987; Movshon, Adelson, Gizzi & Newsome, 1985; Born & Bradley, 2005). Furthermore electrophysiological studies of the response properties of V5/MT neurons have revealed that this area is highly specialised for encoding global motion, as opposed to local motion signals (e.g. Zeki, 1974; Van Essen, Maunsell & Bixby, 1981; Albright, Desimone & Gross, 1984; Newsome & Paré, 1988).

For example, random dot kinematograms (RDKs) containing a coherently translating global motion signal, embedded within a field of randomly moving elements, have been used to demonstrate a strong positive correlation between V5/MT neural responses and primate behavioural performance on a psychophysical global motion task (Britten, Shadlen, Newsome & Movshon, 1993).

It has been reported that up to 90 % of cells in area MT of the macaque are sensitive to motion direction (Albright, 1993) and suppression induced by motion opposite to the preferred direction is prevalent in many cells. Lesions to this area result in a range of deficits selective to visual motion perception, such as reduced direction discrimination (Newsome & Paré, 1988) and impairments of visual pursuit movement (Dürsteler & Wurtz, 1988). Area V5/MT has a columnar organisation, with preferred direction remaining consistent throughout the cortical layers, but varying along the columns (Albright, Desimone & Gross, 1984). Neurons in some columns have a centre-surround directional organisation whereas others have asymmetrical receptive fields (Xiao, Raiguel, Marcar & Orban, 1997). The directional bandwidth of V5/MT neurons (half-width at half-height) is estimated to be ~ 50 to 60 deg (Maunsell & Van Essen, 1983; Albright, 1984; Lagae, Raiguel & Orban, 1993).

V5/MT cells have been categorised into component cells and pattern cells (Movshon et al., 1985). Movshon and colleagues used plaid stimuli to demonstrate that some V5/MT cells respond optimally to *combinations* of

simple stimuli. Plaid stimuli are generated by superimposing two sinusoidal (or square wave) gratings of different orientations. When in motion, plaids are typically perceived as moving in a direction that is midway between the directions of the two component gratings. This direction corresponds to the movement of the 'corners' within the plaid where the two gratings cross. It was found in this electrophysiological study that cells in area V1 and approximately one third of cells in V5/MT respond vigorously to the motion direction of the component gratings of a plaid stimulus, that is, to the directions orthogonal to the component grating orientations. These cells were termed 'component' cells. However, approximately one third of V5/MT cells responded optimally to the direction of the combined pattern rather than to the component gratings, representing the first stage in the visual system to respond to the direction of a stimulus independently of the orientations of its components. These cells were termed 'pattern' cells. These direction-selective pattern cells receive input from the component V5/MT cells, which in turn, receive input from area V1 cells that similarly respond to component direction. The rest of V5/MT cells were found to be intermediate. This continuum suggests that global motion perception of a whole object is achieved by the combination of component motion signals from the component direction-selective cells of V1 and V5/MT, and by pattern direction-selective cells in V5/MT (e.g. Smith, Majaj & Movshon, 2005; Majaj, Carandini & Movshon 2007).

To determine velocity, spatial frequency, temporal frequency and direction of motion all need to be combined (Heeger, 1987; Simoncelli & Heeger, 1998). It

has been found that some V1 cells are selective for temporal frequency, regardless of the stimulus spatial frequency (Foster, Gaska, Nagler & Pollen, 1985), implying that V1 cells are not speed-tuned and that spatial and temporal information are encoded separately. However, it has been reported that some V5/MT neurons are sensitive to object speed (e.g. Perrone & Thiele, 2001). In Perrone & Thiele's (2001) study, macaque V5/MT cell responses were recorded whilst gratings of different spatial and temporal frequencies were viewed. It was found that cells responded selectively to particular combinations of spatiotemporal frequencies. This implies that spatial and temporal information is processed inseparably in V5/MT cells. It has since been reported that only a minority of V5/MT cells are speed tuned when tested with simple sinusoidal gratings, but that more V5/MT cells show good speed-tuning to spatially broadband stimuli that have more in common with real-world objects (Priebe, Cassanello & Lisberger, 2003). Neurons in V5/MT are typically bandpass tuned for speed, with preferred speed ranging from ~ 5 deg/s to ~ 30 deg/s (Maunsell & Van Essen, 1983). Random dot kinematograms have proved useful for investigating the perception of global motion. Williams & Sekuler (1984) proposed that local motions of individual dots were initially detected independently, then combined across space, and finally over time to extract the global motion signal. This has since received support (Williams, Phillips & Sekuler, 1986; Williams & Phillips, 1987; Smith, Snowden & Milne, 1994) and models of global motion perception have been developed (e.g. Watamaniuk, Sekuler & Williams, 1989; Williams, Tweten & Sekuler, 1991, Jazayeri & Movshon, 2007; Webb, Ledgeway & McGraw, 2007).

Adjacent to area V5/MT is the medial superior temporal cortical area (MST), which contains neurons that respond selectively to more complex global motion representations, such as radial (expanding vs. contracting) and rotational (anticlockwise vs. clockwise) components of optic flow fields (Tanaka, Fukada & Saito, 1989; Duffy & Wurtz, 1991a; Duffy & Wurtz, 1991b). Neurons with centre-surround receptive fields in MT preferentially project to dorsal MST [MSTd], whereas MT neurons with asymmetric receptive fields preferentially project to lateral MST [MSTl] (Duffy, 2004). MSTl neurons show size- and speed-dependent selectivity – when a moving dot pattern is small (less than ~ 20 deg diameter), preference for one direction will be evoked, but when the pattern is large, preference will be for the opposite direction (Tanaka, Sugita, Moriya & Saito, 1993). At intermediate sizes responses are instead modulated by speed, such that direction preference is determined by the image speed. Neurons in MSTd respond preferentially to very large stimuli (circular diameters greater than 40 deg), and either show preferences for individual directions of optic flow (for example, translational, circular or radial), or for combinations of two of these motion types, or combinations of all three of these motion types (Duffy & Wurtz, 1991a; Duffy & Wurtz, 1991b).

In terms of the human visual system several neuroimaging studies have demonstrated a homologue of the monkey global motion complex, often referred to as V5/MT+, suggested to contain both MT plus adjacent motion-sensitive areas including MST (e.g. Zeki et al., 1991; Watson et al., 1993; Tootell et al., 1995; Heeger et al., 1999; Huk et al., 2002). Moreover, area

V5/MT+, but not area V1, shows stronger activation to coherent global motion than to random motion (Braddick, O'Brien, Wattem-Bell, Atkinson & Hartley, 2001), and neural responses increase linearly with changes in the level of motion coherence (Rees, Friston & Koch, 2000). Functional magnetic resonance imaging (fMRI) has also revealed an area within V5/MT+ that responds to translational global motion, and this neural activity is separate and distinct from that arising from another area within V5/MT+ that responds to radial and rotational global motion (Morrone, Tosetti, Montanaro, Fiorentini, Cioni & Burr, 2000; Smith, Wall, Williams & Singh, 2006; Wall, Lingnau, Ashida & Smith, 2008). This suggests that hierarchical processing, which is typical of information exchange between V1 and V5/MT is also evident between V5/MT and MST, since MST receives input from V5/MT neurons (Maunsell & Van Essen, 1983). In support of this, a recent imaging study using electroencephalography (EEG) reported significantly stronger "later" responses elicited by V5/MT complexes for rotational motion than for translational motion, consistent with a hierarchical model of analysis for increasingly complex global motion features (Delon-Martin, Gobbele, Buchner, Haug, Antal, Darvas & Paulus, 2006).

Traditionally it has been proposed that two distinct types of motion analysing occur in human visual processing to extract the local motion of objects moving across the visual field, for example the so-called "short-range" and "long-range" motion-detecting systems (Braddick, 1974; Braddick, 1980; Anstis, 1978; Anstis, 1980). The short-range system is identified with the responses of directionally selective neurons to variations in spatio-temporal intensity

changes in the retinal image, and it thought to be responsible for the processing of apparent motion with small (lower than ~ 0.25 deg) spatial displacements, and short (less than ~ 100 ms) temporal intervals between successive stimulus presentations (Braddick, 1973, 1974). The short-range process produces motion aftereffects (Banks & Kane, 1972; Anstis & Mather, 1985) but motion is not perceived when successive stimuli are presented dichoptically (Braddick, 1974), or when stimulus patterns are defined by chromatic as opposed to luminance contrast (Ramachandran & Gregory, 1978). The long-range system, however, is thought to reflect high-level processing which involves computing correspondences between features, and is thought to be responsible for the processing of apparent motion with spatial displacements of many degrees (Zeemann & Roelofs, 1953), and longer temporal intervals (up to ~ 500ms) between stimulus presentations (Mather, 1989). The long-range process produces little or no motion aftereffects (Banks & Kane, 1972; Anstis, 1980; Anstis & Mather, 1985), but motion is perceived when stimulus patterns are defined by chromatic contrast (Ramachandran & Gregory, 1978), and when successive stimuli are presented dichoptically (Shipley, Kenney & King, 1945).

Random-dot field stimuli have been typically used to study the short-range motion system, whereby pairs of random-dot fields presented successively were identical except that a central square region was shifted horizontally in one stimulus. The offset of the central square was not apparent when the stimuli were viewed separately (Anstis, 1980). When appropriate spatial and temporal conditions were used, successive presentation of the two dot patterns

had the effect of producing apparent motion of the central region moving rightwards and leftwards when each stimulus was presented in quick succession. As the central square was not visible until the local dots have been compared and motion has been perceived, it is assumed that the motion perception is not mediated by long-range feature-tracking mechanisms. Long-range motion processing is typically studied using stimuli comprising localised objects that are oscillated over larger spatial and temporal separations that are thought not to activate short-range motion detectors.

More recently, it has been argued that distinctions between motion-detecting systems should be based on processing rather than stimulus differences (Cavanagh & Mather, 1989), and that 'passive' and 'active' motion processes can potentially account for the detection of motion stimuli previously classified as short- and long-range (Cavanagh, 1992). It is proposed that passive processes are pre-attentive and involve low-level detectors, whereas active processes are post-attentive and involve feature detectors.

A feature-detecting model based on computing the correspondence between stimulus features – the Minimal Mapping Theory – was developed by Ullman (1979), and is comparable to the long-range motion detecting system. According to this theory, correspondences are computed between elements of a visual stimulus (for example, edges and corners). When more complex stimuli are used the problem of correspondence occurs (Braddick, 1974), which refers to the question of how successively presented points are matched up to each other. In Ulmann's model, an affinity measure is calculated for every possible

match, where elements that are similar and have been displaced over a smaller spatial separation are more likely to be a correct match, and have a greater affinity. The output of the model is an overall global prediction which favours local matches with strong affinities. A shortcoming of this model is that little is known about how elements of the visual stimulus are extracted and the extent of similarity needed between successive presentations to support the perception of apparent motion. However, although relatively little is known about the physiological basis of feature matching, there is evidence that regions in the inferotemporal cortex of the monkey respond selectively to object features (such as corners) in the retinal image (e.g. Fujita, Tanaka, Ito & Cheng, 1992), which could potentially be involved in the feature extraction of Ulmann's model.

One of the earliest and most influential low-level motion detection models was developed by Reichardt (1961), and is based on the visual system of insects. Reichardt's model operates on a "delay-and-compare" principle whereby a motion sensor compares a time-shifted version of the same signal in two regions of space. A direction-selective subunit with a pair of receptors that sample two different points in the visual field, is the simplest form of the model. Each subunit prefers motion in a particular direction. A translating motion stimulus activates one receptor before the other receptor, and the outputs of the two receptors are multiplied (correlated). If the internal delay matches the external delay between the inputs to the receptors, motion is signalled by the sub-unit: motion in the preferred direction evokes a positive output and motion in the non-preferred direction is signalled by a negative

output of the subunit. By subtracting the outputs of two subunits that prefer opposite directions the local direction and strength of motion can be computed. A major shortcoming of this model, as applied to higher mammals such as cats and monkeys, is that physiological studies have demonstrated that neither the retina nor LGN contain cells that are sensitive to the direction of motion (e.g. Hubel & Wiesel, 1961; Shapley & Lennie, 1985). Cells in V1 that are directionally selective, however, have receptive fields that respond to larger areas of the visual field as opposed to single points. Furthermore, the Reichardt detector suffers from spatial aliasing: motion in the wrong direction is signalled when the distance between each receptor is between 0.5 and 1.0 spatial periods. Another disadvantage is that the outputs of many Reichardt detectors need to be combined to determine the overall perception of motion, and how this might be achieved is left unspecified in the original model.

To overcome the limitations of the Reichardt detector as a model of human vision, Van Santen & Sperling (1984, 1985) developed the model further, and their model is known as the Elaborated Reichardt detector (ERD), and is shown in Figure 1.8. The receptors of the ERD are linear, spatial frequency-selective receptive fields separated by a quarter of a cycle to prevent the spatial aliasing problem of the earlier model. Consequently, the receptive fields of the input spatial filters are in quadrature phase (have a phase difference of 90 deg). In addition, to eliminate temporal aliasing the temporal delay filters can be modified so that all temporal frequencies are delayed by a quarter of a cycle. The spatial and temporal filters are proposed to be separable to allow independent operation. An important distinction between the ERD and the

earlier Reichardt model is that the ERD contains a 'voting rule', which specifies how the outputs from multiple units each with different spatial filtering properties are combined to model the final response of the visual system to motion. While the ERD can account for psychophysical findings that cannot be predicted by the earlier Reichardt model, it must be noted that the model can only predict direction and not the speed of the motion.

It is important to note that several other models of lower-level motion detection have been proposed that share much in common with the ERD. For example, the influential Motion Energy Model (Adelson & Bergen, 1985), the Scalar Motion Sensor model (Watson & Ahumada, 1985) and spatiotemporal

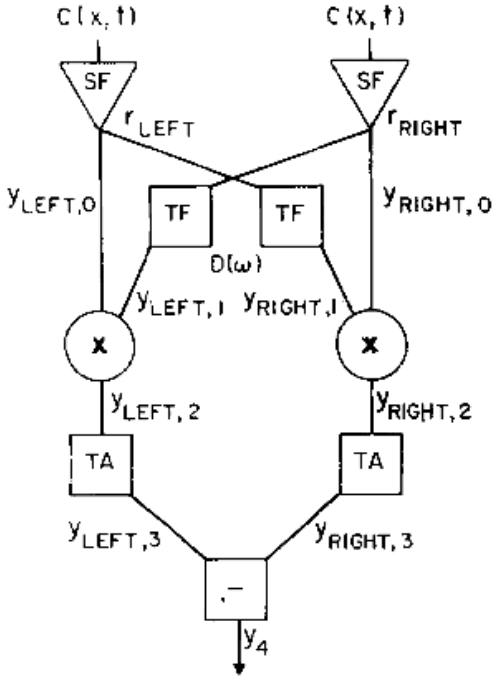

Figure 1.8. The Elaborated Reichardt detector (ERD). The input luminance pattern with contrast *c (x, t)* is sampled by linear spatial filters *SF* with responses *r* at locations *x*. *Y* represents the signal at each stage, *TF* is a time-variant filter and *X* is the multiplication unit. *TA* represents a temporal integration operation. Taken from van Santen & Sperling (1985).

gradient models (e.g. Marr & Ullman, 1981). Although these models operate upon slightly different principles, Van Santen & Sperling (1985) have shown that they can be made formally equivalent to the ERD model.

1.1.5 Feedback mechanisms

Feedback models of orientation selectivity were discussed earlier in this chapter, where the output of a group of V1 cells modifies the response of the 'downstream' simple cells which in turn project back 'upstream', in a feedback loop. In these models, the orientation bandwidth of the 'lower' simple cells becomes narrower over time. Feedback circuits exist within and between cortical areas in almost equal numbers to feedforward projections (Felleman & Van Essen, 1991; Johnson & Burkhalter, 1996; Kennedy, Barone & Falchier, 2000). The precise functional role of feedback connections, however, is still somewhat unclear.

The physiological role of feedback has been studied in monkeys by reversible cooling of higher cortical areas while recording the responses of lower visual areas. For example, when feedback inputs from area V2 or V3 to V1 were disrupted, responses of V1 neurons to stimuli moving within their classical receptive field were inhibited (Sandell & Schiller, 1982), or had less suppression to stimuli outside the receptive field (Hupe, James, Payne, Lombar, Girard & Bullier, 1998). This suggests that feedback connections between areas V2, V3 and V1 are involved in the discrimination of objects relative to the background. There is also indirect evidence that feedback

connections mediate top-down influence that result from attention, memory and imagery (e.g. Ishai & Sagi, 1995; McAdams & Maunsell, 2000; Naya, Yoshida & Miyashita, 2001). However the role of feedback – especially with regard to motion processing in human vision – is still largely unknown, and future research is needed to address this issue.

1.2 Transcranial magnetic stimulation

1.2.1 Principles of TMS

Transcranial magnetic stimulation (TMS) is a non-invasive technique used to modulate the activity of cortical neurons using time-varying magnetic fields, developed by Barker and colleagues (Barker & Freeston, 1985; Barker, Freeston, Jalinous, Merton & Morton, 1985; Barker, Jalinous & Freeston, 1985). In 1831 Michael Faraday described the principle of electromagnetic induction, which is the mechanism behind TMS systems. When an electrical current is passed through a wire loop, or coil, it creates a magnetic field that is perpendicular to the orientation of the coil (Figure 1.9). A changing electrical current produces a changing magnetic field, which generates an electric field, which in turn induces a secondary electrical 'eddy' current in a nearby conductive medium, such as cortical tissue. This secondary current travels in

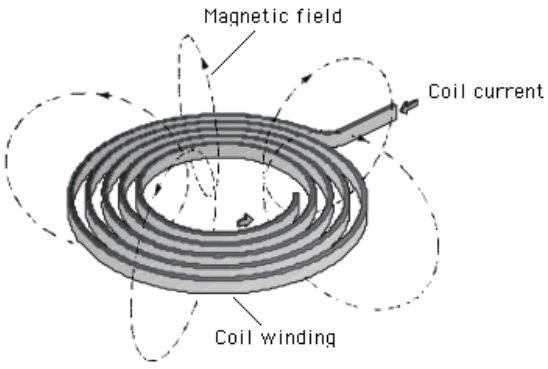

Figure 1.9. Inside a TMS coil, a high voltage electrical current is passed through a length of copper wound into a coil. This creates a magnetic field around the coil that is perpendicular to the orientation of the coil. Taken from Jalinous (1998).

the opposite direction to that of the primary current as a consequence of Lenz's law (Figure 1.10), and can cause a physiological response by depolarising neurons and thus triggering action potentials. Under normal conditions, when a nerve cell membrane is sufficiently depolarised by an increase in voltage (for example, from a resting potential of around -75 mV to around -50 mV), action potentials are typically initiated at the axon hillock next to the cell body (Stuart, Spruston, Sakmann & Häusser, 1997). The flow of an action potential along an axon membrane has been described qualitatively by *cable theory*, in which the neuron is treated as a perfectly cylindrical, electrically passive transmission cable that can be described by a partial differential equation (Hodgkin & Ruston, 1946). Cable theory has also been used in computational models to describe the activation of neurons by TMS, where it has been suggested that the efficacy of neural stimulation is determined by the spatial derivative of the electric field parallel to the neuron (e.g. Reilly, 1989; Roth & Basser, 1990) [see Figure 1.11b – note that the action potential is initiated at a

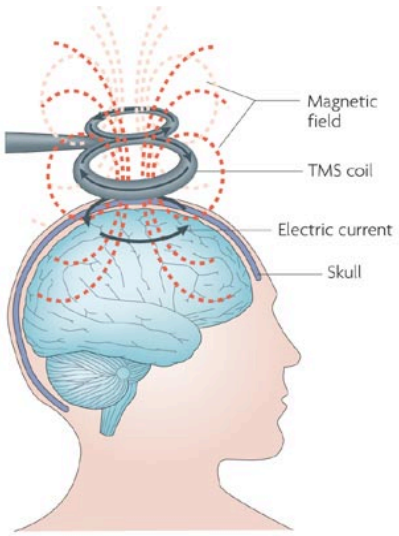

Figure 1.10. The magnetic field passes without attenuation through the skull, and evokes a secondary current in cortical tissue, which travels in the opposite direction to the current in the coil. Taken from Ridding & Rothwell (2007).

point along the axon]. However, models using cable theory analyse infinitely long axons, which is highly inappropriate for modelling the effect of TMS on human cortex as neurons have relatively short dimensions relative to the stimulating coils. It has also been reported that neural excitation occurs when the electrical field is homogeneous – provided that the neuron bends (Amassian, Eberle, Maccabee & Cracco, 1992). Amassian and colleagues applied single TMS pulses to a plastic human skull within which was a peripheral nerve (mammalian or amphibian) immersed in isotonic saline solution. The nerve was recorded out of the volume conductor when straight, and also when bends had been introduced in the nerve trajectory to resemble

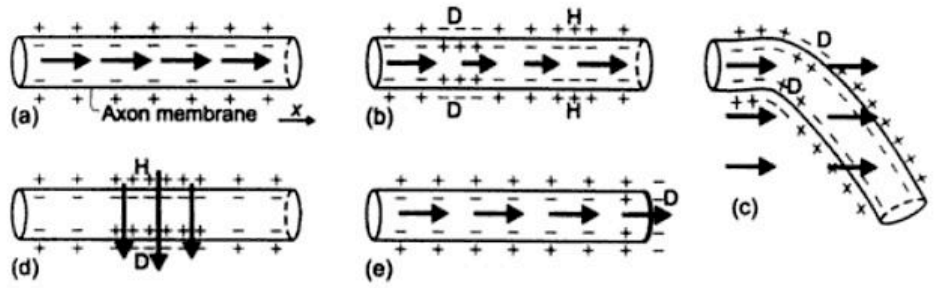

Figure 1.11. Modes of neural stimulation by an electric field. Depolarisation occurs at points along the membrane experiencing current efflux; arrows indicate current flow. When the axon lies in the direction of a uniform electric field, there is no change in transmembrane current (a). In (b), there is a gradient change in transmembrane potential due to a non-uniform field along the axon. The site where excitation first occurs will be the one in which the depolarisation is maximal (in this case, towards the left where the voltage is highest). In (c), the gradient change in transmembrane current is brought about by the spatial variation (bending) of the nerve fibre rather than inhomogeneities in the electric field. The neuron in (d) lies in a transverse orientation to the electric field, and hyperpolarisation and depolarisation occur across the membrane in the direction of the field. Changes in activation at the axon terminal are shown in (e). Depolarisation and hyperpolarisation are represented by D and H respectively. Taken from Ruohonen & Illmoniemi, (1999).

those of corticospinal tract fibres originating in the motor cortex. It was calculated that the excitation of straight nerves occurs near the peak electric field, whereas the activation of bent nerves occurs at the positive peak of the spatial derivative (that is, where the nerve bends in relation to the direction of the electric field) [see Figure 1.11c]. This finding has since been confirmed by a simulation study on pyramidal tract neurons (Salvador, Silva, Basser & Miranda, 2008). A separate study using similar methodology to that of Amassian et al. (1992) also reported that when a nerve is bent and the induced current is directed along the nerve toward the bend, the threshold of excitation is reduced at the bend (Maccabee, Amassian, Eberle & Cracco, 1993). Furthermore, Maccabee et al. (1993) report that increasing the angle of the bend in the nerve from 0 deg to more than 90 deg produced a graded decrease in activation threshold. Additionally, simulation and *in vitro* studies imply that activation threshold is decreased where the axon terminates (e.g. Nagarajan, Durand & Warman, 1993), or has been cut (Maccabee et al., 1993) [Figure 1.11e]. It is proposed that the excitation of finite neural structures by electric fields can be characterised by two driving functions: one is due to the field gradient at neural membranes (either along or across the membrane as in Figures 1.11b and d) and the other is due to the boundaries of neural structures, such as bends, branching, and axons terminating on boutons or cell bodies (as in Figures 1.11c and e) [Nagarajan et al., 1993; Reilly & Diamant 2003].

1.2.2 Stimulation parameters

The magnitude and distribution of the magnetic field, the associated electric field and the induced secondary current depend on a number of stimulation parameters such as the waveform, amplitude and direction of the current in the coil, the coil geometry and size, and the conductivity profile of the head.

1.2.2.1 Pulse waveform

Magnetic stimulators are composed of only a few main elements: a high voltage generator producing currents of up to ~ 8000 amps, a capacitor that stores the required current ready to be discharged, an inductor – the stimulating coil – through which an alternating electrical current may be passed, and a switch to connect the capacitor and the inductor (coil). At the beginning of a TMS pulse, all the energy is stored in the capacitor. When the capacitor discharges, the current flows and all the energy is transferred to the coil. The discharge can be monophasic or biphasic in waveform (see Figure 1.12). To summarise, the monophasic waveform (Figure 1.12a) is created by a unidirectional current through the stimulating coil. The induced voltage in the coil increases very steeply at the start of the pulse, then decreases over ~ 100 μs, after which the coil current slowly dissipates over ~ 300 μs (Hovey, Houseman & Jalinous, 2003; Sommer, Alfaro, Rummel, Speck, Lang, Tings & Paulus, 2006). Only in the initial part of the pulse is the induced voltage high enough to depolarise membranes. Because current in the coil is unidirectional,

the direction of the induced current in the cortex is also unidirectional (as is discussed later).

Biphasic pulses (depicted in Figure 1.12b) are produced by the discharge current flowing through the coil in one direction, and then in the reverse direction. The first quarter cycle of the induced voltage curve is similar to that of the monophasic pulse, but in the biphasic pulse the second and third quarter cycles continue to contribute to the changing magnetic field, which evokes an electric field (Bohning, 2000; Di Lazzaro, Oliviero, Mazzone, Insola, Pilato, Saturno, Accurso, Tonali & Rothwell, 2001). In fact there is evidence to suggest that the later components of the biphasic pulse have a greater effect than the initial one, possibly because of the accumulation of induced charge in the cortex (Corthout, Barker & Cowey, 2001). Because currents are evoked in both directions in the coil, induced currents are evoked in both directions in the

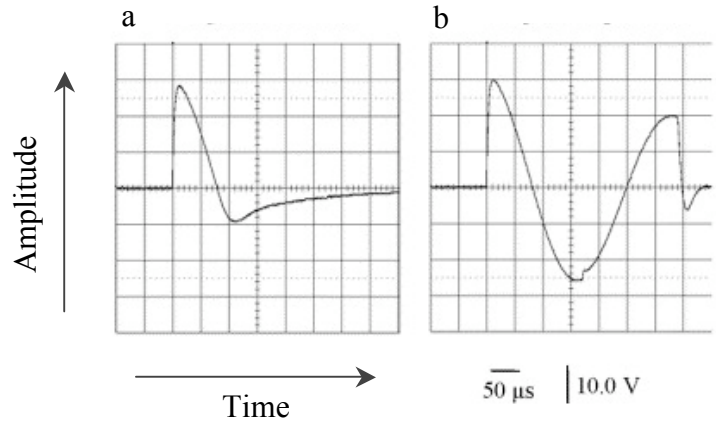

Figure 1.12. Currents induced in a coil by MagStim transcranial magnetic stimulators *(The MagStim Company Ltd., Whitland, UK)*, measured with an oscilloscope. The monophasic pulse (a) was created with a *Magstim 200* stimulator. The biphasic pulse (b) was created with a *Magstim Rapid* stimulator. Taken from Sommer et al. (2006.)

cortex (as is discussed later). Early TMS machines had monophasic current waveforms, but now biphasic waveforms are the default waveforms in most stimulators (Sommer & Paulus, 2008). Biphasic waveforms return up to 60 % of the original energy to the capacitor, enabling capacitors to recharge more quickly, and for pulses to be delivered in rapid succession (Jalinous, 1991; Barker, 1999) whereas in monophasic pulses the current slowly dissipates rather than recharging the capacitor. More importantly, biphasic waveforms have been reported to induce secondary currents in neural tissue at lower magnetic field intensities (McRobbie & Forster, 1984), and induce action potentials in nerve cells at a lower power than monophasic pulses (Wada, Kubota, Maita, Yamamoto, Yamaguchi, Andoh, Kawakami, Okumura & Takenaka, 1996). It has also been reported that the waveform influences the effectiveness of a TMS pulse in human cortex. For example, motor thresholds (commonly defined as the lowest magnetic field strength that can reliably elicit a muscular response) are lower when biphasic pulses are delivered to the motor cortex compared to when monophasic pulses are delivered to the same area (e.g. Niehaus, Meyer & Weyh, 2000; Kammer, Beck, Thielscher, Laubis-Herrmann & Topka, 2001). Similarly, thresholds for the perception of phosphenes (illusory flashes of light following TMS of the visual cortex) are lower when biphasic TMS pulses are delivered over the visual cortex, compared with monophasic pulses (e.g. Corthout et al., 2001; Kammer, Beck, Erb & Grodd, 2001; Kammer, Vorwerg & Herrnberger, 2007).

1.2.2.2 Direction of current

Many studies have investigated the influence of current direction in monophasic TMS pulses on motor threshold. It is widely recognised that motor thresholds are lower when the induced current flows anteriorly in the motor cortex, than when it flows in any other direction (e.g. Chiappa, Cros & Cohen, 1991; Bohning, 2000). This might relate to the orientation of pyramidal tract neurons and their axons (Brasil-Neto, Cohen, Panizza, Nilsson, Roth & Hallett, 1992). However, it has also been reported that in the case of biphasic waveforms, motor thresholds were lower when the initial induced current flowed in a posterior-to-anterior direction than when in an anterior-to-posterior direction (Kammer et al., 2001b). This is consistent with the theory that the later components of the biphasic pulse have at least as large an affect as the initial component (Corthout et al., 2001).

In the visual cortex, phosphene thresholds have been reported to be lower when monophasic pulses are delivered inducing a latero-medial current in the cortex, compared with other directions of current flow (Kammer et al., 2001a). Biphasic pulses produce lower phosphene thresholds than monophasic pulses, but there is no discernable preference for anterior-to-posterior or posterior-to-anterior current direction, and both of these directions produce lower phosphene thresholds than when the current is elicited along a vertical plane (Kammer et al., 2007).

1.2.2.3 Stimulating coil geometry

The geometry of the stimulating coil sets fundamental constraints on the shape of the magnetic field, and therefore the induced cortical current. Circular coils produce a uniform magnetic field directly under the coil winding. Double (also known as 'butterfly' or 'figure of eight') coils comprise two circular coils of copper wire placed next to each other in the same plane, with currents travelling in opposite directions. This produces greater field strength where the two windings interact (Figure 1.13). These differences in the magnetic field shape can be exploited for optimally stimulating different cortical areas. As the maximal magnetic field produced by a double coil is more focal than that stimulate area V5/MT, which is believed to be in the region of 1 cm in diameter (e.g. Beckers & Zeki, 1995; Walsh, Ellison, Battelli & Cowey, 1998; Stewart, Battelli, Walsh & Cowey, 1999; Theoret, Kobayashi, Ganis, Di Capua & Pascual-Leone, 2002; Sack, Kohler, Linden, Goelbel & Muckli, 2006;

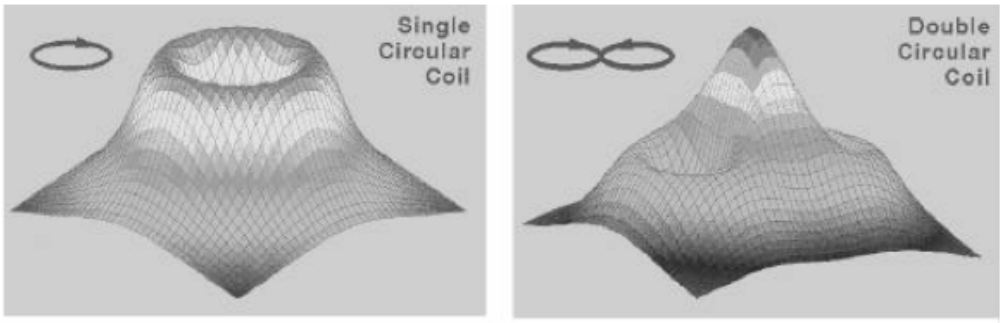

Figure 1.13. The induced magnetic field strength directly under a circular coil (left) and a double coil (right). The magnetic field induced by the circular coil is maximal under the coil winding, and no field is elicited under the centre of the coil. In contrast, the magnetic field induced by each coil winding in the double coil interacts to produce a higher magnetic field strength under the centre of the stimulating coil. (Taken from Jalinous (1998) *MagStim Guide to Magnetic Stimulation*.)

produced by a single circular coil, double coils are now routinely used to Laycock, Crewther, Fitzgerald & Crewther, 2007; McKeefry, Burton, Vakrou, Barrett & Morland, 2008). Also, as the curvature of the head creates a gap between the outer coil windings and the scalp, it is unlikely that the magnetic field produced by the outer windings will have any measurable affect on cortical tissue, as the strength of the induced magnetic field depletes with the square of the distance from the stimulating coil surface. As circular coils have a much broader area of peak magnetic field they are often used to stimulate area V1 in both hemispheres simultaneously (e.g. Amassian, Cracco, Maccabee, Cracco, Rudell & Eberle, 1989; Beckers & Zeki, 1995; Corthout, Uttl, Ziemann, Cowey & Hallet, 1999; Laycock et al., 2007). As only a segment of the circular coil is placed over the desired region of the scalp, most of the coil winding is angled away from the head and is unlikely to induce a current in cortical tissue.

1.2.2.4 Rate of stimulation

TMS can be delivered in either single- or repetitive-pulse mode. Single-pulse TMS refers to a pulse rate of ≤ 1 Hz (Wassermann, 1998), and due to the restricted duration of the effect of one pulse of TMS, is generally delivered "online", that is, during performance of a task at a precise point in time. The main advantage of using the single-pulse mode to modulate neural processing, is that is has the most sensitive temporal resolution. However, this becomes a disadvantage if the appropriate time to deliver the pulse is unclear (Walsh & Cowey, 2000). There are currently several forms of repetitive TMS (hereafter

referred to as rTMS). Broadly, rTMS refers to a pulse rate of > 1 Hz, where pulses can be delivered "online" during task performance, or "offline" for an extended period of time before a behavioural measure is taken. There are many rTMS protocols, such as delivering 'slow rate' 1 Hz TMS for an extended period (such as 30 minutes), or delivering 'rapid rate' rTMS (for example up to 25 Hz 'trains') over short periods (for example 500 ms), with the parameters varied being magnetic field strength, frequency and train duration (number of pulses). All types of rTMS have an increased risk of inducing a seizure compared to single pulse TMS (see Wassermann, 1998, for a review).

1.2.3 Studying the brain-behaviour relationship

1.2.3.1 Functional necessity

Since it was first developed by Barker et al. (1985), TMS has been widely used in the study of attention (e.g. Walsh et al., 1998), learning (e.g. Pascual-Leone, Grafman & Hallett, 1995), plasticity (e.g. Walsh, Ashbridge & Cowey, 1998), awareness (e.g. Cowey & Walsh, 2000), language (e.g. Pascual-Leone, Gates & Dhuna, 1991) and perception (see Kammer [2006] for review). By applying a TMS pulse, or a series of pulses over a cortical region that is involved in a particular cognitive function, one can produce a transient 'virtual lesion', and measure its behavioural consequences. This allows one to determine the functional necessity of a particular brain area for task performance.

1.2.3.2 Chronometry

By delivering a TMS pulse at a precise point in time relative to a task-relevant stimulus, the timing of the critical disruption of a cortical region can be established. Walsh & Cowey (2000) suggest that the time at which delivery of a TMS pulse produces a maximum performance deficit is likely to differ from the estimates of peak activation found using other neuroscientific measures. For example, estimates of the onset of activation of cortical areas in event-related potential or magnoencephalography studies typically relate to the peak response of an area, as the signal is required to build up before it can be detected. However, it is likely that the modulatory effects of TMS on neural behaviour can effectively abort the accumulation of the signal and therefore interfere with processing before the peak response latency is reached (Walsh & Cowey, 2000).

1.2.3.3 Neural pathways / connectivity

The fact that the effects of TMS rapidly spread to functionally connected cortical areas via transynaptic connections, has been reported in several studies using TMS in combination with functional magnetic resonance imaging (fMRI) [Bohning, Shastri, McConnell, Nahas, Lorberbaum, Roberts, Teneback, Vincent & George, 1999], positron emission tomography (PET) [Paus, Jech, Thompson, Comeau, Peters & Evans, 1997] and electroencephalography (EEG) [Ilmoniemi, Virtnen, Ruohonen, Karhu, Aronen, Näätänen & Katila, 1997]. This has been exploited to demonstrate

connectivity between cortical regions. For example, a combined TMS/EEG study reported a contralateral response in right V1 20 ms after a magnetic pulse was delivered to left V1 (Ilmoniemi et al., 1997).

1.2.4 TMS of visual cortex

1.2.4.1 Modulating perception of stationary stimuli

TMS has proved to be a particularly useful tool for studying the neural circuitry mediating human visual processing. It was first found to suppress visual perception by Amassian and colleagues (1989), who reported that when single-pulse TMS was delivered over occipital cortex between 40 ms to 60 ms, or between 120 ms to 140 ms after the onset of three random letters, the letters were correctly reported. When TMS was delivered between 80 ms to 100 ms after the onset of the letters, however, "a blur or nothing was seen". This report of the suppressive effects of TMS on visual perception paved the way for many more TMS studies of vision. In 1993, Amassian and colleagues used single-pulse TMS to abolish the effect of a visual mask on target detection: when TMS was delivered 80 ms to 100 ms after the mask, target letters could be correctly identified, yet without TMS they could not. This study also utilised a control TMS condition in which the coil was held away from the head to confirm that TMS-induced visual suppression was not caused by the sound of the coil discharging (Amassian, Cracco, Maccabee, Cracco, Rudell & Eberle, 1993).

Since then, TMS has been widely used to disrupt neural activity in human primary visual cortex (e.g. Masur, Papke & Oberwittler, 1993; Kammer & Nusseck, 1998; Kastner, Demmer & Ziemann, 1998; Corthout, Uttl, Walsh, Hallett & Cowey, 1999; Corthout, Uttl, Ziemann, Cowey & Hallett, 1999; Corthout, Uttl, Juan, Hallett & Cowey, 2000; Corthout, Hallett & Cowey, 2003; Kammer, Puls, Strasburger, Hill & Wichmann, 2005; Kammer, Puls, Erb & Grodd, 2005; Silvanto, Muggleton, Cowey & Walsh, 2007; Harris, Clifford & Miniussi, 2008). These studies are discussed in detail in the relevant experimental chapters.

1.2.4.2 Modulating perception of moving stimuli

As mentioned earlier in section 1 of this chapter, neuroimaging studies have provided unequivocal evidence for the role of area V5/MT in visual motion processing in humans (e.g. Zeki et al., 1991; Watson et al., 1993; Tootell et al., 1995; Heeger et al., 1999; Huk et al., 2002). Many TMS studies support this assertion by providing evidence that TMS of area V5/MT selectively disrupts motion processing. For example, TMS of area V5/MT improved performance in visual search tasks that required attention to colour or form, but impaired performance when attention to motion was required (Walsh et al., 1998). Participants of Walsh et al.'s (1998) study were required to detect whether a target was present or absent from visual search arrays, where translational motion was either relevant or irrelevant to the task. It was found that TMS increased reaction time when motion was relevant to the search task, but that reaction time actually decreased compared to trials completed in the absence of

TMS when motion was irrelevant. This was discussed as evidence that different visual areas compete for resources (although the authors do not specify what these are) and by disrupting activity in area V5/MT, areas that process colour and form are disinhibited.

It has also been found that single-pulse TMS delivered over area V5/MT disrupts speed discrimination (Matthews, Luber, Qian & Lisanby, 2001), and rTMS over V5/MT can abolish the perception of a motion aftereffect (Theoret et al., 2002). Many other TMS studies provide further support for the role of V5/MT in motion perception (e.g. Beckers & Homberg, 1992; Hotson, Braun, Herzberg & Boman, 1994; Beckers & Zeki, 1995; Anand, Olson & Hotson, 1998; Hotson & Anand, 1999; d'Alfonso, van Honk, Schutter, Caffe, Postma, & de Haan, 2002; Silvanto, Lavie & Walsh, 2005; Sack, Kohler, Linden, Goebel & Muckli, 2006; Laycock et al., 2007). These studies are discussed in detail in the relevant experimental chapters.

1.3 Unresolved Issues

Although the use of TMS as a tool for studying human visual processing has received a considerable amount of attention in recent years, there are still a number of unresolved issues that require further investigation. The experiments described in this thesis set out to resolve some of the outstanding issues described below.

1.3.1 Temporal window for disruption of processing in area V5/MT

The temporal window during which the delivery of a TMS pulse modulates visual performance is typically different to the activation latency of the cortical region estimated by other investigative methods such as EEG or MEG. The critical temporal window for performance disruption is thought to reflect the period when TMS-induced neural activity interacts with task-specific activity to, for example, prevent the accumulation of the signal in a cortical region (Pascual-Leone, Walsh & Rothwell, 2000). The temporal window for TMS-induced disruption of processing in area V1 (around 100 ms after the visual stimulus onset) is agreed upon in the vast majority of studies. The critical period for TMS-induced disruption of visual processing in area V5/MT, however, is far from clear. Previous reports vary widely in their estimates of the critical disruption window(s) for area V5/MT (ranging from 200 ms prior to, to 200 ms after the onset of the visual stimulus). Given that the visual system requires only around 150 ms after stimulus onset to encode relatively complex visual scenes (Hegdé, 2008) this extended period of disruption is somewhat puzzling. There is also considerable variability in the estimations of the duration of the temporal window(s) for disruption of processing in area V5/MT.

Variations in the onset of critical disruption window(s) for area V5/MT processing have previously been attributed to differences in visual stimuli, such as contrast, although this has not before been addressed empirically. The disparity in estimates of the onset and duration of the temporal disruption

windows may also be, in part, attributed to differences in the latencies at which TMS was delivered relative to the visual stimulus in previous studies.

Another current area of debate is the significance of the critical temporal window(s) during which TMS of area V5/MT disrupts performance, with regards to the visual processing pathway. For example, some studies have attributed a particular temporal disruption window after the onset of a visual stimulus to reflect the arrival of the visual signal to area V5/MT from 'lower' visual areas via the feedforward pathway (Sack et al., 2006). Alternatively, other studies have described the same period as reflecting the arrival of the visual signal to area V5/MT from 'higher' areas of the processing pathway, such as the frontal eye fields, through feedback circuits (Laycock et al., 2007). Furthermore, it has been suggested that some temporal window(s) during which TMS disrupts motion processing are a result of non-cortical, muscular side effects of TMS such as eye-blinks, and therefore do not represent a cortical modulation of visual perception. However, which – if any – of these potential explanations is valid remains unclear.

All previous studies of disruption to motion perception have used translational motion, and TMS disruption of complex types of global motion, such as radial or rotational motion has to date, not been investigated. This is surprising as it has been shown in several imaging studies that a separate and distinct part of the human V5/MT complex responds specifically to radial and rotational motion (e.g. Morrone et al., 2000; Smith et al., 2006; Wall et al., 2008). Complex motion types are assumed to involve an additional hierarchical level

of analysis, therefore it might be expected that the critical window for area V5/MT TMS disruption to complex motion processing might have a different temporal onset or duration to that of simple translational motion processing. It is also currently unknown whether there might be multiple temporal windows during which delivery of a TMS pulse to area V5/MT pulse modulates processing of complex motion stimuli, as has been suggested for simple motion types.

1.3.2 Magnetic field strength

Previous studies suggest that field strength is an important consideration for TMS studies of visual perception in humans (e.g. Masur et al., 1993; Kastner et al., 1998; Kammer et al., 2005b), yet this has not been systematically investigated. Physiological studies have shown that the effect of TMS on single neurons in feline cortex is dependent on field strength (e.g. Moliadze, Zhao, Eysel & Funke, 2003). However, the physiological effect of TMS field strength in human visual cortex and how this relates to visual performance is currently unknown.

Behavioural studies in humans have reported that the size of the motor response after delivery of a TMS pulse to the motor cortex is dependent on field strength (e.g. Stewart, Walsh & Rothwell, 2001). Additionally, changes in field strength elicit changes in the intensity and/or frequency of perceived visual phosphenes (e.g. Kammer et al., 2001a). But it is as yet unclear how changes in field strength relate to modulation of visual perception. Many

studies of TMS disruption of visual processing deliver TMS pulses at one field strength to all participants (without – in many cases – specifying why that particular field strength was chosen). However, a frequent finding is that some individuals are considerably more susceptible to TMS disruption of visual processing than others.

To overcome this issue, some studies have used a multiple of individuals' phosphene threshold in an attempt to calibrate the strength of the TMS pulse to individual susceptibility to TMS, although variation in the degree of TMS disruption of visual perception between participants is still often reported. Differences in phosphene thresholds indicate that sensitivity to TMS varies between individuals, but the reliability of phosphene threshold measurements is at best questionable. For example, the methods employed are typically at risk of experimenter bias, and test–retest reliability is not reported. Furthermore, no studies to date have investigated phosphene threshold in relation to TMS disruption to visual perception as a function of magnetic field strength, and so the relationship between them is unknown.

In addition, the limited studies that have investigated the influence of field strength on visual perception have investigated this in relation to detection thresholds (e.g. Masur et al., 1993; Kastner et al., 1998; Kammer et al., 2005a). There have been no studies to date on the effect of TMS on fine discrimination judgments of spatial stimuli, such as orientation discrimination.

1.3.3 The mechanism of TMS disruption

The mechanism behind TMS disruption of visual perception in humans is largely unknown. Physiological studies suggest that the pattern of activity and suppression of neurons following a TMS pulse is complex, and is also dependent on the visual stimulus. For example, in feline cortex, after a TMS pulse was delivered, firing rate for a stimulus moving in the non-preferred direction was increased, and was also facilitated for stimuli presented in the periphery of the classical receptive field that elicited little or no activity in the absence of TMS (Moliadze et al., 2003). This excitatory effect has been likened to an increase in neural "noise" which could mask the visual signal.

Alternatively, it has been reported that the primary affect of TMS is to suppress neural firing. For example, this is known as the 'cortical silent period' after TMS is delivered to the human motor cortex (e.g. Calancie et al., 1987; Orth & Rothwell, 2004). Single cell studies have also reported that in feline cortex, the spike rate for a stimulus moving in the preferred direction was reduced following a TMS pulse delivered to the visual cortex (Moliadze et al., 2003). This inhibitory effect has been likened to a reduction in the strength of the signal being carried by neurons.

Behavioural studies in humans have suggested that TMS suppresses the neural signal related to the target, and this has been characterised as a decrease in the effective contrast of the stimulus. However, the few studies that have investigated this issue have used a contrast-based detection task, and while it

has been reported that increasing stimulus contrast can abolish the affects of TMS on visual processing, it cannot be assumed that increasing stimulus contrast can overcome TMS disruption for all types of stimulus and task (for example, discrimination tasks using above-threshold stimuli).

Furthermore, the idea that TMS reduces the effective strength of the visual signal has previously only been discussed in relation to stimulus contrast. An extension of this argument would render it possible, however, that TMS causes a reduction in other factors contributing to effective signal strength – such as stimulus size or duration – rather than a specific reduction of perceived contrast. This under-researched but fundamentally important issue clearly requires further attention.

Chapter 2: General methods

This chapter describes the general psychophysical and TMS procedures used in experimental Chapters 3 to 7. Detailed methods are described at the beginning of each experimental chapter.

2.1 Psychophysical methods

2.1.1 Psychophysical theory

The application of psychophysical methods allows the measurement of the sensitivity of sensory systems to physical stimuli. By rigorously controlling the physical stimuli presented to observers, one can ascertain the rules used by neural systems to generate the subsequent perception of the stimuli (Fechner, 1860). Psychophysical methods are therefore ideal for the quantification of the influence of TMS on visual perception.

2.1.1.1 Methods

The method of constant stimuli was used all experiments described in this thesis. The method of constant stimuli involves the presentation of a fixed set of stimulus values that vary along one dimension. As in all psychophysical experiments, the observer's task was to make a response after every stimulus presentation. Psychometric functions, or 'frequency of seeing curves', were

generated to measure individual sensitivities to the varied dimension of the physical stimulus. If enough measurements are taken, the psychometric functions often follow an S shape, termed an *ogive***.** Biological systems are not fixed, and instead, comprise a number of sources of noise. Consequently, many measurements must be taken to ensure random fluctuations (in, for example, neural firing or light intensity) do not bias the overall perceptual outcome. Because performance on perceptual tasks forms a continuum, a pre-defined level of performance was taken as the threshold level (such as the stimulus intensity that supports a correct response rate of mid-way between chance level performance and 'perfect' performance).

2.1.1.2 Absolute and difference thresholds

Two types of thresholds were measured in the experiments in this thesis. An absolute threshold may be defined as a particular level of a physical stimulus that results in a particular perceptual outcome, for example, the stimulus intensity that supports a correct response rate of 75 % (see Figure 3.3 in Chapter 3 for an example). A difference threshold may be defined as the smallest change along one dimension of a physical stimulus that can be reliably discriminated, known as the just noticeable difference (JND), for example, the smallest difference in orientation that can be reliably discriminated as different from vertical (see Figure 5.4 in Chapter 5 for an example).

2.1.1.3 Types of perceptual decision

A one-interval two-alternative forced choice paradigm was used in all experiments except for Experiment 7 (which measured phosphene thresholds), in which a 'yes/no' paradigm was used. A forced-choice paradigm requires observers to guess an attribute of a stimulus even when they feel there was not enough information to confidently make a perceptual decision. This is fundamentally different from a 'yes/no' paradigm for which the observer is required to make a judgement regarding the presence or absence of a stimulus.

2.1.1.4 Stimulus range and step size

It is important that an appropriate range of constant stimuli values is used in conjunction with the method of constant stimuli, to generate the 'frequency of seeing curve'. For example, in order to measure absolute thresholds, the stimulus must be varied so that it produces a continuum between close to 100 % correct answers on some trials and close to chance-level performance on others. On tasks that measure JND, the stimulus must be varied such that responses range from approximately 100 % to 0 % response rate for one of the two options (for example, producing a continuum between nearly always responding "clockwise" to rarely responding "clockwise" on an orientation judgement task). All psychometric functions were fitted using the 'method of least squares' using the software *Kaleidagraph 3.6 (Synergy Software)*.

2.1.2 Equipment

All experimental stimuli were generated using an *Apple Macintosh G4* computer using custom software written in the C programming language. Visual stimuli were presented on a *Viglen* 22 inch cathode ray tube (CRT) display with a screen resolution of 1024 x 768 pixels and a vertical refresh rate of 75 Hz. The CRT display had a mean luminance of 73.52 cd/m^2 and was gamma-corrected with the aid of look-up-tables (see Monitor Calibration, below).

2.1.2.1 Monitor Calibration

In most CRT displays the luminance of a given point over the phosphorescent screen is not proportional to the input voltage to the red, blue and green guns. Instead, it is proportional an expansive function of the input voltage, known as gamma (g). The value of gamma varies across monitors but is usually in the region of 1.8 to 2.5 (e.g. Robson, 1998). On a typical uncorrected CTR display the RGB value of (0.5, 0.5, 0.5) results in a luminance output of about 22 % of the luminance when the RGB value is (1.0, 1.0, 1.0). In psychophysical studies of visual perception, it is necessary to present stimuli at a known luminance with standardised luminance increments. The relationship between voltage input and luminance output was characterised using a photometer as well as a psychophysical procedure, and corrected.

2.1.2.2 Calibration using a photometer

The luminance (cd/m^2) of a steady state, circular test patch (diameter = 256 pixels) was measured using a *SpectraScan® PR650* spectrophotometer (*Photo Research® Inc. Chatsworth, CA)*. The photometer was placed tightly to the screen of the monitor used in all experiments, and luminance of pixel values was measured at 17 increments from minimum (0; "black") to maximum (255; "white") output. Each pixel value was measured three times. Figure 2.1 depicts the gamma function, fitted with the equation:

$$y = ax^{\wedge g} + b \tag{2.1}$$

where *a* is a constant, *g* is gamma and *b* is the minimum luminance.

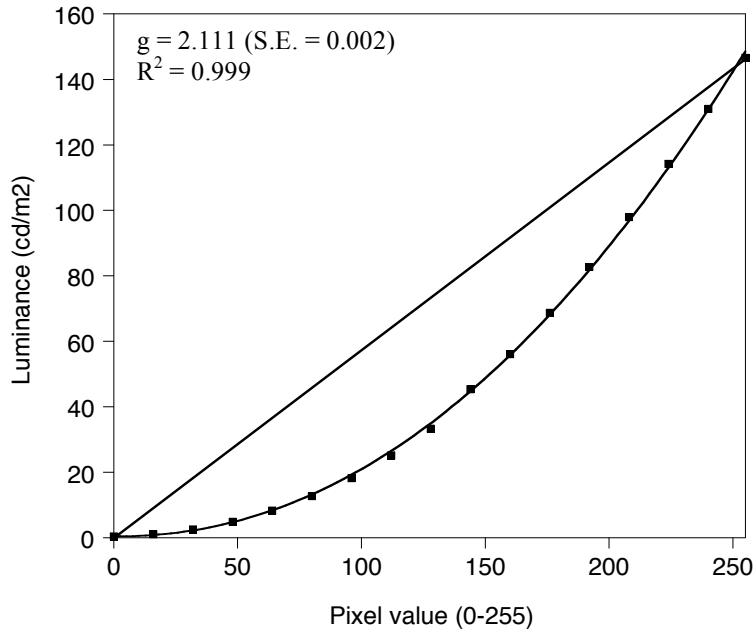

Figure 2.1. An example gamma (g) function of the *Viglen* 22" monitor displaying the luminance level for each of the 256 pixel levels from 0 ("black") to 255 ("white") (squares, fitted with Equation 2.1). A uniform increase in luminance level for each pixel is shown for comparison (shown as a straight line).

2.1.2.3 Calibration using psychophysical observer

In addition to using a photometer, gamma correction can be achieved using psychophysical observers (Ledgeway & Smith, 1994). Motion sequences were constructed in which images alternated between a sinusoidal luminance variation of a two-dimensional static noise field (first-order motion) and a sinusoidal contrast variation of a two-dimensional static noise field (second-order motion). When the spatial phase of the two stimulus types is offset by 0.25 spatial periods in consecutive images, the direction of motion cannot be determined unless there is a significant luminance non-linearity present in the second-order images. It was confirmed that the observers were not able to identify motion direction under these conditions, indicating that luminance non-linearities were minimal. Variations of this technique have been used to measure and check the adequacy of gamma-correction (e.g. Lu & Sperling, 2001). The measured gamma using the psychophysical procedure confirmed the measured gamma using the photometer, and the mean gamma from the two observers and the photometer was computed (Figure 2.2).

The contents of a gamma-correction look-up table were thus changed using the power function:

$$y = 255 * \left(\frac{x}{255} \right)^{\wedge \frac{1}{g}} \tag{2.2}$$

where y is the final eight-bit output value of the gamma-correction LUT, x is the uncorrected eight-bit input value of the gamma-correction LUT, and g is

the correction factor (the mean gamma computed for the two psychophysical observers and the photometer).

2.2 TMS methods

2.2.1 TMS Equipment

A *Magstim Rapid* stimulator (*The Magstim Company Ltd.*) was used in all experiments, which produces a biphasic current, and a magnetic field of up to 2.5 Tesla (T).

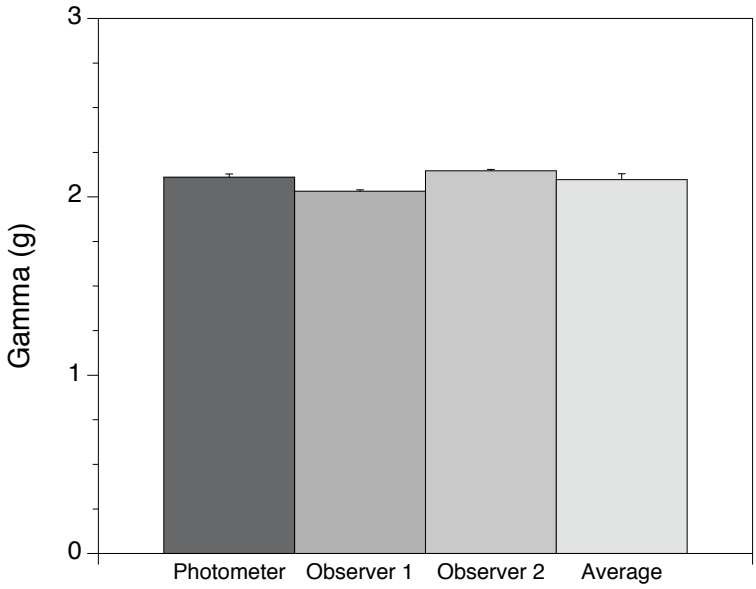

Figure 2.2. A histogram showing the measured gamma (*g*) using a *SpectraScan PR650* spectrophotometer, the results for two observers using the psychophysical gamma correction procedure (mean of 5 trials for each observer) and the mean value for all above measurements of gamma. Error bars represent ± 1 SEM.

2.2.1.1 Stimulating coils

As discussed in section 1.2 of Chapter 1, different coil geometries produce corresponding differences in the shape of the induced magnetic field (see Figure 1.13 in Chapter 1). These differences in the magnetic field shape can be exploited for optimally stimulating different cortical areas. The stimulating coils used in the TMS experiments presented in this thesis are two custom-made 55 mm double coils (for stimulation of area V5/MT) and a high power 90 mm circular coil (for stimulation of area V1) [Figure 2.3]. The double coils are polyurethane coated, and have been constructed without the outer plastic casing that standard coils have, so that the coil winding is in closer proximity to the cortex. This results in increased stimulating efficiency as the induced magnetic field is greatest next to the coil and rapidly falls off. These smaller

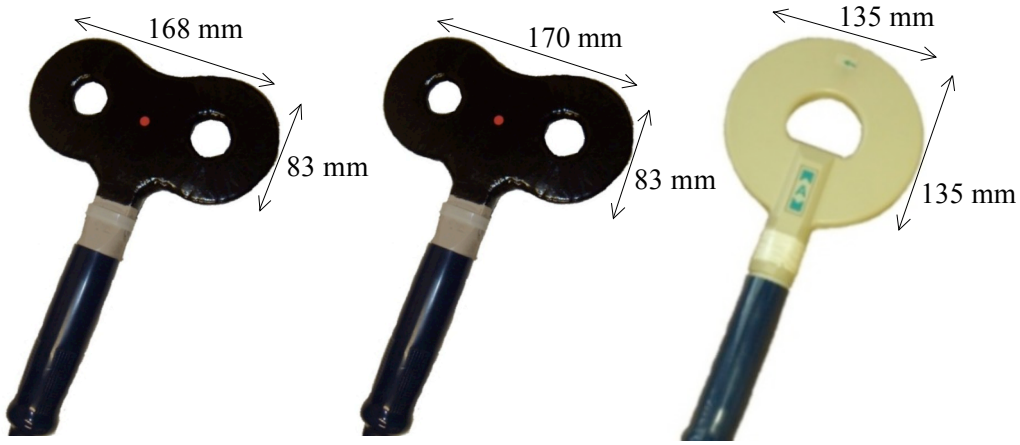

Figure 2.3. The three stimulating coils used in all TMS experiments presented in this thesis. The two 55 mm custom double coils (left and middle) have been made without the outer casing and so the maximal magnetic field they produce has a closer proximity to the cortex. The high power 90 mm circular coil (right) comprises one copper coil that is much larger than either coil winding in the double coils, contained in protective plastic casing. All coils have a 2 m cable that connects to the capacitor.

coils are more focal in their stimulation, but the depth of stimulation is not as large, so greater proximity to the target site is an advantage. The advantage to a larger circular coil size (aside from being able to stimulate both hemispheres) is that it has a higher copper mass and a lower electrical resistance. It therefore has a higher heat capacity and can deliver many more TMS pulses before the coil overheats, and the internal heat sensor turns the power off. See Table 2.1 for the technical specifications of the coils used.

A biphasic TMS current was used in all experiments, In the *Magstim Rapid* stimulator the discharge current (of up to 8000 amps) lasts up to 1 ms in the coil, although 90 % of the discharge occurs within the first 100 μs. This fast discharge rate is crucial, as it is the rate of change in the magnetic field that is the determining factor in the efficacy of the induced electrical current in cortical tissue (Figure 2.4).

Coil type	Diameter of coil winding (mm)	Max field strength (T)	Inductance (μH)	Number of pulses at 100% power before over-heating
Custom double 55 mm	83	2.47	24.73	56
Custom double 55 mm	83	2.43	25.45	56
Circular high power 90 mm	135	2.00	23.30	143

Table 2.1. The technical specifications of the coils used in TMS experiments. Due to the limited number of pulses that can be delivered by a double coil before it overheats, two identical custom double coils were used alternately so that one of the stimulating coils could cool down while the other was in use (Information taken from *Magstim Coils & Accessories Operating Manual*).

2.2.1.2 Triggering the coil

Single-pulse TMS was used in all TMS experiments. A pulse could be delivered before, during or after the presentation of a visual stimulus by displaying a small high luminance square near the bottom right corner of the CRT display. Onset of this square (which was not visible to participants) activated a photodiode that was configured to trigger the discharge of the TMS apparatus in response to a flash of light. The timing of the delivery of a TMS

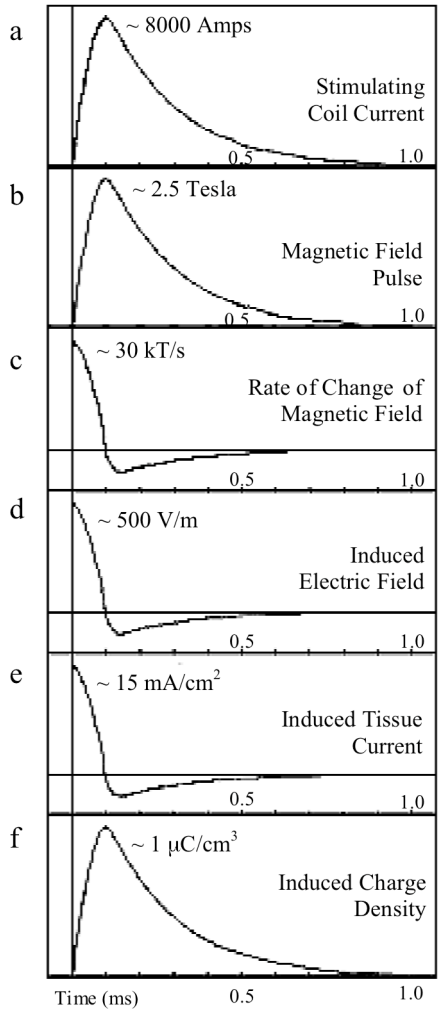

Figure 2.4. The waveforms produced during a single TMS pulse. The capacitor generates an electrical current of up to 8 kA, which is discharged into the stimulator coil (a). As a result, a magnetic field of up to 2.5 T is produced, with a rise time of ~ 100μs and a total duration of 1 ms (b). This creates a high rate of change in the magnetic field, crucial for effective stimulation (c). The fluctuation of the magnetic field causes an electrical current (d), which creates neural activity (e). The change in induced charge density in the cortex is negligible, and dissipates within ~ 1 ms. Taken from Jalinous, 1998 *(Magstim Guide to Magnetic Stimulation)*.

pulse is expressed as the stimulus onset asynchrony (SOA) between the onset of the visual stimulus and the TMS pulse. As the luminance square was presented near the bottom of the screen, the onset of the square occurs when the stimulus has been completely drawn for that particular frame. When the stimulus has been fully drawn, this is taken to be time 0 ms with regard to the onset of the (whole) visual stimulus.

2.2.2 Coil localisation

The site for magnetic stimulation was determined using a combination of functional and anatomical magnetic resonance images and phosphene-induction techniques. The coil can be navigated to stimulate a desired cortical area, by locating the desired region during an fMRI scan and then using neuronavigation software such as *BrainVoyager QX* to locate the corresponding area on the participants' scalp. The participant's own anatomical MR image is therefore used to guide the positioning of the stimulating coil.

2.2.2.1 MRI measurements: Stimuli and design

Visual stimuli were back-projected from an LCD-projector onto a screen at the participants' feet. In the scanner, participants viewed stimuli through angled mirrors fixed to the head coil. The two stimulus conditions used to identify V5/MT were: (1) moving white dots alternating between expanding and contracting motion every 1 second (stimulus size ~ 20 deg x 16 deg; dot

diameter 0.02 deg; dot velocity ~ 5 deg/s), and (2) stationary white dots with the same parameters as in condition (1).

The two experimental conditions (moving and stationary dots) were presented alternately in 20 blocks of 12 seconds duration (total 240 s); two scans were collected for each subject. To control for attention during the scans, participants performed a two-interval forced choice task at fixation, in which they were required to detect the dimming of the fixation cross.

2.2.2.2 MR Imaging

Functional MRI data was collected at 3T on the *Philips Intera Achieva* system, at the Sir Peter Mansfield Magnetic Resonance Centre (The University of Nottingham) using an 8-channel coil (*Noval Medical*). A gradient-recalled echo-planar-imaging (GE-EPI) sequence was used with the following parameters: 20 slices oriented approximately parallel to calcarine sulcus; TR, 1500 ms; TE, 40 ms; voxel size, 3 mm isotropic; FOV 192 mm x 192 mm x 60 mm. Participants' heads were stabilized by use of a vacuum pillow (*Vacuform, Schmidt, Germany*) and additional foam padding. In addition, a high-resolution (1 mm isotropic voxels) anatomical scan for TMS-neuronavigation, surface reconstruction, inflation and flattening, was collected with a T1-weighted magnetization-prepared rapid-acquisition gradient-echo (MPRAGE) sequence.

2.2.2.3 MRI data analysis

Data were analysed using a combination of custom software (*TFI/SurfRelax*; Larsson, 2001), *Matlab* (*The Mathworks, Natick, USA), BrainVoyager QX (BrainInnovation, Maastricht, The Netherlands*) and *FSL (FMRIB, Oxford*). Pre-processing of the functional data included the following steps: (1) three-dimensional motion correction, and (2) linear-trend removal and temporal high-pass filtering at 0.01 Hz. The statistical analysis of the BOLD signal was performed with a general linear model. For every voxel, the time course of the BOLD signal was regressed on a predictor (box-car function) representing the experimental conditions (moving and stationary dots). The predictor time course was convolved with a standard haemodynamic response function (double gamma) to account for the shape and delay of the haemodynamic response.

2.2.2.4 Coil neuronavigation

Localisation of the TMS stimulation site with respect to functional activation was achieved following the methodology described by Sack et al. (2006) using a three-dimensional ultrasound digitizer system *CMS20S (Zebris Medical GmbH)* in conjunction with *BrainVoyager QX* software. Miniature transmitters were attached to the participant's head, which continuously sent ultrasonic pulses to a receiving device. The travel time of the pulses from the transmitters to the receiver indicated their relative spatial position in three-dimensional space. The relative spatial positions of the transmitters were linked to fixed

landmarks on the participant's head (the nasion and the two incisurae intertragicae) to create a participant-based co-ordinate frame. These landmarks were specified using a digitizer pen, which also transmits ultrasonic pulses to indicate its relative spatial position. The participant-based co-ordinate frame was then co-registered to the MRI-based co-ordinate frame by linking anatomical landmarks on the participant's real head to the same landmarks on the head representation (mesh). After this co-registration, movement of the digitizer pen with respect to the head was visualised in real time using the *BrainVoyager QX* software. By overlaying functional MRI data on to the anatomical reconstruction of the brain and head, the point on the scalp directly over functionally active visual cortical areas were then located.

After the location on the scalp overlying a visual cortical area was found using neuronavigation, a grid of points 5 mm apart was then marked on the scalp around the initial marker, and single TMS pulses were delivered over each point. Participants were asked to report whenever they saw a phosphene(s). Coil locations that elicited phosphenes were investigated further with a finer grid of stimulation points, to determine the location and coil angle at which stimulation produced the clearest, most stable phosphenes.

2.2.2.5 Coil orientation

During area V5/MT stimulation the handle of the double coil was parallel to the horizontal plane and pointing toward the occiput (as in Hotson & Anand, 1999; Sack et al., 2006) [Figure 2.6a]. For V5/MT stimulation the initial

evoked cortical current was in a lateral-to-medial direction. For area V1 stimulation, the handle of the circular coil was oriented vertically upwards and 'side A' was placed against the scalp (Figure 2.6b). The direction of the induced current in the cortex was initially clockwise (stimulating right then left hemisphere V1, as the lower rim of the coil made contact with the scalp), followed by a current in the opposite direction.

2.2.3 Spatial resolution of TMS

The functional magnetic field depth produced by the TMS equipment used in all experiments in this thesis is estimated to be up to 10 mm to 20 mm: the peak field strength within 10 mm is nearly constant (Jalinous, 1995), and field

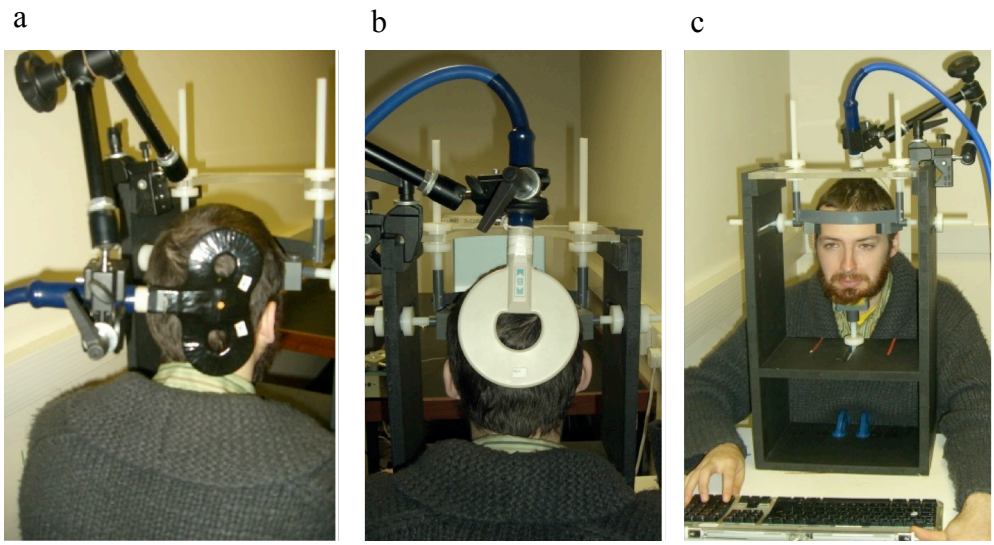

Figure 2.6. Coil location sites for participant RWD. *a* The custom double coil was used for all area V5/MT TMS, the centre of the coil (marked with an orange spot) was positioned 40 mm superior and 47 mm lateral (right) to the centre of the inion. *b* The circular coil was used for all area V1 TMS, and was positioned so the lower edge of the lower rim of the coil was located 25 mm superior to the centre of the inion. *c* The headrest supported the head with adjustable chin, temple and forehead rests to minimise head movements.

strength depletes with the square of the distance from the coil surface (Hovey, Houseman & Jalinous, 2003). The induced currents in cortical tissue evoke neural excitation, but the magnitude and distribution of the induced currents in the human brain are largely unknown. As there have been no in vivo studies measuring the induced current distribution in the human brain, estimates of the spatial resolution of TMS come from theoretical models, phantom experiments, and 'functional resolution'.

2.2.3.1 Magnitude of induced electric currents: theoretical models

Several homogenous models of induced electric currents have been suggested (e.g Roth & Basser, 1990; Ueno, Tashiro & Harada, 1998), but these do not take into consideration tissue inhomogeneities and structural asymmetries, both of which affect the induced current (Terao & Ugawa, 2002; Wagner, Rushmore, Eden & Valero-Cabre, 2009). To overcome this issue, Wagner and colleagues generated MRI-based finite head models, and used eddy current solver software to describe the currents induced in the cortex during magnetic stimulation (Wagner, Eden, Fregni, Valero-Cabre, Ramos-Estebanez, Pronio-Stelluto, Grodzinsky, Zahn & Pascual-Leone, 2008). When a double coil was placed over the motor cortex (and dorsal lateral prefrontal cortex) the maximum cortical current density had decayed by approximately 33 % at a distance of 12.4 mm (and 14.5 mm) from the scalp. Wagner et al. (2008) also modelled the effect of cortical atrophy on the induced currents and found evidence that, as expected, the induced current densities in the cortex decreased in magnitude as the distance from the scalp to the cortex increased.

This sheds some light on the individual differences in the magnitude of the effect of TMS often observed across participants (e.g. Masur et al., 1993; Kastner et al., 1998). However, the precise relationship between current density and neural activation is as yet unknown (Epstein, 2008), and so theoretical induced current models only have limited use for describing the neural consequences of TMS.

2.2.3.2 Phantom studies

Phantom studies either directly measure magnetic fields generated by different coil configurations (e.g. Cohen, Roth, Nilsson, Dang, Panizza, Bandinelli, Friauf & Hallett, 1990), or the induced currents in saline baths (e.g. Tay, Battocletti, Sances, Swiontek & Kurakami, 1989; Maccabee, Amassian, Eberle, Rudell, Cracco, Lai & Somasundarum, 1991). Cohen et al. (1990) reported that for a 90 mm circular coil (similar to that used to stimulate area V1 in the experiments in this thesis) the electric field was maximal around the outer edge of the coil, and was therefore induced over a relatively large area. For a 40 mm double coil (similar, albeit a little smaller, to that used to stimulate area V5/MT in the experiments in this thesis) the electric field was maximal in the centre of the coil (between the two windings) and dropped to 50 %, 27 % and 16 % at 2 cm, 3 cm and 4 cm from the centre of the coil respectively, relative to its value 1 cm under the centre. A similar result was found by Maccabee et al. (1991), who measured the electric fields in a saline bath generated by a circular 92 mm coil and a 50 mm double coil. For the circular coil the electric field was greatest over the coil winding, attenuated

rapidly toward the centre of the coil, but remained prominent moving outward from the windings, signalling a very large and diffuse electric field. The electric field generated by the double coil was greatest in the centre (between the two windings) but were much less pronounced at locations peripheral to the coil windings. The results of phantom studies generally agree that double coils induce a much more focal electric field than that induced by circular coils.

A key problem with phantom studies is that they are often conducted in systems that do not represent tissue inhomogeneities, the non-symetrical nature of the human head, and the electrical properties of biological structures. The induced field is dependent on anatomical and geometrical structure and small structural differences alter the field considerably.

2.2.3.3 Functional resolution of TMS: motor cortex

Several studies have reported the ability of TMS to functionally distinguish scalp sites 1.5 cm (Schluter, Rushworth, Mills & Passingham, 1999) or 1 cm (Amassian, Cracco & Maccabee, 1989; Brasil-Neto, McShane, Fuhr, Hallett & Cohen, 1992) apart. Schluter et al., (1999) used a 70 mm double coil to stimulate 1 cm posterior to, and 0.5 cm, 1 cm, 1.5 cm or 2 cm anterior to the 'hot-spot' for the hand representation of the motor cortex. Stimulation was delivered at a variety of latencies relative to the onset of a visual target, and volunteers performed a choice reaction time task, in which they were required to respond with either their middle or index finger according to the shape presented to them. A significant interaction was found between TMS location

and onset latency, indicating that TMS over the different cortical areas was dependent on the time of delivery.

Amassian et al. (1989) also delivered focal stimulation (using a double coil) over the motor cortex, to elicit movements in the relaxed index finger. At threshold stimulation, moving the coil 1 cm from the optimal site resulted in the loss of finger movement. Stimulation delivered using a circular coil, however, resulted in muscular responses in multiple fingers simultaneously, although altering the angle of the coil allowed the investigators to evoke muscular responses in different combinations of fingers. This finding agrees with the results of phantom studies that the electric field produced by double coils is much more focal than that produced by circular coils.

A later study by Brasil-Neto et al. (1992) used a 45 mm double coil to topographically map the human motor cortex, whilst recording motor evoked potentials from deltoid, biceps, brachii, abductor polis brevis and flexor carpi radialis muscles in five volunteers. Brasil-Neto and colleagues were able to distinguish between the effects of TMS on scalp positions 0.5 cm to 1 cm apart.

2.2.3.4 Functional resolution of TMS: visual cortex

Amassian and colleagues (1989) reported that when TMS was delivered with the lower edge of a circular coil 2 cm superior to the inion, correct identification of a horizontal array of three letters was reduced (Amassian,

Cracco, Maccabee, Cracco, Rudell & Eberle, 1989). The authors went on to report that when the midpoint of the lower rim of the coil was moved 3 cm to the right (or left) of the midline, the incidence of correctly reporting the right-hand (or left-hand) letter increased. When the coil was moved slightly rostral to the optimal suppression site, only the bottoms of the letters in the horizontal display were suppressed. Furthermore, when the three letters were displayed in a vertical array, moving the coil 3 cm superior to the optimal site resulted in the correct identification of the top but not the bottom letter of the display. This provides strong evidence that TMS can alter activity in sub-sections of the retinotopic map within visual cortical area.

This has since been corroborated by findings by Meyer, Diehl, Steinmetz, Britton & Benecke (1991) and Kammer (1999), who report that moving the coil from left to right over the occipital pole resulted in the position of elicited phosphenes in the visual field moving from right to left, and vice versa. It must also be pointed out that Meyer and colleagues used a circular coil for their stimulation, which indicates that the functional resolution of the circular coil is not as coarse as might be predicted by phantom studies. This is probably due to the fact that phantom studies measure the electric field produced by the entire coil, whereas in practise, only a section of the coil winding is placed on the scalp.

It has been suggested that higher field strengths result in a greater spread of induced electric currents through the cortex which results in reduced resolution of functional maps (Gugino, Romero, Aglio, Titone, Ramirez, Pascual-Leone,

Grimson, Weisenfeld, Kikinis & Shenton, 2001). This could explain the finding that with increasing magnetic field strength phosphenes covered a larger area in the visual field (Kammer et al., 2005b).

In conclusion, the relationship between the magnetic field, the extent of the induced electric field and the anatomical specificity of the effect of the current is complex, and yet to be fully understood (Walsh & Rushworth, 1998; Maccabee & Amassian, 2008). However, several studies have shown that the functional resolution of TMS over visual and motor cortex appears to be in the order of ~ 1 cm to 2 cm, which is consistent with the estimates of the functional magnetic field for the TMS equipment used in the experiments in this thesis (Jalinous 1995). Furthermore, focality can generally be increased by using double as opposed to circular coils. Caution must be exercised when interpreting focality, however, as the effects of TMS have been demonstrated to spread rapidly to distinct and distant cortical areas via transsynaptic connections (Ilmoniemi et al., 1997; Paus et al., 1997; Bohning et al., 1999), as discussed earlier.

2.2.4 Safety

There are known risks involved when using TMS, the largest concern being the induction of a seizure. However, there are known contributors to this risk and if these are avoided, the chance of invoking a seizure are very unlikely. These risk factors concern the participant as well as the frequency and intensity of stimulation.

2.2.4.1 Contraindications

Participants were screened using the Transcranial Magnetic Stimulation Adult Safety Screen (Keel, Smith & Wassermann, 2000), to which there were no affirmative answers. The safety screen excluded participants who had any metal implants or fragments in their head (excluding dental plates), cardiac pacemakers, a history of epilepsy, a family history of epilepsy, neurological disease (such as stroke, brain tumour, or multiple sclerosis), neurosurgery or brain-related condition, frequent or severe headaches, anyone who is currently taking medication for neurological or psychological reasons, anyone who may be pregnant, or anyone who has had an adverse reaction to TMS. In addition to this, we also excluded anyone with a history of drug or alcohol abuse, anyone who was sleep-deprived and anyone under the age of 18 years old, although TMS has now been used on children as young as 6 years old (Garvey & Mall, 2008). All participants gave written informed consent after being introduced to the equipment and the procedure.

2.2.4.2 Pulse rate

Single pulse TMS (< 0.3 Hz) was used in all experiments. Single pulse TMS generally refers to a pulse rate of < 1Hz. In the experiments presented here, one TMS pulse was delivered per visual stimulus presentation, and an inter-trial interval of 2.5 s between successive stimulus presentations ensured the rate of stimulation was always considerably lower than 1 Hz. This is well

within the safety guidelines stipulating rates of safe stimulation (Wassermann, 1998).

Chapter 3: An investigation into the temporal properties of translational global motion processing

3.1 Introduction

Despite the impressive temporal resolution offered by TMS, the critical window of disruption for area V5/MT in motion-based tasks is far from clear. Taken together, previous reports indicate a very broad period for critical disruption of V5/MT, approximately ± 200 ms relative to stimulus onset. Many studies differ considerably in their estimates of the critical temporal window for disruption. For example, Beckers & Homberg (1992) reported that a TMS pulse delivered to area V5/MT between 20 ms before and 20 ms after the onset of a visual stimulus, produced complete motion blindness. Similarly, Beckers & Zeki (1995) report disruption to motion processing when TMS was delivered to V5/MT between 20 ms before and 10 ms after visual stimulus onset. The greatest stimulus onset asynchrony (that is, the latency of the delivery of a TMS pulse relative to the onset of a visual target, hereafter known as SOA) at which a TMS pulse was delivered in these two studies was 160 ms (Beckers & Homberg, 1992) and 100 ms (Beckers & Zeki, 1995) after the onset of the visual stimulus. A later temporal window relative to stimulus onset during which delivery of a TMS pulse disrupted motion processing was reported in subsequent studies, however, at SOAs of between approximately 100 ms and 150 ms (Hotson et al., 1994), 120 ms and 200 ms (Anand et al., 1998) and 100 ms to 175 ms (Hotson & Anand, 1999) after visual stimulus

onset. The earliest SOA at which a TMS pulse was delivered in these two studies was 50 ms or 60 ms after onset of the visual stimulus. Hotson & Anand (1999) noted that their study did not provide any information about "early" V5/MT activation (around stimulus onset) and Beckers & Zeki's (1995) study did not provide information about "late" activation (after stimulus offset). Hence, part of the discrepancy in the literature is simply that the temporal windows during which TMS pulses were delivered were too temporally narrow to reveal the full disruption profile.

Furthermore, the SOAs at which TMS pulses were delivered tended to be relatively coarsely sampled, for example, in 20 ms or larger increments (Beckers & Homberg, 1992; Anand et al., 1998; Walsh et al., 1998; Hotson & Anand, 1999). It is therefore possible that discrete temporal periods in which performance may be modulated by TMS are not revealed or masked by course sampling.

In addition to differences in sampling, many studies use very different stimulus configurations to investigate the extent of TMS-induced disruption. This is another potential source of variance to the estimated effects of TMS. A major problem with some stimuli previously used to investigate area V5/MT processing is that potentially the task could be performed without spatio-temporal integration over extensive regions of visual space. For example, in a study by Silvanto et al. (2005), RDK elements were displaced by only one pixel per frame. Similarly, RDKs which contain 100 % coherence (Laycock et al., 2007) could be ocularly tracked to determine direction of motion. To

ensure the functional activation of area V5/MT, a task involving the integration of local motion signals across an extended region of space should be employed (Newsome & Paré, 1988; Britten et al., 1993). However, as the task needs to be sensitive to disruption by TMS, potential ceiling and floor effects needs to be considered to avoid null results (Matthews et al., 2001).

The effective temporal window for TMS disruption may also be affected by other properties of the motion stimulus. For example, the temporal responses of visual neurons are heavily dependant on stimulus contrast at both pre-cortical (Shapley & Victor, 1978; Maunsell, Ghose, Assad, McAdams, Boudreau & Noeranger, 1999) and cortical (Albrecht, 1995; Reich, Mechler & Victor, 2001) levels. Specifically, response latencies – defined as the amount of time between the onset of a stimulus and the onset of a neural response (Maunsell & Gibson, 1992) – decrease as stimulus contrast increases in V1 cells (Albrecht, 1995; Reich et al., 2001). These stimulus-based changes in temporal response are likely to be manifest at higher cortical areas such as V5/MT, V2 and V3 all of which receive direct input from V1 (Zeki, 1969; Maunsell & Van Essen, 1983).

There is not general agreement regarding the validity of an "early" temporal window in which delivery of a TMS pulse disrupts motion processing, as it has been previously explained as a TMS-induced, non-cortical, muscular artefact (for example, an eye blink) [e.g. Corthout et al., 2003; Sack et al., 2006].

Aims

The primary aim of the experiments described in this chapter was to determine the critical period for disruption of translational global motion processing in area V5/MT by TMS. A second objective was to determine whether TMS delivered over a non-visual cortical region induced a muscular artefact that could disrupt performance. Finally, the contrast of the visual stimulus was changed to establish the effect of contrast on TMS-induced disruption to global motion processing.

3.2 Experiment 1: A psychophysical investigation of the summation period for translational global motion processing

3.2.1 Introduction

3.2.1.1 Previous TMS studies

There is a notable variation in the duration of the RDKs employed in previous TMS studies of motion perception, but often no explanation is given as to why a particular duration was used (Beckers & Zeki, 1995; Anand et al., 1998; Hotson & Anand, 1999; Matthews et al., 2001; d'Alfonso et al., 2002). Previous RDK durations vary from 28 ms (Beckers & Zeki, 1995) to 200 ms (Matthews et al., 2001). In the study conducted by Matthews et al. (2001), RDKs were comprised of a sequence of 24 frames (200 ms duration) and there was little or no disruptive effect of TMS on participants' direction

discrimination. One plausible interpretation of this result is that the relatively long duration of the visual stimulus out-lasted the effects of a single TMS pulse. Indeed, the authors observed that on their speed discrimination task, the disruptive effect of TMS decreased as SOA increased, which was probably a function of an increased number of stimulus frames having been summated before the pulse was delivered. An alternative explanation is that the results were confounded by a ceiling effect, and the task was not sensitive enough to reveal disruption by TMS.

3.2.1.2 Psychophysics

Burr & Santoro (2001) investigated coherence threshold (defined as the number of coherently-moving dots producing a correct direction discrimination rate of 75 %) for RDKs depicting translational global motion as a function of duration. It was found that thresholds decreased as duration was increased above 75 ms (3 frames) until a critical duration was reached, after which coherence threshold was asymptotic. In a second experiment, Burr & Santoro investigated coherence sensitivity as a function of duration when the global motion signal was embedded temporally between two periods of randomly moving dots, to ensure that sensitivity was dependent on the duration of the global motion signal.

Adopting this approach in the current study, the minimum number of global motion frames needed to produce asymptotic performance on the task was determined, and indicated the summation period for global direction detection

(Barlow, 1958; Burr & Santoro, 2001). The function describing the relationship between the duration of the global motion sequence and coherence threshold was then used to determine the duration at which sensitivity could be readily modulated while avoiding potential ceiling and floor effects when used in conjunction with TMS.

3.2.2 Methods

3.2.2.1 Observers

Four volunteers (mean age = 29.4 years; range = 23 to 38 years) participated in the study. All participants had normal or corrected-to-normal (N = 2) vision. LKS is the author while the other participants were naïve to the goals of the study.

3.2.2.2 Visual Stimuli

Global motion random dot kinematograms (RDKs) were computer generated using an *Apple Macintosh G4* and displayed on a *Viglen* 22 inch cathode ray tube monitor (see *Equipment* section of Chapter 2: General Methods). Each RDK was composed of a sequence of either 22 or 23 image fames (frame duration = 26.67 ms) which when presented consecutively produced continuous apparent motion. RDKs comprised 100 non-overlapping "black" dots (diameter = 7 arcmins; drift rate, if sustained = 1.76 deg/s) presented within a frameless circular aperture (diameter = 6 deg) on a mid-grey

background (luminance = 73.52 cd/m^2; 0.99 Weber contrast). Properties of the dots were chosen on the basis of pilot studies and previous investigations of global motion perception (Simmers, Ledgeway, Hess & McGraw, 2003) to ensure that dots were not subject to 'false matches' across successive displacements and the correspondence problem minimised (Williams & Sekuler, 1984).

On the first frame of each RDK, dots were randomly positioned and were displaced by 2.81 arcmins on each subsequent frame. When a dot reached the edge of the circular display window it was repositioned in a random spatial position within the presentation window in the following frame. Dots were either constrained to move globally along a translational (up/down) trajectory ("signal" dots) or were displaced in random directions on each frame ("noise" dots). The strength of the global motion signal, which we term the "coherence", could be varied by manipulating the proportion of "signal" dots to "noise" dots (Figure 3.1). On every displacement in the global motion sequence each dot had an equal chance of being selected as a "signal" dot (e.g. Newsome & Paré, 1988; Edwards & Badcock, 1994). For example, at a global motion coherence level of 10 %, 10 dots would be displaced coherently over one frame transition, but a new sample of 10 dots would be randomly selected to carry the signal into the next frame. At this level of motion coherence, the probability of a dot carrying the signal over two successive frames is 1 %. This minimised local 'motion streak' cues (Geisler, 1999) so that spatio-temporal information over the entire display must be integrated to encode global direction. The integration of local motion signals over an extended region of

visual space is thought to be a key function of neurons in V5/MT with large receptive fields. The necessary integration of many local motion signals renders the task ideal for ensuring functional activation of area V5/MT (Britten et al., 1993).

Each RDK contained a global motion sequence of variable duration (where a fixed proportion of dots were "signal" dots) embedded temporally between two random motion sequences (which consisted of 100 % "noise" dots) to limit the deleterious influence of abrupt motion onset/offset transients (Newsome & Paré, 1988; Burr & Santoro, 2001). The total number of image frames (random-coherent-random) in each RDK was constant irrespective of the duration of the global motion sequence, which ranged from 2 to 22 frames

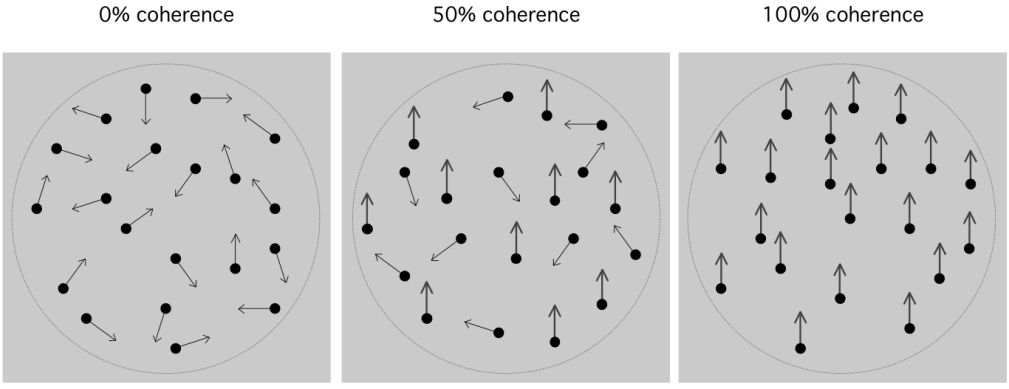

Figure 3.1. Schematic representation of global motion stimuli. When coherence is set to 0 %, left, all dots are "noise" dots and there is no net global motion. At 100 % coherence, right, all dots are "signal" dots and are displaced along the same global trajectory (in this case, upwards). At intermediate coherence levels, centre, a fixed proportion (e.g. 50 %) of dots are "signal" dots and are displaced coherently while the rest are displaced in random directions.

(Figure 3.2). As each RDK had a similar duration and number of dot displacements, global motion coherence thresholds were dependant on the duration of the global motion signal (Barlow & Tripathy, 1997; Burr & Santoro, 2001). Immediately prior to, and after, the presentation of each motion stimulus, a prominent fixation cross was presented in the centre of the display to maintain stable fixation and prevent ocular tracking of the stimulus.

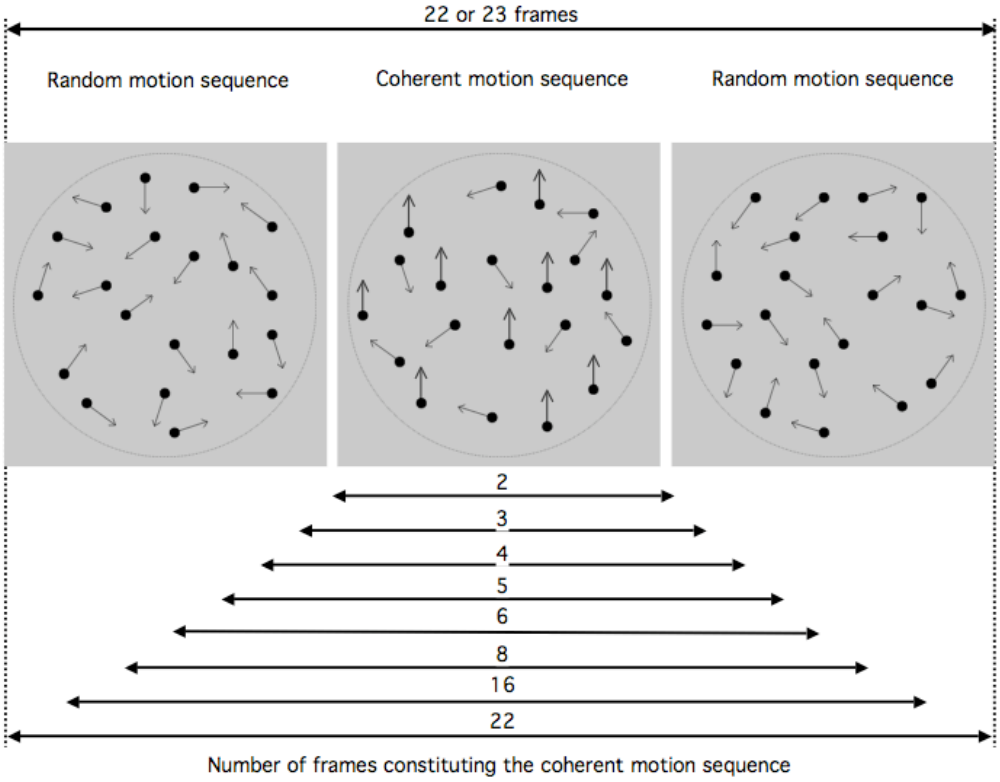

Figure 3.2. Each RDK (comprised of 22 or 23 image frames) contained a global motion sequence of between 2 and 22 frames where a fixed proportion of dots carried the signal. The global motion sequence was preceded and followed by 0 % coherence motion frames, to bring overall RDK frame number to 22 or 23 frames. The exception was the 22 frame global motion sequence which was not preceded or followed by random motion.

3.2.2.3 Visual psychophysics

Global motion direction discrimination was measured using a one-interval, two-alternative forced choice task ("up" vs. "down") in conjunction with the method of constant stimuli. Psychometric functions were generated by presenting seven percentages of "signal" dots that produced a continuum between chance and ~ 100 % correct performance. Threshold was defined as the percentage of "signal" dots required to produce a correct response rate of 75 % correct. In a single run, each of the seven coherence levels was presented randomly ten times. A single run lasted ~ 2.5 mins. Each participant completed four runs for each of the global motion sequences comprising 2, 3, 4, 5, 6, 8, 16 and 22 frames.

3.2.3 Results and discussion

The percentage of correct directional judgements was plotted as a function of global motion coherence (percentage of "signal" dots). Global motion thresholds were extracted using a logistic function of the form:

$$y = 50 + \frac{50}{1 + \left(\exp - \left(\frac{x - t}{s}\right)\right)} \tag{3.1}$$

where t represents the percentage of "signal" dots supporting 75 % correct responding (taken as threshold), and s represents the slope of the curve (see Figure 3.3 for an example psychometric function). Global motion thresholds

(*t*) were then plotted as a function of number of frames in the global motion sequence (Figure 3.4). It can be seen in Figure 3.4 that global motion thresholds decrease as the number of global motion frames is increased above two until a critical value is reached, after which thresholds are approximately asymptotic. Global motion thresholds appear to be stable when the number of global motion frames was increased above about 10 frames (266 ms).

More importantly, it can be seen in Figure 3.4 that global motion thresholds increase steeply when the number of global motion frames is lower than around four frames. The optimal number of global motion frames to be used in conjunction with TMS should ideally fall on the rising part of the curve to ensure that potential ceiling effects are avoided and baseline global motion

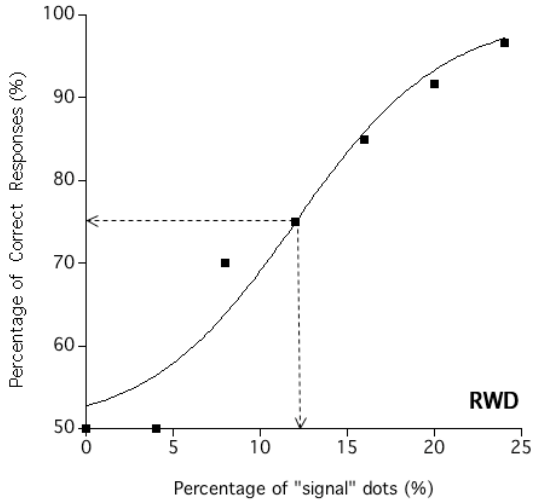

Figure 3.3. An example of a psychometric function for one participant, fitted with Equation 3.1, to extract the 75 % threshold (indicated with the broken lines).

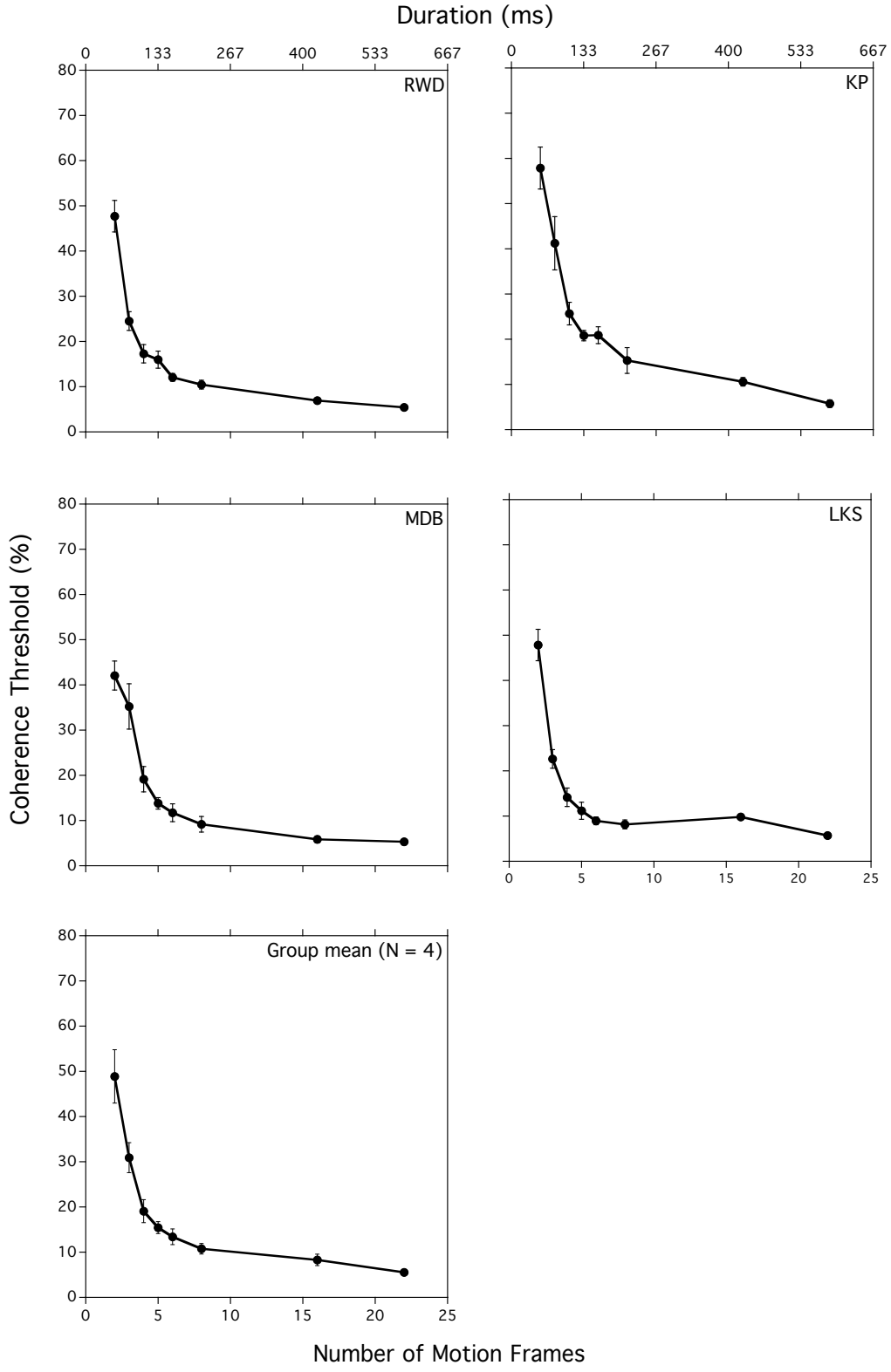

Figure 3.4. Coherence thresholds (% "signal" dots needed to support 75 % correct responding) for translational global motion, plotted as a function of number of global motion frames. Coherence thresholds decrease rapidly as the number of global motion frames increase until a critical frame number is reached, after which thresholds are generally invariant of the number of motion frames. Error bars represent the SE.

thresholds are sensitive to disruption. Accordingly, 3 global motion frames (duration 80 ms) were used for all global motion stimuli used in conjunction with TMS (preceded and followed by a ten-frame random motion sequence, to limit the influence of onset/offset transients). It can also be seen from Figure 3.4 that the marked rapid increase in coherence threshold when the number of global motion frames less then approximately four is similar for all participants.

3.3 Experiment 2: Investigating the critical period for disruption of translational global motion processing in area V5/MT

3.3.1 Introduction

As has been discussed earlier, investigating a broad range of SOAs in a single study is crucial to the complete characterisation of the TMS disruption profile. Evidence from previous studies suggests that a TMS pulse delivered over area V5/MT can disrupt motion processing in two or more epochs. An *early* period (at or close to motion onset) has been reported in some studies (Beckers and Homberg, 1992; Beckers & Zeki, 1995) while others report a *late* period, which ranged between 60 ms to 200 ms after stimulus onset (Hotson & Anand, 1999; Silvanto et al., 2005; Anand et al., 2008).

The timing of the periods of disruption, when not attributed to non-cortical effects of TMS (such as blinking), are often interpreted in terms of feedforward and feedback mechanisms known to exist between motion-sensitive areas of the visual cortex, but with very different estimates of latencies. For example, Beckers and Zeki (1995) concluded that motion information can reach area V5/MT before area V1, as they found that delivering TMS to area V1 60 ms and 70 ms after motion onset, and to V5/MT between 20 ms prior to, and 10 ms after motion onset, decreased motion direction discrimination. These results were explained on the basis of a subcortical pathway that is thought to transmit to area V5/MT directly, bypassing area V1. Primate studies have provided anatomical and physiological evidence of significant projections from sub-cortical structures such as the LGN and pulvinar directly to V5/MT (Girard, Salin & Bullier, 1992; Sincich et al., 2004). However, activation of a fast pathway to area V5/MT is thought to be speed-dependent, only occurring when stimulus speed is greater than ~ 20 deg/s (ffytche, Guy & Zeki, 1995; Holliday et al., 1997; Azzopardi & Cowey, 2001), which is twice that of the stimulus speed (11 deg/s) used by Beckers and Zeki (1995). Furthermore, the presence of a fast subcortical pathway to area V5/MT to humans remains controversial (Anderson et al., 1996) [see section 3.6, General discussion, for a full discussion of this].

Two recent studies, however, found two critical periods during which delivery of a TMS pulse to area V5/MT impairs the ability to discriminate the direction of translationally-moving stimuli (Sack et al., 2006; Laycock et al., 2007).

However, although these two studies observe a decrease in direction discrimination at around 150 ms after stimulus onset, each study attributes this critical period to different cortical processes. Sack et al. speculate that this latency coincides with estimates of V5/MT onset latency from MEG studies, whereas Laycock et al. argue that TMS disruption at SOAs of around 150 ms is too late to represent feedforward processing, and is more likely to reflect feedback from higher cortical areas such as the frontal eye fields or parietal cortex.

Aims

This experiment sought to re-evaluate the situation by measuring the fine disruption profile over an extended period relative to global motion onset.

3.3.2 Methods

3.3.2.1 Observers

Five observers participated in this investigation: SB was naïve to the purpose of the investigation, as were RWD, KP, and MDB who also participated in Experiment 1. PVM was an experienced psychophysical observer. All participants reliably perceived phosphenes after single-pulse stimulation (80 % maximum stimulator output, ~ 1.95 T) over the location of area V5/MT, as determined by Sack et al. (2006). Participants gave no affirmative responses to any items on the Transcranial Magnetic Stimulation Adult Safety Screen (Keel

et al., 2000), and gave written informed consent after being introduced to the equipment and procedure.

3.3.2.2 Visual Stimuli

Visual stimuli used in conjunction with TMS comprised RDKs made up of a three-frame global motion sequence (80 ms) presented at each observer's individual coherence threshold (RWD, 26 %; KP, 28 %; MDB, 28 %; SB, 23 %; PVM, 33 %), preceded and followed by 10 random motion frames (266.65 ms) giving an overall duration of 613.3 ms. All other stimulus parameters were as described in Experiment 1.

3.3.2.3 TMS coil localisation

The coil position and orientation for area V5/MT stimulation was localised using a combination of functional and anatomical MRI measurements and phosphene-induction methods. After the location on the scalp overlying area V5/MT was found using neuronavigation (see Coil localisation section in Chapter 2: General Methods) [see Figure 3.5], a 3 x 3 grid of points 5 mm apart was then marked on the scalp around the initial point, and single TMS pulses (80 % of maximum output; ~ 1.95 T) were delivered over each point. Participants were asked to report whenever they saw a phosphene(s). Coil locations that elicited phosphenes that appeared in the centre of the left hemifield were investigated further with a finer grid of stimulation points, to determine the location and coil angle at which stimulation produced the most

frequent and stable phosphenes (see Table 3.1 for comparison of stimulation sites). The right hemisphere was chosen for investigation because phosphenes could be reliably induced by right hemisphere stimulation in all participants (c.f. Theoret et al., 2002; McKeefry et al., 2008).

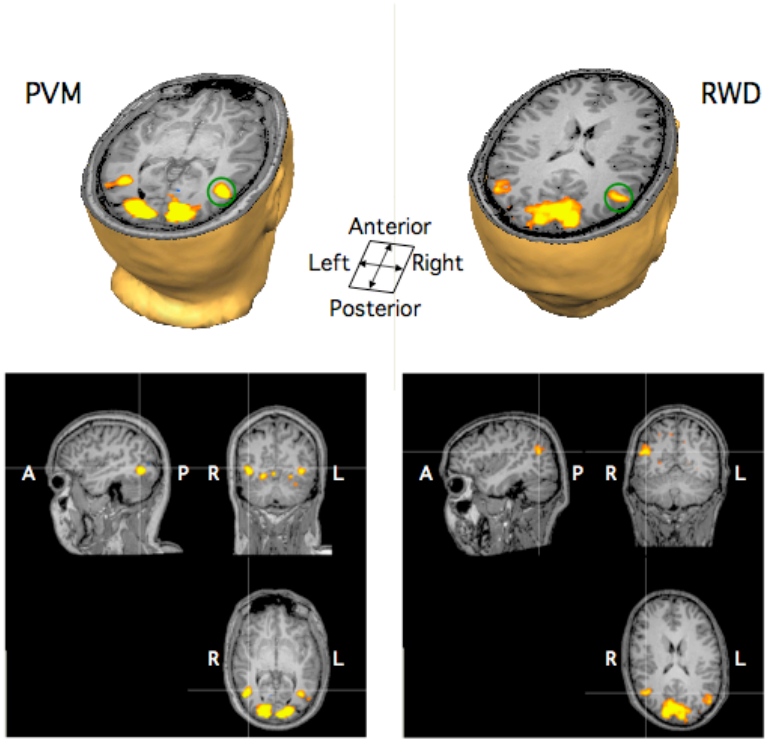

Figure 3.5. Functional identification of area V5/MT for two participants. Voxels with significant activation in response to moving dots vs. stationary dots are shown on anatomical scans using a pseudocolour overlay. Areas of most significant activation ($p_{(\text{uncorrected})} < 0.0001$) are shown for two observers (PVM, RWD). (Top) Axial slices through head reconstructions at the level of right V5/MT (marked with green circles) with an axis of head orientation for reference. (Bottom) Right hemisphere V5/MT marked on sagittal, coronal, and transverse cross-sections through the high-resolution anatomical image for participants PVM and RWD. Images are displayed in radiological convention (R, right; L, left; A, anterior; P, posterior).

3.3.2.4 TMS procedure

Participants sat in a dimly illuminated laboratory with their head stabilised in a custom-made wooden headrest, which minimised head movement. Biphasic TMS pulses were delivered with one of two custom 55 mm double coils. The handle was parallel to the horizontal plane and pointed toward the back of the head (Hotson et al., 1994; Sack et al., 2005), and was clamped securely in place. Participants were offered earplugs to wear for the TMS trials. The delivery of TMS was time-locked to the vertical refresh rate of the monitor. A single pulse could be delivered before, during or after the presentation of the global motion sequence by displaying a small high luminance square in the bottom right corner of the monitor. Onset of this square (which was not visible to participants) activated a photodiode that was configured to trigger the discharge of the TMS apparatus. Single pulses were delivered at a rate of one pulse per RDK stimulus presentation, with a 2.5 second inter-trial-interval between participants' response and the onset of the next RDK stimulus. TMS was delivered at forty different stimulus onset asynchronies (SOAs) [from -266 ms to +253 ms] relative to the onset of the global motion sequence (see Figure 3.6), with one hundred repetitions per SOA. Sessions were run in blocks of fifty RDK stimuli presentations; forty with TMS, interleaved with ten without as a control measure. Each block of fifty trials lasted approximately four minutes. This is well within the safety guidelines stipulating rates of safe stimulation (Wassermann, 1998).

3.3.3 Results and discussion

In Figure 3.7 the results for each individual participant are plotted separately and the group mean data (N = 5) are also shown. Although there is some variability in the individual participant responses, all participants showed a decrease in performance (a reduction in the percentage of correct responses) on TMS trials. Indeed the data for each participant clearly reveal two discrete

Study	Participant	Anterior (mm)	Lateral (mm)
Sack et al. (2005)	1	34	54
	2	37	63
	3	21	61
	4	41	55
	5	40	63
Beckers & Zeki (1995)	Mean (N=5)	30-40	60
Beckers & Homberg (1992)	Mean (N=4)	50	50-60
Silvanto et al. (1995)	Mean (N=5)	31	51
Theoret et al. (2002)	Mean (N=12)	30	50
Present Study	KP	33	50
	MDB	50	55
	PVM	27	50
	RWD	40	47
	SB	60	70
	Mean (N=5)	42	54.4

Table 3.1. Location of area V5/MT stimulation site for each participant relative to inion, compared to previous studies. Overall mean location of area V5/MT stimulation site reported in previous studies = 35.4 mm anterior, 54 mm lateral from inion.

temporal windows where delivery of a single TMS pulse modulates task performance. To quantify the location, height and width of each temporal window, the individual data were fitted with a bimodal function composed of the sum of two inverted Gaussian functions as follows:

$$y = \exp\left\{-\left[(x-a)/b\right]^2 \ln 2\right\}c + \exp\left\{-\left[(x-d)/e\right]^2 \ln 2\right\}f + g \qquad (3.2)$$

where x is TMS onset (in ms), a and d are TMS onsets that cause maximal disruption, b and e are the Gaussian bandwidths (half-width, half-height), c and f are the amplitudes (heights) of each Gaussian and g is the performance level for which TMS disruption is minimal. The group data and curve fit, derived from the means of the fitted parameter values, (Figure 3.7, bottom-right panel) clearly illustrate two important findings. First, there exists a relatively broad

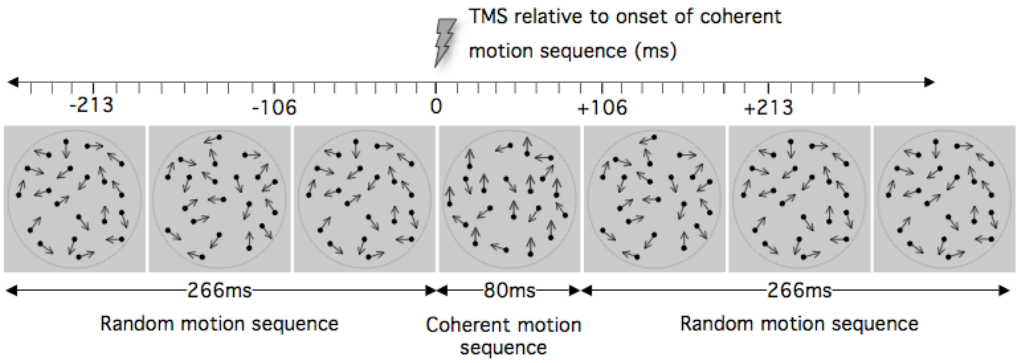

Figure 3.6. Single-pulse TMS was delivered once per RDK stimulus presentation sequence at one of 40 latencies relative to the onset of the global motion sequence (ranging from 266 ms prior to, to 253 ms after global motion onset). The onset of the global motion sequence was at 0 ms (duration = 80 ms), and was preceded and followed by random motion sequences, each lasting 266 ms.

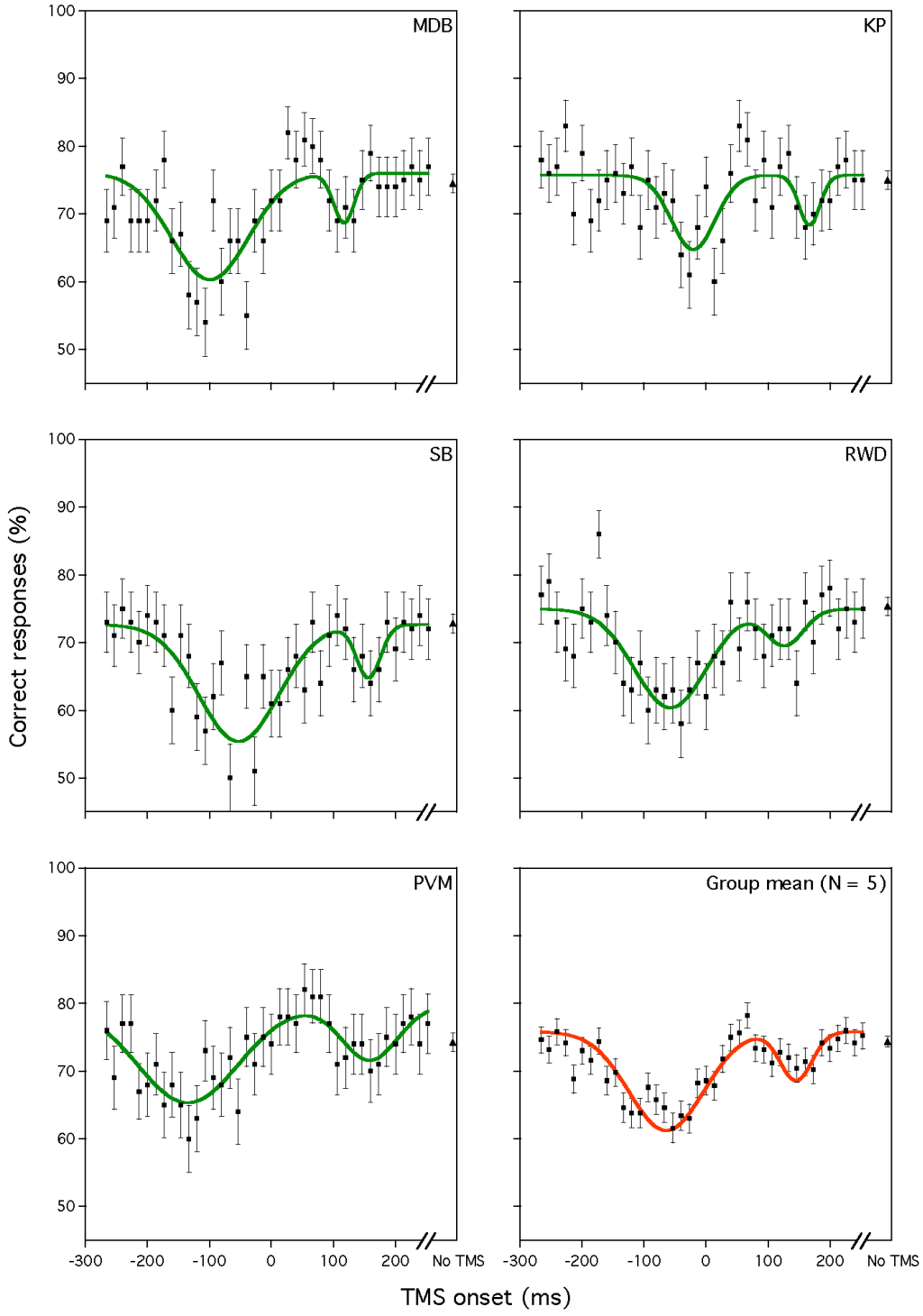

Figure 3.7. Performance as a function of TMS onset asynchrony. The first five panels show individual data, the bottom right panel shows the group mean data (N = 5). 0 ms represents the onset of the global motion sequence. Performance during TMS trials (squares) is impaired relative to no TMS trials (triangles) during two temporal windows - although there are individual differences in the onset and magnitude of the performance deficit. The solid lines show the best-fitting curves, derived from Equation 3.2, to the data and reveal, relative to global motion onset, a broad *early* performance deficit and a less marked *late* deficit. Error bars for individual data represent the SE of the %, error bars for group mean data represent the SEM.

temporal window (mean *b* = 70.8 ms; SEM = 8.7 ms) where peak disruption of processing occurs *before* the global motion sequence is onset (mean *a* = -63.8 ms; SEM = 18.4 ms). Second, a narrower temporal window (mean *e* = 30 ms; SEM = 6.4 ms) is also evident, with a smaller peak deficit occurring *after* the onset of the global motion sequence (mean *d* = +145.6 ms; SEM = 9.8 ms). The mean peak performance deficit (*c*) for the *early* temporal window is 14.5 % (SEM = 1 %) and for the later window the corresponding value (*f*) is 7.2 % (SEM = 0.5 %), although some individual data show larger performance deficits.

The two temporal windows for disruption with TMS concur with previous studies (Sack et al., 2006; Laycock et al., 2007). However, it can be seen when comparing Figure 3.7 to Figures 3.8 and 3.9 that the data presented in the current experiment appears to be considerably more consistent than that presented in the previous two studies. For example, the results from Sack et al.'s experiment only appear to exhibit a relatively modest effect of TMS compared to the results presented here, and this effect of TMS was only observed after the group data was combined. The data collected in Laycock et al's study appear to be highly variable, with participants frequently achieving a correct response rate of 100 % even on TMS trials. Furthermore, the two most variable participants excluded from the analysis, although no reason was provided for this. More critically, the disruption to performance observed when TMS was delivered 150 ms after stimulus onset in Laycock et al.'s first experiment (Figure 3.9, top panel) was not replicated under the same conditions in their second experiment (Figure 3.9, bottom panel).

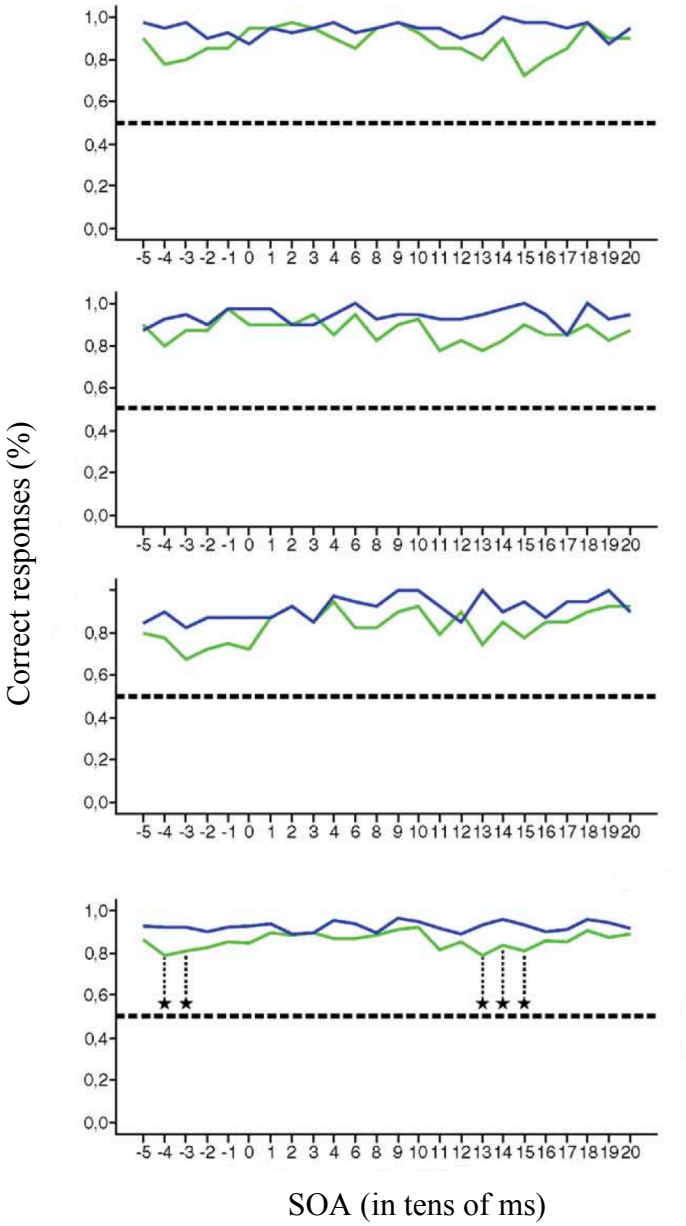

Figure 3.8. Percentage of correct direction judgments for 3 example participants (N = 5), taken from Sack et al.'s study (2006). It can be seen that there was a significant decrease to performance when TMS was delivered to area V5/MT (shown by the green line) 40 ms and 30 ms prior to motion onset (0 ms) and between 130 ms and 160 ms after motion onset (marked with asterisks), compared to when TMS was delivered to a control site (Cz) [shown by the blue line]. However, there was no significant difference between TMS and control trials in individual participants' data.

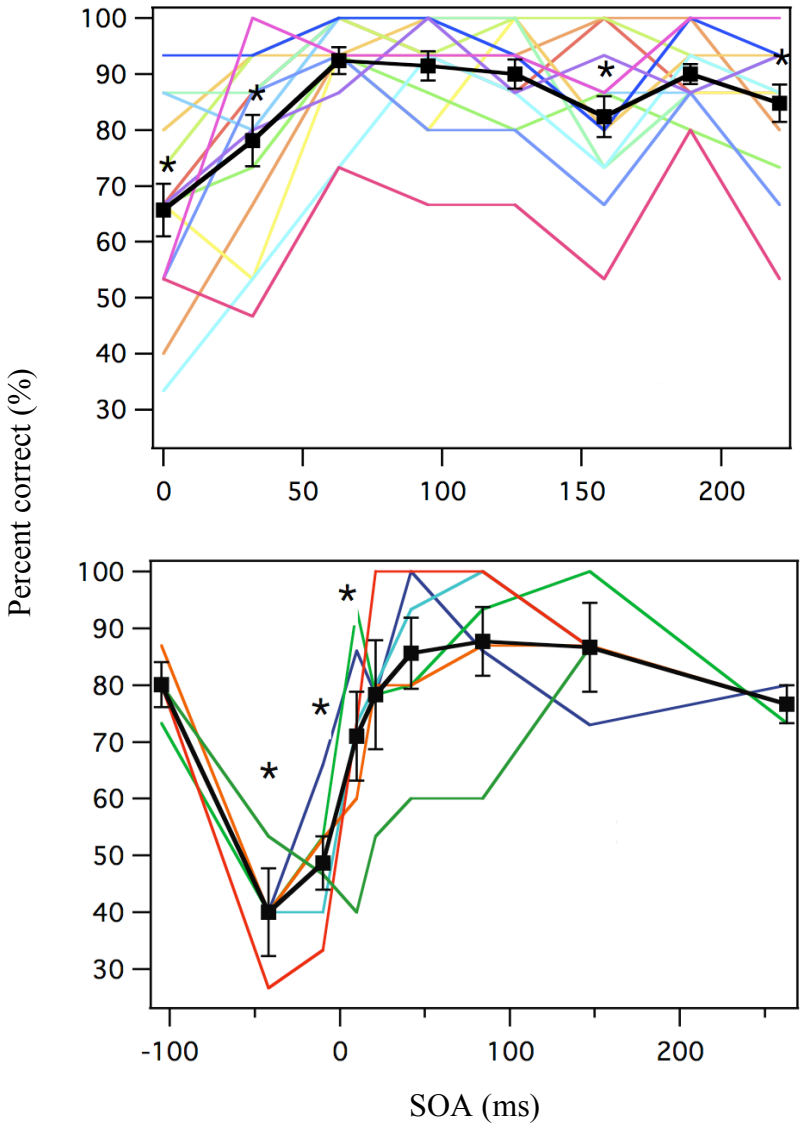

Figure 3.9. Taken from Laycock et al.'s study (2007). Correct directional judgements when TMS was delivered to area V5/MT at positive SOAs (top panel) and both negative and positive SOAs (bottom panel). It can be seen that the responses varied considerably between participants, even though the two most variable participants had been excluded from this analysis, by the authors, as they showed inconsistent results. Asterisks denote significant post-hoc results.

3.4 Experiment 3: Exploring the possibility of TMS-induced eye-blink artefacts

3.4.1 Introduction

Early periods of disruption have previously been attributed to a TMS-induced "eye-blink" artefact (Sack et al., 2006; Corthout et al., 2000; Corthout et al., 2003) although there is little or no evidence this is actually the case. The SOAs at which delivery of a TMS pulse is suggested to initiate an eye-blink are 40 to 30 ms (Sack et al., 2006) and 70 to 50 ms (Corthout et al., 2000; Corthout et al., 2003) before visual stimulus onset.

Beckers & Zeki (1995) speculated that in stimulating area V5/MT they may also have stimulated the posterior bank of the VIIth facial nerve. This may, in turn, have elicited a response in the orbicularis oculi muscles and caused a reflexive eye-blink. Consequently, they delivered 1 T pulses with the coil placed slightly anterior and superior of the ear, as this location was thought to lie directly over the VIIth nerve. The participant (N = 1) received ten pulses each at 0 ms and +10 ms relative to the onset of the visual stimulus, as Beckers & Zeki found that TMS delivered over area V5/MT at these SOAs disrupted motion discrimination. Performance was 100 % correct during this control-site stimulation, which suggests that an eye-blink caused by stimulation of the VIIth nerve is unlikely to have caused the disruption to direction discrimination observed when area V5/MT was stimulated.

The current experiment is an additional control experiment to investigate if a TMS-induced blink artefact can account for the relatively early period of disruption (before global motion onset) found in Experiment 2. TMS pulses were delivered to a non-visual cortical region (motor cortex) and the effect on performance on the global motion task was measured.

3.4.2 Methods

3.4.2.1 Observers

Two volunteers who took part in Experiments 1 and 2 (RWD and MDB) participated in this investigation.

3.4.2.2 Visual stimuli

Global motion stimuli were identical to the visual stimuli used in Experiment 2, and were presented at each observer's individual coherence threshold level.

3.4.2.3 TMS coil localisation

The primary motor cortex, M1, was located using a standard search technique (e.g. Siebner, Peller, Willoch, Minoshima, Boecker, Auer, Drzezga, Conrad & Bartenstein, 2000; Stewart, Walsh & Rothwell, 2001; Gerwig, Kastrup, Meyer & Niehaus, 2003). An initial mark was made on participants' scalps 1 cm anterior and 2 cm lateral (right) of the vertex. Single pulses were then

delivered over a 3 x 3 grid of points (10 mm apart) centred on the initial marker. The coil location used in the experiment was the one at which twitches in the fingers of the left hand were most frequently elicited.

3.4.2.4 TMS procedure

Single pulse TMS was delivered to the right hemisphere primary motor cortex while participants performed global directional judgements for translationally-moving RDKs. TMS pulses were delivered at a time when considerable disruption to performance was observed in Experiment 2 (40 ms prior to the onset of the global motion sequence), and all other TMS procedures were as set out before. Each participant completed two sessions, each comprised of 40 RDK stimuli presentations; 20 with TMS, interleaved with 20 without as a control measure.

As an additional control, a 30 Hz video camera was used to record eye blinks following a TMS pulse for three conditions: TMS of area V5/MT, TMS of motor cortex and sham TMS (coil discharged next to head but not placed on scalp). Each condition was run separately and consisted of 60 stimulations.

3.4.3 Results and discussion

No difference in performance was found between trials in which TMS was delivered to the motor hand area 40 ms prior to global motion onset, and trials with no TMS at all, as shown in Figure 3.10. That is, performance was close to

75 % correct in both conditions. This result makes it extremely unlikely that the performance deficit observed in Experiment 2 when TMS was delivered over area V5/MT prior to global motion onset was caused by a TMS-induced muscular artefact.

The videos from the three conditions: (a) TMS of area V5/MT, (b) TMS of motor cortex and (c) sham TMS were analysed on a frame-by-frame basis. For each of the two participants, the percentage of trials in which a blink occurred within a 2 s window following TMS onset was established for each condition – (a) 0 % and 3.3 %; (b) 10 % and 8.3 % and (c) 5 % and 6.6 %. The fact that

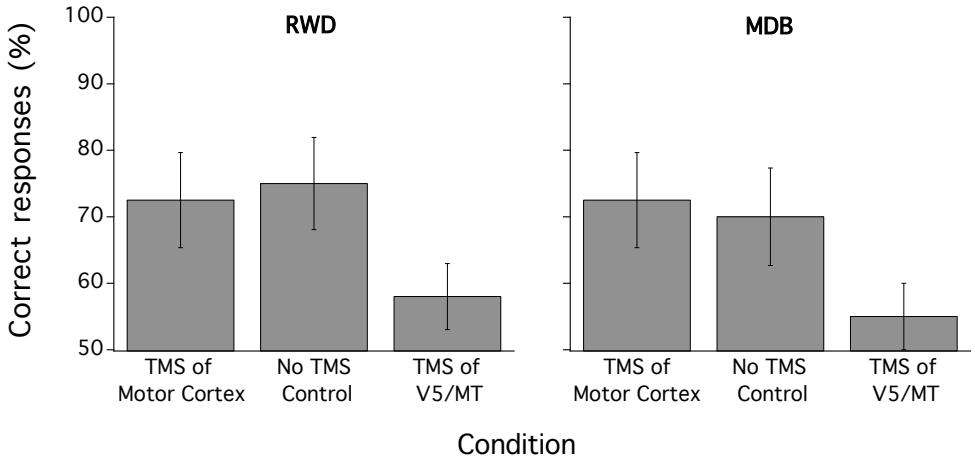

Figure 3.10. The percentage of correct responses for two participants when TMS was delivered over right hemisphere primary motor cortex 40 ms prior to global motion onset. The global motion stimulus used was identical to that when TMS was delivered over area V5/MT (data re-plotted from Experiment 2 for purposes of comparison), yet here performance was similar for TMS and no TMS conditions. Error bars represent the SE of the %.

more eye-blinks occurred within a 2 s window following a TMS pulse with motor cortex stimulation compared to TMS of area V5/MT makes it very unlikely that the disruption to motion perception elicited in this time window is caused by an eye-blink as has been previously suggested (Corthout et al., 2000; Corthout et al., 2003; Sack et al., 2006).

3.5 Experiment 4: The effect of contrast on the critical period for disruption of translational global motion processing in area V5/MT

3.5.1 Introduction

As was mentioned earlier in this chapter, the temporal responses of the visual system are dependent on stimulus contrast. This has been demonstrated behaviourally in humans by an increase in reaction time as contrast was decreased, for detecting the presence of a stimulus (Harwerth & Levi, 1978), or for detecting motion onset (Burr, Fiorentini & Morrone, 1993). The increase in reaction time to lower-contrast stimuli is also reflected in the visually evoked response, measured by EEG, the latency of which is longer for lower than higher contrast stimuli in humans (Vassilev & Manahilov, 1986).

In cat and monkey, the response latencies – defined as the amount of time between the onset of a stimulus and a neural response – for cells in the striate visual cortex were approximately 45 ms shorter after presentation of a higher

contrast (approximately 90 % Michelson contrast) moving grating stimulus than a lower contrast (approximately 3 % Michelson contrast) stimulus, although the exact value varied from cell to cell (Albrecht, 1995). Similarly, Reich and colleagues (2001) measured the response of cells in the primary visual cortex of macaques and report the data collected from one simple cell. Its onset latency was approximately 40 ms when the moving grating stimulus was 100 % contrast, but increased to approximately 68 ms when the contrast of the stimulus was reduced 12.5 %.

In light of this, the current experiment sought to investigate whether the critical temporal window during which TMS disrupted to global motion perception varied as a function of contrast. If neural response latencies change as a function of contrast then this should produce a measurable shift in the peak of disruption.

3.5.2 Methods

3.5.2.1 Observers

Two participants (RWD and MDB) who took part in Experiments 1, 2 and 3 also took part in this investigation. They were naïve as to the purpose of the study.

3.5.2.2 Visual stimuli

All global motion stimulus parameters other than dot luminance (69.5 cd/m^2) were identical to the translationally-moving RDKs described earlier. Prior to the TMS sessions, participants' baseline (no-TMS) coherence thresholds – the percentage of "signal" dots required to support a correct response rate of 75 % – were measured as described in Experiment 1. During the TMS sessions, visual stimuli used in conjunction with TMS comprised RDKs presented at each observer's coherence threshold (38 % and 45 % for RWD and MDB respectively).

3.5.2.3 TMS procedure

Area V5/MT was localised using the same methods as described in Experiment 2. TMS was delivered at thirteen different SOAs (from 253 ms prior to, to 226 ms post global motion onset at 40 ms intervals), with one hundred repetitions per SOA. All other procedures were as described in Experiment 2. Sessions were run in blocks of fifty RDK stimuli presentations; forty with TMS interleaved with ten without as a control measure. Each block of fifty trials lasted approximately four minutes.

3.5.3 Results and discussion

In Figure 3.11 performance for each individual is plotted alongside their results from Experiment 2 (where global motion stimuli were presented at 0.99 Weber

contrast), for purposes of comparison. It can be seen that the *early* and *late* periods of disruption persist at 0.03 Weber contrast, with performance falling close to chance when TMS was delivered during the *early* temporal window in conjunction with lower contrast stimuli. The deficit in performance when TMS was delivered during the *late* window of disruption has a similar magnitude for both contrasts tested, but if anything, may be shifted temporally by approximately 40 ms towards later SOAs for the lower contrast stimulus. This is in agreement with Albrecht's (1995) single cell study in which response latencies were approximately 45 ms longer for lower than higher contrast stimuli.

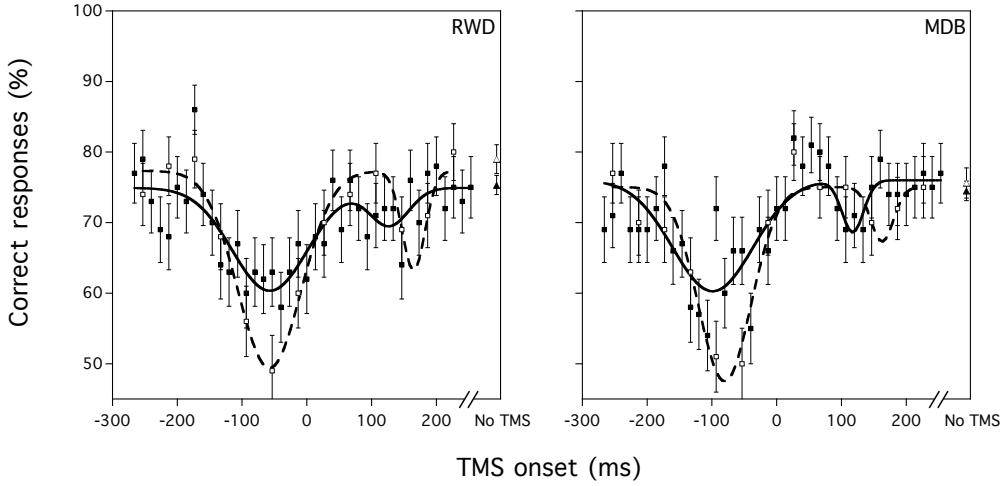

Figure 3.11. The percentage of correct responses for two participants for high contrast (0.99 Weber contrast — filled symbols and solid line) and low contrast (0.03 Weber contrast — open symbols and broken line) global motion stimuli, fitted with Equation 3.2. Performance is disrupted in TMS trials (squares) compared to no TMS trials (triangles) during an *early* (pre-global motion) and a *late* (post-global motion) temporal window. The peak performance deficit during the *early* temporal window is larger for lower contrast stimuli. The performance deficit during the later temporal window is of similar magnitude for both stimulus contrasts, although the peak effect may be temporally shifted towards greater SOAs for the low contrast stimuli. Error bars represent the SE of the percentage.

3.6 Discussion

The results of Experiment 2 clearly reveal two critical epochs during which delivery of a single TMS pulse to area V5/MT disrupts global motion discrimination: an *early* period which is centred, on average, approximately 64 ms prior to the onset of global motion, and a relatively *late* period which occurs approximately 146 ms after the onset of global motion. These two temporal disruption periods are separated by an interval during which delivery of TMS has little or no effect on performance. The earlier period is broader in its temporal extent and single pulse TMS, delivered at or around this time, produces a deficit of approximately twice the magnitude of that which occurs after motion onset. These disruption windows persist at different stimulus contrast levels (Experiment 4).

Several other studies have reported reduced performance on motion-based tasks when TMS is delivered to area V5/MT, but only during either exclusively *early* (Beckers & Homberg, 1992; Beckers & Zeki, 1995) or *late* (Hotson et al., 1994; Anand et al., 1998; Hotson & Anand, 1999) temporal windows. This is primarily because the range of times at which TMS was delivered simply did not extend to both of the critical periods found in the present study, and/or the sampling of the temporal disruption profile was too coarse to reveal the performance drop. Nonetheless as mentioned previously, other studies worthy of note have also reported two critical periods during which delivery of a TMS pulse over area V5/MT impairs the ability to

discriminate the direction of translational global motion (Sack et al., 2006; Laycock et al., 2007). However there are marked differences in both methodology and interpretation between these studies and the present experiments and these are considered below.

Sack and colleagues reported significantly impaired performance when TMS was delivered between 30 to 40 ms prior to, and also 130 to 150 ms following, global motion onset. The timescale of the post-motion onset disruption window is very similar to the current findings, both in terms of when it occurs and the temporal extent of the effect. The authors attributed the later deficit to the direct disruptive action of TMS on the cortical processes mediating integration of motion signals in V5/MT. Sack et al., and others (Corthout et al., 2000; Corthout et al., 2003), have suggested that the *early* performance deficit was most likely the result of a TMS-induced blink artefact, rather than the functional disruption of cortical processing. This was based on the fact that TMS is known to cause motor neurons to depolarise and can produce facial twitching that could potentially include ocular muscles. Although Sack et al. attribute the *early* TMS induced deficit to non-neuronal factors, they state that it was specific to stimulation of V5/MT. At first glance, blink duration (typically around 200 to 300 ms) and the active suppression of visual information associated with eye-blinks (approximately 200 ms) both appear consistent with the temporal extent of the *early* period of TMS disruption (Ridder & Tomlinson, 1993; VanderWerf, Brassinga, Retis, Aramideh & Ongerboer de Visser, 2003). However, Experiment 3 in the current study showed that this initial period of visual disruption is absent for stimulation at a

control site, even though this elicited considerable facial twitching in the participants. More importantly, when the contrast level of the global motion stimulus was reduced in Experiment 4, the peak performance deficit during the *early* temporal window was considerably larger. If the *early* disruption were simply the result of TMS-induced eye-blinks, changing a stimulus characteristic (such as contrast) should not produce a more severe disruption in performance. Sack et al. also reported deficits of similar magnitude when TMS was delivered before and after motion onset (Figure 3.8). In contrast, the results presented here indicate that the *early* performance deficit is always greater in magnitude than the *late* deficit.

Laycock et al. (2007) found significantly reduced accuracy on a global direction discrimination task when TMS was delivered to area V5/MT at time delays between -42 and +10 ms, in addition to +158 ms, relative to motion onset. However, several aspects of their study make interpretation of the results problematic. The authors report the results of two separate experiments. In the first, the duration of the global motion stimulus was set at a level designed to produce thresholds of 80 % correct performance, yet their data clearly show that this threshold level was unstable, with the vast majority of participants performing considerably better than this on the task. As they neglected to measure baseline thresholds (i.e. trials without TMS) during the experiment, it is difficult to separate shifts in participants' baseline performance from TMS induced deficits, unless the latter were very large. To highlight this point, the disruption they reported in their first experiment, occurring after stimulus onset, was not replicated in their second experiment

despite TMS delivery to the same cortical site (area V5/MT) at the same point in time. They did however report a large performance deficit when TMS was delivered to V5/MT before and just after motion onset. Unfortunately, the authors did not specify how the measure of stimulus onset asynchrony was determined with respect to their double-pulse technique. In the present study a single TMS pulse technique was used, in combination with small temporal sampling intervals, so that any motion deficit resulting from TMS to V5/MT could be precisely quantified. Although the results of Experiment 2 are broadly similar to those of Laycock et al., the relatively large and uneven sampling interval they used, coupled with a double-pulse TMS delivery method with unspecified timing, make direct comparison difficult.

Laycock et al. proposed two alternative accounts for the *early* disruption window they find, neither of which is based on eye-blink artefacts. First, they suggest that TMS may disrupt the rapid propagation of motion signals, via a direct pathway from the lateral geniculate nucleus (LGN) to V5/MT, which bypasses primary visual cortex (V1). In support, primate studies have provided anatomical and physiological evidence of significant projections from sub-cortical structures such as the LGN and pulvinar directly to V5/MT (Girard et al., 1992; Sincich et al., 2004). However, activation of a fast pathway to area V5/MT in humans is thought to be speed-dependent, only occurring when stimulus speed is greater than 22 deg/s (ffytche, Guy & Zeki, 1995), which was not the case of the motion stimuli in Laycock et al.'s study, which had a velocity of 1.75 deg. Disruption of this fast motion pathway, if it exists in humans, would be consistent with reduced performance just after motion

onset. The assumption of a subcortical pathway to extrastriate regions in human cortex, however, remains controversial. Anderson, Holliday, Singh & Harding (1996) used MEG to measure human cortical responses to drifting grating stimuli, for a range of spatial (0.25 c/deg to 8.0 c/deg) and temporal (0 Hz to 45 Hz) frequencies. Anderson et al. (1996) reported that the evoked magnetic response to motion from area V1 always preceded that from area V5/MT by ~ 20 ms, and there was no evidence for early human V5/MT responses that might reflect rapid geniculo-prestriate input. Nevertheless, the presence of a pathway that bypasses area V1 is a popular explanation for the sparing of motion detection in the phenomenon of 'blindsight'. Blindsight occurs when people who are perceptually blind in certain areas of their visual field demonstrate the ability to detect, localise or discriminate visual stimuli presented in their field defect. Holliday, Anderson & Harding (1997) used MEG to measure the magnetic responses to stationary and moving (32 deg/s) grating stimuli in observer GY, a well-documented hemianope who lacks the left V1. The authors reported that there was no magnetic response to stationary stimuli presented in the blind contralateral visual field, but a large response peaking at ~ 180 ms to stimuli presented in the ipsilateral visual field. Interestingly, for moving stimuli, there was a response when stimuli were presented in the blind (peaking at 245 ms) in addition to the sighted (peaking at 191 ms and 262 ms) hemifields. The peaks at 245 ms and 262 ms originated in area V5/MT, but the cortical sources for the first peak of the dipole (191 ms) could not be determined. The first peak was likely to have been generated in area V1 as it was in general agreement with the latency of GY's V1 response for stationary stimuli (~ 180 ms), and the temporal separation of the dipole

peaks was similar to that observed for V1 and V5/MT responses in normal observers; approximately 50 ms to 70 ms (Anderson et al, 1996). Holliday et al. (1997) conclude that this study provides evidence for a subcortical input to area V5/MT that subserves residual visual sensitivity to motion in the blind hemifield, although it must be noted that the response in area V5/MT occurs after – not before – that likely to be generated in area V1. A more recent study investigated psychophysical motion detection and direction discrimination for GY and two other patients with blindsight. Azzopardi & Cowey (2001) found that GY and another observer were more sensitive and better able to discriminate moving bars drifting at 32 deg/s and 20 deg/s as opposed to 4 deg/s, although they were unable to discriminate the direction of RDKs and gratings of any speed. Azzapardi & Cowey suggest that this implies that motion processing is severely compromised following damage to area V1, and that this is inconsistent with a theoretical subcortical pathway that fully supports motion perception. To summarise, in normal observers there is evidence that a fast subcortical pathway is activated at speeds above 22 deg/s (ffytche et al., 1995), although this result could not be replicated (Anderson et al., 1996), and observers with damage to area V1 demonstrate some ability to detect some stimuli at speeds greater than 20 deg/s (Holliday et al., 1997; Azzopardi & Cowey, 2001) although perception of many types of motion stimuli (e.g. RDKs) is completely absent (Azzopardi & Cowey, 2001). This therefore implies that the suggested fast pathway provides a largely incomplete representation of motion, and is only activated at speeds of greater than 20 deg/s, if at all. It is therefore unlikely to be the cause of the *early* disruption window observed in Laycock's and in the present study (Experiments 2 and 4).

Laycock et al. also proposed that earlier performance deficits, found prior to motion onset (-42 ms in their case), were unlikely to be associated with motion processing *per se*, but instead may reflect a disruption of attention or expectation. Although disruption of cognitive processes such as attention may lead to some deterioration in performance, it is not clear why this effect would necessarily be restricted to the earliest SOAs tested (prior to motion onset). Indeed a general, TMS-induced, cognitive impairment could not easily explain why performance in the current study returns to baseline levels even when TMS is applied at certain SOAs. Laycock and colleagues also differ from Sack et al. (2006) in their interpretation of the *late* disruption window, found after motion onset. Rather than reflecting the direct influence of TMS on ongoing neural activity at the level of V5/MT, they speculate that this deficit is associated with the disruption of feedback signals from higher cortical regions (e.g. top-down processing from parietal cortex and frontal eye fields) to V5/MT.

Here, a parsimonious and physiologically plausible scheme of how TMS influences direction perception is presented, at different time intervals relative to global motion onset, based upon a simple feedforward-feedback model. The main features of this explanation are outlined schematically in Figure 3.12 and proceed as follows. Following a period of global motion (80 ms, in this study) the first cortical stage of visual analysis takes place in primary visual cortex, or V1 (Hubel & Wiesel, 1968). In order to encode the global direction of motion, V5/MT neurons need to integrate local motion information over successive

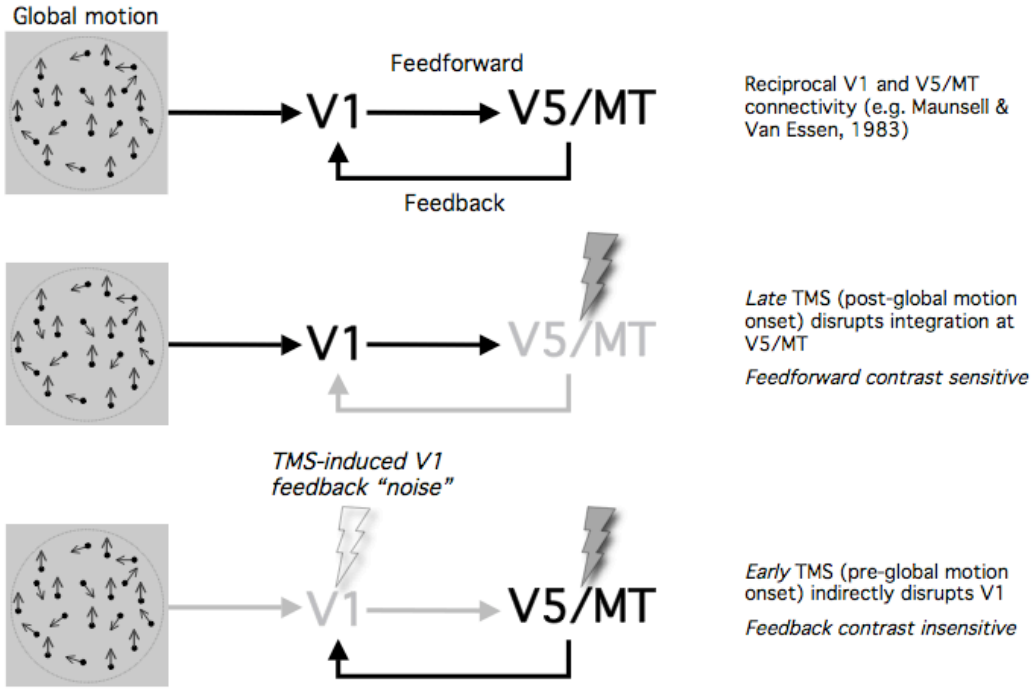

Figure 3.12. An outline of how TMS could disrupt global motion perception within a simple feedforward/feedback framework. During presentation of a coherent motion sequence V1 neurons are activated and then the activation propagates through the visual cortical hierarchy, arriving at area V5/MT sometime later. Disruption of global motion processing in area V5/MT (*late* temporal window) occurs when the presence of TMS-induced neural "noise" coincides with the arrival of task-related activity at area V5/MT, and motion perception is consequently disrupted. Disruption of processing in area V1 (*early* temporal window) occurs when TMS-induced neural activity is transmitted from area V5/MT back to area V1, via recurrent feedback connections. The arrival of indirect V1 feedback "noise" disrupts the local motion signals being processed at the level of V1.

frames, thereby collating information over the entire extent of the coherent sequence (80 ms). Taking these estimates into account and considering a purely feedforward model of information transfer, TMS to V5/MT should disrupt motion signals sometime after the onset of the motion sequence. The precise time at which this disruption will occur will depend on the response latencies of neurons at each of the pre-cortical and cortical visual areas involved. Single cell studies in primates show that estimates of the response latencies of visual neurons vary widely from study to study (for reviews see Bullier, 2001; Bullier 2003) but typically fall within the range approximately 25 to 120 ms for V1 and approximately 45 to 130 ms for V5/MT. Furthermore as the temporal responses of visual neurons can also be influenced by external factors (e.g. stimulus contrast), providing a definitive estimate of the response latency of the different visual areas in humans is not straightforward. Nonetheless it is likely that the *late* period of TMS disruption reflects the impairment to ongoing motion processing at the level of V5/MT.

To explain the *early* deficit in global motion perception a novel, but somewhat speculative, feedback-based approach is proposed. It is well known that the effects of TMS rapidly spread to functionally connected cortical areas via transynaptic connections, as has been demonstrated in several studies using TMS in combination with fMRI (Bohning et al., 1999), PET (Paus et al., 1997) and EEG (Ilmoniemi et al., 1997). For example, a combined TMS/EEG study reported a contralateral response in right occipital cortex 20 ms after a magnetic pulse was delivered to left occipital cortex (Ilmoniemi et al., 1997). As feedback connections are known to exist between areas V5/MT and V1 in

equal numbers (Maunsell & Van Essen, 1983; Shipp & Zeki, 1989), and feedforward and feedback fibres show similar conduction velocities (Nowak, James & Bullier, 1997), one prediction is that the effects of a TMS pulse delivered to area V5/MT will propagate back to area V1 via feedback connections, arriving sometime later.

Importantly, a feedback based explanation of the *early* disruption period (TMS applied prior to global motion) also predicts that the peak of the initial disruption window will be less sensitive to contrast-mediated changes in neural response latency, since unlike the feedforward connections, the propagation of TMS disruption back to V1 will be unaffected by changes in the stimulus characteristics. The results presented in Figure 3.11 appear to support this with only one participant exhibiting a very small shift in the peak deficit before global motion onset, but both participants showing a more pronounced shift for the later deficit found with lower contrast stimuli.

Another notable aspect of the data is the fact that the deficit when TMS is delivered to V5/MT prior to motion onset is greater in magnitude and occurs over a broader range of stimulus onset asynchronies. This is likely to reflect the fact that TMS delivered much later than stimulus onset provides sufficient time for cortical network dynamics to recover and re-stabilise. Additionally, TMS delivered after V5/MT has integrated local motion signals is unlikely to have any effect at all on motion perception as the relevant information will have been transmitted to the next stage of visual analysis. Beckers and Homberg (1992) noted that the window for disruption is broader when TMS is

delivered to V1 as compared with disruption of V5/MT. They conclude that this results from the fact that TMS to V1 disrupts not only local motion signals at V1 but also the arrival of the feedback signals from area V5/MT. Here a similar effect is shown, but critically one that arises without any change in the site of disruptive cortical stimulation.

The feedforward/feedback theory presented in Figure 3.12 is currently qualitative in nature and there is a need for future research to elaborate this idea further. Specifically, there are presently no quantitative computational models that can adequately account for the effects of TMS on human global motion perception. To develop such a model is one of the principle aims of the next chapter (Chapter 4), in addition to investigating the effects of TMS on the perception of more complex types of global motion than have been discussed in the present chapter.

Chapter 4: An investigation into the temporal properties of optic flow global motion processing

4.1 Introduction

Optic flow global motion

In the last Chapter (Experiments 1 to 4), the temporal properties of translational global motion processing were investigated. Although the stimuli in those experiments comprised coherently-moving "signal" dots presented within random dynamic "noise" – and therefore contained many local motion directions – the coherently-moving dots were displaced in the same direction regardless of their location. This type of global motion is regarded as the most simple component of optic flow fields. When moving through the environment, the corresponding deformation of the visual array can be broadly classified into radial motion (expansion and contraction), rotational motion (clockwise and anticlockwise), translation, and combinations of these (spiral motion and other deformations). Unlike translational motion, for rotational and radial motion, coherently-moving elements move in opposing directions in opposite areas of the visual field.

Medial superior temporal area

In order to integrate such spatially separated cues, large receptive fields would be of great benefit. Raiguel, Van Hulle, Xiao, Marcar, Lagae & Orban (1997) reported the mean area of a receptive field of a macaque MT neuron to be ~ 31 deg^2, whereas receptive fields of cells in the neighbouring medial superior temporal area (MST) were ~ 35 times larger than this. Indeed, receptive fields of MST cells can often cover a whole quadrant or more of visual space (Tanaka, Hikosaka, Saito, Yukie, Fukada & Iwai, 1986). MST is often referred to as a "satellite" of area V5/MT or as part of the V5/MT complex (V5/MT+) (Morrone et al., 2000). Single cell studies using monkeys have confirmed that MST has neurons that respond selectively to complex global motion representations, such as radial (expanding/contracting) and rotational (anticlockwise/clockwise) components of optic flow fields (Tanaka et al., 1989; Duffy & Wurtz, 1991a; Duffy & Wurtz, 1991b). This suggests that hierarchical processing, which is typical of information exchange between V1 and V5/MT is also evident between V5/MT and MST, since MST receives input from V5/MT neurons (Maunsell & Van Essen, 1983).

Functional magnetic resonance imaging (fMRI) has revealed in humans an area within V5/MT+ that responds to translational global motion, and this neural activity is separate and distinct from that arising from a more anterior area within V5/MT+ that responds to radial and rotational global motion (Morrone et al., 2000). Similarly, an anterior region in human V5/MT+, presumed MST, was reported to be most strongly driven by complex motions

which contained multiple components of optic flow patterns, such as spiral motion, whereas V5/MT was activated equally by all RDKs, including translational motion (Smith et al., 2006). Another fMRI study employing an adaptation paradigm found that, in human MST, separate neural populations are sensitive to rotational and radial motion (Wall et al., 2008). These authors also found, however, that V5/MT as well as V3a responded specifically to optic flow components, but to a lesser extent than area MST. Wall et al. speculate that V5/MT and V3a may acquire sensitivity to optic flow components as a result of modulatory feedback from MST. In support of this, a recent imaging study using electroencephalography (EEG) reported significantly stronger "later" responses elicited by V5/MT complexes for rotational motion than for translational motion, consistent with a hierarchical model of analysis for increasingly complex global motion features (Delon-Martin et al., 2006).

In light of this, it may be hypothesised that the critical period(s) for TMS disruption of optic flow global motion may occur at a later SOA than for simple translational motion. Furthermore, it is presently unknown if TMS disruption profiles for optic flow patterns also shown *two* distinct epochs similar to global translational motion (see Chapter 3).

Aims

The principle aim of the experiments described in this chapter was to determine the critical periods for disruption of complex (rotational and radial) global motion processing in area V5/MT by applying single-pulse TMS. A secondary aim of this chapter was to develop a quantitative, computational model that can account for the effects of single pulse TMS on global motion processing.

4.2 Experiment 5: A psychophysical investigation of the summation period for optic flow global motion processing

4.2.1 Introduction

It was previously found that the summation period for random-dot moving stimuli was in the order of approximately 100 to 200 ms when contrast sensitivity for direction discrimination was measured as a function of exposure duration (Fredericksen, Verstraten & van de Grind, 1994; Burr & Santoro, 2001). When coherence threshold for direction discrimination was measured as a function of RDK duration, however, thresholds for direction discrimination continue to improve over a longer period, for example, approximately 250 ms (see Experiment 1). This finding is corroborated by a study that measured direction discrimination as a function of the directional bandwidth of local motions for a range of stimulus durations (Watamaniuk et al., 1989). The dot directions for the stimuli in Watamaniuk et al.'s study were drawn from a

Gaussian probability distribution and thus dots underwent a 'random walk' in direction. The authors reported that temporal integration occurred for 500 ms or more.

Watamaniuk and colleagues (1989) suggest that the longer integration periods observed when a task requires local motion signals to be pooled, are indicative of the summating properties of higher cortical areas. This theory was corroborated by the findings that the temporal summation periods for translational and biological motion were approximately 700 ms and 2000 ms respectively (Neri, Morrone & Burr, 1998), as while both motion types activate area V5/MT, biological motion is also processed in higher cortical regions, such as the superior temporal sulcus.

Temporal integration times measured specifically for optic flow global motion stimuli were first reported by Burr & Santoro (2001). These authors found that when the global motion signal was temporally embedded between random motion sequences, the temporal integration period (as indicated by asymptotic coherence thresholds) was similar for rotationally- radially- and translationally-moving RDKs. However, when the global motion stimuli were presented without the random motion sequences, coherence thresholds for translational global motion increased much more steeply, as duration decreased below approximately 1000 ms, than rotational or radial thresholds. The authors concluded that there are at least two different stages of motion analysis with different temporal properties: firstly an early local motion processing stage with a summation period of approximately 200 to 300 ms (which they

measured using contrast sensitivity), and then a subsequent global motion integration stage with a much longer summation period (up to approximately 3000 ms for rotational and radial global motion). As the latter integration period for translational global motion was only 1000 ms, the authors conclude that these different estimates are likely to reflect the functional architecture of the human visual system.

Aims

The experiment presented here (Experiment 5) sought to determine the summation period for two varieties of optic flow global motion. This was partly to ensure suitable stimulus duration was employed subsequently for use in conjunction with TMS (as in Experiments 1 to 4), but also to compare the temporal integration period to that for translational global motion.

4.2.2 Methods

4.2.2.1 Observers

LKS, who took part in Experiment 1, KP who took part in Experiments 1 and 2, and two participants (RWD and MDB) who took part in Experiments 1, 2, 3 and 4, participated in this experiment. All subjects except LKS were naïve as to the purpose of the study.

4.2.2.2 Visual stimuli

Rotational and radial global motion stimuli were identical to translationally-moving stimuli used in Experiments 1 to 4 except that the "signal" dots were constrained to move coherently along either a rotational (clockwise/ anticlockwise) or a radial (expanding/contracting) trajectory. Dot displacement magnitude was always constant across space (2.81 arcmins), that is, dot displacement was not larger nearer the edge of the presentation window, as it would have been for strictly rigid rotational or radial global motion. This ensured that the local dot speeds and jump sizes were identical, regardless of the type of global motion depicted, and allowed direct comparison of the three global motion types, in line with previous studies (Burr & Santoro, 2001; Simmers, Ledgeway, Mansouri, Hutchinson & Hess, 2006). When a dot reached the centre of the display (for radial motion) it was repositioned in a random spatial position within the presentation window in the following frame.

4.2.2.3 Psychophysical procedure

Global motion direction discrimination was measured using a two-alternative forced-choice task in conjunction with the method of constant stimuli, with threshold defined as the percentage of "signal" dots required to produce a correct response rate of 75 %. Performance was measured for global motion sequences comprising either 2, 3, 4, 5, 6, 8, 16 or 22 frames of global motion, flanked by random motion sequences, as described in Experiment 1 (Figure 3.2).

4.2.3 Results and discussion

The percentage of correct directional judgments was plotted as a function of global motion coherence (percentage of "signal" dots), and coherence thresholds were extracted using Equation 3.1. Coherence thresholds are presented for rotational and radial global motion in Figures 4.1 and 4.2 respectively, as a function of global motion duration. It can be seen that global motion thresholds increased steeply as the number of global motion frames decreased below approximately four frames (106 ms) for all participants. When the number of global motion frames exceeded approximately ten frames (266 ms), coherence thresholds were approximately asymptotic. This finding is similar to that of Experiment 1, indicating that the temporal summation period for complex global motion is similar to that for translational global motion, when temporally embedded within random motion sequences. Burr & Santoro (2001) also found temporal integration periods to be similar for translational, rotational and radial global motion when global motion sequences were flanked by random motion. These findings suggest that the random motion is compulsorily integrated with coherent motion over an extended period. As Burr & Santoro demonstrated that when no random motion sequences were present, the summation period for rotational and radial motion was much greater than for translational motion, this suggests that different mechanisms are used in the processing of these different types of motion. However, presenting random motion before and after each global motion type appears to

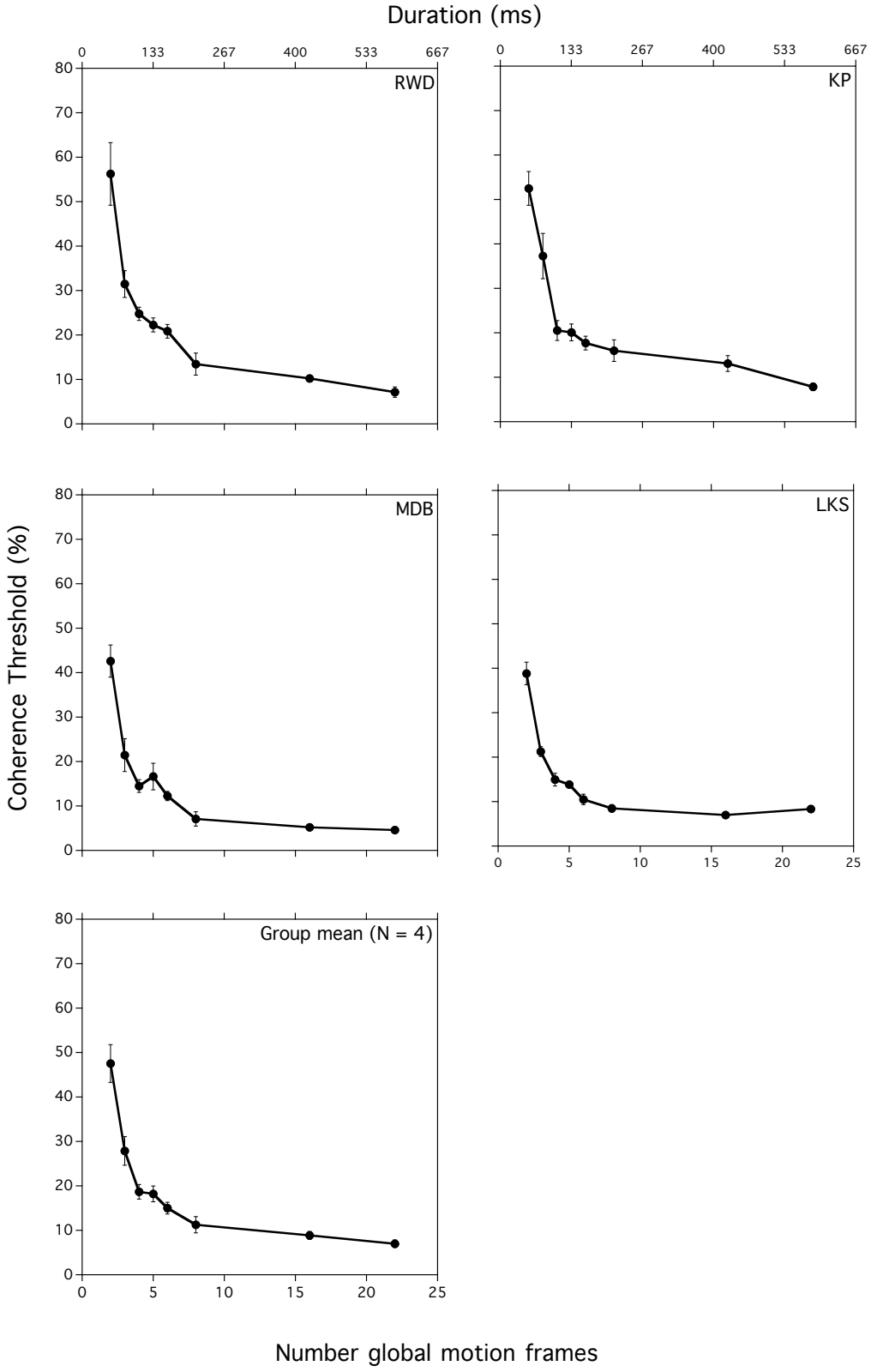

Figure 4.1. Coherence thresholds for rotational global motion, plotted as a function of the number of global motion frames and global motion duration (ms). Error bars represent the SE.

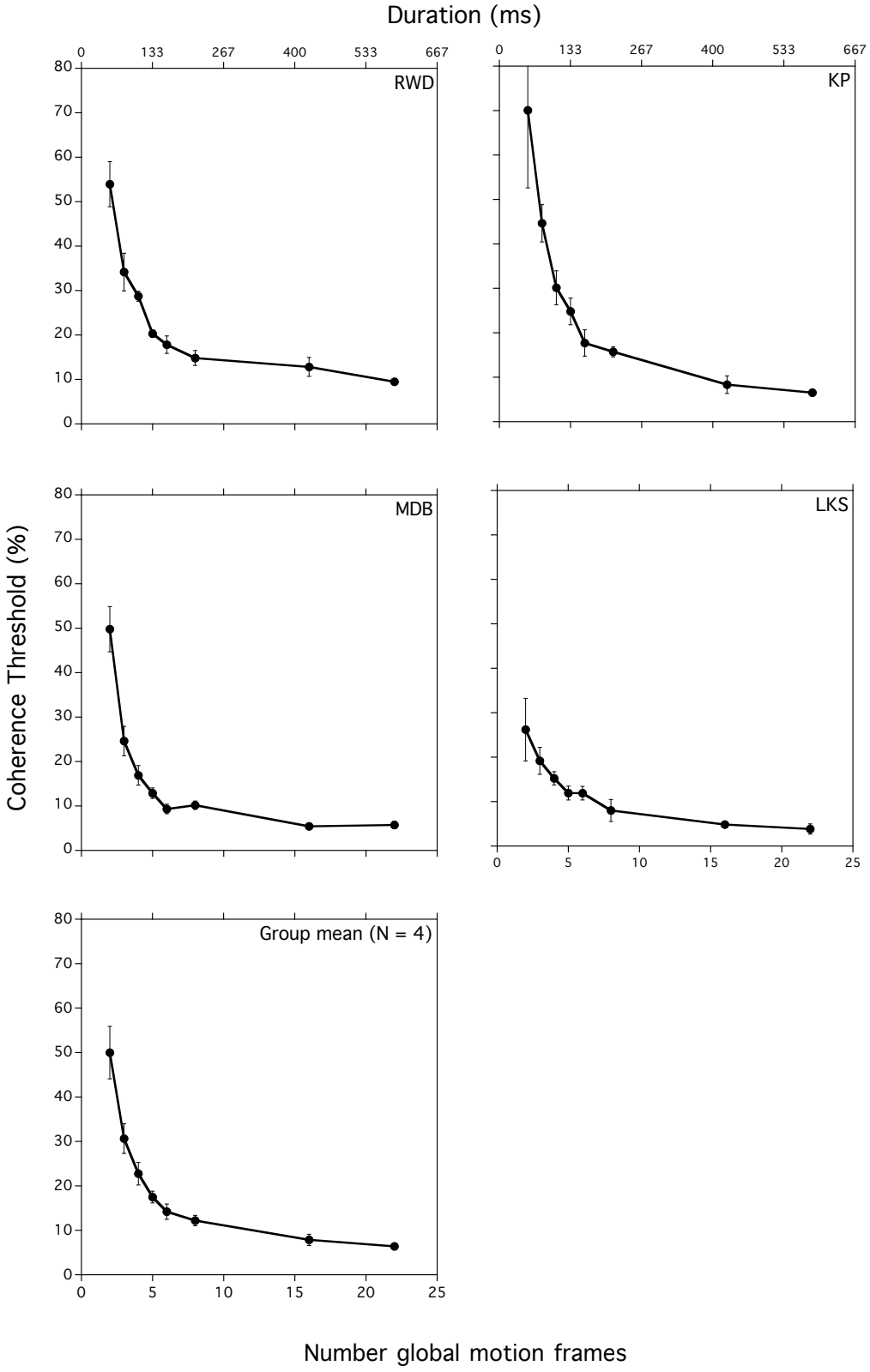

Figure 4.2. Same as Figure 4.1 except that the RDK depicted radial global motion. Error bars represent the SE.

be an effective method for calibrating the integration periods across the different types of global motion. As outlined in Experiments 2 to 4, the optimal number of global motion frames to be used in conjunction with TMS should ideally fall on the rising part of the curve to ensure that potential ceiling effects are avoided and baseline global motion thresholds are sensitive to disruption. Consequently, a three-frame global motion sequence (80 ms) was employed in Experiment 6, preceded and followed by a ten-frame global motion sequence (total stimulus duration = 613.3 ms), as in Experiments 2 to 4. This also allowed for meaningful comparisons in the temporal disruption profile to be made between translational and complex global motion types.

4.3 Experiment 6: The effects of TMS over area V5/MT on optic flow global motion processing

4.3.1 Introduction

This experiment sought to determine whether the TMS temporal disruption profile was similar for complex components of global motion to simple translational global motion. As no studies to date have been published on the affect of TMS on optic flow global motion processing, a number of different hypotheses can be postulated. Firstly, it may be predicted that a *late* disruption window (centred approximately 150 ms after onset of translational global motion) may also be present – and indeed, be broader – for complex global motion types. As optic flow motion signals are subject to additional "higher"

processing after the level of V5/MT – in MST – it seems plausible that TMS over the V5/MT complex* might disrupt the signal either at the V5/MT or MST processing level, creating a wider temporal window in which to disrupt processing. Adopting the assumptions of the preliminary feedforward/ feedback model framework for single-pulse TMS disruption to global motion processing, described in the Discussion section of Chapter 3, it is likely that an *early* temporal window of disruption would also be present as was observed with translational global motion, since the propagation of the effects of TMS back down to area V1 will not be affected by changes in the visual stimulus.

Similarly, it may be speculated that TMS would cause a greater magnitude of disruption for optic flow stimuli (that is, a more pronounced decrease in correct directional judgments) during the *late* temporal window, as ongoing reciprocal processing between V5/MT and MST (as proposed by Wall et al., 2008) may be abolished. For example, TMS may disrupt processing at V5/MT in the feedforward sweep of visual processing, and the effects may linger and disrupt feedback signals from MST.

Finally, it is possible that there will be no difference between the temporal disruption profiles for translational and optic flow global motion, as all global motion stimuli with the same properties (such as speed, contrast and flanking

* As detailed in Chapter 2, section 2.2.2, the spatial resolution of the effects of a single TMS pulse is in the order of ~ 20 mm (e.g. Jalinous, 1995; Hovey et al., 2003). It is therefore not sufficient to selectively disrupt areas V5/MT and MST in humans.

random motion sequences) will be processed in the V5/MT complex after a similar delay for a similar duration.

4.3.2 Methods

4.3.2.1 Observers

Three observers took part in this experiment, all of who also took part in Experiment 5 (RWD, KP and MDB).

4.3.2.2 Visual stimuli

Visual stimuli used in conjunction with TMS comprised RDKs made up of a three-frame global motion sequence (80 ms) presented at each observer's coherence threshold to support 75 % correct response rate (see Table 4.1). This was preceded and followed by 10 random motion frames (266.65 ms) giving an overall stimulus duration of 613.3 ms (as in Experiments 2, 3 and 4). All other visual stimulus parameters were as described in Experiment 5.

4.3.2.3 TMS coil localisation and procedure

The coil position and orientation for area V5/MT stimulation was localised using the same methods as described in Experiment 2. Single pulses were delivered at a rate of one pulse per RDK stimulus presentation, with a 2.5 s inter-trial-interval between participants' response and the onset of the next

RDK stimulus. TMS was delivered at 40 different SOAs (from -266 to +253 ms relative to the onset of the global motion sequence), as in Experiment 2 (see Figure 3.6), with 100 repetitions per SOA. Sessions were run in blocks of 50 RDK stimuli presentations; 40 with TMS, interleaved with 10 without TMS as a control measure. Each block of 50 trials lasted approximately 4 minutes. Participants completed 100 blocks in total for each motion type (rotational and radial), with a maximum of four blocks in one day.

4.2.3 Results and discussion

Direction discrimination data for rotational and radial global motion are shown in Figures 4.3 and 4.4 respectively. The broader *early* (pre-global motion onset) temporal window and the narrower *late* (post-global motion offset) temporal windows of disruption present for translational global motion discrimination are also evident for rotational and radial global motion for all participants. Data were fitted with Equation 3.2, as for translational global motion.

Observer	Rotational motion coherence threshold (%)	Radial motion coherence threshold (%)
MDB	21	24
KP	37	45
RWD	31	34

Table 4.1. Coherence threshold (percentage of "signal" dots to support 75 % correct response rate) for each participant.

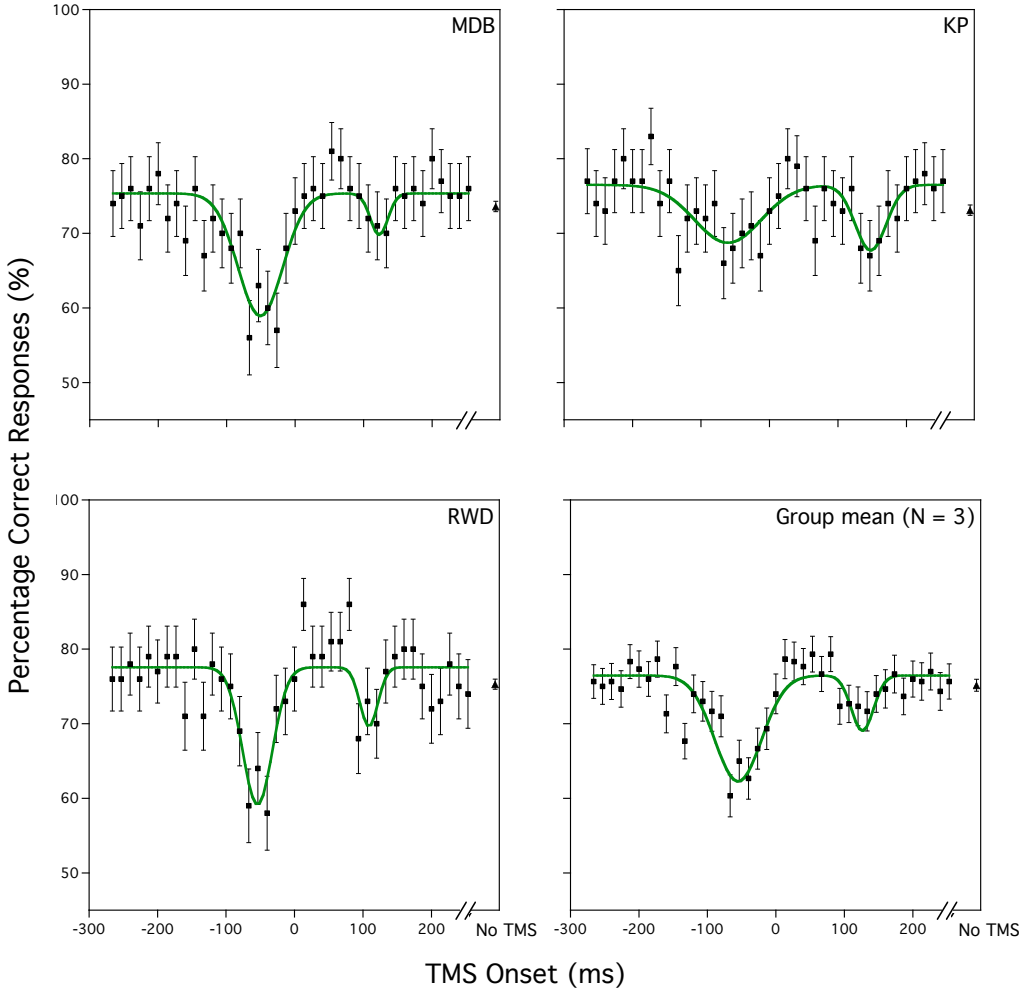

Figure 4.3. Percentage of correct responses for rotational global motion as a function of TMS onset asynchrony. The first three panels show individual data, the bottom right panel shows mean data (N = 3). 0 ms represents the onset of the global motion sequence. Performance during TMS trials (squares) is impaired compared to no TMS trials (triangles) during two temporal windows although there are individual differences in the onset and magnitude of the performance deficits. The solid lines show the best-fitting curves, derived from Equation 3.2, to the data. Error bars for individual data represent the SE of the %, error bars for group mean data represent the SEM.

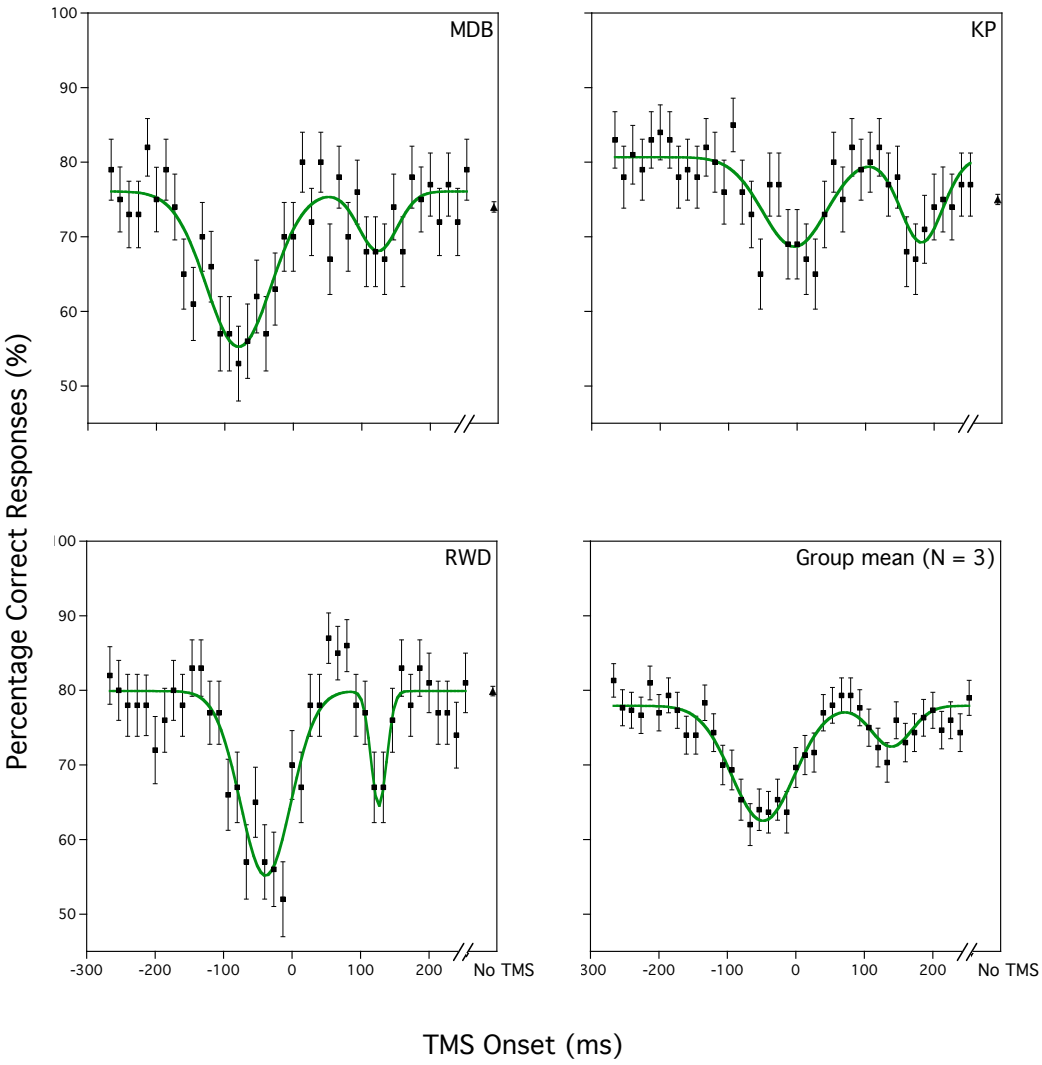

Figure 4.4. Same as Figure 4.3 except that the RDK depicted radial motion.

The combined group data (N = 3) suggest that the early disruption window may, if anything, be temporally narrower for rotational and radial global motion than for translational global motion, although any such differences are relatively modest. The peak disruption latencies derived from Equation 3.2 occur at -40.7 ms (SEM = 21.9 ms) and +144 ms (SEM = 18.9 ms) for radial global motion and -55.1 ms (SEM = 2.9 ms) and +126.4 ms (SEM 11.4 ms) for rotational global motion (relative to global motion onset), with performance returning to 75 % correct responding at approximately +50 ms relative to global motion onset. These critical temporal windows are consistent with those presented in Experiment 2, where the mean peak disruption latencies occurred at -63.8 ms (SEM = 18.4 ms) and +145.6 ms (SEM = 9.8). The similarity of the temporal disruption profiles indicates that all global motion types activate the V5/MT complex after a similar delay. As the peak performance deficit to direction discrimination during the *late* window was similar for all three types of motion, it is unlikely that the TMS pulse differentially disrupted a feedback loop between MST and V5/MT specific for optic flow global motion.

4.4 Discussion

It was found in Experiment 5 that the summation period for complex global motion processing is similar to that of simple translational global motion processing. This is in agreement with the result found by Burr & Santoro (2001), when global motion stimuli were also preceded and followed by random motion sequences. The results of Experiment 6 reveal that the critical

periods of disruption for rotational and radial TMS global motion processing were also similar to that of simple translational global motion processing. Although complex global motion has been shown to occur in a separate and distinct area (MST) to that which processes translational global motion, it is likely that the spatial resolution of TMS is not fine enough to stimulate each of these areas individually in the human visual system. This may primarily be because the size of area V5/MT+ complex is within the effective range of the magnetic field that causes depolarisation of underlying neurons. Huk and colleagues (2002) functionally subdivided human V5/MT+ into the component areas V5/MT and MST using retinotopic mapping, and it was found that the grey matter surface area of V5/MT was larger than that of MST in every (N = 5) participant (on average, 243 mm^2 and 83 mm^2, respectively). Additionally, since it is known that there are many reciprocal connections between areas V5/MT and MST, it is also highly likely that the TMS-induced activity spreads rapidly between these two areas.

Quantitative model

In the previous chapter (Chapter 3), a schematic qualitative model was presented detailing how the disruptive effects of TMS on global motion processing might be accounted for within a physiologically-plausible framework. The data in the current study (Experiment 6) and previous experiments (Experiments 2, 3 and 4) can be explained by a simple quantitative model that encapsulates the feedforward/feedback circuitry outlined in Figure 3.12.

As mentioned previously, it is likely that the *late* period of TMS disruption reflects the impairment to ongoing motion processing at the level of the V5/MT complex, and that the deleterious effect of a single TMS pulse is initially maximal and then gradually falls exponentially to zero over time (Walsh & Cowey, 2000). Consequently, the disruption in performance can be quantified by the following equation:

$$D_{late} = \begin{cases} \sum_{n=1}^{3} \exp\left\{ - \left[(x - a - b - 26.67n)/c \right]^2 \ln 2 \right\} d & x \le a + b + 80 \\ 0 & x > a + b + 80 \end{cases} \quad (4.1)$$

where x is TMS onset (in ms), a is the response latency (in ms) of V1 (i.e. the time at which visual evoked global motion activity first arrives at V1), b is the latency (in ms) of the feedforward connection between V1 and V5/MT, n is frame number (either 1, 2 or 3) containing coherent global motion, c is the half-life (persistence) of the TMS-induced V5/MT "noise" and d is a scaling factor.

As discussed in Chapter 3, it is well known that the effects of TMS spread to functionally connected areas via transynapic connections (Ilmoniemi et al., 1997; Paus et al., 1997; Bohning et al., 1999). Therefore, it is plausible that the effects of a TMS pulse delivered to area V5/MT will propagate back to area V1 some time later. This feedback connection may therefore underlie the *early* period of TMS disruption found in the present and previous chapter. If one reasonably assumes that it takes roughly the same time for information to

travel up the cortical hierarchy from V1 to V5/MT as it does for recurrent signals to return in the opposite direction, then the disruptive influence of TMS-induced feedback "noise" in V1 can be expressed as follows:

$$D_{early} = \begin{cases} \sum_{n=1}^{3} \exp\left\{ - \left[(x + b - a - 26.67n)/e \right]^2 \ln 2 \right\} f & x + b \le a + 80 \\ 0 & x + b > a + 80 \end{cases} \quad (4.2)$$

where x is TMS onset (in ms), a is the latency (in ms) of the feedforward connections between the retina and V1 (i.e. determines the time at which visual evoked global motion stimulation first arrives at V1), b is the latency (in ms) of the feedback connection between V5/MT and V1 (in this case identical to the feedforward latency), n is frame number (either 1, 2 or 3) containing coherent global motion, e is the half-life (persistence) of the TMS-induced V1 feedback "noise" and f is a scaling factor.

Consequently the total TMS-induced disruption for a given TMS onset is then found by combining Equations 4.1 and 4.2 to give:

$$D_{total} = D_{late} + D_{early} + P_{baseline} \quad (4.3)$$

where $P_{baseline}$ is the performance level obtained on the global motion direction task when TMS is absent (ideally approximately 75 % correct).

In this relatively straightforward feedforward/feedback model the degree of disruption produced by a single pulse of TMS is simply a function of the degree of temporal overlap between the presence of TMS-induced "noise" and global motion evoked activity within a particular visual area. Furthermore although few studies have addressed the issue of TMS persistence (embodied by parameters *c* and *e* in Equations 4.1 and 4.2), what little evidence there is suggests that the suppressive effects of a single pulse on visual evoked activity, albeit in feline cortex, can last for up to 200 ms (Moliadze et al., 2003).

Applying the model to the mean data obtained for the three different types of global motion (solid lines shown in Figure 4.5), illustrates clearly that it readily characterises the two periods of *early* and *late* TMS disruption consistently found in the present study [mean values of *a*, *b*, *c*, *d*, *e* and *f* are 30.1 ms (SEM = 4.9 ms), 74.6 ms (SEM = 0.9 ms), 79.4 ms (SEM = 24.1 ms), -3.0 ms (SEM = 0.2 ms), 3.9 ms (SEM = 1.5 ms) and -3.5 ms (SEM = 0.9 ms), respectively and the mean r^2 value of the fits = 0.79 (SEM = 0.03)]. The estimated values of *a* and *b* are comfortably within the range reported by physiological studies of visual latencies within monkey cortex (Bullier, 2001; Bullier, 2003) and similar to onset latencies in humans derived from EEG (Di Russo, Martinez, Sereno, Pitzalis & Hillyard, 2001) and MEG studies (Inui & Kakigi, 2006).

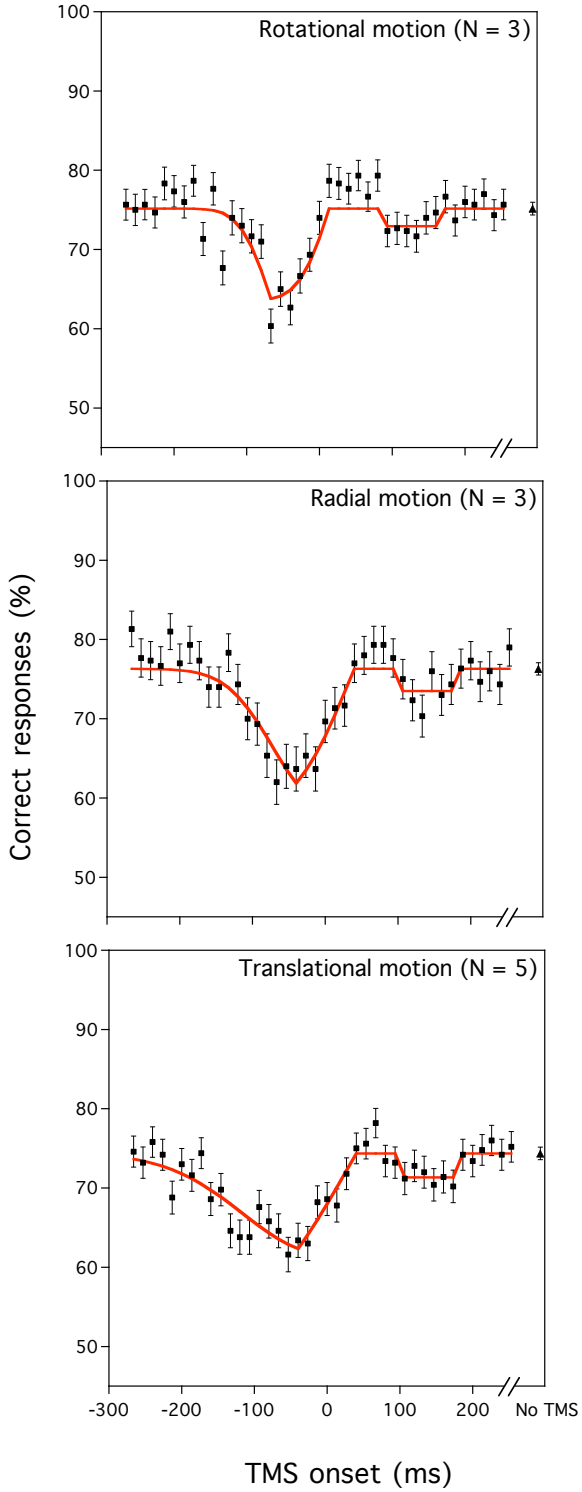

Figure 4.5. Group mean (N = 3) percentage correct responses for rotational (top panel) and radial (middle panel) global motion. For comparison, the group mean correct responses for translational global motion are re-plotted (bottom panel). Solid lines represent the best-fitting curves derived from applying a simple feedforward/ feedback model of TMS disruption to the data (see Equations 4.1, 4.2 and 4.3 and the text for further details). The disruption profiles for each type of global motion show very good agreement. Error bars represent the SE.

It can be concluded from the experiments reported in this chapter, that when the temporal integration periods for simple and complex global motion types are calibrated by temporally embedding the coherent motion sequence between random motion sequences, the time course of activation of area V5/MT is similar. As the magnitude of performance deficit is similar for all motion types, it is likely that the spatial resolution of the functional effects of TMS is too coarse to disrupt processing at individual subdivisions of the human V5/MT complex. Furthermore, the reciprocal connections between areas V5/MT and MST would, in all likelihood, allow TMS-induced activation to propagate through the whole of the V5/MT complex.

Chapter 5: Investigating the sensitivity of the visual cortex to magnetic field strength

5.1 Introduction

TMS delivered over occipital cortex suppresses detection of a visual target, but this effect not only depends on the position of the coil (e.g. Amassian et al., 1989; Kastner et al, 1998), timing of the delivery of the TMS pulse (e.g. Breitmeyer, Ro & Ogmen, 2004; Kammer et al., 2005b), and properties of the visual target (e.g. Masur et al., 1993) but also on the magnetic field strength (e.g. Masur et al., 1993; Kastner et al., 1998; Kammer et al., 2005).

Effect of TMS field strength on visual suppression

One of the earliest studies that delivered TMS over occipital cortex reported that letter identification was disrupted by TMS but there were individual differences regarding the magnitude of disruption (Masur et al., 1993). Masur and colleagues monocularly presented trigrams of three white letters on a dark background very briefly (height = 0.6 deg, Michelson contrast = 95 %, duration = 1 ms) to healthy participants (N = 20) and patients with optic neuritis. Single pulse TMS was delivered at 100 % maximum field strength (1.5 T) at 13 latencies ranging from 20 to 140 ms post-visual stimulus onset in increments of 10 ms. Ten healthy volunteers (50 %) demonstrated a "complete" suppression of visual perception, which was defined as when

correct response rate of letter identification was 0 % for at least one eye, when TMS was delivered between approximately 64 and 83 ms after visual stimulus onset. Six other healthy volunteers demonstrated a "partial" suppression (which was defined as when correct response rate was reduced compared to no-TMS practice trials) when TMS was delivered between approximately 77 ms to 106 ms after onset of the visual stimulus. Unfortunately, Masur et al., do not present individual data regarding the extent of suppression, so the precise differences in performance between the two groups are unknown. For four of the twenty healthy volunteers, however, there was no significant effect of TMS on the number of letters correctly reported at any SOA, where correct response rate remained at approximately 100 %. Two healthy participants who demonstrated "complete" suppression with 100 % field strength (1.5 T) TMS took part in a second experiment in which TMS field intensity was reduced. Reducing the field strength to 90 % (1.35 T) led to "incomplete" suppression of the visual targets (although the extent of this is not reported) and at 75 % maximum field strength (1.125 T) Masur et al. report no effect of TMS on correct response rate compared to no-TMS trials. These combined results indicate that there is potentially a wide range of sensitivity between individuals to the same magnetic field strength (in this case, 1.5 T), and disruption of visual identification appears to be dependent on magnetic field strength.

Several years later, Kastner et al. (1998) delivered single TMS pulses of varying intensity (70 – 100 % maximum field strength [0.98 T to 1.4 T], varied in 5 – 10 % steps) over occipital cortex, to investigate the spatial extent of TMS-induced disruption for detection of small bright dots (diameter = 0.3 deg,

5 cd/m^2, duration = 14.3 ms) on a dark background (0.05 cd/m^2). The locations in which the dots appeared were arranged in "rings" of 12 dots around a central fixation point at distances of 1, 3, 5, 7 or 9 deg from central fixation. If a participant incorrectly indicated they saw a target in one of the 15 catch trials present in every run of 75 trials, the whole run was discarded – this may have inadvertently led to participants being more cautious in their "yes I see it" responses, although the authors do not discuss this. Before the TMS sessions, all participants practised the task sufficiently so that they were performing at 100 % correct response rate. When TMS was delivered at 95 % to 100 % maximum field strength (1.33 T to 1.4 T) detection rate for targets 1 deg to 3 deg from fixation was reduced to less than approximately 50 %. At eccentricities of greater than 3 deg, target detection decreased to less than approximately 30 %, but this effect was mainly restricted to the lower visual field. Only eight out of seventeen participants, however, demonstrated a "reproducible interference" of target detection during TMS trials and were included in this analysis, while the rest of the participants showed little or no suppression. Five participants who did demonstrate a TMS-induced disruption to target detection took part in a second experiment where the TMS intensity was varied from 70 % to 100 % maximum field strength (0.98 T to 1.4 T). Detection rates were measured for targets located 1 deg from fixation in upper and lower visual fields (excluding the horizontal meridian) and 4 deg and 7 deg from fixation in the lower visual field. There was no effect of TMS on performance when TMS field strength less than 80 % maximum (1.12 T), but target detection rate decreased as magnetic field strength increased above 80 % for all participants. Four participants showed a similar pattern of results, where

lower field strengths (less than 80 %) disrupted detection primarily for targets 1 deg from fixation, and higher field strengths disrupted detection of targets presented in the periphery. For targets presented 1 deg from fixation, detection rate was approximately 75 %, 45 % and 25 % for TMS field strengths of 80 % (1.12 T), 90 % (1.26 T) and 100 % of maximum output (1.4 T), respectively. Detection rate was always lower for targets presented 1 deg below fixation than targets presented 1 deg above. Detection rate for targets presented 7 deg below fixation was almost unimpaired by TMS at 80 % maximum field strength, but was decreased to approximately 65 % and 30 % for field strengths of 90 % and 100 % respectively. One participant, however, showed the opposite pattern of results, whereby target detection was suppressed only in the periphery (7 deg) at 85 % field strength, and when field strength increased to 90 % and 100 %, performance was disrupted for targets presented 4 deg from fixation, and the central 1 deg, respectively. These results are similar to those of Masur et al., (1993) in that TMS appears to have little influence on visual perception for some participants, and for those who show TMS suppression, the results are very variable.

In the same series of experiments, Kastner et al. (1998) also investigated participants' phosphene perception. Fourteen out of the seventeen participants perceived phosphenes (compared to eight out of seventeen who demonstrated target suppression during TMS trials), most of whom perceived phosphenes when field strength was approximately 40 % to 60 % of maximum (approximately 0.56 T to 0.84 T) – a much lower field strength than that needed to suppress a visual target (1.12 T or higher). Unfortunately, the

authors do not report which of their participants perceived phosphenes or visual suppression, or whether there was any relationship between these two measures.

A third study that varied magnetic field strength was conducted by Kammer et al. (2005), who used TMS in conjunction with psychophysical methods to estimate the effect of TMS on threshold and slope of the psychometric function depicting percentage correct vs. stimulus contrast. In one experiment, a U-shaped hook target (0.43 deg, duration = 10 ms, luminance varied) was presented in the lower left or right visual field displaced by 0.3 deg or 0.5 deg relative to fixation, to correspond to the area of the visual field in which phosphenes could be elicited for each participant. Background luminance was either 0.3 or 3 cd/m^2. Participants (N = 4) discriminated the orientation of the hook in a single-interval four-alternative forced-choice paradigm, and an adaptive staircase procedure was used to measure contrast thresholds. TMS was delivered from 125 ms before to 205 ms after visual stimulus onset (in increments of 10 ms) or until there was no difference between TMS and baseline (no-TMS) thresholds. TMS was delivered at 80 % field strength (0.88 T) for 3 participants and 100 % (1.1 T) for 1 participant, although the authors do not give the reason for the variations in field strength used for participants. When TMS was delivered within a critical temporal window a pronounced bell-shaped elevation of contrast threshold was observed as a function of TMS latency. The maximum threshold elevation occurred when the TMS pulse was delivered between 101.9 ms and 87.9 ms after stimulus onset, for background luminances of 0.3 cd/m^2 and 3 cd/m^2, respectively.

Kammer et al.'s participants took part in a second experiment in which field strength as well as SOA was varied (background luminance = 3 cd/m^2). The range of TMS intensities used (between 60 – 100 % field strength; 0.66 – 1.1 T) were varied between each participant, but unfortunately the authors do not give any details on the criterion they used to select field strength. Each participant was tested with four (N = 3) or three (N = 1) different field strengths. They reported that contrast threshold increased as a function of TMS field strength for all participants. Compared to baseline (no-TMS) thresholds, the group mean contrast thresholds were elevated by a factor of approximately 1.5 for field strengths of 60 % to 70 % (0.66 T to 0.77 T), approximately 2.5 for field strengths of 70 % to 80% (0.77 T to 0.88 T), approximately 7.5 for field strengths of 80 % to 90% (0.88 T to 0.99 T) and approximately 20 for the highest field strength tested for each participant (85 % to 100%; 0.94 T to 1.11 T). There were, however considerable individual differences in the magnitude of threshold elevation between participants – two participants showed an elevation of contrast threshold by a factor of 28, one of whom was tested with a TMS field strength that was only 85 % of maximum (0.94 T). Another participant showed a maximum elevation of contrast threshold by a factor of 5 when TMS field strength was 100 % (1.11 T). This supports the idea that increasing field strength increases the influence of TMS on visual perception, but there are clearly individual differences in the extent to this.

In addition to increasing the contrast threshold at the most effective SOA, increasing TMS field strength also had the effect of producing elevated

contrast thresholds at shorter SOAs; a greater number of earlier SOAs elicited contrast threshold elevation as TMS field strength was increased. This led the authors to conclude that higher field strengths lead to a longer-lasting effect of TMS, since it can be presumed that there is a fixed critical time window for the interaction between a TMS pulse and visual processing. In one participant, however, contrast threshold elevations were not observed at earlier SOAs, even at high field strengths, as only moderate elevation was observed at the maximal SOA with the maximum field strength.

In their final experiment Kammer et al. (2005) measured the perimetry of visual suppression by measuring contrast threshold for small light spots (10 ms) presented at different locations, which the participant (N = 1) was required to detect. This was to determine whether the contrast threshold elevations induced at earlier SOAs by high field strengths were due to cortical processes or non-cortical side-effects of TMS. TMS pulses were delivered at SOAs of 95 ms (which previously produced a maximal contrast threshold elevation in the previous discrimination experiment) and 25 ms (which produced a smaller threshold elevation in the previous experiment, but only at the highest field strengths). It was found that after TMS was delivered at an SOA of 95 ms thresholds were elevated in the lower left quadrant of the visual field by up to 11.7 cd/m^2, whereas at an SOA of 25 ms a weaker threshold elevation of up to 1.74 cd/m^2 occurred in the same region of the visual field. The rest of the visual field was unaffected. Since the contrast elevation was retinotopic, the threshold elevation observed for earlier SOAs at high field strengths was assumed to be the result of a long-lasting suppression effect.

Physiological effect of TMS of the visual cortex

Moliadze et al. (2003) delivered single TMS pulses over anesthetised feline cortical area 17 (the feline analogue of human visual area V1). The distance between the surface of the coil and the cortex was 10 mm, and at this distance the maximum magnetic field strength was 1.25 T. Single pulse TMS increased the spontaneous and visually evoked firing (to a drifting bar) of simple and complex cells, which lasted up to ~ 500 ms after a pulse of ≥ 80 % maximum field strength (1 T). The duration and magnitude of increased firing rate were dependent on magnetic field strength. At high field strengths, this initial period of increased TMS-induced activation was replaced by a period of almost complete suppression (that is, spike rate was lower than spontaneous firing rate in the absence of TMS) lasting approximately 50 ms to 150 ms. This occurred within 200 ms post-TMS pulse for both spontaneous and visually evoked firing rate. A late and long-lasting period of suppression occurred after the initial period of increased firing rate. Hence, the onset of this second period of suppression occurred approximately 500 ms after the TMS pulse for ≥ 80% field strength and approximately 100 ms after the TMS pulse for ≤ 30% field strength. The duration of the late suppression period was approximately 2 s for both spontaneous and visually evoked firing rate. When a TMS pulse was delivered shortly before a visual response, approximately 200 ms to 50 ms prior to response for the preferred direction, or approximately 50 ms prior to response for the non-preferred direction, the resulting initial increase in firing rate was *more* than the sum of the firing rates when either TMS or a visual stimulus were presented alone. When TMS was delivered a longer time before

a visual response, between 700 and 1200 ms prior to response, there was a decrease in firing rate, compared to no-TMS trials. Late suppression was almost identical for TMS strengths between 30 and 70 %, but the duration and magnitude of the first visual response increased with field strength. Similarly, the duration and magnitude of the first period of suppression (up to 200 ms post-TMS pulse) increased with field strength.

Although magnetic field strength increases linearly with the percentage of maximum stimulator output for Magstim machines (Moliadze et al., 2003; private communication with Dan Phillips, product specialist, *The MagStim Company Ltd., Whitland, UK*), a study measuring human EEG responses to TMS found that evoked activity amplitudes do not increase linearly with field strength (Komssi, Kähkönen, & Ilmoniemi, 2004). When a large number of neurons depolarise simultaneously, post-synaptic potentials can be recorded through scalp EEG. Komssi et al. measured motor threshold, defined as the TMS intensity that evoked a motor-evoked potential of 50 μV on 50 % of trials for abductor digiti minimi muscle in the foot. TMS was delivered to the motor cortex at 60 %, 80 %, 100 % and 120 % of motor threshold for six participants, and a seventh participant was stimulated at lower multiples of their motor threshold as it was very high (capacitor voltage 1850 – 2000 V). Stimulation voltages ranged from 800 to 2040 V as motor thresholds ranged from 1400 to 2000 V. Unfortunately, the authors do not give details of the magnetic field strength used. After delivery of a TMS pulse, an overall brain response, known as a global mean field amplitude, was observed for all field intensities. The response was composed of four peaks, appearing at 15 ± 5 ms (Peak I), 44 ± 10

ms (II), 102 ± 18 ms (III), and 185 ± 13 ms (IV) after the TMS pulse. The overall TMS-evoked EEG response depended non-linearly on TMS field strength, and was most pronounced for peaks I and II. The amplitudes of peaks I and II were very large after TMS at higher stimulus intensities, whereas the amplitude-intensity dependence of peaks III and IV was more linear. The scalp distributions and the latencies of the response, however, were very similar for all TMS field strengths. This implies that a sequence of neural events is initiated after a TMS pulse that is independent of field strength. If this is the case, then TMS pulses delivered at a sub-threshold intensity may also activate the same cortical circuits as higher field strengths. One major difference between higher and lower field strengths, however, may be that the initial cortical volume in which neurons are effectively excited by TMS varies with field strength.

Properties of the magnetic field

The time-varying magnetic field produces an electric field inside and outside the axon (Nagarajan, 1993), and this creates a transmembrane potential (Rudiak & Marg, 1994). If the voltage change is large enough, an action potential is initiated. The effective magnetic field depth is estimated to be 10 mm to 20 mm diameter; the peak field strength is nearly constant within 10 mm (Jalinous, 1995) and depletes with the square distance from the stimulating coil (Hovey et al., 2003). It is currently unknown how the effective magnetic field depth – the volume of cortex in which neurons can be depolarised to a level where an action potential is initiated – varies with the

strength of the magnetic field. For example, the effective field depth may remain constant, but elicit action potentials in a greater number of neurons at field at higher field strengths than at lower field strengths.

Individual differences in sensitivity

Many studies have reported individual differences in sensitivity to TMS, for example, performance is typically disrupted for some, but not all participants (e.g. Masur et al., 1993; Sack et al., 2006). Previous studies deliver TMS pulses using a single TMS field strength for all participants (Beckers & Zeki, 1990), while others have calibrated TMS field strength the field strength required to produce a finger twitch or elicit a visual phosphene. Calibration to the excitability of a cortical region is thought to produce a constant neurophysiological effect of TMS in each individual (Deblieck, Thompson, Iacoboni & Wu, 2008). Individual differences in sensitivity to TMS may contribute to the difference in effects observed in studies that have applied the same magnetic field strength to all participants. Evidence suggests that cortical regions differ in excitability to TMS. For example, many studies have shown that phosphene and motor thresholds are uncorrelated (Stewart et al, 2001; Boroojerdi, Meister, Follys, Sparing, Cohen & Topper, 2002; Gerwig et al., 2003; Kammer et al., 2005; Antal, Arlt, Nitsche, Chadaide & Paulus, 2006). This is of concern as phosphene threshold is commonly thought to be a valid measure of visual cortex excitability, but current guidelines for safety of magnetic stimulation only exist in terms of motor threshold (Wassermann,

1998). In addition to this, phosphene thresholds are not normally measured using conventional psychophysical methods, but employ much less stringent methods that are prone to experimenter bias (e.g. Boroojerdi et al, 2002; Antal et al., 2006).

Aim

The aims of the following experiments in this chapter were to characterise the effect of TMS field strength on discrimination of visual stimuli, to measure phosphene threshold using psychophysical techniques, and to determine the relationship – if any – between phosphene threshold and individual differences in the suppressive influence of TMS on visual perception.

5.2 Experiment 7: Investigating phosphene threshold using the method of constant stimuli

5.2.1 Introduction

Phosphenes thresholds (often determined as the percentage of maximum stimulator output that elicits illusory flashes of light with 50 % of TMS pulses) have been used to calibrate TMS field intensity to individual sensitivity to TMS when stimulating the visual cortex (e.g. Harris et al., 2008). Phosphene thresholds are believed to be a good indicator of an individual's sensitivity to TMS, which is important in practising TMS procedures safely. Phosphene thresholds are assumed to provide an equivalent indication of excitability of

the visual cortex as motor evoked potentials (MEPs) do for the motor cortex. Safety guidelines for TMS parameters are given in terms of motor threshold (often defined as the minimum field strength needed to evoke an EMG response in 5 out of 10 trials), as the motor cortex is thought to be the most epileptogenic of brain areas. It is therefore widely assumed that the motor threshold provides a reasonable indication of susceptibility to seizure induction (Wassermann, 1998).

A recent investigation (Deblieck et al., 2008) found a weak correlation (of 0.53) between phosphene and motor thresholds, but only for active motor thresholds (when the participants squeezed a small cylinder with their hand) and when the participant was dark-adapted for > 45 mins, although there was no correlation between phosphene threshold and motor threshold when the hand was relaxed. The investigators claim to have used psychophysical procedures to measure both types of threshold. However, the method employed was to deliver pulses of suprathreshold strength for eliciting stable phosphenes, and then reducing the TMS intensity in 1 % increments of maximum output. Phosphene threshold was defined as the lowest stimulator intensity at which stable phosphenes were perceived in *at least* 5 out of 10 stimulations. This descending approach was selected to reduce the risk of participants having artificially high phosphene thresholds, but this can lead to systematic biases in performance. Their participants, however, were found to have much higher phosphene thresholds (59 % to 99 % maximum field strength; 1.18 T to 1.98 T) than in most other studies. Deblieck et al. (2008) reported that phosphene thresholds were measurable in 21 out of 27 participants, but six participants

never reported seeing a phosphene, even after a break, and the concept of a phosphene being re-explained to them.

Furthermore, Deblieck et al. (2008) claimed that phosphene and motor thresholds were measured under similar thresholding procedures. However, although the experimenters measured the difference between active and resting motor thresholds, they did not measure threshold for both visually active and resting states; all participants were dark-adapted for 45 minutes before phosphene thresholds were measured. This is potentially a major problem as recent studies have found that the effects of TMS are dependent on the baseline level of excitability or the adapted state of the cortex (e.g. Silvanto et al., 2007).

In the vast majority of studies, phosphene thresholds are not typically measured using controlled psychophysical techniques, instead authors usually employ more crude methods (see Table 5.1). For example, participants are asked to describe the qualities of their perception to the experimenter and "uncertain" responses are classified as absent phosphenes (Deblieck et al., 2008), where a simple "yes/no" paradigm would give rise to a more accurate threshold.

The current study sought to measure phosphene thresholds using a "yes/no" paradigm, in which the TMS field strength was varied in conjunction with the method of constant stimuli. Although "yes/no" paradigms are subject to variations in response criteria between and within participants, the subjective

Study	TMS delivery	Lighting conditions	Threshold measurement	Coil position	Stimulator
Stewart et al. (2001)	Single pulse	Blindfolded	From 60% max field strength, 5% increments or decrements	Handle oriented upwards	Magstim 200, monophasic
Kammer et al. (2001a)	Single pulse	Eyes open, fixating on a monitor screen (0.5 cd/m^2)	Method of constant stimuli, 10 levels interleaved randomly of 2% intervals	Area V2/V3, handle oriented horizontally, current direction reversed	Dantec MagPro, monophasic, and Magstim 200, monophasic
Boroojerdi et al. (2002)	Paired pulse	Blindfolded, dark room	From below phosphene threshold, in 1% increments	Handle oriented upwards	Magstim SuperRapid, biphasic
Gerwig et al. (2003)	Single pulse	Blindfolded, periodic light exposure	From below phosphene threshold, in 5% increments then 2% at random	Handle oriented horizontally	Dantec MagPro, biphasic
Kammer et al. (2005a)	Single pulse	Eyes open, fixating on a monitor screen (0.3 cd/m^2)	Method of constant stimuli, 10 levels interleaved randomly of 2% intervals	Handle oriented horizontally	Dantec MagPro, biphasic
Antal et al. (2006)	Paired pulse	Eyes closed, dark room	From 50% max field strength, increase in 5% steps until a stable phosphene is elicited, then decrease in 5% steps, until no phosphene, then increase in 2% steps until phosphene elicited	2-4cm superior to inion, handle oriented upwards	Dantec MagPro, biphasic
Deblieck et al. (2008)	Single pulse	Light-proof goggles	From above phosphene threshold, in 1% decrements	Handle oriented upwards	Magstim SuperRapid, biphasic

Table 5.1. Techniques for measurement of phosphene threshold used in previous studies.

nature of phosphene perception makes this impossible to avoid. As a measure of the stability of participants' responses, phosphene thresholds for two participants were re-measured at a later time (6 weeks after the initial measurement) to confirm the reliability of the internal criteria used to report the perception of phosphenes. Stewart and colleagues (2001) found that phosphene thresholds were stable within participants across different TMS sessions, but that there was more variability than when motor thresholds were measured in an analogous manner.

'Sham TMS' was not used for several reasons. The primary reason was that in order to randomly interleave control TMS pulses (over a different cortical location) into blocks of TMS trials, either the coil delivering the 'control' pulses would have to be placed somewhere other than the back of the head (as the coils are relatively large, at 14 cm diameter), or the coils would have to be moved in between trials. This would be very impractical, and disruptive to the participant, as the correct positioning of the coil is very time consuming. Variations on coil placement, such as holding the coil angled away from the scalp, positioning the edge of the coil perpendicular to the scalp, holding the coil a distance above the scalp or placing a block of wood between the coil and the scalp were all found to give an unrealistic stimulation in our pilot experiments and in previous studies, and participants are therefore aware of the difference between sham and real TMS trials. This, coupled with the increased localisation time and error, rendered it impractical.

5.2.2 Methods

5.2.2.1 Observers

Five observers took part in this experiment. All participants had taken part in previous TMS experiments and were familiar with the perception of phosphenes. Three observers (KP, RWD and PVM) took part in Experiments 2 and 6. Participants RWD and LKS also took part in a second session six weeks after the initial part of this study.

5.2.2.2 Coil localisation

A circular coil was used (as is standard for stimulation of area V1 in humans) and the location for V1 stimulation was localised using searching phosphene 'hotspot' techniques, as is typical for area V1 stimulation (e.g. Silvanto et al. 2005; Silvanto et al., 2007; Laycock et al., 2007; Harris et al., 2008) [see Table 5.2 for stimulation sites].

5.2.2.3 TMS procedure

Participants sat in a dark room, with their heads secured in a headrest. The circular coil was held securely using a *Manfroto Magic Arm* clamped to the headrest with side A facing the head and the handle oriented upwards. Pulses were delivered separated by ~ 2.5 s. The participant reported whether or not

Study	Participant	Part of coil used for positioning	Superior (mm)	Lateral (mm)	Method of localisation
Amassian et al. (1989)	Mean (N=4)	Circular, lower edge	20	0	To mimic lesions
Amassian et al. (1993)	Mean (N=4)	Circular, lower edge or double, centre	20	0	?
Masur et al. (1993)	Mean (N=20 Normal, N=15 Patients)	Circular 14cm coil, centre	50-70	0	Visual suppression
Beckers & Zeki (1995)	Mean (N=5)	Circular, ?	20-30	0	?
Kammer et al. (1998)	Mean (N=4)	Circular, lower edge	0	0	Visual suppression
Kastner et al. (1998)	Mean (N=18)	Circular, lower margin	20-40	0, 30	Visual suppression
Corthout et al. (1999a)	Mean (N=4)	Circular, lower edge of lower rim	10	0	?
Corthout et al. (2000)	Mean (N=5)	Circular, lower edge of lower rim	10	0	?
Corthout et al. (2003)	Mean (N=3)	Circular, lower edge of lower rim	20	0	?
Kammer et al. (2005)	Mean (N=4)	Double, centre	?	?	Visual Suppression
Jolij & Lamme (2005)	Mean (N=10)	Circular, lower rim	15	0	?
Silvanto et al. (2005)	Mean (N=7)	Double, centre	20	5	Phosphenes
Laycock et al. (2007)	Mean (16)	Circular, ?	21	0	Phosphenes
Silvanto et al. (2007)	Mean (N=5)	Double, centre	10-20	0	Phosphenes
Harris et al. (2008)	Mean (N=9)	Double, centre	10	10	Phosphenes
Present Study	RWD	Circular, lower edge of lower rim	25	0	Phosphenes
	MB		35	0	
	KP		25	0	
	LKS		20	0	
	PVM		25	0	
	Mean (N=5)		26	0	

Table 5.2. Area V1 stimulation site for each participant relative to the inion bone, compared to previous studies. Questions marks (?) denote that information was not supplied in previous studies.

they saw a phosphene(s) ('yes/no') after each pulse, and the next pulse was delivered. The participant had their eyes closed for the duration of the investigation. Pilot testing revealed that wearing blacked-out goggles or a blindfold put pressure on the eyelids and around the eyes, which was both uncomfortable and distracting for the participants.

Ten pulses in total were delivered at each stimulator output intensity, and ten stimulator output levels were tested (as in Kammer et al., 2001). Pilot testing determined the range of output intensities to be tested with each observer. The field strength was selected randomly for every trial.

5.2.2.4 Phosphene descriptions

Phosphenes evoked at the target site were described by all participants as patches of "bright white light", which extended predominantly across the lower visual hemifield in a "butterfly" shape (as in Kammer et al., 2005). In a pilot study, TMS pulses were delivered to participants when they had their eyes open and were fixating on the centre of the monitor, and the phosphenes appeared as two darker patches to the lower left and right of fixation.

5.2.3 Results and discussion

Figure 5.1 shows the responses of five observers after single pulse TMS to area V1. These data have been fitted with the Equation:

$$y = \frac{100}{1 + \left(\exp - \left(\frac{x - t}{s}\right)\right)} \tag{5.1}$$

where t represents the percentage of maximum field strength eliciting phosphenes on 50 % of trials (taken as threshold), and s represents the gradient (slope) of the function (see Figure 5.1). It can be seen that the phosphene perception rate follows a roughly sigmoidal function for most observers, although there are individual differences in the slope of the psychometric functions. Table 5.2 shows each observer's phosphene threshold and the slope of the curve (expressed as the percentage of maximum field strength, and in Tesla units). The mean phosphene threshold for the group (N = 5) is 55.087 % (S.E.M. = 2.200 %) of maximum stimulator output, corresponding to 1.102 T (S.E.M. = 0.044 T).

Figure 5.2 shows the phosphene thresholds for two participants re-tested six weeks after the first threshold measurement was taken. It can be seen that the phosphene thresholds are virtually identical across the two testing phases. For RWD, threshold was 52.231 % (S.E. = 0.174 %) maximum stimulator output, corresponding to 1.045 T (S.E. = 0.003 T) in the initial session, and 51.523 %

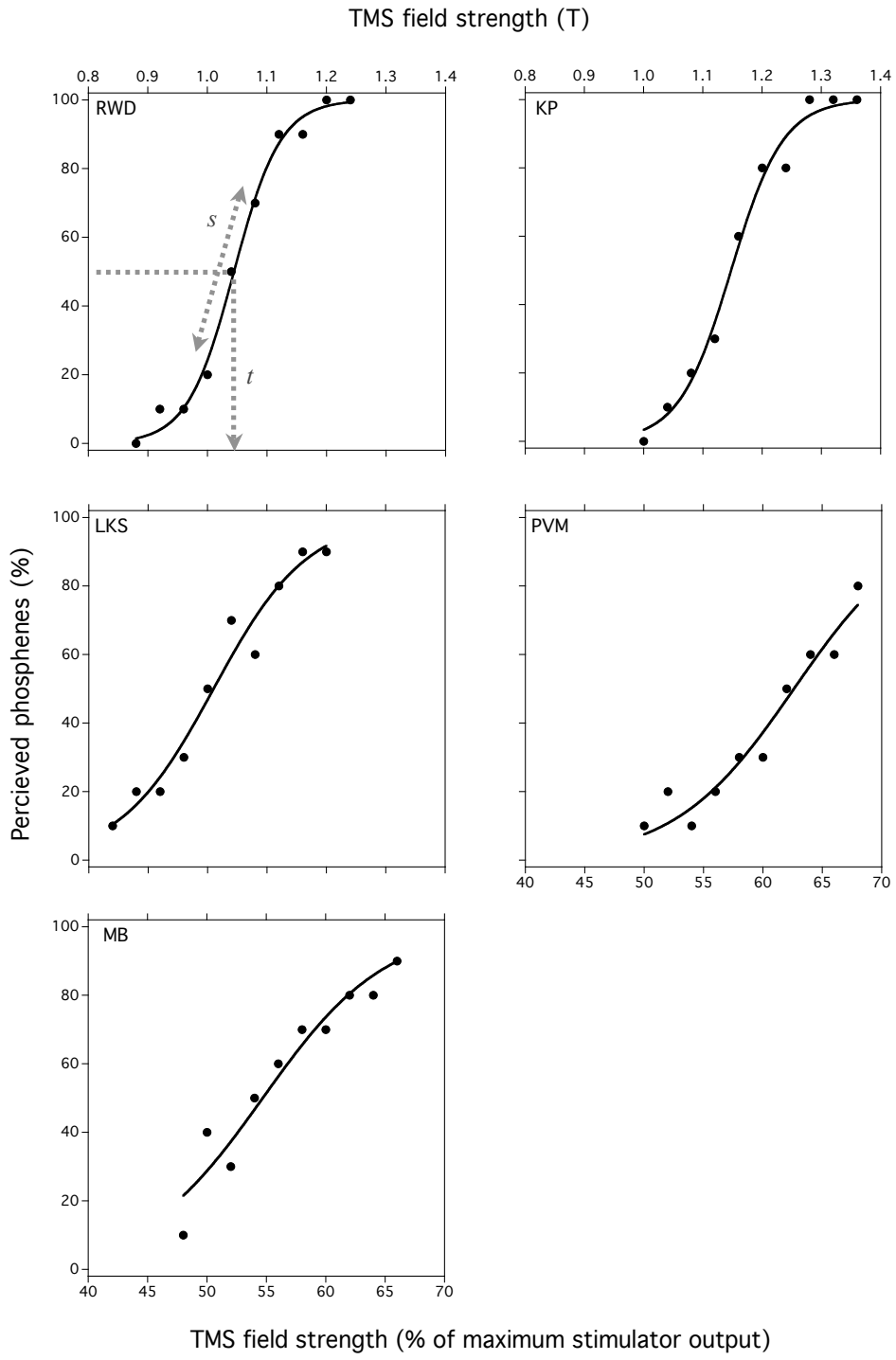

Figure 5.1. The percentage of trials in which phosphenes were perceived, as a function of field strength (T) and percentage of maximum stimulator output (%), for 5 observers. Data have been fitted with Equation 5.1 shown as a solid line: t is the field strength that supports a phosphene perception rate of 50 % and s is the slope of the psychometric function.

(S.E. = 0.283 %) maximum stimulator output, corresponding to 1.030 T (S.E. = 0.006 T) in the re-test phase. For LKS, threshold was 50.506 % (S.E. = 0.433 %) maximum stimulator output, corresponding to 1.010 T (S.E. = 0.020 T) in the initial session, and 51.257 % (S.E. = 0.557 %) maximum stimulator output, corresponding to 1.025 T (S.E. = 0.011 T) in the re-test phase. This finding is similar to that of Stewart et al. (2001) who reported phosphene thresholds to be stable across two sessions, although their participants' phosphene thresholds ranged from between 35 % to 85 % maximum field strength (0.77 T to 1.87 T).

Observer	Threshold, t (% maximum stimulator output)	Slope, s (% maximum stimulator output)	Threshold, t (T)	Slope, s (T)	R^2 value of curve fit
RWD	52.231 (0.174)	1.953 (0.153)	1.045 (0.003)	0.039 (0.003)	0.993
KP	57.383 (0.238)	2.196 (0.212)	1.148 (0.023)	0.044 (0.004)	0.988
LKS	50.506 (0.433)	3.950 (0.428)	1.010 (0.020)	0.079 (0.009)	0.963
PVM	62.618 (0.495)	5.022 (0.555)	1.252 (0.025)	0.100 (0.011)	0.949
MB	52.698 (0.601)	5.168 (0.680)	1.054 (0.021)	0.103 (0.014)	0.930
Group mean (N=5)	55.087 (0.388)	3.658 (0.406)	1.102 (0.018)	0.073 (0.008)	

Table 5.2. Phosphene thresholds (*t* derived from Equation 5.1) and slope (*s* derived form Equation 5.1) of the psychometric function relating phosphene perception rate to field strength, expressed as the percentage of maximum stimulator output and Tesla (T). Numbers in brackets indicate +1S.E. for individual data, and S.E.M. for the group mean.

Although there was some relatively moderate variability in phosphene threshold between participants, the response criterion appears to remain stable, as demonstrated by the re-test thresholds. This indicates that the 'yes/no' task together with the method of constant stimuli is a reliable way of measuring phosphene thresholds. Phosphene thresholds were much lower here (mean = 1.1 T) than those found previously using a descending approach (1.18 T – 1.98 T; Deblieck et al., 2008).

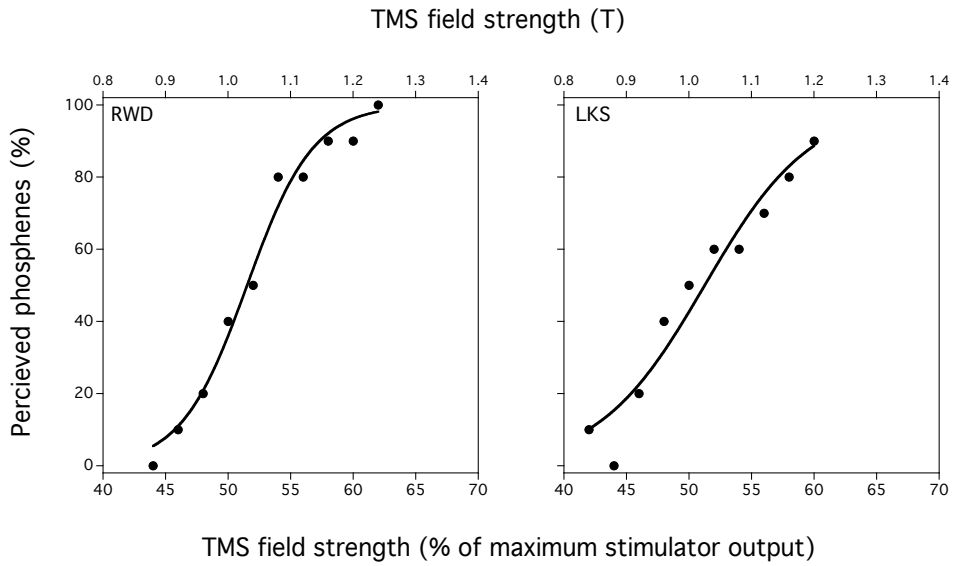

Figure 5.2. As Figure 5.1, except these data were collected in a re-test phase, six weeks after those presented in Figure 5.1 were collected.

5.3 Experiment 8: The effects of TMS field strength on orientation coding

5.3.1 Introduction

As the results of Experiment 7 demonstrate that phosphene threshold varied between observers, it can be predicted that the field strength required to disrupt performance on visual tasks also varies between observers. Whereas previous TMS studies have used a detection approach to measure the influence of field strength (Masur et al., 1993; Kastner et al., 1998), it could be postulated that measuring a discrimination threshold, such as orientation discrimination, might be a more sensitive measure of the effect of TMS. For example, it might give rise to a measurable affect of TMS in all as opposed to just some observers. Measuring the percentage of correct responses can result in a ceiling or floor effect, whereas the measurement of a discrimination threshold gives a quantitative response.

5.3.2 Methods

5.3.2.1 Observers

Four observers took part in this experiment, all of who also took part in Experiment 7.

5.3.2.2 Visual stimuli

Viewing was binocular at a distance of 192 cm. Visual stimuli were conventional Gabor patches and consisted of oriented sinusoidal gratings (2 c/deg; 12 % Michelson contrast) presented within a Gaussian envelope (SD = 0.08 deg) on a mid-grey background (73.5 cd/m^2). The duration of each visual stimulus was 66 ms. On each presentation, the spatial phase of the grating was selected randomly. Each Gabor was presented foveally, in the centre of a black annulus, which was presented continuously (see Figure 5.3). The participants were instructed to fixate at the centre of the annulus at the start of every trial to aid stable fixation and reduce any uncertainty concerning the location of the oriented stimulus. Foveal presentation was chosen as it has previously been found that single-pulse TMS delivered over area V1 produces visual field defects at fixation (Amassian et al., 1989; Kastner et al., 1998).

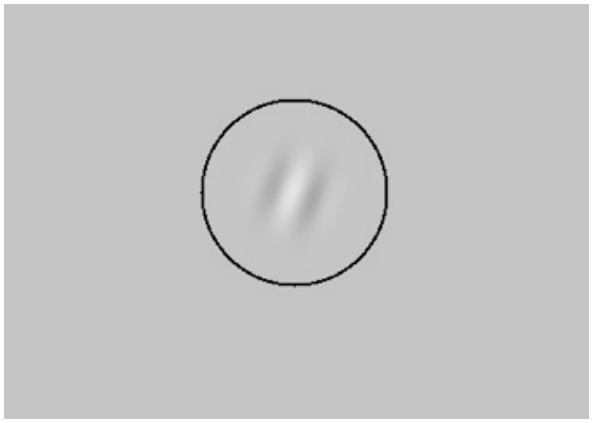

Figure 5.3. An example of the oriented Gabor stimuli used. The black annulus was displayed continuously. Participants fixated the centre of the annulus to reduce uncertainty concerning the location of the stimuli. An annulus was chosen instead of a central fixation cross, to avoid afterimages occurring at the same retinal location as the visual stimulus.

5.3.2.3 Psychophysics

A one-interval, two-alternative forced choice paradigm was employed, in conjunction with the method of constant stimuli, whereby participants judged the orientation of a Gabor patch as either clockwise or anti-clockwise of vertical. There was one of seven possible orientations in any trial, centred around vertical, and the step size was varied between participants to produce an appropriate range of responses from 100 % to 0 % "clockwise" responses. In a single run of trials, each of the seven orientations was presented ten times in a random order. Four runs of trials (280 trials) were completed by each participant for magnetic field strength tested.

5.3.2.4 Coil localisation and TMS procedure

Participants sat in a dark room with their heads secured in a headrest. The high-power 90 mm circular coil was held securely using a *Manfroto Magic Arm* clamped to the headrest with the handle oriented upwards, as in Experiment 7. The delivery of the TMS pulse was time-locked to the vertical refresh rate of the monitor with a 2.5 s inter-trial-interval between each response and the onset of the next stimulus. Single pulse TMS was delivered at a rate of once per stimulus presentation, delivered 107 ms after stimulus onset. The timing for the delivery of the TMS pulse was based on the results of pilot testing of all four participants, and on the basis of previous research that has found ~ 100 ms post visual stimulus onset to be an effective time delay to suppress visual perception (e.g. Amassian et al., 1989; Miller, Fendrich,

Eliassen, Demirel & Gazzaniga, 1996; Kastner et al. 1998; Kammer et al., 2005). Sessions were run in blocks of 70 stimulus presentations. Each block of 70 trials lasted approximately 4 minutes – this effective rate of stimulation (< 0.3 Hz) is well within the safety guidelines for rates of stimulation (Wassermann, 1998). Participants completed 32 blocks each, with a maximum of four blocks in one day.

TMS was delivered at 15 %, 30 %, 60 %, 70 %, 85 %, 87 %, 90 % and 100 % maximum output in all participants (which corresponded to 0.30 T, 0.60 T, 1.20 T, 1.40 T, 1.70 T, 1.74 T, 1.80 and 2.00 T).

5.2.3 Results and discussion

The percentage of "clockwise" responses was plotted as a function of Gabor orientation. Orientation JNDs were extracted using a logistic function of the form:

$$y = 100 + \frac{100}{1 + \left(\exp - \left(\frac{PSE - x}{JND}\right)\right)} \tag{5.2}$$

where PSE represents the point of subjective equality (in this case, subjective "vertical"), and JND is the orientation discrimination threshold (Figure 5.4). Orientation JNDs were then plotted as a function of TMS field strength (Figure 5.5) and data were fitted with the equation:

$$y = ax^b + c \tag{5.3}$$

where x is field strength and a, b and c are constants. It can be seen in Figure 5.5 that JNDs are approximately constant when TMS field strength is below a critical value, approximately 80 % maximum field strength (1.6 T). When field strength exceeds this critical value, JNDs either rise very steeply as TMS intensity increases (as shown by participants RWD and KP), or have a more shallow incline (as shown by participants LKS and PVM). Participants RWD and KP undertook TMS trials at 100 % (2 T) stimulator output, but psychometric functions could not be fitted to these data as most responses were at chance level (~ 50 % "clockwise" responses for all orientations), demonstrating a much greater level of suppression to that shown by PVM and LKS. Therefore only data for the other two participants are presented at this field strength.

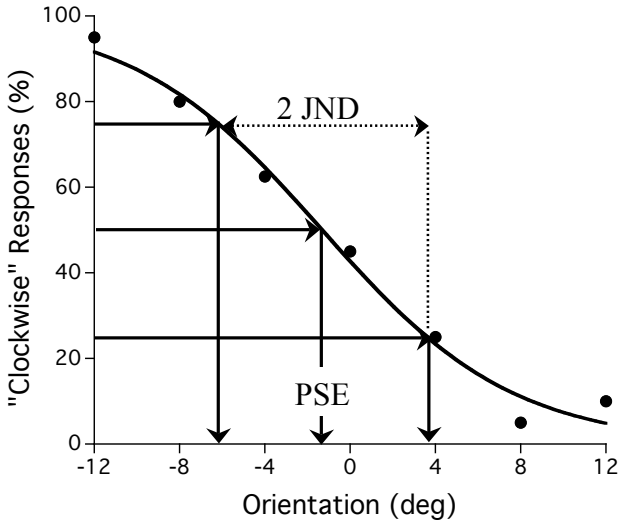

Figure 5.4. An example of a psychometric function for one participant, fitted with Equation 5.2, to extract JNDs. Negative values indicate an orientation clockwise of vertical, as is standard in visual psychophysical experiments.

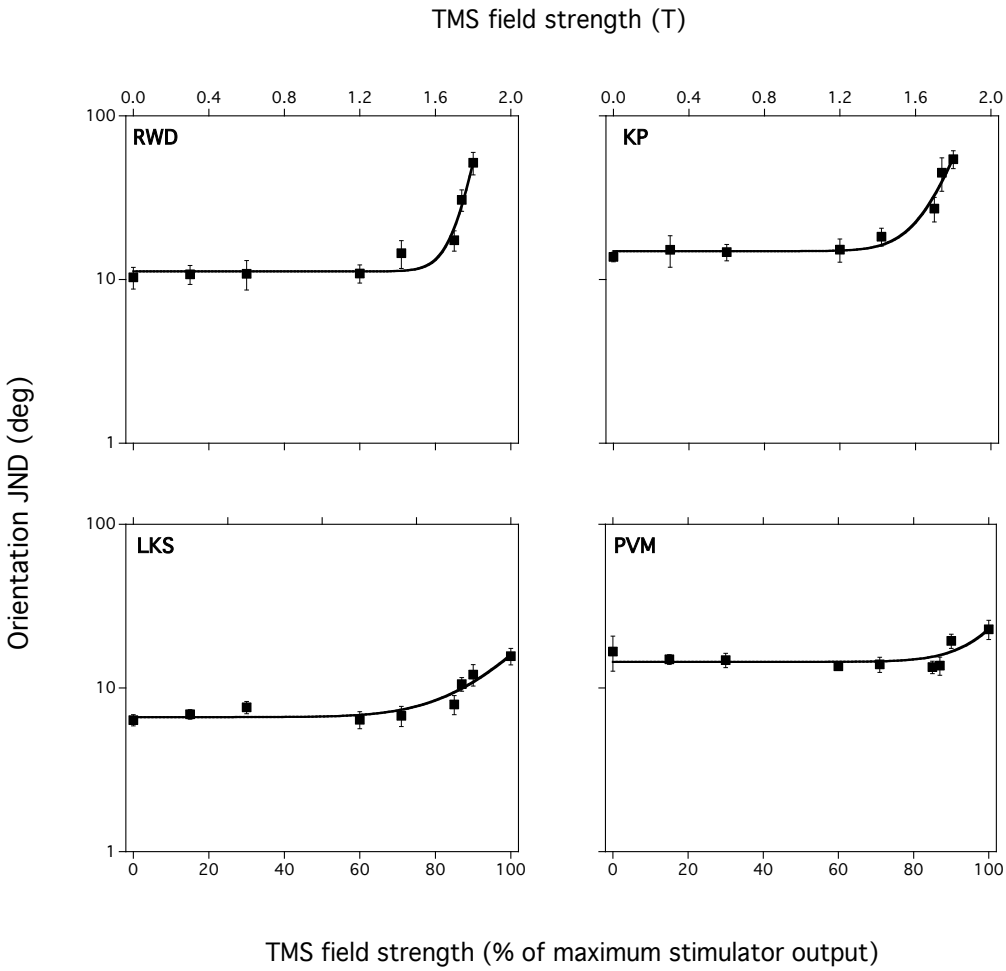

Figure 5.4. Orientation JNDs plotted as a function of magnetic field strength, for four observers. All data have been fitted with Equation 5.3, shown as a solid line. There is little or no effect on orientation JNDs when magnetic field strength is below ~ 80 % maximum (~ 1.6 T). When magnetic field strength is increased above ~ 80 % maximum, JNDs increase steeply for observers RWD and KP but less so for observers LKS and PVM. Error bars represent ± 1 SE.

The rise in orientation JNDs for all observers when TMS field intensity was ≥ ~ 80 % of maximum (1.6 T) is comparible to the results of the detection studies described earlier: Masur et al. (1993) reported that field strengths of 1.125 T had little or no effect on correct response rate, however, field strengths of 1.35 T and 1.5 T led to an 'incomplete' or 'complete' suppression respectively. Similarly, field strengths of 1.12 T, 1.26 T and 1.4 T reduced correct responding to 75 %, 45 % and 25 % levels respectively (Kastner et al., 1998). For both of these previous studies, correct response rate was 100 % in the absence of TMS. In the study conducted by Kammer and collegues (2005), contrast threshold was elevated as a function of TMS field strength, but this effect was very variable between participants.

5.4 Discussion

The results of Experiment 7 demonstrate modest variability in phosphene thresholds between participants, and that (for the two participants that were re-tested) they appeared to be stable over time. The main findings of Experiment 8 were that the influence of TMS on visual perception was dependent on the field strength, with no measurable effect of TMS when field strength was below 1.8 T (80 % maximum). Above a critical field strength, all participants showed sensitivity to the disruptive influence of TMS, the magnitude of which was dependent on field strength. Two participants (KP and RWD) appeared to be more sensitive to increases in field strength above ~ 1.8 T than the other participants (LKS and PVM). This sensitivity could not be predicted by

phosphene thresholds as LKS had the lowest (1.010 T, SE = 0.020 T) whereas PVM had the highest (1.252 T, SE = 0.025 T) threshold.

The magnetic field strength needed to evoke an "excitatory" perception of phosphenes is lower for all participants than the field strength needed to disrupt processing of a visual stimulus, that is, to have an "inhibitory" effect. It has previously been reported that individuals perceive phosphenes at around 40 % to 60 % maximum field strength (0.784 T to 0.80 T), but that detection of visual targets is only affected when TMS field strength is above 80 % (1.12 T) [Kastner et al., 1998]. It has been speculated that neurons in the same cortical region may also have different thresholds to electrical stimulation, and so lower magnetic field strengths may activate a more limited selection of neurons than higher field strengths (Ridding & Rothwell, 2007).

The individual differences may be in part explained by anatomical variations. For example, Andrews, Halpern & Purves (1997) found a two- to three-fold difference in size of area V1 across 15 neurologically normal human brains obtained at autopsy, which they describe as having "extravagant interindividual variations". In addition to the difference in the volume and surface area of area V1 between individuals, substantial differences have been reported within individuals. Mechelli, Friston, Frackowiak & Price (2005) used voxel-based morphometry for characterising structural human brain differences *in vivo*, and found that while the density in medial and extrastriate regions in one hemisphere were good predictors of the density of the equivalent structure in the other hemisphere, this was not the case for area V1.

The density of area V1 in one hemisphere did not co-vary with the density of the same region in the contralateral hemisphere, an effect that appeared to be specific to area V1.

In human brains, area V1 is located nearly entirely on the medial surface of the occipital lobe, with around two thirds of the area lying within the walls of the calcerine sulcus (Stensaas, Eddington & Dobelle, 1974). The outcome of this is that area V1 is more "buried" in some individuals (e.g. Rademacher, Caviness, Steinmetz & Galaburda, 1993; Zilles, Schleicher, Langemann, Amunts, Morosan, Palomero-Gallagher, Schormann, Mohlberg, Buergel & Steinmetz, 1997). Furthermore, the course of the calcerine sulcus varies widely between individuals (Polyak, 1957, Stensaas et al., 1974; Ono, Kubik & Abernathy, 1990; Andrews et al., 1997), which may have important implications for the effects of TMS. In Wagner et al.'s (2008) theoretical model of the effect of cortical brain atrophy on TMS-induced currents (discussed in more detail in section 2.2.3, Spatial resolution of TMS), the effects of widening sulci was explored. Wagner et al. report that the behaviour of current density was far less predictable along widened sulci borders, in general, the current density was increased in regions proximal to the widened sulci (within ~ 1 cm). The authors comment that these effects could theoretically occur in normal sulcal regions.

As the most part of area V1 is situated on the medial surface of the occipital lobe, only a small and interindividually variable portion is located on the surface of the occipital lobe, and therefore close to the scalp (Masur et al.,

1993). Because of the quadratic function between the distance from the coil and the decay of the induced electric field strength, only dorsal parts of the visual cortex are reached with TMS (Kammer, 2006). This is supported by evidence from an fMRI investigation of retinotopic architecture of early visual cortical areas, where it was found that the dorsal parts of the occipital cortex next to the skull represent only the lower parts of the visual field (Kammer et al., 2005b). This goes some way to explaining the increased effectiveness of TMS masking for stimuli presented in the lower visual field.

It is entirely feasible that the depth of the magnetic field that is thought to modulate neural processes (in the order of ~ 10mm to 20 mm [Jalinous, 1991; Hovey et al., 2003]) may not be large enough to directly affect V1 neurons in some individuals. In addition to this, the precise physiological effect of TMS in human visual cortex – and how this might be dependent on anatomical and geometrical structures – remains elusive.

Chapter 6: Is TMS disruption to visual processing caused by a decrease in signal strength or an increase in noise?

6.1 Introduction

6.1.1 TMS of human visual cortex

As discussed in Chapter 5, TMS of area V1 has been widely used to causally investigate visual processing. However, the precise mechanism behind TMS disruption remains uncertain. For example, one view is that the "virtual lesion" paradigm suppresses the neural signal related to the target, which can be likened to a reduction in perceived visibility (Kammer et al., 2005b; Harris et al., 2008). Alternatively, other evidence suggests that TMS induces neural noise, thereby reducing the signal-to-noise ratio, which results in an overall increase in discrimination threshold (Kammer & Nusseck, 1998).

This problem was first addressed in 1998 by Kammer & Nusseck, who from a series of experiments concluded that TMS increases the noise level in the visual system, which results in an elevation in contrast threshold. In their first experiment, Kammer & Nusseck measured participants' (N = 2) contrast threshold, defined as the stimulus contrast that supports 78 % correct orientation identification of a Landolt C presented for 21 ms (using a four-

alternative forced-choice procedure in conjunction with the method of constant stimuli). Under the control (no TMS) condition, mean contrast threshold was 0.95 and 1.07 log units (Weber contrast) for the two participants. The functions were shifted for both subjects when TMS was delivered 120 ms after visual stimulus onset, and mean contrast threshold increased to 2.15 and 1.91 log units (Weber contrast) respectively. Furthermore, compared with no-TMS trials, the steepness of the threshold function in TMS trials was distinctly flattened for one participant, and slightly flattened for the other participant. The second experiment employed the same visual stimuli, but contrast threshold was measured using an adaptive staircase technique to minimise the number of trials. Contrast threshold was measured for each participant (N = 4) without TMS, and also with TMS delivered 40 ms, 80 ms, 120 ms, 160 ms and 200 ms after the onset of the visual stimulus. TMS raised contrast thresholds in a bell-shaped function, where the maximum mean threshold elevation occurred when TMS was delivered 120 ms after stimulus onset. The authors note, however, that there was a "remarkable difference" in threshold elevation between the two runs for two (50 %) of the participants. The maximum threshold elevation was much greater in the first run for one participant, but much greater in the second run for another participant, but no suggestions were made as to the cause of this effect. In their final experiment, Kammer & Nusseck measured the percentage of participants' (N = 3) correct responses for orientation identification of a Landolt C, when TMS was delivered between 40 ms and 200 ms post stimulus onset in 20 ms steps, and also at 400 ms post visual stimulus onset. The effect of TMS was measured for three (N = 1) or five (N = 2) different contrast levels. Variation of SOA resulted in a typical

inverse bell-shaped modulation of percentage of correct responses. At the highest contrasts tested (~ 1.50 to 2.0 log units Weber contrast), participants achieved ~ 100 % correct performance at TMS SOAs of between 40 ms and 100 ms post visual stimulus onset, and of 180 ms, 200 ms and 400 ms post visual stimulus onset. Correct performance was, for one participant, reduced to 40 % correct (chance level = 25 %) when TMS was delivered 120 ms after visual stimulus onset. The other two participants also showed the greatest deficit to performance when TMS was delivered 120 ms after visual stimulus onset, but the deficit was not as large, although their exact results were not reported. When all three participants were tested using the same (lower) stimulus contrasts, there was great variation in the performance modulation induced by TMS. For example, at 1.58 log units Weber contrast, TL (naïve observer) achieved approximately 100 % correct performance for all TMS SOAs except for when TMS was delivered 120 ms after visual stimulus onset, where performance dropped to approximately 75 % correct. For the other two observers (the two authors), performance dropped to chance level (25 % correct) and was affected over a much broader temporal window (40 ms to 180 ms post stimulus onset for one observer, and 80 ms to 180 ms post stimulus onset for the other). In all participants, however, increasing stimulus contrast decreased the performance deficit in addition to narrowing the effective temporal window in which delivery of a TMS pulse modulated performance.

Kammer & Nusseck (1998) noted that all of the participants perceived phosphenes during the TMS trials. They conclude that with respect to the visual signal coming from the retina, TMS-induced cortical phosphenes are to

be considered as noise, and that the increase in noise is the likely cause of the elevation in contrast thresholds. However, a linear increase in additive noise should shift contrast thresholds without changing the slope of the contrast threshold function – but this is not what was observed. The authors speculated, therefore, that in addition to increasing noise level (phosphenes), TMS also reduces the magnitude of the signal coming from the retina.

A re-examination of this issue came in 2005, by Kammer and colleagues. Kammer et al. (2005b) measured contrast thresholds for orientation identification of a Landolt C stimulus, whilst also varying background luminance, TMS onset asynchrony relative to the visual stimulus, and TMS field strength (the methods used by Kammer et al. are described fully in Chapter 5). To summarise their results: the effect of TMS on orientation identification could be reliably determined as an elevation in contrast threshold; contrast threshold was dependent on SOA and was modulated in a bell-shaped manner, with a maximum effect when TMS was delivered approximately 100 ms after stimulus onset; higher TMS field strengths raised contrast thresholds even at the shortest SOAs, which caused a deformation of the bell-shaped function (discussed in Chapter 5); when results were combined across all participants (N = 4) for the "highest few" TMS field strengths and across "several SOAs" (between 75 ms and 115 ms post stimulus onset), it was found that the slope of the function relating contrast threshold to orientation identification was decreased by a factor of ~ 2 compared to the control (no TMS) condition. As an increase in contrast threshold was found in the TMS conditions in addition to a decrease in the slope of the threshold function (as

was also found in one, and to some extent, both observers in the study by Kammer & Nusseck, 1998), the authors speculated that in terms of signal detection theory, TMS appears to shift the mean of the internal noise to a higher level in addition to increasing the variance of the internal noise.

Kammer et al. (2005b) commented that their results are not consistent with the earlier "added noise" explanation for a TMS-induced increase in contrast thresholds. The earlier study by Kammer & Nusseck (1998) suggested that TMS disrupts visual processes via an excitatory mechanism – the TMS-induced "phosphene signal" competes with the retinal signal. However, Kammer et al. (2005) postulated that TMS acts via an *inhibitory* mechanism, for two reasons. Firstly, the threshold modulation effect produced with the highest field strengths tested appeared to have a longer duration in the visual system than that of lower field strengths, causing a deformation of the bell-shaped function at shorter SOAs. This is comparable to the dependence of the motor system on TMS intensity, where the duration of the silent period increases with magnetic field strength (Fuhr, Agostino & Hallet, 1991; Inghilleri, Berardelli, Cruccu & Manfredi, 1993). Secondly, the field strength that produces phosphenes is much lower than that needed to modulate contrast threshold, and one would expect similar thresholds for phosphene perception and visual disruption if the disruption effect is based purely on neural excitation.

It has since been proposed that the effect TMS has on populations of neurons – whether it be excitatory or inhibitory – is dependent on the initial cortical

activation state (Silvanto et al., 2007). Silvanto and colleagues combined TMS of V1 with an adaptation paradigm, and reported that after adapting to a colour for 30 s (e.g. “red”) and then viewing a “white” screen on which the afterimage is seen (e.g. “green”), TMS-induced phosphenes appeared to take on the colour of the adapting stimulus. In a second experiment, participants (N = 5) adapted to diagonal lines of 45 deg clockwise or anticlockwise of vertical, that were either black and green or black and red (stripe width = 0.25 deg) in a rectangular aperture (6 deg horizontal, by 3 deg vertical). Adapting stimuli were followed by a test stimulus of either the same or different colour (stripes of either black and red or black and green) and either the same or different orientation (clockwise or anticlockwise of vertical). Silvanto et al. reported that when TMS was delivered during the test grating presentation, performance was significantly improved compared to the no-TMS conditions if the test grating was fully congruent with the adapting stimulus (i.e. same colour and orientation). Furthermore, performance was significantly impaired compared to no-TMS conditions if the test grating was fully incongruent to the adaptor (i.e. different colour and orientation). The authors suggest that attributes that are encoded by the least active neural population (that has been adapted) are perceptually facilitated by TMS. While their results do not rule out the possibility that TMS preferentially inhibits the most active neurons, Silvanto et al. maintain that this is unlikely as the primary effect of TMS is to excite neurons. Single-unit studies, however, contradict this assumption (e.g. Moliadze et al., 2003) as is discussed later.

Very recently, Harris et al. (2008) used an added-noise paradigm to determine whether TMS adds noise to visual processing, decreases the strength of the visual signal, or a combination of these two possibilities. Harris et al. presented Gabor patches (duration = 40 ms, spatial frequency = 1.6 c/deg) tilted 45 deg either clockwise or anticlockwise of vertical to participants (N = 9) who were required to identify the orientation of the stimulus (using a two-alternative forced choice task). The contrast of the Gabor was varied according to an adaptive staircase technique, to measure participants' discrimination thresholds (defined as the contrast which supported 80.3 % correct responding). Thresholds were measured while TMS was delivered 106 ms after visual stimulus onset to either the occipital cortex, or Cz (according to the International 10-20 EEG system), and for three, four or five different levels of image noise. Noise was added to the image by superimposing spatial white noise (added as single pixels) drawn from a uniform distribution onto the grating. This "equivalent noise" paradigm was first developed by Barlow (1956) and assumes that visual performance is limited by internal noise in the visual system, and exploits the additivity of variance in the stimulus and variance in the visual system. The strength of the stimulus (T) was expressed in terms of contrast and was linearly related to the total level of noise (internal noise plus stimulus noise) [Barlow, 1956]. The contrast threshold power (T^2) was linearly related to the variance of the total noise. Consequently, the authors propose that if TMS added a further source of noise to visual processing, this would be observed as a parallel shift of the line relating T^2 to variance of image noise (three to five levels), compared to no-TMS conditions. If TMS reduced the efficiency of the visual system without adding any noise,

this would be observed as an increase in slope of the line relating T^2 to variance of image noise. If TMS added a source of noise and reduced the signal strength, this would be observed as both a parallel shift and an increase in slope.

Harris et al. (2008) reported that TMS interacted with image noise in a multiplicative manner (increasing the slope), which suggests that TMS disrupts visual processing by reducing the effective signal strength – and there was no support for the hypothesis that TMS added neural noise. These results, however, are based on the shift of the line relating T^2 to variance of image noise when TMS was delivered to occipital cortex compared to when it was delivered to Cz, rather than the control (no-TMS) condition, for which data are not shown. It could be reasonably argued, considering that the effects of TMS rapidly propagate to other areas (Ilmoniemi et al., 1997; Paus et al., 1997; Bohning et al., 1999), that TMS of Cz may have produced a small increase in threshold across all stimulus conditions, which may have produced a parallel shift of the line relating T^2 to variance of image noise compared to no-TMS conditions. If this is the case, then a similar parallel shift produced by TMS of occipital cortex may go unnoticed. Indeed, two participants (out of nine) do show a parallel shift of the line relating T^2 to variance of image noise compared to no-TMS conditions, which is indicative of the presence of TMS-induced noise. Furthermore, the lines relating T^2 to variance of image noise are based on only a very limited set of (three to five) data points, representing levels of image noise tested. The potential problem is the difficulty in reliably

determining the change in slope and position of the function relating T^2 to variance of image noise for each participant, based on so few points.

The field strength used by Harris et al. was 110 % of individual participants' phosphene threshold. Unfortunately, the definition of, and technique for measuring phosphene threshold was not mentioned, nor any information about the absolute field strengths actually used. This is problematic, as phosphene threshold can be measured in a number of different ways, and the effect of TMS on disruption to visual perception is critically dependent on field strength, as was discussed in Chapter 5. Harris et al. commented on the large variability between participants in terms of the effects of TMS on performance, but do not discuss this in relation to individual phosphene thresholds.

6.1.2 Physiological evidence

As mentioned earlier in this chapter, the affect of TMS on visual detection has been described in terms of signal detection theory as shifting the mean of the internal noise to a higher level in addition to increasing the variance of the internal noise (Kammer et al., 2005). Recent single-unit studies have provided support for both an increase in firing rate and an increase in response variance of neurons in feline primary visual cortex following a single TMS pulse, although the response profile is complex and depends on a number of factors (Moliadze et al., 2003). A detailed discussion of the neural consequences of TMS reported by Moliadze et al. is provided in Chapter 5. To summarise the points relevant to this discussion, after a single TMS pulse was delivered over

feline primary visual cortex: spike rate for a stimulus moving in the preferred direction was reduced; spike rate for the non-preferred direction was increased; spike rate was strongly facilitated for stimuli at the periphery of the classical receptive field that elicited little or no activity prior to TMS; and spontaneous activity was strongly facilitated and suppressed in cycles. From these results it can be seen that TMS can potentially suppress a visual signal (as demonstrated by the decrease in spike rate for the preferred direction), and add neural noise (demonstrated by the increase in firing rate for non-preferred direction, non-optimally positioned stimuli, and spontaneous firing).

6.1.3 Summary

Behavioural studies have concluded that TMS disrupts visual processing by increasing noise in the visual system either in the form of phosphenes produced by spontaneous firing of all neurons (Kammer & Nusseck, 1998), or by preferentially exciting neurons that are least active (Silvanto et al., 2007). Alternatively, there is also evidence to suggest that TMS reduces the strength of the visual signal (Kammer et al., 2005; Harris et al., 2008). The limited physiological evidence there is on the neural consequences of single-pulse TMS appears to support both of these theories (Moliadze, 2003). These potential affects of TMS on neuronal behaviour are depicted in Figure 6.1.

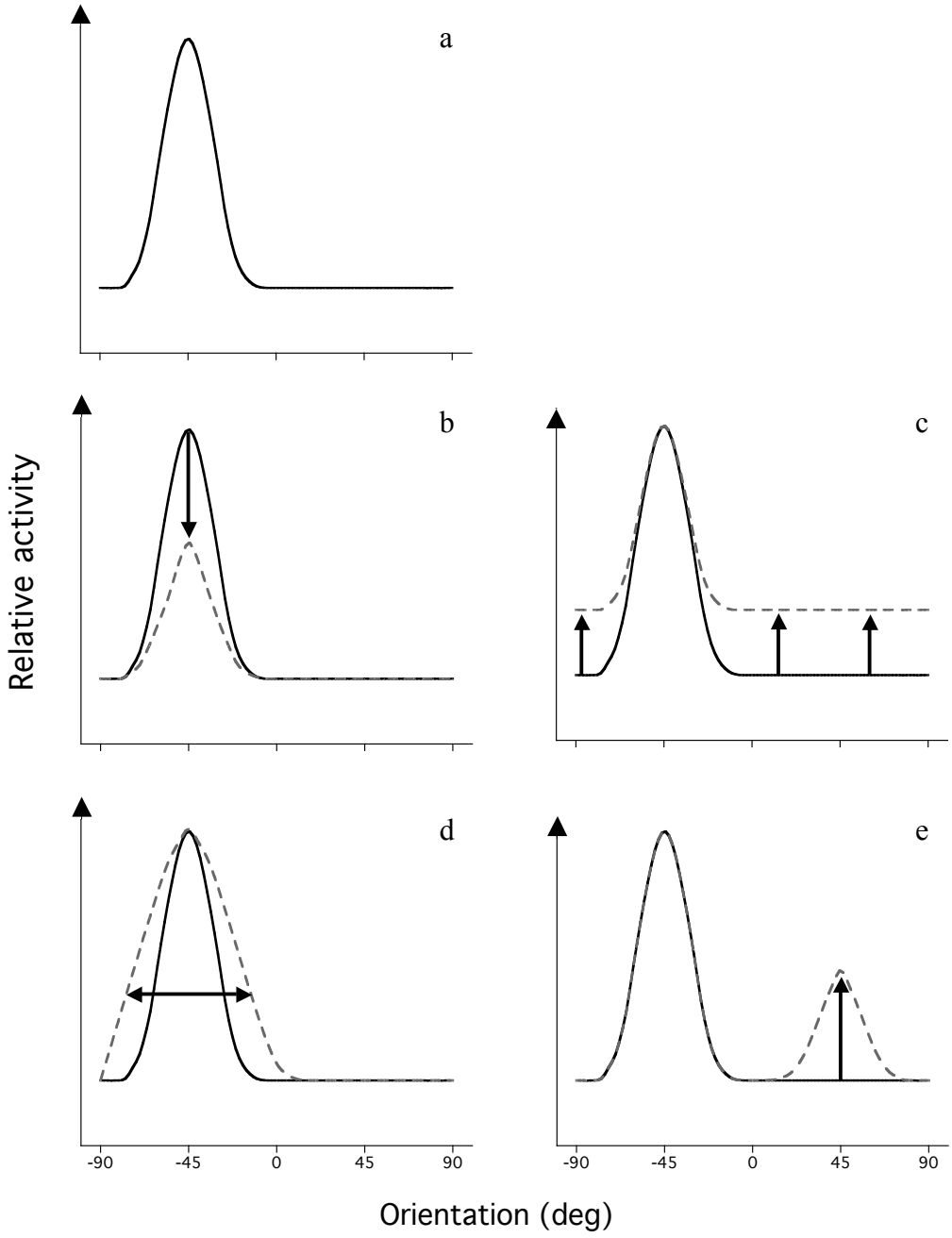

Figure 6.1. A representation of some of the ways that TMS could potentially affect the responses of a single cell to oriented stimuli. An illustration of a tuning curve under normal conditions is shown (solid line), with hypothetical examples of how this might change under TMS conditions (broken line). The response in no-TMS trials (a) is based on the mean responses of a simple cell in feline cortex to 80 % contrast drifting gratings of optimum spatial frequency, as reported by Skottun et al. (1989). TMS may reduce the maximum response to a stimulus of preferred orientation by, for example, interrupting the complex pattern of firing that signals the stimulus (b); increase the level of uncorrelated firing, observed as an increase in 'background noise' (c); increase the variance of the cell's response, by increasing the response to stimuli on the edge of the tuning curve (d); or preferentially increase the response to non-optimal stimuli (e).

Aim

The principle aim of the experiments contained within this chapter is to determine whether the disruption to visual processing from single-pulse TMS of area V1 can be characterised as an increase in contrast threshold, as has been previously claimed (Kammer & Nusseck, 1998; Kammer et al., 2005), and whether elevated thresholds can be attributed to a decrease in signal strength or an increase in neural noise.

6.2 Experiment 9: A psychophysical investigation of orientation discrimination as a function of stimulus contrast

6.2.1 Introduction

Orientation tuning is possibly the most studied feature of V1 neurons (Ferster, 2004), and in higher mammals many cells in primary visual cortex respond best to a particular orientation (e.g. Hubel & Wiesel, 1959; Hubel & Wiesel, 1968; Bradley, Skottun, Ohzawa, Sclar & Freeman, 1987). Orientation sensitivity is dependent on perceived contrast, and this effect can be measured psychophysically. Consequently, orientation sensitivity appears to be a suitable measure for investigating the mechanisms underlying V1 processing, and the nature of the modulation of visual processing by TMS (which will be examined in Experiment 10).

As discussed in Chapter 1, orientation discrimination is dependent on a number of different stimulus parameters, such as duration, spatial frequency, contrast and the orientation bandwidth of the stimulus. Skottun et al. (1987) measured the affect of contrast on human psychophysical orientation discrimination, in addition to single-unit responses in the feline primary visual cortex. Skottun and colleagues reported that psychophysical orientation sensitivity did not continue to increase with contrast, but reached a plateau, despite the fact that the firing rate of many neurons continued to increase as contrast increased. Specifically, orientation discrimination improved as contrast increased above detection threshold, until a critical contrast (typically ~ 10 % Michelson contrast) is reached, after which performance was asymptotic (typical maximum discrimination performance was approximately 0.4 deg to 0.7 deg). However, maximum discrimination performance was observed in some cases at very low contrasts, for example, one participant had a similar orientation discrimination threshold (0.5 deg) for 3 % and 80 % contrast gratings. In the feline primary visual cortex, the response amplitude of many neurons increased linearly with log contrast over most of the visible range, although some cells showed response saturation at medium contrasts.

Aim

The aim of Experiment 9 is to characterise the function relating orientation just noticeable differences (JNDs) to stimulus contrast levels.

6.2.2 Methods

6.2.2.1 Observers

Four experienced psychophysical observers participated in this study, two (RWD, KP) were naïve to the goals of the study. All had normal or corrected-to-normal vision.

6.2.2.2 Visual stimuli

Viewing was binocular at a distance of 192 cm. Visual stimuli were conventional Gabor patches and consisted of oriented sinusoidal gratings (2 c/deg) presented within a Gaussian envelope on a mid-grey background (73.5 cd/m^2). On each presentation, the spatial phase of the grating was selected randomly. Each Gabor was presented foveally, in the centre of a black annulus, which was presented continuously (see Figure 5.3, Experiment 8). The participants were instructed to fixate at the centre of the annulus at the start of every trial to aid stable fixation, and reduce any uncertainty concerning the location of the oriented stimulus. Orientation discrimination was measured, as a function of Gabor grating contrast for two Gaussian envelope sizes (SD = 0.08 deg and 0.25 deg). Using two envelope sizes allowed the influence of the orientation bandwidth (ambiguity) of the stimulus to be investigated, as decreasing stimulus size broadens stimulus orientation bandwidth (Graham, 1989), as shown in Figure 6.2. Gabor stimuli were presented for 67 ms at

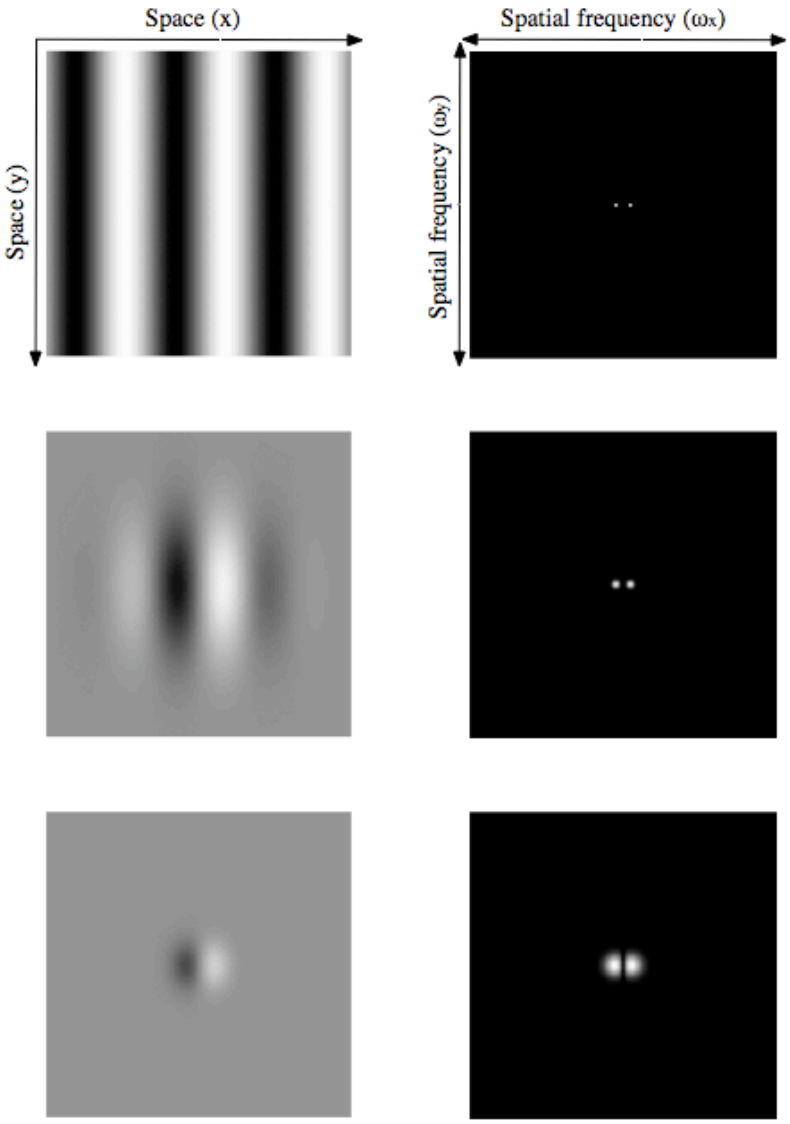

Figure 6.2. Space-space (x-y) plots (left) demonstrating the construction of Gabor patches analogous to those used in the actual experiment. To the right of each image is a power spectrum, computed by applying a fast Fourier transform to the 128 x 128 pixel array representing that image. The spectrum represents the power (amplitude squared) at each orientation and spatial frequency, with brighter values indicating greater power. For clarity, the d.c. components are omitted and the intensity values have been scaled to cover the available range of brightness. The sinusoidal grating pattern (top left) has a spectrum that is both spatially and orientationally narrowband. Multiplying the grating with a two-dimensional Gaussian window results in a Gabor patch (middle and bottom) that has power at a range of orientations (and spatial frequencies). The orientation bandwidth is inversely related to the standard deviation of the Gaussian window and thus for the smallest Gabor patch (bottom left) the orientation of the Gabor patch is most ambiguous.

approximately 100 %, 50 %, 25 %, 12 %, 6 %, 4 %, 2 % and 1 % Michelson contrasts.

6.2.2.3 Psychophysics

A one-interval two-alternative forced choice paradigm was employed, in conjunction with the method of constant stimuli, whereby participants judged the orientation of the Gabor patch as either clockwise, or anti-clockwise of vertical. There was one of seven possible orientations in any trial, centred around vertical, and the step size was varied between participants to produce an appropriate range of responses from 100 % to 0 % "clockwise" responses. In a single run of trials, each of the seven orientations was presented ten times in a random order. Four runs of trials (280 trials) were completed by each participant for each contrast and for each stimulus size.

6.2.3 Results and discussion

Orientation JNDs were extracted using Equation 5.2, as in Experiment 8, and plotted as a function of stimulus contrast (Figure 6.3). Data were fitted with a two-limbed function (c.f. Burr & Santoro, 2001) of the form:

$$y = \left[\frac{\left(\mathrm{sgn}(a-x)+1\right)\left(\frac{a}{x}\right)^{c} + \mathrm{sgn}(x-a)+1}{2} \right] b \qquad (6.1)$$

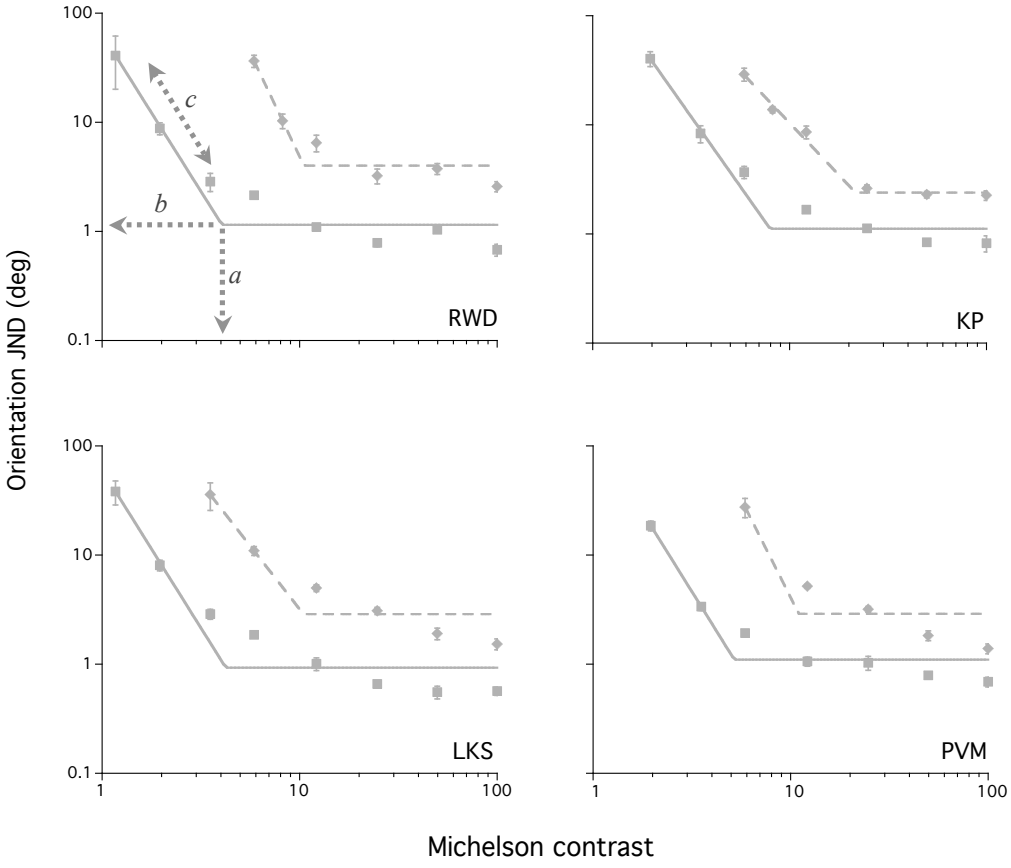

Figure 6.3. JNDs for orientation discrimination as a function of Gabor contrast for four participants. Squares represent JNDs for larger Gabor patches (SD = 0.25 deg) and diamonds represent JNDs for smaller Gabor patches (SD = 0.08 deg). All data have been fitted with Equation 6.1, shown as a solid line for larger Gabor patches and a broken line for smaller Gabor patches. JNDs decrease steeply as contrast increases until a critical contrast is reached, after which JNDs are not dependent on contrast. Error bars represent the SE.

Where sgn is the signum function and is equal to either +1, 0 or -1 depending on whether the argument in the parentheses is >0, 0 or <0, respectively, *a* is the critical contrast beyond which contrast is no longer a limiting factor on performance, *b* is the minimum JND at which performance asymptotes, and *c* is the slope of the descending limb of the function (see Figure 6.3, top left).

It can be seen in Figure 6.3 that for both Gabor envelope sizes, JND data follow a similar trend: at the lowest contrasts tested, there is a steep decrease in JND as contrast increases. When contrast exceeds a critical value, however, performance asymptotes and is essentially invariant of stimulus contrast. This is consistent with previous studies (e.g. Skottun et al., 1987; Mareschal & Shapley, 2004). The data presented in Figure 6.3 are presented on logarithmic axes, which tend to compress differences at higher values along the *y* axis and emphasise relatively modest differences at the lower values.

Figure 6.3 shows that the function describing orientation JNDs for the smaller Gabor size (SD = 0.08 deg) is displaced to higher values along both the contrast and orientation JND axes compared to that for the larger Gabor size (SD = 0.25 deg). The shift along the contrast axis is demonstrated by the lateral shift in the transition point where performance changes from a descending to an asymptotic JND (*a*) [see Tables 6.1 and 6.2]. Participants' JNDs were asymptotic by approximately 4.2 % to 8.0 % and 10.5 % to 21.7 % Michelson contrast for the larger and smaller Gabor sizes respectively. Skottun et al. (1987) report asymptotic performance after contrast increased above around 5 – 10 %.

Participant	***a*** Critical contrast (%)	***a*** Critical contrast SE (%)	***b*** Optimal JND threshold (deg)	***b*** Optimal JND SE (deg)	***c*** Slope	***c*** Slope SE	R^2 of curve fit
RWD	4.045	0.005	1.150	0.342	2.878	0.153	0.998
KP	7.970	0.012	1.115	0.342	2.560	0.136	0.998
LKS	4.229	0.006	0.929	0.358	2.893	0.172	0.997
PVM	5.190	0.006	1.100	0.219	2.904	0.251	0.996

Table 6.1. Parameters extracted from the curve fit derived from Equation 6.1 describing the relationship between orientation discrimination and stimulus contrast in the absence of TMS, for the Gabor stimulus with a SD of 0.25 deg.

Participant	***a*** Critical contrast (%)	***a*** Critical contrast SE (%)	***b*** Optimal JND threshold (deg)	***b*** Optimal JND SE (deg)	***c*** Slope	***c*** Slope SE	R^2 of curve fit
RWD	12.354	0.020	3.187	1.251	3.274	0.483	0.984
KP	21.651	0.042	2.392	0.694	1.906	0.188	0.992
LKS	13.371	0.035	2.174	0.963	2.098	0.250	0.990
PVM	17.852	0.029	2.136	0.541	2.303	0.254	0.996

Table 6.2. Parameters extracted from the curve fit derived from Equation 6.1 describing the relationship between orientation discrimination and stimulus contrast in the absence of TMS, for the Gabor stimulus with a SD of 0.08 deg.

An upward shift of JND data along the orientation JND axis is demonstrated by an increase in asymptotic performance level (*b*). Minimum orientation discrimination thresholds were ~ 0.9 deg to 1.2 deg for the larger Gabor size, and ~ 2.1 deg to 3.2 deg for the smaller Gabor size (see Tables 6.1 and 6.2). These thresholds are larger than those reported by Skottun et al. (1987), where minimum orientation thresholds were approximately 0.4 deg to 0.7 deg. The lower thresholds found by Skottun et al. are most likely a result of their larger stimulus window which subtended 4 deg diameter, compared to the visible window used in this experiment, which subtended ~ 1 deg or ~ 0.3 deg diameter (for larger and smaller Gabor sizes, respectively), or the longer stimulus duration in their study (500 ms compared to 67 ms here).

The lateral shift of the JND data along the contrast axis (*a*) for the smaller compared to the larger Gabor envelope size can be explained in terms of a reduction in spatial energy (Kukkonen, Rouamo, Tiippana & Nasanen, 1993), as described by Bloch's or the Bunsen-Roscoe law (Response = Intensity x Time). Consequently, as the duration was constant (67 ms), intensity (in this case contrast) must be increased for the smaller stimulus to elicit the same response (JND) as the larger stimulus.

The upward shift of the function for the smaller compared to the larger Gabor size is consistent with the fact that orientation bandwidth increases as stimulus size decreases (Grahem, 1989), and that orientation thresholds increase with orientation bandwidth (Beaudot & Mullen, 2006).

6.3 Experiment 10: The effects of TMS over area V1 on orientation processing as a function of stimulus contrast

6.3.1 Introduction

Having characterised the relationship between baseline orientation JND and stimulus contrast, the mechanism behind TMS disruption to visual processing can be ascertained by observing the direction of any shifts that occur in the function describing JND vs. contrast compared to baseline (no-TMS) conditions.

If performance in TMS trials is limited by perceived contrast (a reduction in visibility), then it would expected the relationship between orientation JND and stimulus contrast for TMS trials to be well described by a laterally-translated version (toward a higher contrast) of the function measured in the absence of TMS. If, however, performance in TMS trials is limited by orientation uncertainty (without a decrease in visibility), then we would expect the function describing JND vs. contrast for TMS trials to be well described by an upwardly-translated version (toward higher JND) of the relationship between JND and stimulus contrast for no-TMS trials.

Aims

The principle aim of Experiment 10 is to determine what effect TMS has on the function describing orientation JND for a range of contrasts as in Experiment 9.

6.3.2 Methods

6.3.2.1 Observers

The four observers that participated in this experiment also participated in Experiment 9. All participants had no contraindications on the TMS Safety Screen (Keel et al., 2000).

6.3.2.2 Visual stimuli

Oriented Gabor visual stimuli were identical to those used in Experiment 9. Step size was tailored for each participant to produce an appropriate range of responses from 100 % to 0 % "clockwise" responses.

6.3.2.3 TMS procedure

The high power circular coil was positioned over area V1 as in Experiments 7 and 8. Pulses were delivered at 1.8 T (90 % maximum stimulator output), as it was found in Experiment 8 that TMS field strengths of greater than approximately 1.6 T (80 % maximum output) disrupted orientation

discrimination. The delivery of TMS was time-locked to the vertical refresh rate of the monitor. Single pulses were delivered at a rate of one pulse per Gabor stimulus presentation, with a 2.5 s inter-trial-interval between each response and the onset of the next stimulus. TMS was delivered 107 ms after the visual stimulus onset. The timing for the delivery of the TMS pulse was based on the results of pilot testing of all four participants, and on the basis that previous research has found ~ 100 ms post visual stimulus onset to be an effective time delay to suppress visual perception (Amassian et al., 1989; Miller et al., 1996; Kastner et al., 1998; Kammer et al., 2005). Sessions were run in blocks of 70 stimulus presentations. Each block of 70 trials lasted approximately 4 minutes – this is well within the safety guidelines stipulating rates of safe stimulation (Wassermann, 1998). Participants completed 36 blocks each, with a maximum of four blocks in one day.

6.3.3 Results and discussion

Orientation JNDs were extracted using Equation 5.2, as in Experiment 8, and plotted as a function of stimulus contrast (Figure 6.4). Data were fitted with Equation 6.1, as in Experiment 9. It can be seen in Figure 6.4 that for TMS trials, compared to no-TMS trials, the function describing JND vs. contrast has shifted laterally along the *x* axis, towards a higher contrast, for all observers (as can be seen when comparing the 'critical contrast' (*a*) values in Tables 6.3 and 6.4 with those in Tables 6.1 and 6.2, in Experiment 9). This is true for both stimulus envelope sizes. For example, critical contrasts (above which JNDs are

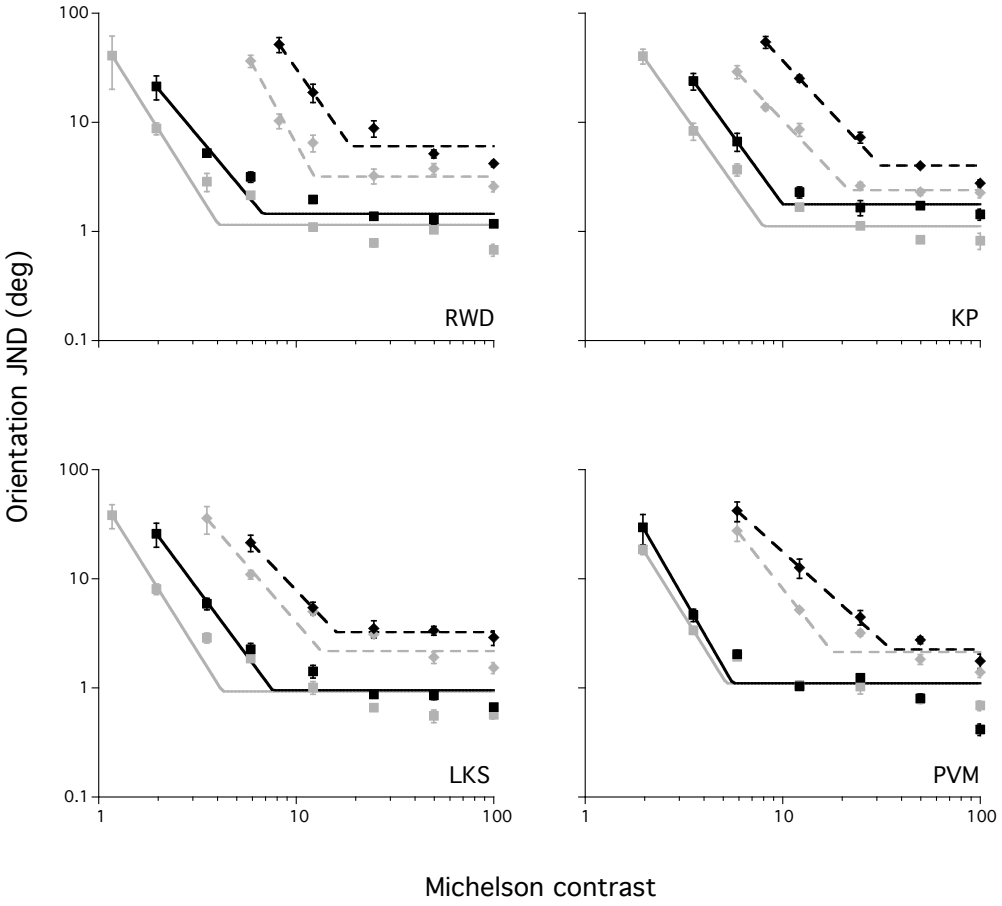

Figure 6.4. JNDs for orientation discrimination as a function of contrast for four participants during TMS trials compared to baseline (no-TMS) trials. Performance in TMS trials (black symbols) is impaired compared to no TMS trials (grey symbols: data from Experiment 9 are re-plotted for purposes of comparison). Squares represent JNDs for larger Gabor patches (SD = 0.25 deg) and diamonds represent JNDs for smaller Gabor patches (SD = 0.08 deg). All data have been fitted with Equation 6.1, shown as a solid line for larger Gabor patches and a broken line for smaller Gabor patches. JNDs improve as contrast increases until a critical contrast is reached, after which JNDs are invariant to further changes in stimulus contrast. Error bars represent the SE.

Participant	***a*** Critical contrast (%)	***a*** Critical contrast SE	***b*** Optimal JND (deg)	***b*** Optimal JND SE (deg)	***c*** Slope	***c*** Slope SE	R^2 of curve fit
RWD	6.779	0.011	1.451	0.383	2.163	0.194	0.993
KP	9.983	0.006	1.777	0.183	2.499	0.111	0.999
LKS	7.592	0.007	0.953	0.197	2.438	0.098	0.999
PVM	5.578	0.006	1.106	0.270	3.145	0.223	0.998

Table 6.3. Parameters extracted from the curve fit derived from Equation 6.1 describing the relationship between orientation discrimination and stimulus contrast during TMS trials, for the Gabor stimulus with a SD of 0.25 deg.

Participant	***a*** Critical contrast (%)	***a*** Critical contrast SE (%)	***b*** Optimal JND (deg)	***b*** Optimal JND SE (deg)	***c*** Slope	***c*** Slope SE	R^2 of curve fit
RWD	18.889	0.027	6.049	1.413	2.571	0.352	0.992
KP	31.262	0.038	4.022	0.787	1.943	0.100	0.999
LKS	15.937	0.008	3.249	0.183	1.892	0.083	0.999
PVM	35.445	0.046	2.253	0.417	1.628	0.056	0.999

Table 6.4. Parameters extracted from the curve fit derived from Equation 6.1 describing the relationship between orientation discrimination and stimulus contrast during TMS trials, for the Gabor stimulus with a SD of 0.08 deg.

relatively invariant of contrast) were between ~ 4.2 % and ~ 8.0 % contrast and ~ 10.5 % and ~ 21.7 % contrast in baseline conditions (Experiment 9) for larger and smaller envelope sizes, but increased to between ~ 5.5 % and ~ 10.0 % contrast and ~ 15.9 % and 35.4 % contrast in TMS conditions (current experiment), for larger and smaller envelope sizes respectively. This is consistent with the theory that TMS raises contrast thresholds (Kammer & Nusseck, 1998; Kammer et al., 2005), or more generally, decreases the effective signal strength.

For observers RWD and KP, however, there is also an upward shift (along the *y* axis) in the data for TMS conditions compared to baseline conditions, that cannot be overcome by increasing contrast. For example, for the larger envelope size, JNDs were ~ 1.12 deg and ~ 1.14 deg in baseline conditions (Experiment 9), but were ~ 1.78 deg and ~ 1.79 deg in TMS conditions (current experiment) for participants KP and RWD respectively. For the smaller envelope size, JNDs were ~ 2.30 deg and ~ 3.19 deg in baseline conditions, but were ~ 4.02 deg and ~ 6.05 deg in TMS conditions for participants KP and RWD. This overall decrement in maximum discrimination performance is consistent with the theory that TMS induces neural noise by, for example, increasing uncorrelated spontaneous firing or increasing spike rate for non-optimal stimuli (Moliadze et al., 2003; Silvanto et al, 2007). In terms of population coding, an increase in the firing of neurons selective for non-optimal orientations may increase internal noise by causing the population orientation tuning response to appear to become broader. This would result in an upward shift in the function describing JND, as error rates would increase,

as dictated by signal detection theory (Green & Swets, 1966), and discrimination becomes less sensitive in spite of the contrast. For participants LKS and PVM, however, there is comparatively little shift of the function along the *y* axis: optimal JNDs for the larger envelope were ~ 0.93 deg and ~ 1.10 deg in baseline conditions (Experiment 9), and ~ 0.95 deg and ~ 1.11 deg in TMS conditions for participants LKS and PVM respectively. For the smaller envelope size, baseline JNDs were ~ 2.89 deg and ~ 2.14 deg, compared with ~ 3.25 deg and ~ 2.25 deg for participants LKS and PVM.

Figure 6.5 demonstrates the relationship between the orientation and contrast shifts for each participant. The contrast shift in orientation JND for TMS trials compared to baseline trials is represented along the *x* axis, and is determined by the ratio:

$$\frac{TMSa}{BLa} \tag{6.2}$$

where *TMSa* and *BLa* are the critical contrasts (*a*) as extracted from the curve fit derived from Equation 6.1 for the TMS and the baseline (no-TMS) conditions, respectively. The orientation shift represented along the *y* axis, determined by the ratio:

$$\frac{TMSb}{BLb} \tag{6.3}$$

where *TMSb* and *BLb* are the optimal orientation JNDs (*b*) as extracted from the curve fit derived from Equation 6.1, for TMS and baseline conditions respectively. If either ratio equals 1, the values derived for the baseline and the TMS conditions are equal and there is no shift. If the resulting ratio is greater

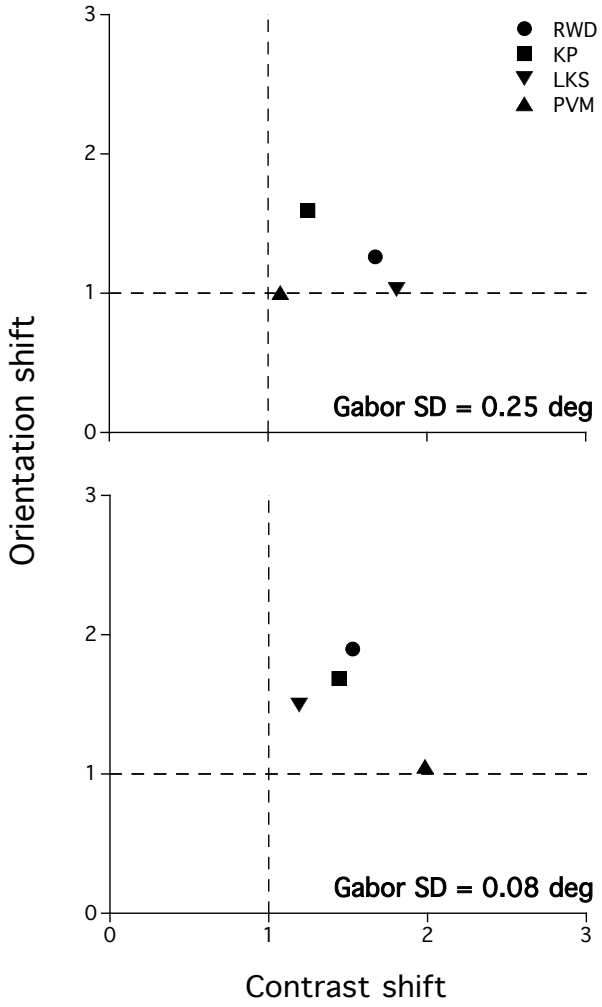

Figure 6.5. The relationship between contrast (*a*) and orientation (*b*) shifts in the JND data for TMS compared to baseline conditions. Plots show shifts for larger (top) and smaller (bottom) Gabor envelope sizes. A contrast shift of 1 (shown by the vertical broken line) indicates that the critical contrast (*a* in Equation 6.1) was equal for the two conditions, and a contrast shift greater then 1 indicates that the critical contrast was higher in the TMS conditions compared to baseline conditions (in the absence of TMS). An orientation shift of 1 (indicated by the horizontal broken line) indicates that optimal orientation JNDs (*b* in Equation 6.1) were equal for the two conditions, and an orientation shift greater than 1 indicates that performance was worse in TMS conditions.

then 1, then the value derived for the TMS condition is greater than that for the baseline condition, and the opposite is true if the value is less than 1. It can be seen in Figure 6.5 that for the larger Gabor size, observers KP (circle) and RWD (square) show both contrast and an orientation shifts, whereas observer LKS (diamond) shows only a contrast shift and observer PVM (triangle) shows little or no shift in the TMS compared to no-TMS trials. For the smaller Gabor size, KP, RWD and LKS show both contrast and an orientation shifts, whereas PVM show only a contrast shift.

6.4 Discussion

The main findings of the experiments presented in this chapter are as follows: firstly, the shape of the function describing orientation JNDs is similar to that reported by Skottun et al. (1987), in that performance improves as stimulus contrast increases, but reaches maximum levels at relatively low contrasts. This effect is likely to be caused by the fact that the response of many V1 neurons increases with contrast, but maximum response is reached at low to medium contrasts (e.g. Skottun et al. 1987). The plateau in JND represents the level of internal noise (Maraschal & Shapley, 2004), which reflects the existence of an absolute threshold in the absence of external (contrast) noise.

Secondly, TMS induces a contrast shift of the function describing orientation JND in all four participants. Compared to the baseline JNDs, performance continued to improve in TMS conditions until a higher critical contrast was reached after which performance saturated. This supports the idea that the

effect of TMS on visual processing can be characterised as an increase in contrast threshold, as proposed by Kammer and colleagues (Kammer & Nusseck, 1998; Kammer et al., 2005), who found that increasing stimulus contrast reduced the effects of TMS on visual processing. This may be caused by a decrease in visual signal strength in the cortex, as it is has been reported that TMS reduces firing rate for preferred stimuli (Moliadze, 2003), and is likely to interrupt the complex pattern of activity that signals the stimulus (Silvanto et al., 2007). A signal reduction account would explain the lateral shift in the descending part of the function describing orientation JNDs as it may be postulated that at low contrasts when neurons have not reached maximum response, TMS has the effect of reducing this response further, as if effectively reducing the contrast of the stimulus. On the plateau part of the function, TMS-induced reduction of contrast may have little effect on perception if most neurons are responding maximally.

Thirdly, TMS induced an orientation-based noise shift for two participants for both stimulus sizes (RWD and KP). Performance in TMS conditions for these two observers never reached their performance level in baseline conditions. This implies that the level of internal noise has increased (e.g. Maraschal & Shapley, 2004) as this effect exists on the plateau part of the function describing orientation JNDs even at 100 % stimulus contrast, which is much greater than the critical contrasts for either participant (where performance changed from descending JNDs to asymptotic JNDs). This increase in noise level may have been caused by a number of excitatory effects that TMS has on single cells as reported by Moliadze et al. (2003), such as an increase in firing

rate for non-preferred stimuli, increased firing rate for stimuli positioned in the periphery of the receptive field (which would not normally elicit a response), or an increase in spontaneous firing rate. This increased-noise theory is supported by Silvanto et al., (2007), who postulate that TMS preferentially activates neurons that are closer to resting potential (that is, neurons that are not activated by a visual stimulus). This would have the effect of creating a complementary pattern of activity across neurons to that induced by a stimulus, and could explain an overall decrease in performance such as that found for participants KP and RWD in Experiment 10.

Although it was proposed by Kammer & Nusseck (1998) that the effects of TMS on visual processing are likely to be a result of an increase in noise level (as the result of cortical phosphenes), it was also reported in their study, and in the later study by Kammer et al. (2005) that the effect of TMS on visual processing could be reduced and even abolished by increasing the contrast of the stimulus. This is not the case here for participants KP and RWD, as JNDs were increased in TMS compared to baseline conditions even at 100 % contrast. The orientation shift of JNDs also contradicts the results of Harris et al. (2008), who reported that the only effect of TMS on visual processing is that of a reduction of contrast. However, in their study, contrast thresholds were measured as a function of the level of contrast noise added to the stimulus; no other type of noise was measured. In Experiment 10, orientation discrimination was measured as a function of contrast, and so the effect of contrast could be differentiated from any other type of 'orientation' based noise affecting discrimination. Furthermore, Harris et al. claim that their data

show no evidence that TMS increases noise levels, and instead suggest the only mechanism by which it compromises visual processing is that of reducing the signal. As discussed earlier in this chapter, they compare their function (which relates contrast threshold to the level of image noise) gained when TMS was delivered V1, to when TMS was delivered to Cz. As they do not present baseline data for the function (when TMS is not delivered), it is unclear whether TMS to Cz could be increasing internal noise, which would mask any noise produced when TMS is delivered over area V1. Furthermore, two (out of nine) of their participants do in fact show a parallel shift in the function (which infers that TMS adds a further source of noise) in addition to the increase in the slope of the function (which infers that TMS reduces signal strength, that is, contrast) that is observed in all of their participants, although they do not offer an explanation for this.

This finding reflects the results of Experiment 10: that all participants demonstrate a TMS-induced reduction in signal strength, yet two also demonstrate the presence of TMS-induced noise. Individual differences in the effects of TMS on visual processing are reported frequently (for discussion, see Chapter 5). For example, in addition to the effect reported by Harris et al., Kammer & Nusseck (1998) report that TMS-induced elevations in contrast thresholds are more pronounced in some participants than others, and Kammer et al. (2005) report that contrast threshold is greatly elevated in some participants by relatively low magnetic field strengths, whereas thresholds in other participants are only slightly elevated by much higher field strengths. Indeed, it was reported in Experiment 8 that orientation JNDs increased much

more steeply with increasing field strength for participants KP and RWD than for participants LKS and RWD. This finding, combined with the findings of Experiment 10, could imply that not only do individuals have different levels of sensitivity (or "susceptibility", Masur et al., 1993) to TMS field strength, but that field strength determines the effect by which TMS alters perceptual processes (that is reducing the signal, or increasing noise).

Since it was found in Experiment 9 that the function describing baseline (no-TMS) JNDs vs. contrast for the smallest Gabor patch was shifted both laterally and upwards compared to that for the larger Gabor patch, it is possible that the perceptual effect of TMS is to reduce the patch size, which in turn, effectively increases the orientation ambiguity of the stimulus.

Conclusion

The aim of the experiments presented in this chapter was to tease apart the underlying mechanisms by which a TMS pulse modulates normal visual processing. Experiment 9 determined the function describing orientation JNDs over a range of contrasts. Experiment 10 demonstrated that TMS produced a contrast-based shift of JNDs for all observers, consistent with a 'signal-reduction' account. However, the effects of TMS on orientation discrimination are not entirely accountable by a TMS-induced reduction in effective stimulus contrast – as there was an upward shift of JNDs for two observers in addition to the contrast shift. That is, increasing the signal strength could overcome the effects of TMS for two observers, but importantly, not for two other observers. This is consistent with an 'increased noise' account, and contradicts the

prediction that the effects of TMS on visual processing can be characterised entirely as an increase in contrast threshold (Kammer & Nusseck, 1998, Kammer et al., 2005). Furthermore, it is entirely possible that the TMS-induced reduction in signal strength could be characterised as a deficit in a different stimulus characteristic, such as stimulus duration, but this is currently unknown, and will be investigated in the next chapter.

Chapter 7: Investigating orientation discrimination as a function of exposure duration

7.1 Introduction

One of the main findings of Chapter 6 was the presence of a contrast re-scaling of orientation discrimination thresholds for all participants in the TMS trials compared with the baseline (no-TMS) trials. This supports the idea that the affect of TMS on visual processing can be characterised as a reduction in effective stimulus contrast (Kammer et al., 2005; Harris et al., 2008). However, it is possible that this effect is a consequence of a TMS-induced reduction in the integrated energy of the visual stimulus in a more general manner than simply contrast reduction. For example, the visual response to a stimulus is related not only to contrast but also other factors such as duration, size and whether it is viewed monocularly or binocularly (Bearse & Freeman, 1994). Indeed, it has been shown that orientation discrimination is dependent on size (Westheimer, 1998) and duration (Bearse & Freeman, 1994; Zlatkova, Vassilev & Mitov, 2000). Consequently, it seems equally plausible that TMS might reduce the effective exposure duration of a stimulus: it is known that TMS temporarily disrupts neural function, for example, by causing a brief period of almost complete suppression of activity following a single TMS pulse (Moliadze et al., 2003). This interference with the ongoing temporal response could conceivably compromise the temporal integration of a stimulus.

A second reason why it is likely that the effect of TMS on visual processing cannot be described solely as just a reduction in effective stimulus contrast is that two participants of Experiment 10 demonstrated an upward (orientation) shift in function relating orientation JNDs to stimulus contrast in addition to the contrast re-scaling. The cause of the orientation shift is unclear. It was speculated in Chapter 6 that the orientation shift observed for participants RWD and KP could be the consequence of an injection of TMS-induced noise, such as uncorrelated neural firing, increased firing rate for stimuli in the periphery of the receptive field, or even a preferential response to non-optimal stimuli (Moliadze et al., 2003), as depicted in Figure 6.1.

Aims

The principle aim of the experiments contained within this chapter is to determine whether the modulation of visual processing by TMS can be described as a reduction in effective exposure duration. If TMS elicits a duration-based shift in orientation discrimination thresholds, it can be assumed that the reduction of stimulus energy by TMS is more general than a simple reduction in perceived contrast.

7.2 Experiment 11: A psychophysical investigation of orientation discrimination as a function of exposure duration

7.2.1 Introduction

The effect of exposure duration on sensitivity to visual stimuli, or in other words, temporal summation, depends on a number of factors such as stimulus area (Graham & Margaria, 1935; Barlow, 1958), background intensity (Barlow, 1958), spatial frequency (Tulunay-Keesey & Jones, 1976; Breitmeyer & Ganz, 1977; Legge, 1978), method of viewing, such as monocularly or binocularly (Bearse & Freeman, 1994), type of stimulus modulation such as contrast or luminance (Ledgeway & Hess, 2002), and task type, such as detection or discrimination (Zlatkova et al., 2002).

The period of temporal summation has been reported to vary for sinusoidal gratings of different spatial frequencies (Legge, 1978; Breitmeyer & Ganz, 1977). For example, Legge (1978) reported that at spatial frequencies of 1.5 c/deg or greater, contrast detection thresholds decreased as power functions of stimulus duration in two stages – a brief steep threshold decrease until approximately 100 ms to 200 ms, after which the decline was longer and shallower – and then reached an asymptotic level near 1000 ms. Below 1.5 c/deg, a similar brief and steep decline in threshold was observed, but threshold was independent of duration beyond 100 ms. Similarly, Breitmeyer & Ganz (1977) reported that the critical duration for temporal summation

increased from approximately 60 ms to 200 ms as spatial frequency increased from 0.5 c/deg to 16 c/deg. The variation in the duration of the temporal summation period is thought to provide support for the existence of sustained and transient mechanisms in human vision, on the assumption that transient and sustained channels operate at lower and higher spatial frequencies respectively (Tolhurst, 1975). These results therefore imply that transient channels have a shorter integration time than sustained channels. However, Tulunay-Keesey & Jones (1976) reported that contrast threshold decreased for any spatial frequency (between 1.5 c/deg and 10 c/deg) as a function of exposure duration up to 50 ms, after which there was a gradual decline in threshold until it become asymptotic at approximately 1000 ms. The disparity in these results is somewhat puzzling as the stimulus used by Tulunay-Keesey & Jones was smaller (3.8 deg by 2.9 deg) than those used by either Legge (10 deg diameter) or Breitmeyer & Ganz (4 deg by 6 deg), yet it is a well-documented phenomenon that the limit of temporal summation is reached earlier with a relatively large stimulus than with a smaller stimulus (Graham & Margaria, 1935; Barlow, 1958).

The period of temporal summation is inversely related to stimulus energy, and effective stimulus energy is assumed to be higher for stimuli of greater spatial extent, higher contrast, longer exposure duration, or when viewing is binocular as opposed to monocular (Bearse & Freeman, 1994). Binocular summation is an improvement in performance with binocular compared with monocular viewing, and is maximal at stimulus contrasts of around 1 % and absent at contrasts above approximately 30 % (Home, 1978). To determine whether

binocular summation is dependent only on stimulus contrast, or on the general integrated energy of the stimulus, Bearse & Freeman measured orientation discrimination thresholds for one-dimensional, difference-of-Gaussians (approximately 2 deg length, 0.4 deg width, dominant spatial frequency in cross-section was 5 c/deg) as a function of exposure duration and stimulus contrast. Binocular summation for briefly presented stimuli (50 ms) was greatest at low contrasts but orientation discrimination thresholds for monocular and binocular viewing were equal at contrasts above 15 %. More importantly, binocular summation for low contrast stimuli (8 %) was greatest at short stimulus durations, but there was no difference between monocular and binocular thresholds at durations of 100 ms or more. Therefore, binocular summation in orientation discrimination is greatest for low-energy stimuli. The shorter temporal summation period for binocular compared with monocular viewing is comparable to the shorter summation period for larger compared with smaller stimuli (e.g. Graham & Margaria, 1935; Barlow, 1958), as both effectively increase stimulus energy.

It has also been reported that temporal summation for orientation identification depends on the whether the task is a simple detection or a discrimination, and whether the discrimination judgment is coarse or fine (Zlatkova et al., 2000). In a series of experiments, Zlatkova and colleagues presented white bars to observers, which were of varying orientations compared to a reference stimulus. It was found that intensity-dependent (luminance) changes in reaction time were similar for detection tasks and coarse discrimination tasks (orientation difference of 15 deg or more between test and reference stimuli),

and that the temporal summation was similar for both tasks (approximately 30 ms). For the fine discrimination task (orientation differences less than 15 deg), there was a greater affect of stimulus intensity on reaction time, and the period of temporal summation was also increased compared with detection and coarse discrimination tasks (to approximately 100 ms). The temporal differences are proposed to provide support for differences in processing, for example, that the mechanism of fine identification requires additional processing that is not available immediately after stimulus presentation.

It can be seen from the reports discussed above that there are complicated interrelations between temporal summation and other stimulus properties, and that critical duration is variable depending on the task.

Aim

The aim of this initial experiment was to characterise the function relating orientation JNDs to stimulus duration.

7.2.2 Methods

7.2.2.1 Observers

The four observers (RWD, KP, LKS and PVM) who took part in this experiment had participated in Experiments 9 and 10. Participants RWD and KP were naïve as to the purpose of the experiment.

7.2.2.2 Visual Stimuli

Viewing was binocular at a distance of 192 cm. Visual stimuli were conventional Gabor patches, and consisted of oriented sinusoidal gratings (12 % Michelson contrast, 2 c/deg) presented within a Gaussian envelope (SD = 0.08 deg) on a mid-grey background (luminance = 73.52 cd/m^2). On each stimulus presentation, the spatial phase of the grating was selected randomly. Each Gabor was presented foveally in the centre of a black annulus, which was presented continuously (see Figure 5.3 in Experiment 8 for an example of an oriented Gabor stimulus). The participants were instructed to fixate at the centre of the annulus at the start of every trial to aid stable fixation and reduce any uncertainty concerning the location of the oriented stimulus. Gabors were presented for 853 ms, 427 ms, 213 ms, 107 ms, 80 ms, 53 ms, 40 ms, 27 ms and 13 ms, which corresponded to 64, 32, 16, 8, 6, 4, 3, 2 and 1 screen refresh respectively.

7.2.2.3 Psychophysics

A one-interval, two-alternative forced choice paradigm was employed in conjunction with the method of constant stimuli. Participants judged the orientation of the Gabor patch grating as either clockwise or anticlockwise of vertical. There was one of seven possible orientations on any one trial, centred around vertical, and the step size was tailored to each participant to produce an appropriate range of responses from 100 % to 0 % "clockwise" responses. In a single run of trials, each of the seven orientations was presented ten times, in a

random order. Four runs of trials (in total 280 trials) were completed by each participant for each stimulus duration.

7.2.3 Results and discussion

The percentage of "clockwise" responses was plotted as a function of Gabor orientation. Orientation JNDs were extracted using Equation 5.2 as in Experiment 8. Orientation JNDs were then plotted as a function of Gabor duration (Figure 7.1), and data were fitted with a two-limbed function (c.f. Burr & Santoro, 2001) of the form:

$$y = \left[\frac{\left(\mathrm{sgn}(a-x)+1\right)\left(\frac{a}{x}\right)^{c} + \mathrm{sgn}(x-a)+1}{2} \right] b \qquad (7.1)$$

where sgn is the signum function and is equal to either +1, 0 or -1 depending on whether the argument in the parentheses is >0, 0 or <0, respectively, *a* is the critical duration beyond which duration no longer limits performance, *b* is the minimum JND at which performance asymptotes, and *c* is the slope of the descending limb of the function (see Figure 7.1, top left).

It can be seen in Figure 7.1 that the JND data for all participants follow a similar trend: at the shortest durations tested, there is a steep decrease in JND as duration increases above 13 ms. When duration exceeds a particular value,

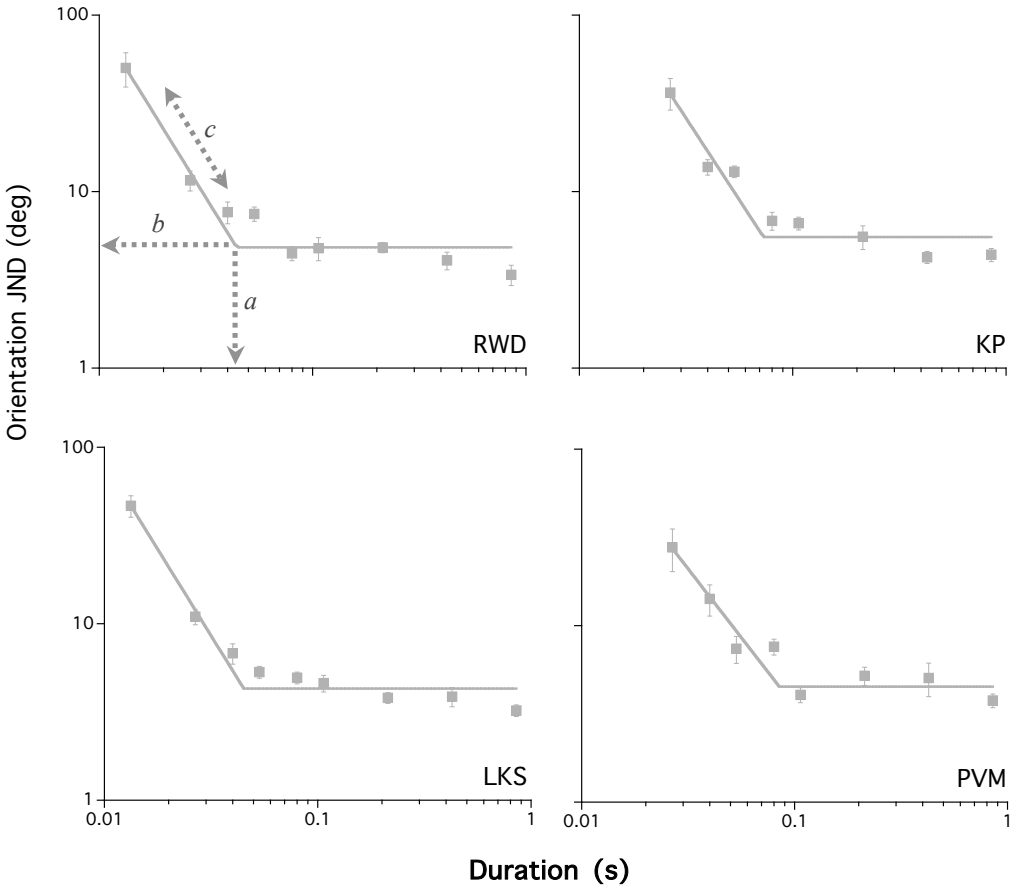

Figure 7.1. Orientation JNDs as a function of stimulus duration for four participants. All data have been fitted with Equation 7.1, shown as a solid line. After a critical duration (*a*), orientation discrimination reached a plateau and was not dependent on exposure duration (*b*). Before the critical duration, JNDs decreased steeply as duration increased (*c*). Error bars represent the SE.

however, performance becomes asymptotic, and is essentially invariant of stimulus duration. Note, data presented in Figure 7.1 are on logarithmic axes, which tend to compress differences at the higher values along the *y* axis and emphasise relatively modest differences at the lower values.

The critical durations for temporal summation (parameter *a* derived from Equation 7.1) for each participant in the present study are shown in Table 7.1. The critical durations for orientation discrimination temporal summation found in the present study (between 39 ms and 85 ms) fall within the range of those found in previous studies. For example, Bearse & Freeman (1994) found that using binocular viewing conditions, orientation discrimination thresholds were asymptotic at stimulus durations of 50 ms for one participant and 100 ms for the other two participants. For the "fine discrimination" condition in Zlatkova et al.'s investigation, the summation period for the two participants was 83 ms

Participant	***a*** Critical duration (s)	***a*** Critical duration SE (s)	***b*** Optimal JND (deg)	***b*** Optimal JND SE (deg)	***c*** Slope	***c*** Slope SE	R^2 of curve fit
RWD	0.044	0.005	4.836	0.643	1.957	0.148	0.992
KP	0.073	0.012	5.529	1.003	1.854	0.261	0.969
LKS	0.045	0.004	4.295	0.411	1.959	0.102	0.996
PVM	0.085	0.014	4.518	0.789	1.558	0.179	0.973

Table 7.1. Parameters extracted from the curve fit derived from Equation 7.1, describing the relationship between orientation discrimination and exposure duration for baseline (no-TMS) conditions.

and 100 ms. For orientation-detection tasks, Tulunay-Keesey & Jones (1976) reported the critical duration for temporal summation to be 50 ms, with a gradual decrease in threshold for up to 1 s, for all spatial frequencies (1 c/deg to 10 c/deg). Breitmeyer & Ganz (1977) tested a range of spatial frequencies, but for the spatial frequency (2.5 c/deg) most similar to that used in the present experiment (2 c/deg) their two participants demonstrated critical durations of 60 ms and 80 ms, after which performance was not dependent on exposure duration. Lastly, the critical durations for the most similar conditions to the present study (spatial frequency of 1.5 c/deg and 3 c/deg), reported by Legge (1978) were approximately 100 ms. As is the case in previous studies, the participants differ slightly in the extent of the dependence on the stimulus duration.

7.3 Experiment 12: The effects of TMS over area V1 on orientation processing as a function of stimulus duration

7.3.1 Introduction

Having characterised the relationship between orientation JNDs and exposure duration (Experiment 11), the mechanism behind TMS disruption to visual perception may be observed as shifts of the function relating orientation JND to stimulus duration. The present experiment is analogous in design to Experiment 10, in which the influence of TMS on orientation JNDs was investigated as a function of stimulus contrast. To briefly summarise the

results of Experiment 10, a contrast shift was observed for all four participants, which was interpreted as support for the theory that TMS reduces perceived stimulus contrast (Kammer & Nusseck, 1998; Kammer et al., 2005). However, the results of Experiment 10 do not eliminate the possibility that TMS instead disrupts the fidelity of other factors contributing to stimulus energy, such as duration or size, and that the effect is not in fact specific to contrast as previously suggested (Kammer et al., 2005; Harris et al., 2008).

If TMS affects visual processing by (say) reducing the effective exposure duration, it can be predicted that the relationship between orientation JNDs and stimulus duration for TMS trials would be well described by a rightwards shift along the duration axis of the same function measured in the absence of TMS. If, however, performance in TMS trials is limited by orientation uncertainty that is not related to the effective exposure duration, it can be predicted that this would be observed as an upwards shift of the function relating JND to stimulus duration along the orientation axis.

Aim

The aim of this experiment was to determine the affect that TMS has on the relationship between orientation discrimination and exposure duration.

7.3.2 Methods

7.3.2.1 Observers

The same four observers who took part in Experiment 11 participated in this experiment.

7.3.2.2 Visual Stimuli and procedure

The visual stimuli used in the present experiment were identical to those employed in Experiment 11. Four runs of trials (in total 280 trials) were completed by each participant for every stimulus duration.

7.3.2.3 TMS procedure

The 90 mm high-power circular coil was positioned over area V1, as described in Experiment 8 (Chapter 5). Single pulses were delivered at 90 % of maximum field strength (1.8 T) at a rate of once per Gabor stimulus presentation. Pulses were delivered 107 ms after onset of the visual stimulus, as in Experiments 8 and 10. At the end of each trial, the participant was required to make an orientation judgment (clockwise or anticlockwise of vertical) via a button press. There was then a 2.5 s delay between the participant's response and the start of the next trial. Sessions were run in blocks of 70 stimulus presentations, each lasting approximately 4 mins. This effective rate of stimulation is well within the safety guidelines for rate of

stimulation (Wassermann, 1998). Participants completed 36 blocks each, with a maximum of four blocks in one day.

7.3.3 Results and discussion

Orientation JNDs were extracted using Equation 5.2, as in Experiment 8, and plotted as a function of stimulus duration (Figure 7.2). Data were fitted with Equation 7.1. Figure 7.2 shows the data for TMS trials, and also baseline (no-TMS) data re-plotted from Experiment 11 as a comparison. It can be seen in Figure 7.2 that there is a lateral (rightwards) shift of the function relating JND to exposure duration along the duration axis, in TMS trials compared to baseline trials, for all participants. This is consistent with the idea that TMS interrupts temporal integration of a visual stimulus, and effectively reduces exposure duration. The critical duration for temporal summation in TMS trials compared to control conditions increased by 19 ms and 21 ms for participants LKS and PVM respectively (see Table 7.2), and continued to decrease up to the highest exposure duration tested (853 ms) for participants RWD and KP, although thresholds for TMS trials were gradually approaching those of control trials at the higher durations (Figure 7.2). The shape of the response function relating orientation JND to exposure duration for participants RWD and KP resembles those described by Legge (1978) and Tulunay-Keesey & Jones, 1976): both of those studies found that detection thresholds for sinusoidal gratings decrease steeply over lower stimulus durations, then have a more gradual decline until approximately 1 s, after which performance ceased to be dependent on stimulus duration. An upward shift of the function relating

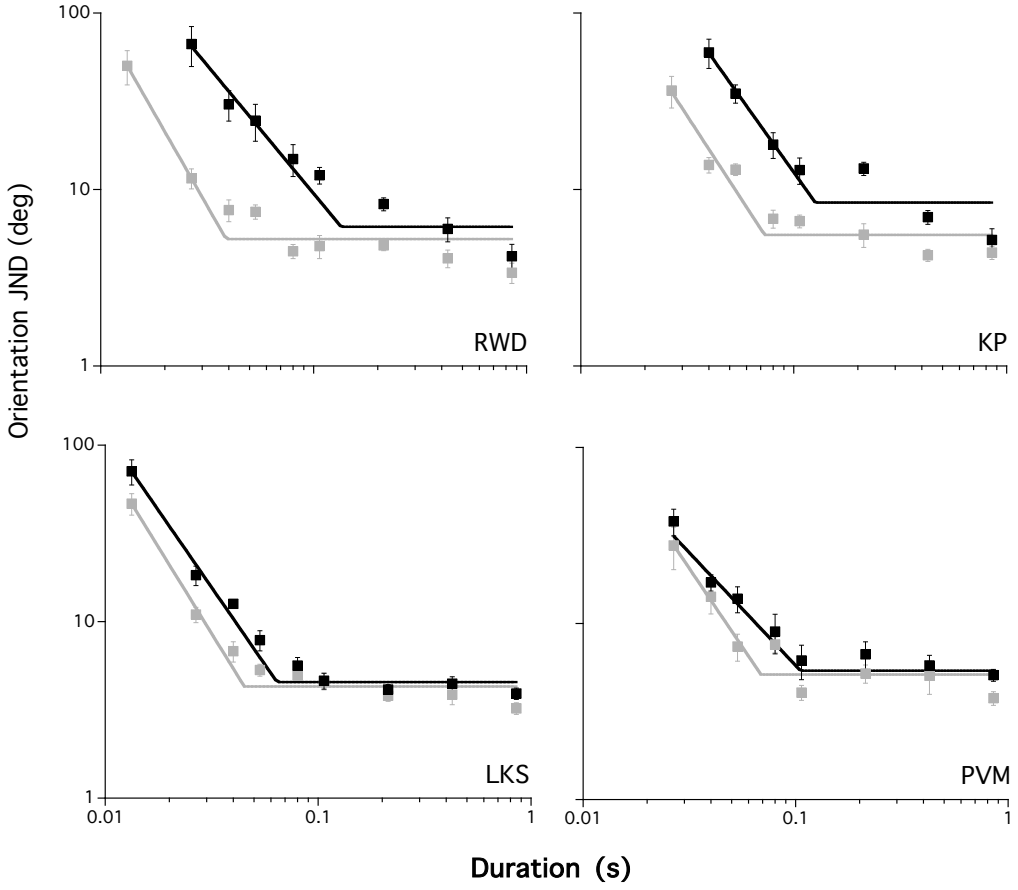

Figure 7.2. Orientation JNDs as a function of stimulus duration for four participants during TMS trials. Performance in TMS trials (black symbols) is impaired compared to no TMS trials (grey symbols: data from Experiment 11 is re-plotted for purposes of comparison). All data have been fitted with Equation 7.1, shown as a solid line. It can be seen that a rightwards shift along the duration axis is present for all four participants for the TMS compared to the baseline condition. For participants RWD and KP, performance with TMS does not reach baseline levels, but gradually decreases as a function of exposure duration. Error bars represent the SE.

orientation JND to duration along the orientation axis was also observed for participants RWD and KP for the TMS conditions compared with the control conditions, although this may be caused in part by the fact that performance may not have reached asymptotic levels in the TMS trials for the durations tested here. The data for individual participants presented in Figure 7.2 show similarities to the data presented in Figure 6.5 in Experiment 10 (Chapter 6), where orientation discrimination was measured as a function of stimulus contrast. In both the present experiment and Experiment 10, the relationship between orientation discrimination and signal strength (contrast or duration) has been re-scaled to a higher signal strength for all four participants, and also upward along the orientation axis for participants RWD and KP for TMS trials compared to control conditions.

Participant	***a*** Critical duration (s)	***a*** Critical duration SE (s)	***b*** Optimal JND (deg)	***b*** Optimal JND SE (deg)	***c*** Slope	***c*** Slope SE	R^2 of curve fit
RWD	0.135	0.035	6.147	1.978	1.454	0.140	0.980
KP	0.126	0.022	8.436	1.825	1.694	0.186	0.983
LKS	0.064	0.008	4.551	0.752	1.747	0.086	0.995
PVM	0.106	0.024	5.395	0.331	1.280	0.296	0.943

Table 7.2. Parameters extracted from the curve fit derived from Equation 7.1, describing the relationship between orientation discrimination and exposure duration for the TMS conditions.

Figure 7.3 demonstrates the relationship between the orientation and duration shifts for each participant. The duration shift in orientation JND for TMS trials compared to baseline trials is represented along the *x* axis, and is determined by the ratio:

$$\frac{TMSa}{BLa} \tag{7.2}$$

where *TMSa* and *BLa* are the critical durations (*a*) as extracted from the curve fit derived from Equation 7.1 for the TMS and the baseline (no-TMS) conditions, respectively.

The orientation shift represented along the *y* axis, determined by the ratio:

$$\frac{TMSb}{BLb} \tag{7.3}$$

where *TMSb* and *BLb* are the optimal orientation JNDs (*b*) as extracted from the curve fit derived from Equation 7.1, for TMS and baseline conditions respectively. If either ratio equals 1, the values derived for the baseline and the TMS conditions are equal and there is no shift. If the resulting ratio is greater than 1, then the value derived for the TMS condition is greater than that for the baseline condition, and the opposite is true if the value is less than 1. It can be seen in Figure 7.3 that all participants show duration shifts of varying degrees.

Participants RWD and KP have greater duration shifts than the other participants. Participants RWD and KP also demonstrate an orientation shift, although this is not as large as the duration shift for these two participants. Little on no orientation shift is present for observers LKS and PVM.

As all of the participants of this experiment demonstrate a duration shift of some degree, this supports the theory that TMS reduces the integrated energy of a visual stimulus in a more general manner than the simple contrast reduction account proposed by Kammer & Nusseck (1998) and Kammer et al. (2005). However, these data also suggest the presence of an orientation shift

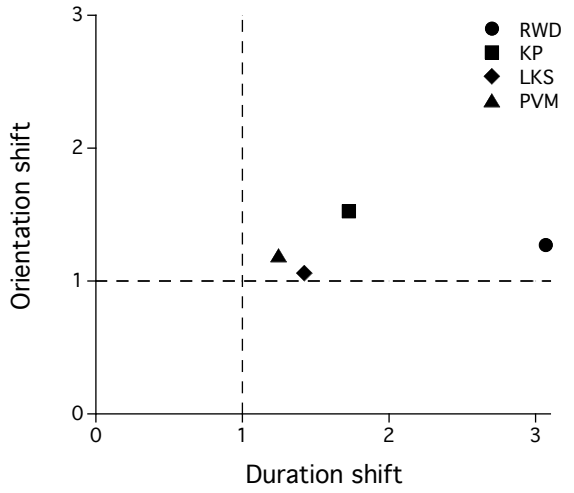

Figure 7.3. The relationship between the orientation shift and the duration shift in JND data for TMS vs. baseline trials. A duration shift of 1 (shown by the vertical broken line) indicates that the critical duration (*a* in Equation 7.1) was equal for the two conditions, a duration shift higher than 1 indicates that the critical duration was higher in the TMS condition and the opposite is true if the value lower than 1. An orientation shift of 1 (shown by the horizontal broken line) indicates that optimal orientation JNDs (*b* in Equation 7.1) were equal for the two conditions; an orientation shift higher than 1 indicates that performance was worse in the TMS condition, and the opposite is true if the value is lower than 1.

for two observers, which might not be overcome by increasing the stimulus duration. Interestingly, the two observers whose JNDs do not return to baseline levels in the current experiment also demonstrated an orientation shift in TMS trials in Experiment 10.

7.4 Experiment 13: A psychophysical investigation of orientation processing as a function of stimulus duration for low contrast stimuli

7.4.1 Introduction

It was reported in Experiment 10 that the effect of TMS on visual processing can, in part, be characterised as an increase in contrast threshold, although two participants showed an increase in orientation JND that could not be accounted for by a TMS-induced contrast deficit. In Experiment 12 it was reported that the effect of TMS could be characterised as a decrease in the effective exposure duration, although data for two participants suggested that the increase in orientation JND might not be entirely accounted for by a duration-based deficit to performance. Taken together, these results suggest that the effect of TMS on visual processing might be a general reduction of the stimulus energy, rather than a specific reduction of perceived contrast.

It has been suggested that Bloch's Law, which formally states that Luminance x Duration = Constant, can be applied to stimulus contrast, rather than

luminance *per se* (e.g. Breitmeyer & Ganz, 1977; Tulunay-Keesey & Jones, 1976). Due to the reciprocal nature of stimulus strength (contrast or luminance) and duration in terms of detection thresholds, it is possible that the duration-based shift observed in Experiment 12 might in fact be caused indirectly by a TMS-induced reduction in perceived contrast. For example, if TMS reduced the perceived contrast this would result in stimuli effectively having a lower stimulus energy, which results in a longer temporal integration period (e.g. Graham & Margaria, 1935; Barlow, 1958; Bearse & Freeman, 1994). Importantly, this would be observed as a duration-based shift of the relationship between orientation JND and exposure duration in TMS trials.

To establish how the relationship describing orientation JND to exposure duration would change with a reduction in the effective contrast, orientation JNDs were measured for all stimulus durations used in Experiments 11 and 12 for stimuli of a lower contrast (in the absence of TMS).

7.4.2 Methods

7.4.2.1 Observers

The same four observers who took part in Experiments 11 and 12 also participated in the present experiment.

7.4.2.2 Visual Stimuli and psychophysics

All stimulus parameters were identical to those described in Experiment 11, except for the Gabor carrier grating contrast, which was reduced by approximately half to 5.8 % in the present experiment (c.f. 12 % in Experiments 11 and 12). The step size was tailored to each participant to produce an appropriate range of responses from 100 % to 0 % "clockwise" judgements. Four runs of trials (in total 280 trials) were completed by each participant for each stimulus duration.

7.4.3 Results and discussion

The percentage of "clockwise" responses was plotted as a function of Gabor orientation, and orientation JNDs were extracted using Equation 5.2, as in Experiment 8. Orientation JNDs were then plotted as a function of Gabor duration (Figure 7.4), and data were fitted with Equation 7.1. Figure 7.4 shows the data collected in the present experiment for lower contrast (5.8 %) stimuli, with the baseline and TMS data for higher contrast (12 %) stimuli from Experiments 11 and 12, plotted for purposes of comparison. It can be seen in Figure 7.4 that the JNDs are translated along both the duration and the orientation axes for the low contrast (5.8 %) condition, compared with the high contrast (12 %) no-TMS condition for all participants. An upward shift of JND data is also shown by all participants in the 5.8 % contrast condition compared with the TMS condition (which were collected at 12 % contrast).

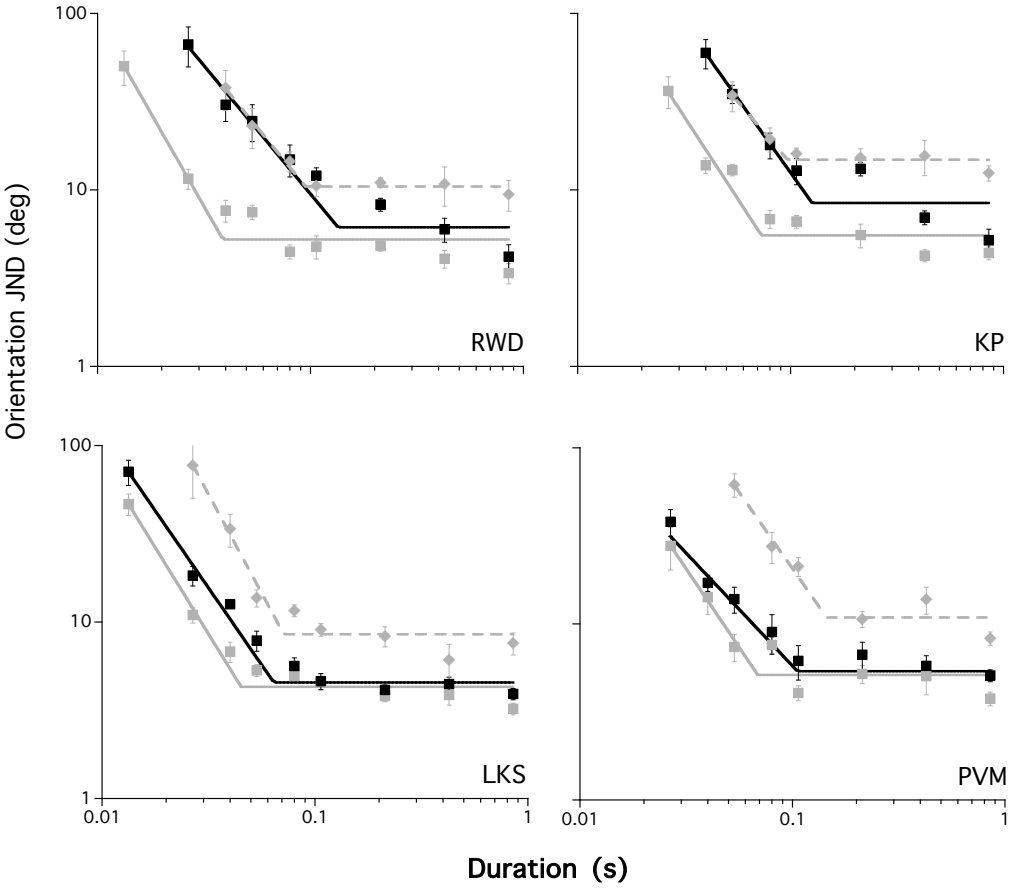

Figure 7.4. JNDs for orientation discrimination as a function of stimulus duration for four participants for lower contrast (5.8 %) stimuli. Performance in lower-contrast trials (grey diamonds, broken line) is impaired compared to 12 % contrast baseline conditions (grey squares, unbroken line: re-plotted from Experiment 11 for purposes of comparison) and TMS conditions (black squares, unbroken line: re-plotted from Experiment 12 for comparison). All data have been fitted with Equation 7.1. Error bars represent the SE.

Interestingly, for participants RWD and KP, reducing the contrast of the stimuli resulted in a shorter period of temporal summation to that found when the higher contrast stimuli were used in conjunction with TMS. For example, it can be seen in Table 7.3 that the critical durations (*a*) for participants RWD and KP for the low contrast conditions were 97 ms and 95 ms, and in the TMS conditions they were 135 ms and 126 ms respectively (Table 7.2), but without TMS they were 44 ms and 73 ms (Table 7.1) for the higher contrast. This demonstrates that the effect of both TMS and contrast reduction is to produce a duration shift of the relationship between JND and exposure duration. However, reducing the contrast of the stimulus produces an orientation shift that could not be overcome by additional temporal summation, that is, the optimal JND threshold was higher for lower contrast stimuli.

Participant	***a*** Kneepoint (s)	***a*** Kneepoint SE (s)	***b*** Optimal JND (deg)	***b*** Optimal JND SE (deg)	***c*** Slope	***c*** Slope SE	R^2 of curve fit
RWD	0.095	0.006	10.445	0.554	1.473	0.113	0.992
KP	0.097	0.009	14.829	0.806	1.407	0.235	0.975
LKS	0.071	0.006	8.533	1.096	2.243	0.157	0.993
PVM	0.144	0.021	10.896	1.861	1.730	0.207	0.984

Table 7.3. Parameters extracted from the curve fit derived from Equation 7.1, describing the relationship between orientation discrimination and exposure duration for low-contrast baseline (no-TMS) conditions.

Figure 7.5a shows the relationship between the duration (*a*) and orientation (*b*) shifts (as derived from Equation 7.1) for each participant for 5.8 % contrast vs. 12 % contrast baseline conditions. The ratios are calculated in a similar manner as shown for Figure 7.3. Figure 7.5b shows the relationship between the duration and orientation shifts for 5.8 % contrast vs. TMS conditions, calculated in the same way.

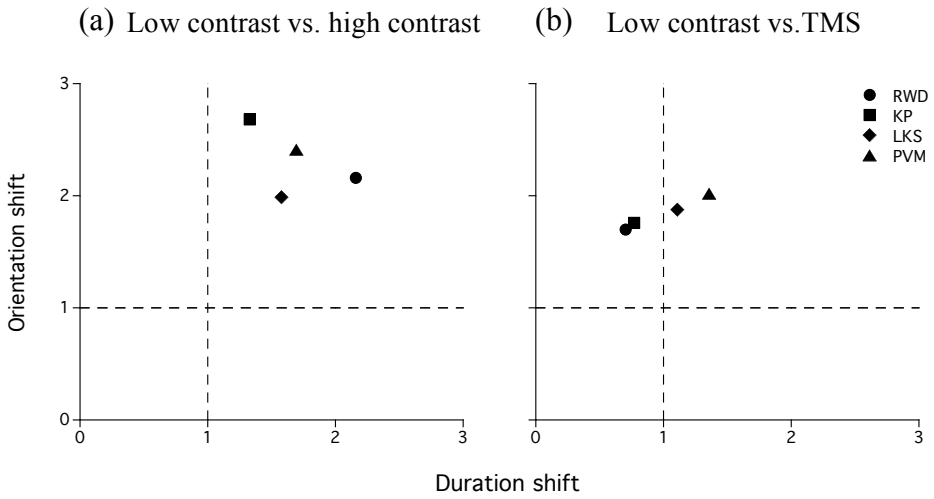

Figure 7.5. The relationship between the orientation shift and the duration shift of the function relating JND to exposure duration for lower contrast (5.8 %) no-TMS trials vs. higher contrast (12 %) no-TMS trials (a), and lower contrast no-TMS trials vs. higher contrast TMS trials (b). A duration shift of 1 (shown by the vertical broken line) indicates that the critical duration (*a* in Equation 7.1) was equal for the two conditions, a duration shift higher than 1 indicates that the critical duration was higher in the lower contrast condition and the opposite is true if the value lower than 1. An orientation shift of 1 (shown by the horizontal broken line) indicates that optimal orientation JNDs (*b* in Equation 7.1) were equal for the two conditions; an orientation shift greater than 1 indicates that performance was worse in the lower contrast condition, and the opposite is true if the value is less than 1.

It can be seen in Figure 7.5 that as expected, data from the lower contrast (5.8 %) condition are shifted along both the orientation and duration axes compared to the higher contrast (12 %) condition (a). The lower stimulus energy of the 5.8 % contrast low contrast condition is likely to result in a longer temporal summation period, which may be observed as a duration shift in orientation JNDs (Barlow, 1958; Bearse & Freeman, 1994). The shift along the orientation axis for low contrast JNDs is likely to be a result of the increased orientation ambiguity caused by the marked decrease in stimulus contrast/visibility, which cannot be overcome by increasing stimulus duration.

When data from the lower contrast condition are compared with TMS data (collected at 12 % contrast), it can be seen that the largest shift is along the orientation axis for all participants. The critical duration is reduced in the lower contrast compared to the TMS conditions (shown by a duration shift of less than 1) for participants RWD and KP, but is increased for participants LKS and PVM.

The fact that optimum orientation JNDs are lower for the TMS conditions than the 5.8 % contrast condition, even though the temporal summation period seems to be longer, could be due to the effect of the brief TMS pulse dissipating over the time course of the stimulus, and consequently modulating only part of the response to the visual stimulus. This could go some way toward explaining the extended period of temporal summation observed for participants RWD and KP in Experiment 12.

7.5 Experiment 14: Investigating the effect of reducing TMS field strength on orientation discrimination

7.5.1 Introduction

The results of Experiments 10 and 12, demonstrate that TMS appears to influence orientation discrimination in two ways. Firstly, a stimulus intensity (contrast or duration) shift was observed for all participants for all conditions. Secondly, an overall orientation threshold shift was observed for two participants (KP and RWD). Magnetic field strength was also found to influence orientation discrimination, as demonstrated in Experiment 8, whereby there was little or no affect of TMS on orientation JNDs at field strengths below approximately 1.6 T (80 % maximum field strength). When TMS field strength was increased above 1.6 T, however, orientation discrimination thresholds increased steeply as a function of field strength for two participants (RWD and KP), or more gradually for two other participants (LKS and PVM) [see Figure 5.4, Experiment 8]. As participants RWD and KP appear to have considerably higher sensitivity to TMS field strength than the other participants, the aim of the current experiment was to investigate whether this contributed to the orientation-based shifts observed in Experiments 10 and 12.

7.5.2 Methods

7.5.2.1 Observers

Two observers who were naïve as to the goals of the study, KP and RWD, took part in this experiment.

7.5.2.2 Visual Stimuli and psychophysics

Visual stimuli (Gabor patches of 12 % Michelson contrast) and procedures were identical to those employed in Experiments 11 and 12. Four runs of trials (in total 280 trials) were completed by each participant for each stimulus duration. Sessions were run in blocks of 70 stimulus presentations. In total, participants completed 28 blocks each, with a maximum of four blocks in one day.

7.5.2.3 TMS procedure

Area V1 was localised as described in Experiment 7, and single TMS pulses were delivered 107 ms after stimulus onset at 1.6 T (80 % maximum field strength) [c.f. Experiments 10 and 12, where TMS was delivered at 1.8 T (90 % maximum field strength)]. This field strength was selected as it fell on the rising part of the curve relating magnetic field strength to orientation discrimination (Figure 5.4, Experiment 8).

7.5.3 Results and discussion

Orientation JNDs were extracted using Equation 5.2, as in Experiment 8, and plotted as a function of stimulus duration (Figure 7.6). Data were fitted with Equation 7.1. It can be seen in Figure 7.6 that there is a duration-based shift in the relationship between orientation discrimination and exposure duration for lower field strength (1.6 T) TMS trials compared with baseline (no-TMS) trials. The critical duration has increased from 44 ms and 73 ms for baseline conditions, to 104 ms and 120 ms for 1.6 T TMS conditions for participants RWD and KP respectively (see Table 7.4). However, the critical duration is marginally lower than observed when TMS was delivered at 1.8 T (Experiment 12), where critical durations were 135 ms and 126 ms for RWD and KP, respectively. More importantly, there is little or no orientation shift for 1.6 T TMS trials compared with baseline trials – optimal JNDs for RWD and KP are similar in 1.6 T TMS trials (5.430 deg and 5.561 deg) to those measured in the absence of TMS (4.836 deg and 5.529 deg).

Figure 7.7 demonstrates the relationship between the duration (*a*) orientation (*b*) shifts (as derived from Equation 7.1) for each participant for 1.6 T TMS condition vs. baseline conditions in the absence of TMS. The ratios were calculated as shown for Figure 7.3 in Experiment 11. It can be seen in Figure 7.7 that data collected at 1.6 T magnetic field strength for participants RWD and KP demonstrates a duration shift in the relationship between threshold and duration compared to no-TMS conditions, but little or no orientation shift, unlike data collected at 1.8 T field strength.

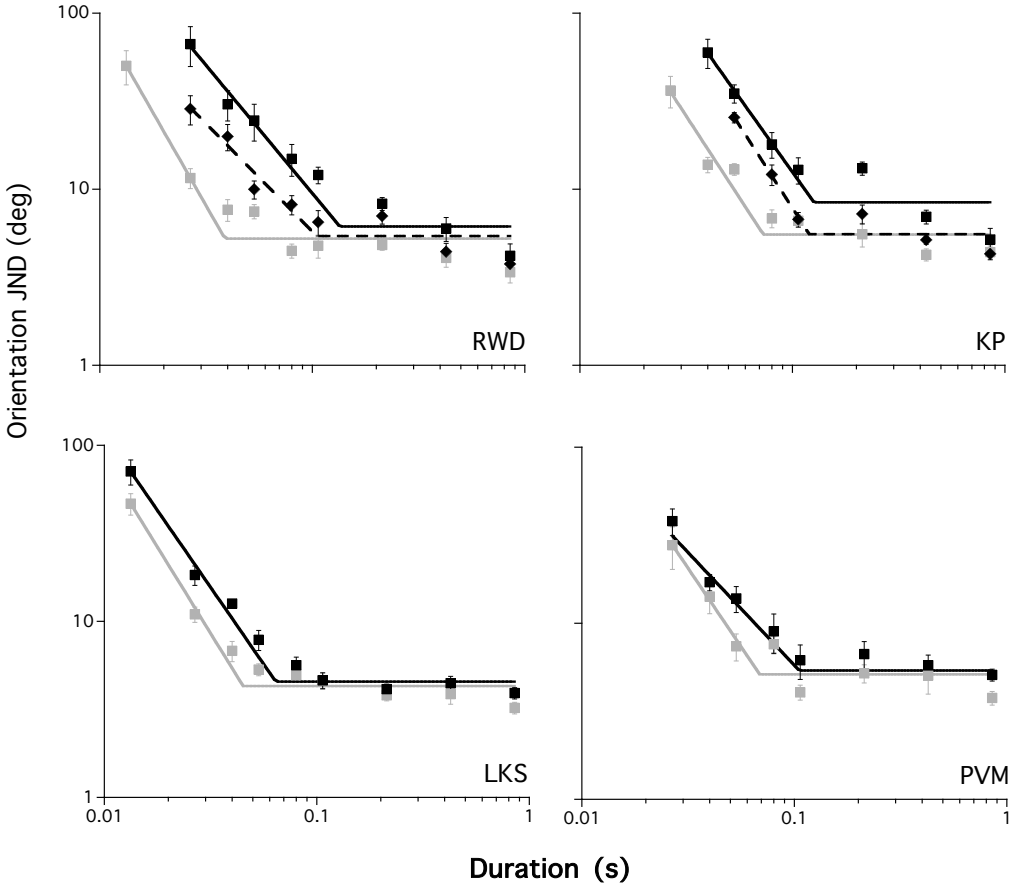

Figure 7.6. JNDs for orientation discrimination as a function of stimulus duration for participants RWD and KP during reduced field strength (1.6 T) TMS trials. Data for participants LKS and PVM are re-plotted from Experiments 11 and 12 for purposes of comparison. All data have been fitted with Equation 7.1. For RWD and KP, performance in lower field strength (1.6 T) TMS trials (black diamonds, broken line) is shifted along the duration axis (*a* in Equation 7.1) compared to baseline (no-TMS) trials (grey squares and line), but the duration shift is not as large as in higher field strength (1.8 T) trials (black squares and solid line). Furthermore, there is little or no orientation shift (*b* in Equation 7.1) in 1.6 T TMS trials compared with baseline trials. Error bars represent the SE.

Participant	***a*** Kneepoint (s)	***a*** Kneepoint S.E. (s)	***b*** Optimal JND (deg)	***b*** Optimal JND S.E. (deg)	***c*** Slope	***c*** Slope S.E.	R^2 of curve fit
RWD	0.104	0.023	5.430	0.981	1.225	0.171	0.964
KP	0.120	0.013	5.561	0.720	1.883	0.206	0.985

Table 7.4. Parameters extracted from the curve fit derived from Equation 7.1, describing the relationship between orientation discrimination and exposure duration for lower field strength (1.6 T, 80 % maximum field strength) TMS trials.

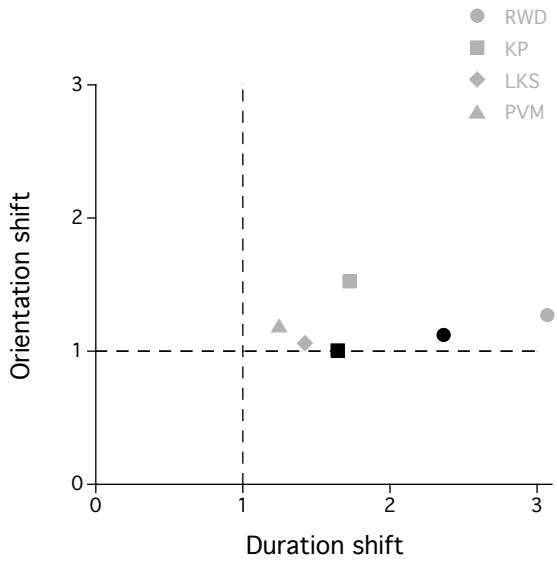

Figure 7.7. The relationship between the orientation shift and the duration shift for orientation JNDs for 1.6 T field strength vs. baseline conditions (black symbols). Data collected with 1.8 T field strength (grey symbols) are re-plotted from Experiment 12 for purposes of comparison.

Taken together, the results of the current experiment and those of Experiment 12 indicate that the affect of TMS on orientation discrimination – whether it is characterised by a duration or an orientation shift – is separable depending on the magnetic field strength, and sensitivity to field strength. For example, whereas participants RWD and KP demonstrated orientation shifts in addition to duration shifts when TMS was delivered at 1.8 T, only duration shifts were observed when TMS was delivered at 1.6 T. As only duration shifts were observed for participants PVM and LKS when TMS was delivered at 1.8 T, and given the decreased sensitivity of these participants to TMS field strength (Experiment 8), it seems plausible that some individuals are more sensitive to TMS than others. Indeed, this is a common speculation in TMS studies of visual perception (e.g. Masur et al., 1993; Kastner et al., 1998; Sack et al., 2006; Harris et al., 2008), but the perceptual outcome has not been characterised previously.

7.6 General discussion

The main findings of the experiments reported in this chapter (Experiments 11 to 14) are as follows: firstly, the relationship between orientation discrimination and exposure duration in baseline (no-TMS) trials was similar to that reported by previous studies, in that performance improved as stimulus duration increases until a critical duration is reached, after which performance was invariant to changes in duration (Tulunay-Keesey & Jones, 1976; Breitmeyer & Ganz, 1977; Legge, 1978; Loshin & Jones, 1982; Bearse &

Freeman, 1994; Savage, 1996). When TMS was delivered over area V1, there was a temporal re-scaling of the orientation JND vs. duration function. Two participants (LKS and PVM) demonstrated a moderately increased critical duration – where performance changes from being duration-dependent, to effectively duration-independent – in TMS conditions compared with baseline conditions. This is consistent with the theory that TMS effectively reduces the encoded stimulus energy. For example, a duration re-scaling effect has been reported when stimulus energy is decreased, such as when stimulus size (Graham & Margaria, 1935; Barlow, 1958) or luminance (Savage, 1996) is reduced, or when viewing is monocular (Bearse & Freeman, 1994). Two other participants (RWD and KP), however, demonstrated a much larger increase in critical duration in TMS conditions compared with baseline (no-TMS) conditions, with a gradual transition from descending to asymptotic thresholds. A gradual change in threshold as a function of stimulus duration has been previously reported: Tulunay-Keesey & Jones (1976) reported that sensitivity to vertically-oriented sinusoidal gratings initially increased rapidly as a function of stimulus duration, but when duration was greater than approximately 50 ms to 100 ms, sensitivity increased gradually up to around 1 s, after which performance was asymptotic. It has similarly been reported that thresholds for detecting sinusoidal gratings of between 1.5 c/deg and 12 c/deg decrease as a function of duration in two stages: firstly, a brief period of steeply decreasing threshold as duration increases to between approximately 80 ms to 150 ms (depending on spatial frequency), followed by a longer secondary decline in threshold until around 1 s when performance becomes asymptotic (Legge, 1978). The steep threshold decrease is attributed by Legge

to temporal summation, whereas the gradual decline is attributed to probability summation. The theory of probability summation dictates that noise may influence the visibility of a temporally extended signal, by influencing the probability that the threshold will be exceeded in each instant. The overall probability that the stimulus is detected must therefore take into account all of the momentary probabilities (Watson, 1979). As it is known from single cell studies of feline visual cortex that TMS evokes a complex pattern of increased firing and suppression (Moliadze, et al., 2003), it seems plausible that the gradual decrease in orientation JND over an extended period (as is observed for participants RWD and KP in Experiment 12) is related to TMS-induced noise, and can be explained by probability summation. However, only two participants appear to exhibit a longer, gradual increase in sensitivity in the TMS conditions, whereas the other two participants' performance reaches baseline (no-TMS) levels at much shorter stimulus durations, by comparison.

The increased temporal summation period observed in TMS trials for participants RWD and KP was also apparent when compared with data collected at a lower contrast (5.8 % compared with 12 % contrast). The fact that the critical duration was longer in TMS trials – at a higher contrast – makes it likely that TMS can be characterised as a reduction of stimulus energy, as stimuli with lower energy typically give rise to longer integration periods (e.g. Graham & Margaria, 1935; Barlow, 1958). Although this could, in theory, be caused indirectly by a TMS-induced reduction of effective stimulus contrast, it is unlikely that the influence of TMS on visual processing can be entirely accounted for by a reduction of contrast as the data in

Experiment 10 demonstrate an upwards shift in threshold that cannot be overcome by increasing stimulus contrast. Furthermore, as the two participants who showed an orientation shift also demonstrated a similar effect in Experiment 12 (which measured orientation JNDs as a function of duration), and who were also more sensitive to magnetic field strength (Experiment 8), it is plausible that participants RWD and KP were more sensitive to TMS-induced "noise", rather then just a reduction in signal strength.

Chapter 8: General discussion

8.1 Summary of main findings

8.1.1 Two critical periods for V5/MT disruption

The results of Experiment 2 clearly revealed two distinct epochs during which delivery of single-pulse TMS (1.8 T) to area V5/MT disrupted translational global motion processing: an *early* period which was centred, on average, 64 ms prior to the onset of global motion, and a *late* period which occurred approximately 146 ms after the onset of global motion. Two other studies have also reported two critical periods during which delivery of a TMS pulse over area V5/MT impairs the ability to discriminate the direction of translational global motion (Sack et al., 2006; Laycock et al., 2007). However, there are marked differences in the methodology and interpretation between these studies and the experiments described in Chapter 3 (Experiments 1, 2, 3 and 4). Sack and colleagues (2006) reported significantly impaired performance when TMS was delivered between 30 – 40 ms prior to, and also 130 – 150 ms following global motion onset. The authors attributed the later deficit to the direct disruptive action of TMS on the cortical processes mediating motion processing in area V5/MT, and the earlier period to an eyeblink artefact – although they provide no evidence to support this. Laycock and colleagues (2007) reported significantly reduced accuracy on a global direction discrimination task when TMS was delivered over area V5/MT between -42

ms and +10 ms, and also +158 ms relative to global motion onset, although notably in their second experiment the later disruption window was not replicated. Laycock et al. attributed the later deficit to the disruption of feedback signals from higher cortical regions to area V5/MT. The earlier period was attributed to either a disruption in attention/expectation, or disruption of the rapid propagation of motion signals via a direct pathway to V5/MT, which bypasses area V1.

8.1.2 Interpretation of the early *temporal window*

Importantly, Experiment 3 in Chapter 3 provided evidence that the *early* period of disruption cannot be attributed to an eye-blink artefact. This has not before been investigated, but has been widely assumed to be the cause of an *early* temporal disruption period (e.g. Sack et al., 2006; Corthout et al., 2000; Corthout et al., 2003). The evidence that the *early* period was not caused by muscular artefact has implications for the theoretical relevance of this temporal window. Laycock and colleagues speculated that the *early* period was caused by disruption in V5/MT of rapidly propagated motion signals, transmitted via a direct pathway from sub-cortical structures such as the LGN and pulvinar directly to area V5/MT. However, this seems unlikely, as evidence suggests that a direct pathway in humans is only activated by relatively high-speed motion of greater than ~ 20 deg/s (ffytche et al., 1995; Holliday et al., 1997; Azzopardi & Cowey, 2001), if at all (Anderson et al., 2001). Laycock et al. offer an alternative explanation for the earlier period of disruption – that TMS disrupts attention/expectation. However, this explanation is ruled out by the

results of Experiment 3 in Chapter 3, in which delivery of TMS over a control site failed to produce a disruption to performance.

To explain the *early* temporal window it is suggested in Chapter 3 of this thesis that the effects of the TMS pulse delivered over area V5/MT propagate back down to V1 via feedback connections, and disrupt the feedforward sweep at 'lower' levels in the motion processing hierarchy. The *early* window is temporally much broader, and the performance deficit is much greater, than that which occurs later. This is consistent with the idea that the effects of TMS spread to functionally connected areas (e.g. Ilmoniemi et al., 1997; Paus et al., 1997; Bohning et al., 1999). For example, in macaques, area V5/MT has strong feedback connections to many visual areas and sub-cortical structures such as the LGN and pulvinar (see Felleman & Van Essen, 1991). It therefore seems feasible that the fidelity of the motion signal is disrupted in multiple areas – including V1 – by a TMS pulse, giving rise to a larger performance deficit. Indeed, TMS delivered after the motion signal has been encoded in a particular visual area is unlikely to have as large an effect on motion perception, as the relevant information will already have been transmitted to the next stage of visual analysis. Furthermore, it is possible that the effects of TMS at multiple cortical sites are additive, which might result in a broader temporal envelope. Additionally, it is unknown whether the effects of TMS are related to the volume of cortical tissue they act on, for example, V1 is reported to be the largest single cortical area (see Felleman & Van Essen, 1991) and it is feasible that the 'reverberating volleys' are active for longer due to the many horizontal connections within area V1.

8.1.3 Effect of stimulus contrast on V5/MT disruption

Variations in critical temporal windows have previously been explained in terms of differences in stimulus parameters (see Sack et al., 2006; Laycock et al., 2007), however, the effect of stimulus contrast on TMS-induced disruption of motion processing in area V5/MT had not been previously reported. Experiment 4 of this thesis revealed that when global motion stimuli were presented at a lower contrast (0.03 Weber contrast), the *late* temporal window was shifted by approximately 40 ms compared to the higher contrast condition (0.99 Weber contrast), to occur approximately 180 ms after global motion onset. This implies that lower contrast stimuli give rise to longer activation latencies in V5/MT, and goes some way toward explaining the variation in temporal disruption windows reported in previous studies.

Compared to the higher contrast condition, the deficit to performance when TMS is delivered within the *early* temporal window was much greater in the lower contrast condition. This may partly be because V1 cells are sensitive to contrast (e.g. Dean, 1981; Albrecht & Hamilton, 1982; Sclar, Maunsell & Lennie, 1990; Carandini, Heeger & Movshon, 1997) – the *late* period does not demonstrate such a change in deficit, which may be because V5/MT cells area relatively contrast insensitive (e.g. Nakayama, 1985). This also provides further evidence that the *early* period is due to a disruption of cortical processes, as if it were simply the result of TMS-induced eye blinks, changing a stimulus characteristic (e.g. contrast) should not lead to a more severe deficit in performance.

8.1.4 Disruption of complex global motion perception

It is widely assumed that optic flow patterns are analysed in cortical areas distinct from those involved in translational global motion perception (e.g. Tanaka et al., 1989; Duffy & Wurtz, 1991a; Duffy & Wurtz, 1991b; Delon-Martin et al., 2006). As the affect of single-pulse TMS delivered over area V5/MT on components of optic flow patterns had not been previously reported, this was investigated in Chapter 4 of this thesis. The results of Experiment 6 clearly revealed two separate and distinct epochs during which delivery of single-pulse TMS (1.6 T) to area V5/MT disrupted rotational and radial global motion processing, and these were similar in latency and duration to those observed in Experiment 2, with translational global motion. Although neuroimaging studies have revealed an area within the V5/MT complex (medial superior temporal area, or MST) that responds selectively to components of optic flow, and is separate and distinct to an area that responds selectively to translational global motion (e.g. Morrone et al., 2000), it is highly likely that the spatial resolution of TMS is too course to stimulate each region separately. It has also been reported, however, that human V5/MT also shows weak selective responses to specific optic flow structures (Smith et al., 2006; Wall et al., 2008), and it is possible that some of this apparent specificity to optic flow in V5/MT is inherited from feedback connections from MST. Consequently the *late* period may reflect a feedback "loop" between V5/MT and MST.

8.1.5 Sensitivity to magnetic field strength

Experiment 7 revealed that phosphene threshold varied moderately between participants, as has been found in previous studies (e.g. Kammer et al., 2001; Stewart et al., 2001; Kammer et al., 2005; Antal et al., 2006), and that it appeared to be stable over time, indicating that the 'yes/no' task together with the method of constant stimuli was a reliable way of measuring phosphene thresholds.

Sensitivity to different levels of magnetic field strength, in terms of disruption to visual perception, was investigated in Experiment 8, where it was found that that there was little or no effect of single-pulse TMS delivered over area V1 on orientation discrimination when the field strength was below approximately 1.6 T. The fact that there was no discernable effect for fine visual discriminations when TMS was delivered at moderately high field strengths (1.6 T was equal to 80 % of the maximum stimulator output) is likely to contribute to the variable degree of TMS disruption reported in previous studies. Above a critical field strength, however, all participants showed sensitivity to the disruptive influence of TMS, which was dependent on field strength, and orientation discrimination thresholds became poorer as field strength increased above approximately 1.6 T. Interestingly, above the critical field strength, two observers in Experiment 8 showed sensitivity to the disruptive influence of TMS that had a higher dependence on field strength than that showed for two other participants. A similar finding has been reported previously in terms of detection thresholds, and it has been suggested

that some individuals are simply more susceptible to the influence of TMS on visual perception (e.g. Masur et al., 1993; Kammer et al., 2005). Although the exact reasons for this remain elusive, it is possibly a result of anatomical differences.

Taken together, the results of Experiments 7 and 8 suggested that phosphene thresholds were not related to sensitivity to field strength on a visual discrimination task, for V1 stimulation. This has considerable implications for TMS studies of visual perception, as field strength has previously been set as a multiple of phosphene threshold in an effort to calibrate the pulse output with individual sensitivity to TMS (e.g. Harris et al., 2008). In light of the data presented in Chapter 5 (Experiments 7 and 8), however, it would be more informative to use a single field strength for all participants, preferably close to maximum output, as this would demonstrate individual differences in susceptibility more clearly.

8.1.6 The effect of TMS can be only partially explained as a reduction of contrast

It was found in Experiment 10 that single-pulse TMS delivered at 1.8 T over area V1 produced a contrast rescaling effect for orientation discrimination thresholds for all participants. This supports the hypothesis that TMS reduces the signal strength and that this phenomenon can be characterised as a decrease in perceived contrast (Kammer et al., 2005; Harris et al., 2008). The effect was

most prominent at lower stimulus contrasts – this is likely to be because this was where TMS had the biggest influence on psychophysical thresholds. Additionally, an 'orientation' shift – when thresholds in TMS conditions never returned to baseline levels – was observed for two participants, but not two others. Importantly, the two observers who demonstrated the orientation shift were also the participants who were more susceptible to TMS-induced disruption to visual perception (see Experiment 8).

The 'orientation' shift shown by two observers provided new evidence that the affect of TMS cannot simply be overcome by increasing the stimulus contrast, as was previously thought (Kammer et al., 2005; Harris et al., 2008). This finding is consistent with the idea that TMS may induce task-specific noise (e.g. Kammer & Nusseck, 1998; Silvanto et al., 2007).

8.1.7 Are signal reduction and task-specific noise separable?

To determine whether the contrast-rescaling effect of TMS reported in Experiment 10 could be attributed to a general decrease in signal strength (rather than contrast *per se*), orientation discrimination at different stimulus durations was investigated in Chapter 7 (Experiments 11, 12, 13 and 14). The influence of TMS on temporal summation has not previously been investigated. Single-pulse TMS delivered over area V1 at 1.8 T field strength produced a duration rescaling effect for all participants in Experiment 12. The cause of the duration rescaling effect may be that TMS directly compromises temporal summation. For example, it is known that TMS temporarily disables

neural function by causing a brief period of almost complete suppression of firing following a single TMS pulse (Moliadze et al., 2003). This interference with the ongoing temporal response could plausibly compromise temporal integration of the stimulus. An alternative interpretation to the contrast effect is that TMS reduces the encoded stimulus energy in general. For example, a duration rescaling effect has been reported when stimulus energy is decreased, such as when stimulus size (Graham & Margaria, 1935; Barlow, 1958) or luminance (Savage, 1996) is reduced.

Experiment 12 reported a moderate duration rescaling effect for two participants, but a much larger increase in critical duration and an 'orientation' shift – when thresholds did not reach those in the absence of TMS – for two other participants. Importantly, again the two observers who demonstrated the 'orientation' shift were the same two who demonstrated an 'orientation' shift in Experiment 10 and also were more susceptible to TMS-induced disruption to visual perception. It is possible that this effect could be attributed to a secondary (indirect) effect of TMS on perceived contrast.

In Experiment 14, the TMS field strength was reduced to 1.6 T (as opposed to 1.8 T, used in Experiments 10 and 12) and delivered over area V1 of the two TMS-susceptible individuals who demonstrated orientation shifts in Experiments 10 and 12. A duration rescaling effect without an orientation shift was observed for both participants, and data resembled that of the other subjects at 1.8 T field strength.

This suggests there may be two differential effects of TMS on visual perception: at lower field strengths, TMS may reduce the fidelity of the visual signal, whereas at higher field strengths the signal may be masked by an increase in neural noise. These effects appear to be separable, dependent on field strength and individual susceptibility to TMS.

8.2 Future research directions

Following the novel findings presented in this thesis, the following issues warrant further investigation.

8.2.1 Area V5/MT: Coarse vs. fine discrimination

Empirical evidence in the form of reaction times suggests that fine discriminations take place over a longer temporal period than coarse discriminations (e.g. Zlatkova et al., 2000). This may reflect additional processing stages required for fine discriminations. In Experiments 1, 2, 3, 4, 5 and 6, global motion direction discrimination was measured using a two-alternative forced choice task where the participants responded to whether the direction of motion was in one of two opposite directions (e.g. up vs. down, clockwise vs. anticlockwise, expanding vs. contracting). It would therefore be interesting to investigate the temporal disruption profile of area V5/MT for global motion processing, using a fine discrimination task. For example, the 'signal' dots could be constrained to translate along a trajectory oriented

clockwise or anticlockwise of vertical, and participants respond to the orientation of motion axis (e.g. 'clockwise' vs. 'anticlockwise' of vertical). It might be predicted using the model described in Chapter 4 that if the extra processing needed for fine discriminations occurred in the feedforward sweep of information processing, that the *late* temporal disruption window might be shifted later in time compared to when coarse discriminations are made. Alternatively, the extended period of processing might occur in V5/MT, and in this case, the *late* disruption window might be temporally broader than that for course discrimination. By measuring coarse discrimination (e.g. 'up' vs. 'down' motion direction discrimination) and fine discrimination (e.g. 'clockwise' vs. 'anticlockwise' motion axis discrimination) after each trial, the temporal disruption profile for the different types of motion discrimination could be unravelled.

8.2.2 Area V5/MT: First-order vs. second-order motion

To date, second-order (e.g. contrast-defined) motion has not been disrupted using single-pulse TMS. This may also have a different time course of processing compared to first-order (luminance defined) motion. For example, reaction times for second-order motion are typically considerably longer than those for first-order stimuli (Ellemburg, Lavoie, Lewis, Maurer, Lepore & Guillemot, 2003; Ledgeway & Hutchinson, 2008) and it has been suggested that second-order motion extraction is subject to either processing delays (e.g. Wilson, Fererra & Yo, 1992), or sluggish temporal responses (e.g. Derrington, Badcock & Henning, 1993). It is thought that processing of global direction of

second-order stimuli is not completed in area V1, which responds primarily to luminance-defined stimuli only (e.g. Albright, 1992). It might be predicted from the model described in Chapter 4 that for second-order motion stimuli, the *late* window disruption window may occur later than for first-order motion stimuli.

8.2.3 Sub-cortical motion pathway

It has been suggested that similar to monkey cortex, there is a 'fast' sub-cortical motion pathway in human cortex that bypasses area V1 and connects the SC directly with area V5/MT (e.g. ffytche et al., 1995; Chawla, Phillips, Buechel, Edwards & Friston, 1998). This pathway is thought to be activated by relatively high-speed motion of 22 deg/s or more (ffytche et al., 1995), although, this has not yet been investigated systematically with TMS. It would therefore be very interesting to measure the temporal disruption profile for area V5/MT for a range of stimulus speeds, ranging from considerably below to above 22 deg/sec. This may provide further evidence for the fast pathway in humans.

8.2.4 The spatial extent of visual disruption

The spatial extent of the disruptive effects of TMS on visual perception is also currently unknown. For example, in Experiment 10 it was reported that there was a TMS-induced contrast rescaling for all participants. However, it is unknown whether this reflects a global rescaling of contrast across the whole

visual field, or whether it is constrained, say, to the central visual field. The spatial extent of the effect may also be dependent on the area stimulated. As V5/MT receptive fields are typically ten-fold larger in diameter than those of area V1 (e.g. Gattass & Gross, 1981; Albright & Desimone, 1987), it may be the case that stimulation of area V5/MT typically disrupts processing of a larger area of the visual field than stimulation of area V1. Furthermore, it has been reported that phosphenes can be elicited in different parts of the visual field by manipulating the position of the coil over area V1 (Marg & Rudiak, 1994). This implies that perceptual affects of TMS might be constrained retinotopically to some extent, and it would be interesting to determine whether this is also the case with TMS disruption to visual perception.

8.2.5 Specificity of TMS disruption

In Experiments 10 and 12 it was reported that TMS induces orientation coding deficits that cannot be accounted for by changes in the effective of contrast or duration alone. However, it is likely that this effect is not specific to orientation processing and may be present for other visual dimensions and tasks. This could be tested by replicating Experiments 10 and 12 using, for example, a spatial frequency discrimination task rather than an orientation discrimination task, to establish the generality of the phenomenon.

8.2.6 The effect of TMS on duration encoding

It was reported in Experiments 12 and 14 that TMS induced a duration-rescaling effect on orientation discrimination. It cannot be ruled out by the experiments presented in this thesis that the duration-rescaling effect is not simply a reflection of Bloch's Law (with the primary affect of TMS being a reduction in, for example, contrast or stimulus size). To determine whether TMS impairs temporal summation *per se* a future study could directly investigate duration judgements for contrast- and size-matched stimuli (with and without TMS). For example, two stimuli of equal size matched for contrast (that is, that appear to be of equal contrast in both the control and TMS conditions) could be presented consecutively, with a TMS pulse delivered at a time that would maximally disrupt one of the stimulus presentations. If there is no difference in the perceived duration of the two stimuli, it can be concluded that the primary affect of TMS on visual perception is a reduction in contrast. If the stimulus which was paired with a TMS pulse appeared to be of shorter duration than the control stimulus, it can be assumed that TMS influences either the perceived size or duration of visual stimuli. This could be then investigated using pairs of stimuli of equal contrast matched for size (that is, that appear to be of equal size in control and TMS conditions). If the stimulus paired with a TMS pulse appeared to be of shorter duration than the control stimulus, it could be postulated that TMS does indeed influence temporal summation of visual stimuli.

8.2.7 Separating the disruptive effects of TMS on visual perception

In Experiments 10, 12 and 14, it was reported that two influences of TMS on visual perception (a reduction of visual signal strength and an increase in noise) were separable, dependent on TMS field strength, and also individual susceptibility. This could be confirmed by replicating the study by Harris et al. (2008), which reported that there was no evidence for TMS-induced noise on orientation identification. Harris et al. delivered single pulse TMS to all of their participants at 110 % of each individual's phosphene threshold, although the authors do not report phosphene threshold or the field strengths used in their experiment. However, it was found in Experiments 7 and 8 of this thesis that phosphene thresholds (approximately 1.0 T) were considerably lower than the magnetic field strength necessary for disruption of orientation discrimination JNDs (approximately 1.6 T). It is therefore likely that the field strengths used by Harris et al. were not high enough to elicit an increase in task-related noise. Using their paradigm, it would be predicted that at lower field strengths there would be a shift of the data that would be consistent with a signal-reduction account. At higher field strengths, however, it would be predicted that there would be a shift of the data that would be consistent with an increased-noise account, which was actually observed to a small extent for two of their participants. Using the same field strengths for all participants would also give an indication of individual susceptibility to the influence of TMS on visual perception (which was found not to be related to phosphene threshold in Experiment 7, Chapter 5).

8.2.8 Using rTMS to increase task-specific noise

One possible outcome of the experiment proposed above, is that some participants are less susceptible to the modulation of visual processing by TMS, as was found in Experiments 10 and 12. In this instance, the use of rTMS may be considered in future studies. For example, a brief train of TMS pulses (e.g. 3 pulses delivered at 10 Hz) may produce a similar effect of TMS-induced 'noise' in less susceptible individuals to that of a single TMS pulse on more susceptible individuals. Furthermore, it has been suggested that neural activity following a period of rTMS is dependent on the rate of rTMS. Empirical evidence suggests that after high-frequency rTMS neural activity is increased compared with baseline activity, but after low-frequency rTMS, neural activity is reduced (e.g. Maeda, Keenan, Tormos, Topka & Pascual-Leone, 2000). This finding could be exploited for the investigation of the mechanism of TMS disruption to visual processing in humans.

8.3 Concluding remarks

The experiments contained within this thesis report the effects of single-pulse TMS delivered over the human visual cortex, and the behavioural consequences that result. It was previously assumed that the temporal resolution of single-pulse TMS was discrete, yet the experiments presented here show that the disruptive effects can persist for quite some time. These experiments also show that single-pulse can reliably disrupt visual processing,

but there are individual differences in susceptibility. Further research is needed to determine the cause of these differences.

Chapter 9: References

Adelson, E. H. & Bergen, J. R. (1985). Spatiotemporal energy models for the perception of motion. *Journal of the Optical Society of America A, 2*: 284-299.

Albrecht, D. G. (1995). Visual cortex neurons in monkey and cat: Effect of contrast on the spatial and temporal phase transfer functions. *Visual Neuroscience, 12*: 1191-1210.

Albrecht, D. G. & Hamilton, D. B. (1982). Striate cortex of monkey and cat: contrast response function. *Journal of Neurophysiology, 48 (1)*: 217-237.

Albright, T. D. (1993). Cortical processing of visual motion and its role in the stabilization of gaze. In F. A. Miles & J. Wallman (Eds.), *Visual motion and its role in the stabilization of gaze.* Amsterdam: Elsevier. pp. 177-201.

Albright, T. D. (1984). Direction and orientation selectivity of neurons in visual area MT of the macaque. *Journal of Neurophysiology, 52 (6)*: 1106-1130.

Albright, T. D. & Desimone, R. (1987) Local precision of visuotopic organization in the middle temporal area (MT) of the macaque. *Experimental Brain Research, 65*: 582-592.

Albright, T. D., Desimone, R. & Gross, C. G. (1984). Columnar organization of directionally selective cells in visual area MT of the macaque. *Journal of Neurophysiology, 51 (1)*: 16-31.

Amassian, V. E., Cracco, R. Q., Maccabee, P. J. (1989). Focal stimulation of human cerebral cortex with the magnetic coil: a comparison with electrical stimulation. *Electroencephalography and Clinical Neurophysiology, 74 (6)*: 401-416.

Amassian, V. E., Cracco, R. Q., Maccabee, P. J., Cracco, J. B., Rudell, A. & Eberle, L. (1989). Suppression of visual perception by magnetic coil stimulation of human occipital cortex. *Electroencephalography and Clinical Neurophysiology, 74*: 458-462.

Amassian, V. E., Cracco, R. Q., Maccabee, P. J., Cracco, J. B., Rudell, A. & Eberle, L. (1993). Unmasking human visual perception with the magnetic coil and its relationship to hemispheric asymmetry. *Brain Research, 605*: 312-316.

Amassian, V. E., Eberle, L., Maccabee, P. J. & Cracco, R. Q. (1992). Modelling magnetic coil excitation of human cerebral cortex with a peripheral nerve immersed in a brain-shaped volume conductor: the significance of fiber bending in excitation. *Electroencephalography Clinical Neurophysiology, 85 (5)*: 291-301.

Anand, S., Olson, J. D. & Hotson, J. R. (1998). Tracing the timing of human analysis of motion and chromatic signals from occipital to temporo-parieto-occipital cortex: A transcranial magnetic stimulation study. *Vision Research, 38*: 2619-2627.

Anderson, S. J. & Burr, D. C. (1985). Spatial and temporal selectivity of the human motion detection system. *Vision Research, 25(8)*: 1147-1154.

Anderson, S. J., Holliday, I. E., Singh, K. D. & Harding, G. F. (1996). Localization and functional analysis of human cortical area V5 using magneto-encephalography. *Proceedings of Biological Sciences, 263 (1369)*: 423-431.

Andrews, T. J., Halpern, S. D. & Purves, D. (1997). Correlated size variations in human visual cortex, lateral geniculate nucleus, and optic tract. *Journal of Neuroscience, 17 (8)*: 2859-2868.

Anstis, S. M. (1978). Apparent movement. In H.-L. Teuber, R. H. Held, & H. W. Leibowitz (Eds.), *Handbook of sensory physiology: Vol. 8. Perception*. New York: Springer.

Anstis, S. M (1980). The perception of apparent movement. *Philosophical transactions of the Royal Society of London. Series B, Biological sciences, 290 (1038)*: 153-168.

Anstis, S. M. & Mather, G. (1985). Effects of luminance and contrast on direction of ambiguous apparent motion. *Perception, 14 (2):*167-179.

Antal, A., Arlt, S., Nitsche, M. A., Chadaide, Z. & Paulus, W. (2006). Higher variability of phosphene thresholds in migraineurs than in controls: A consecutive transcranial magnetic stimulation study. *Cephalalgia, 26*: 865-870.

Azzopardi, P. & Cowey, A. (2001). Motion discrimination in cortically blind patients. *Brain, 124 (1)*: 30-46.

Banks, W. P. & Kane, D. A. (1972). Discontinuity of seen motion reduces the visual motion aftereffect. *Perception & Psychophysics, 12*: 69-72.

Barker, A. T. (1999). The history and basic principles of magnetic nerve stimulation. *Electroencephalography and Clinical Neurophysiology Supplement, 51* : 3–21.

Barker, A. T., Freeston, I. L. (1985). Medical applications of electric and magnetic fields. *Electron Power 31(10)*: 757-760.

Barker, A. T., Freeston, I. L., Jalinous, R., Merton, P. A. & Morton, H.B. (1985). Magnetic stimulation of the human brain. *Journal of Physiology (Lond.), 369*: 3P.

Barker, A. T., Jalinous, R. & Freeston, I. L. (1985). Non-invasive magnetic stimulation of human motor cortex. *Lancet, 1 (8437)*: 1106-1107.

Barlow, H. B. (1956). Retinal noise and absolute threshold. *Journal of the Optical Society of America, 46*: 634-639.

Barlow, H. B. (1958). Temporal and spatial summation in human vision at different background intensities. *Journal of Physiology, 141*: 337-350.

Barlow, H. B. & Tripathy, S. P. (1997). Correspondence noise and signal pooling in the detection of coherent visual motion. *The Journal of Neuroscience, 17 (20)*: 7954-7966.

Baylor, D. A. & Fettiplace, R. (1976). Transmission of signals from photoreceptors to ganglion cells in the eye of the turtle. *Cold Spring Harbour Symposium on Quantitative Biology, 40*: 529-536.

Bearse, M. A. & Freeman, R. D. (1994). Binocular summation in orientation discrimination depends on stimulus contrast and duration. *Vision Research, 34 (1)*: 19-29.

Beaudot, W. H. & Mullen, K. T. (2006). Orientation discrimination in human vision: psychophysics and modeling. *Vision Research, 46 (1-2)*: 26-46.

Beckers, G. & Homberg, V. (1992). Cerebral visual motion blindness: Transitory akinetopsia induced by transcranial magnetic stimulation of human area V5. *Proceedings of the Royal Society of London B, 249*: 173-178.

Beckers, G. & Zeki, S. (1995). The consequences of inactivating areas V1 and V5 on visual motion perception. *Brain, 118*: 49-60.

Ben-Yishai, R., Bar-Or, R. L. & Sompolinsky, H. (1995). Theory of orientation tuning in visual cortex. *Proceedings of the National Academy of Science USA, 92 (9)*: 3844-3848.

Blakemore, C. & Campbell, F. W. (1969a). On the existence of neurones in the human visual system selectively sensitive to the orientation and size of retinal images. *Journal of Physiology, 203*: 237-260.

Blakemore, C. & Campbell, F. W. (1969b). Adaptation to spatial stimuli. *Journal of Physiology, 200 (1)*: 11-13.

Bohning, D. E. (2000). Introduction and overview of TMS physics. In: M. S. George & R. H. Belmaker (Eds), *Transcranial magnetic stimulation in neuropsychiatry.* Washington DC and London: American Psychiatric Press, Inc. pp 13-14

Bohning, D. E., Shastri, A., McConnell. K. A., Nahas, Z., Lorberbaum, J. P., Roberts, D. R., Teneback, C., Vincent, D. J. & George, M. A. (1999). A combined TMS/fMRI study of intensity-independent TMS over motor cortex. *Biological Psychiatry, 45*: 385-394.

Born, R. T. & Bradley, D. C. (2005). Structure and function of visual area MT. *Annual Review of Neuroscience, 28*: 157-189.

Boroojerdi, B., Meister, I. G., Foltys, H., Sparing, R., Cohen, L. G. & Topper, R. (2002). Visual and motor excitability: A transcranial magnetic stimulation study. *Clinical Neurophysiology, 113*: 1501-1504.

Bowling, D. B. & Michael, C. R. (1980). Projection patterns of single physiologically characterised optic tract fibres in cat. *Nature, 286*: 899-902.

Braddick O. J. (1973). The masking of apparent motion in random-dot patterns. *Vision Research, 13 (2)*: 355-369.

Braddick, O. J. (1974). A short-range process in apparent motion. *Vision Research, 14 (7)*: 519-527.

Braddick, O. J. (1980). Low-level and high-level processes in apparent motion. *Philosophical Transactions of the Royal Society of London B Biological Sciences, 290 (1038)*: 137-151.

Braddick, O. J., O'Brien, J. M. D., Wattem-Bell, J., Atkinson, J. & Hartley, T. (2001). Brain areas sensitive to coherent visual motion. *Perception, 30*: 61-72.

Bradley, A., Skottun, B. C., Ohzawa, I., Sclar, G. & Freeman, R. D. (1987). Visual orientation and spatial frequency discrimination: A comparison of single neurons and behavior. *Journal of Neurophysiology, 57 (3)*: 755-772.

Brasil-Neto, J. P., Cohen, L. G., Panizza, M., Nilsson, J., Roth, B. J. & Hallett, M. (1992). Optimal focal transcranial magnetic activation of the human motor cortex: effects of coil orientation, shape of the induced current pulse, and stimulus intensity. *Journal of Clinical Neurophysiology, 9 (1)*: 132-136.

Breitmeyer, B. G. & Ganz, L. (1977). Temporal studies with flashed gratings: inferences about human transient and sustained channels. *Vision Research, 17 (7)*: 861-865.

Breitmeyer, B. G., Ro, T. & Ogmen, H. (2004). A comparison of masking by visual and transcranial magnetic stimulation: Implications for the study of conscious and unconscious visual processing. *Consciousness and Cognition, 13*: 829-843.

Britten, K. H., Shadlen, M. N., Newsome, W. T. & Movshon, J. A. (1993). Responses of neurons in macaque MT to stochastic motion signals. *Visual Neuroscience, 10*: 1157-1169.

Bullier, J. (2001). Integrated model of visual processing. *Brain Research, Review, 36*: 96-107.

Bullier J. (2003). Hierarchies of cortical areas. In: *The Primate Visual System,* J. H. Kaas, C. E. Collins (Eds.) CRC Press, Boca Raton, pp. 181–204.

Burr, D. C., Fiorentini, A. & Morrone, C. (1998). Reaction time to motion onset of luminance and chromatic gratings is determined by perceived speed. *Vision Research, 38 (23)*: 3681-3690.

Burr, D. C. & Santoro, L. (2001). Temporal integration of optic flow, measured by contrast and coherence thresholds. *Vision Research, 41*: 1891-1899.

Burr, D. C. & Wijesundra, S. A. (1991). Orientation discrimination depends on spatial frequency. *Vision Research, 31 (7/8)*: 1449-1452.

Callaway, E. M. & Wiser, A. K. (1996). Contribution of individual layer 2-5 spiny neurons to local circuits in macaque primary visual cortex. *Visual Neuroscience, 13 (5)*: 907-922.

Campbell, F. W., Cooper, G. F. & Enroth-Cugell, C. (1969). The spatial selectivity of the visual cells of the cat. *Journal of Physiology, 203 (1)*: 223-235.

Campbell, F. W. & Kulikowski, J. J. (1966). Orientational selectivity of the human visual system. *Journal of Physiology, 187 (2)*: 437-445.

Campbell, F. W. & Robson, J. G. (1968). Application of Fourier analysis to the visibility of gratings. *Journal of Physiology, 197 (3)*: 551-566.

Carandini, M., Heeger, D. J. & Movshon, J. A. (1997). Linearity and normalization in simple cells of the macaque primary visual cortex. *Journal of Neuroscience, 17 (21)*: 8621-8644.

Cavanagh, P. (1992). Attention-based motion perception. *Science, 257*: 1563-1565.

Cavanagh, P. & Mather, G. (1989). Motion: The long and short of it. *Spatial Vision, 4*: 103-129.

Chance, F. S., Nelson, S. B. & Abbott, L. F. (1998). Synaptic depression and the temporal response characteristics of V1 cells. *Journal of Neuroscience, 18*: 4785-4799.

Chawla, D., Phillips, J., Buechel, C., Edwards, R. & Friston, K. J. (1998). Speed-dependent motion-sensitive responses in V5: an fMRI study. *Neuroimage, 7 (2)*: 86-96.

Chiappa, K. H., Cros, D. & Cohen, D. (1991). Magnetic stimulation: determination of coil current flow direction. *Neurology, 41 (7)*: 1154-1155.

Chung, S. & Ferster, D. (1998). Strength and orientation tuning of the thalamic input to simple cells revealed by electrically evoked cortical suppression. *Neuron, 20 (6)*: 1177-1189.

Cohen, L. G., Roth, B. J., Nilsson, J., Dang, N., Panizza, M., Bandinelli, S., Friauf ,W. & Hallett, M. (1990). Effects of coil design on delivery of focal magnetic stimulation. Technical considerations. *Electroencephalography and Clinical Neurophysiology, 75 (4)*: 350-357.

Cooper, G. F. & Robson, J. G. (1968). Successive transformations of spatial information in the visual system. National Physical Laboratory Symposium on Pattern Recognition. *IEE Conference Proceedings, 42*: 134-143.

Corthout, E., Barker, A. T. & Cowey, A. (2001). Transcranial magnetic stimulation: Which part of the waveform causes the stimulation? *Experimental Brain Research, 141*: 128-132.

Corthout, E., Hallett, M. & Cowey, A. (2003). Interference with vision by TMS over the occipital pole: A forth period. *Neuroreport, 14 (4)*: 651-655.

Corthout, E., Uttl, B., Juan, C. H., Hallet, M. & Cowey, A. (2000). Suppression of vision by transcranial magnetic stimulation: A third mechanism. *Neuroreport, 11 (11)*: 2345-2349.

Corthout, E., Uttl, B., Walsh, V., Hallett, M. & Cowey, A. (1999a). Timing of activity in early visual cortex as revealed by transcranial magnetic stimulation. *Neuroreport, 10 (12)*: 2631-2634.

Corthout, E., Uttl, B., Ziemann, U., Cowey, A. & Hallet, M. (1999b). Two periods of processing in the (circum)striate visual cortex as revealed by transcranial magnetic stimulation. *Neuropsychologia, 37*: 137-145.

Cowey, A. & Walsh, V. (2000). Magnetically induced phosphenes in sighted, blind and blindsighted observers. *Neuroreport, 11 (14)*: 3269-3273.

Cragg, B. G. (1969). The topography of the afferent projections in the circumstriate visual cortex of the monkey studied by the Nauta method. *Vision Research, 9 (7)*: 733-47.

Curcio, C. A., Sloan, K. R., Kalina, R. E. & Hendrickson, A. E. (1990). Human photoreceptor topography. *Journal of Computational Neurology, 292*: 497-523.

d'Alfonso, A. A. L., van Honk, J., Schutter, D. J. L. G., Caffé, A. R., Postma, A. & de Haan, E. H. F. (2002). Spatial and temporal characteristics of visual motion perception involving V5 visual cortex. *Neurological Research, 24*: 266-270.

Dean, A. F. (1981). The relationship between response amplitude and contrast for cat striate cortical neurones. *Journal of Physiology, 318*: 413-427.

Deblieck., C. Thompson, B., Iacoboni, M. & Wu, A. D. (2008). Correlation between motor and phosphene thresholds: A transcranial magnetic stimulation study. *Human Brain Mapping, 29*: 662-670.

Delon-Martin, C., Gobbele, R., Buchner, H., Haug, B. A., Antal, A., Darvas, F. & Paulus, W. (2006). Temporal pattern of source activities evoked by different types of motion onset stimuli. *NeuroImage, 31*: 1567-1579.

Derrington, A. M., Badcock, D. R. & Henning, G. B. (1993). Discriminating the direction of second-order motion at short stimulus durations. *Vision Research, 33 (13)*: 1785-1794.

Derrington, A. M. & Lennie, P. (1984). Spatial and temporal contrast sensitivities of neurones in lateral geniculate nucleus of macaque. *Journal of Physiology, 357*: 219-240.

Desimone, R. & Schein, S. J. (1987). Visual properties of neurons in area V4 of the macaque: sensitivity to stimulus form. *Journal of Neurophysiology, 57 (3)*: 835-868.

De Valois, R. L., Albrecht, D. G., Thorell, L. G. (1982) Spatial frequency selectivity of cells in macaque visual cortex. *Vision Research 22 (5)*: 545-559.

DeYoe, E. A. & Van Essen, D. C. (1988). Concurrent processing streams in monkey visual cortex. *Trends in Neurosciences, 11 (5)*: 219-226.

Di Lazzaro, V., Oliviero, A. Mazzone, P., Insola, A., Pilato, F., Santurno, E., Accurso, A., Tonali, P. & Rothwell, J. C. (2001). Comparison of descending volleys evoked by monophasic and biphasic magnetic stimulation of the motor cortex in conscious humans. *Experimental Brain Research, 141*: 121-127.

Di Russo, F., Martinez, A., Sereno, M. I., Pitzalis, S. & Hillyard, S. A. (2001). Cortical sources of the early components of the visually evoked potential. *Human Brain Mapping, 15*: 95-111.

Douglas, R. J., Koch, C., Mahowald, M., Martin, K. A. & Suarez, H. H. (1995). Recurrent excitation in neocortical circuits. *Science, 269 (5226)*: 981-985.

Dragoi, V., Sharma, J., Miller, E. K. & Sur, M. (2002). Dynamics of neuronal sensitivity in the visual cortex and local feature discrimination. *Nature Neuroscience, 5 (9)*: 883-891.

Dubner, R. & Zeki, S. M. (1971). Response properties and receptive fields of cells in an anatomically defined region of the superior temporal sulcus in the monkey. *Brain Research, 35*: 528-532.

Duffy, C. J. (2004). The cortical analysis of optic flow. In: L. M. Chalupa & J. S. Werner (Eds.), *The visual neurosciences* (Vol. 2). Cambridge, MA: MIT Press. pp. 1260-1283.

Duffy, C. J. & Wurtz, R. H. (1991a). Sensitivity of MST neurons to optic flow stimuli. I. A continuum of response selectivity to large-field stimuli. *Journal of Neurophysiology, 65 (6)*: 1329-1345.

Duffy, C. J. & Wurtz, R. H. (1991b). Sensitivity of MST neurons to optic flow stimuli. II. Mechanisms of response selectivity revealed by small field stimuli. *Journal of Neurophysiology, 65 (6)*: 1346-1359.

Dürsteler, M. R. & Wurtz, R. H. (1988). Pursuit and optokinetic deficits following chemical lesions of cortical areas MT and MST. *Journal of Neurophysiology, 60 (3)*: 940-965.

Edwards, M. & Badcock, D. R. (1994). Global motion perception: Interaction of the ON and OFF pathways. *Vision Research, 34 (21)*: 2849-2858.

Ellemberg, D., Lavoie, K., Lewis, T. L., Maurer, D., Lepore, F. & Guillemot, J. -P. (2003). Longer VEP latencies and slower reaction times to the onset of second-order motion than to the onset of first-order motion. *Vision Research, 43 (6)*: 651-658

Enroth-Cugell, C. & Jones, R. W. (1963). Responses of cat retinal ganglion cells to exponentially changing light intensities. *Journal of Neurophysiology, 26*: 894-907.

Epstein, C. M. (2008). TMS stimulation coils. In: E. M. Wassermann, C. M. Epstein, U. Ziemann, V. Walsh, T. Paus & S. H. Lisanby (Eds). *The Oxford handbook of Transcranial magnetic stimulation.* New York: Oxford University Press.

Fang. F., Murray, S. O., Kersten, D. & He, S. (2005). Orientation-tuned FMRI adaptation in human visual cortex. *Journal of Neurophysiology, 94 (6)*: 4188-4495.

Fechner, G. T. (1860). *Elemente der Psychophysik.* Leipzig: Breitkopf und Härtel, 2. (Reprinted, Bristol: Thoemmes Press, 1999).

Felleman, D. J. & Van Essen, D. C. (1991). Distributed hierarchical processing in the primate cerebral cortex. *Cerebral Cortex, 1*: 1-47.

Ferster, D. (2004) Assembly of receptive field in primary visual cortex, In: L. M. Chalupa & J. S. Werner. (Eds.) *The Visual Neurosciences*. Cambridge: MIT Press.

Ferster, D., Chung, S. & Wheat, H. (1996). Orientation selectivity of thalamic input to simple cells of cat visual cortex. *Nature, 380 (6571)*: 249-252.

ffytche, D. H., Guy, C. N. & Zeki, S. (1995). The parallel visual motion inputs into areas V1 and V5 of human cerebral cortex. *Brain, 118*: 1375-1394.

Fitzpatrick, D., Lund, J. S. & Blasdel, G. G. (1985). Intrinsic connections of macaque striate cortex: Afferent and efferent connections of lamina 4C. *Journal of Neuroscience, 5*: 3329-3349.

Foster, K. H., Gaska, J. P., Nagler, M. & Pollen, D. A. (1985). Spatial and temporal frequency selectivity of neurones in visual cortical areas V1 and V2 of the macaque monkey. *Journal of Physiology, 365*: 331-363.

Fredericksen, R. E., Verstraten, F. A. J. & Van de Grind, W. A. (1994). Temporal integration of random dot apparent motion information in human central vision. *Vision Research, 34 (4)*: 461-476.

Fuhr, P., Agostino, R. & Hallett, M. (1991). Spinal motor neuron excitability during the silent period after cortical stimulation. *Electroencephalography and Clinical Neurophysiology, 81(4)*: 257-262.

Fujita, I., Tanaka, K., Ito, M. & Cheng, K. (1992). Columns for visual features of objects in monkey inferotemporal cortex. *Nature, 360*: 343-346.

Gallant, J. L., Connor, C. E., Rakshit, S., Lewis, J. W. & Van Essen, D. C. (1996). Neural responses to polar, hyperbolic, and Cartesian gratings in area V4 of the macaque monkey. *Journal of Neurophysiology, 76(4)*: 2718-2739.

Gardner, J. L., Anzai, A., Ohzawa, I. & Freeman, R. D. (1999). Linear and non-linear contributions to orientation tuning of simple cells in the cat's striate cortex. *Visual Neuroscience, 16*: 1115 – 1121.

Garvey, M. A. & Mall, V. (2008). Transcranial magnetic stimulation in children. *Clinical Neurophysiology, 119 (5)*: 973-984.

Gattass, R. & Gross, C.G. (1981). Visual topography of striate projection zone (MT) in posterior superior temporal sulcus of the macaque. *Journal of Neurophysiology, 46*: 621-638.

Geisler, W. S. (1999). Motion streaks provide a spatial code for motion direction. *Nature, 400*: 65-69.

Geisler, W. S. & Albrecht, D. G. (1997). Visual cortex neurons in monkeys and cats: detection, discrimination, and identification. *Visual Neuroscience, 14 (5)*: 897-919.

Geisler, W. S. & Albrecht, D. G. (2000). Spatial vision, In: K. K. De Valois, (Ed.) *Handbook of Perception and Cognition, Seeing, 2nd Edition.* New York: Academic Press, pp 79-128.

Gerwig, M., Kastrup, O., Meyer, B. U. & Niehaus, L. (2003). Evaluation of cortical excitability by motor and phosphene thresholds in transcranial magnetic stimulation. *Journal of the Neurological Sciences, 215*: 75-78.

Gilbert, C. D. (1977). Laminar differences in receptive field properties of cells in cat primary visual cortex. *Journal of Physiology, 268 (2)*: 391-421.

Gillespie, D. C., Lampl, I., Anderson, J. S. & Ferster, D. (2001). Dynamics of the orientation-tuned membrane potential response in cat primary visual cortex. *Nature Neuroscience, 4 (10)*: 1014-1019.

Girard, P., Salin, P. A. & Bullier, J. (1992). Response selectivity of neurons in area MT of the macaque monkey during reversible inactivation of area V1. *Journal of Neurophysiology, 67 (6)*: 1437-1446.

Graham, C. H. & Margaria, R. (1935). Area and the intensity time relation in the peripheral retina. *American Journal of Physiology, 113*: 299-305.

Grahem, N. V. S. (1989). *Visual Pattern Analyzers*. New York: Oxford University Press.

Green, D. M. and Swets, J. A. (1966). *Signal detection theory and psychophysics.* New York: Wiley.

Gugino, L. D., Romero, J. R., Aglio, L., Titone, D., Ramirez, M., Pascual-Leone, A., Grimson, E., Weisenfeld, N., Kikinis, R. & Shenton, M. E. (2001). Transcranial magnetic stimulation coregistered with MRI: a comparison of a guided versus blind stimulation technique and its effect on evoked compound muscle action potentials. *Clinical Neurophysiology, 112 (10)*: 1781-792.

Harris, J. A., Clifford, C. W. G. & Miniussi, C. (2008). The functional effect of transcranial magnetic stimulation: Signal suppression or neural noise generation? *Journal of Cognitive Neuroscience, 20 (4)*: 734-740.

Hart Jr, W. M. (1992). The temporal responsiveness of vision. In: W. M. Hart Jr (Ed.) *Adler's Physiology of the Eye.* St. Louis: Mosby Yearbook. pp 548-578.

Hartline, H. K., Wagner, H. G. & Ratliff, F. (1956). Inhibition in the eye of Limulus. *The Journal of General Physiology, 39 (5)*: 651-673.

Harwerth, R. S. & Levi, D. M. (1978). Reaction time as a measure of suprathreshold grating detection. *Vision Research, 18 (11)*: 1579-1586.

Heeger, D. J. (1987). Model for the extraction of image flow. *Journal of the Optical Society of America A, 4 (8)*: 1455-1471.

Heeger, D. J., Boynton, G. M., Demb, J. B., Seidemann, E. & Newsome, W. T. (1999). Motion opponency in visual cortex. *The Journal of Neuroscience, 19 (16)*: 7162-7174.

Hegdé, J. (2008). Time course of visual perception: Coarse-to-fine processing and beyond. *Progress in Neurobiology, 84*: 405-439.

Hendry, S. H & Reid, R. C. (2000). The koniocellular pathway in primate vision. *Annual Review of Neuroscience, 23*: 127-153.

Hendry, S. H. & Yoshioka, T. (1994). A neurochemically distinct third channel in the macaque dorsal lateral geniculate nucleus. *Science, 264 (5158)*: 575-577.

Hodgkin, A. L., Rushton, W. A. H. (1946). The electrical constants of a crustacean nerve fibre. *Proceedings of the Royal Society of London B, 133*: 97-132.

Holliday, I. E., Anderson, S. J. & Harding, G. F. (1997). Magneto-encephalographic evidence for non-geniculostriate visual input to human cortical area V5. *Neuropsychologia, 35 (8)*: 1139-1146.

Home, R. (1978). Binocular summation: a study of contrast sensitivity, visual acuity and recognition. *Vision Research, 18 (5)*: 579-585.

Horwitz, G. D. & Newsome, W. T. (1999). Separate signals for target selection and movement specification in the superior colliculus. *Science, 284(5417)*: 1158-1161.

Hotson, J. R. & Anand, S. (1999). The selectivity and timing of motion processing in human temporo-parieto-occipital cortex: A transcranial magnetic stimulation study. *Neuropsychologia, 37*: 169-179.

Hotson, J., Braun, D., Herzberg, W. & Boman, D. (1994). Transcranial magnetic stimulation of extrastriate cortex degrades human motion detection. *Vision Research, 34 (16)*: 2115-2123.

Hovey, C., Houseman, P. & Jalinous, R. (2003). *The New Guide to Magnetic Stimulation.* Whitland: Wales: MagStim.

Hoyt, W. T. & Luis, O. (1963). The primate optic chiasm. Details of visual fibre organisation studied by silver impregnation techniques. *Archives of Ophthalmology, 70*: 69-85.

Hubel, D. H. (1959). Single unit activity in striate cortex of unrestrained cats. *Journal of Physiology, 147*: 226-238.

Hubel, D. H. & Wiesel, T.N. (1959). Receptive fields of single neurones in the cat's striate cortex. *Journal of Physiology, 148*: 574-591.

Hubel, D. H. & Wiesel, T.N. (1961). Integrative action in the cat's lateral geniculate body. *Journal of Physiology (London), 155*: 385-398.

Hubel, D. H. & Wiesel, T.N. (1962). Receptive fields, binocular interaction and functional architecture in the cat's visual cortex. *Journal of Physiology, 160*: 106-154.

Hubel, D. H. & Wiesel, T. N. (1968). Receptive fields and functional architecture of monkey striate cortex. *Journal of Physiology, 195 (1)*: 215-243.

Huk, A. C. Dougherty, R. F. & Heeger, D. J. (2002). Retinotopy and functional subdivision of human areas MT and MST. *Journal of Neuroscience, 22 (16)*: 7195-7205.

Hupé, J. M., James, A. C., Payne, B. R., Lomber, S. G., Girard, P. & Bullier, J. (1998). Cortical feedback improves discrimination between figure and background by V1, V2 and V3 neurons. *Nature, 394 (6695)*: 784-787.

Ilmoniemi, R. J., Virtnen, J., Ruohonen, J., Karhu, J., Aronen, H. J., Näätänen, R., Katila, T. (1997). Neuronal responses to magnetic stimulation reveal cortical reactivity and connectivity. *NeuroReport, 8*: 3537-3540.

Inghilleri, M., Berardelli, A., Cruccu, G. & Manfredi, M. (1993). Silent period evoked by transcranial magnetic stimulation of the human cortex and cervicomedullary myoclonus. *Electroencephalography and Clinical Neuro-physiology, 109*: 70-72.

Inui, K. & Kakigi, R. (2006). Temporal analysis of the flow from V1 to the extrastriate cortex in humans. *Journal of Neurophysiology, 96*: 775-784.

Ishai, A. & Sagi, D. (1995). Common mechanisms of visual imagery and perception. *Science, 268 (5218)*: 1772-1774.

Jalinous, R. (1991). Technical and practical aspects of magnetic nerve stimulation. *Journal of Clinical Neurophysiology, 8 (1)*: 10-25.

Jalinous, R. (1998). *Guide to Magnetic Stimulation.* Whitland: Wales: MagStim.

Jazayeri, M. & Movshon, J. A. (2007). Integration of sensory evidence in motion discrimination. *Journal of Vision, 7 (12)*: 7.1-7.

Johnson, R. R. & Burkhalter, A. (1996). Microcircuitry of forward and feedback connections within rat visual cortex. *Journal of Computational Neurology, 368 (3)*: 383-398.

Jones, J. P. & Palmer, L. A. (1987). The two-dimensional spatial structure of simple receptive fields in cat striate cortex. *Journal of Neurophysiology, 58*: 1187-1211.

Kammer, T. (2006). Masking visual stimuli by transcranial magnetic stimulation. *Psychological Research*, *71 (6)*: 659-666.

Kammer, T., Beck, S., Erb, M. & Grodd, W. (2001a). The influence of current direction on phosphene thresholds evoked by transcranial magnetic stimulation. *Clinical Neurophysiology, 112*: 2015-2021.

Kammer, T., Beck, S., Thielscher, A., Laubis-Herrmann, U. & Topka, H. (2001b). Motor thresholds in humans: A transcranial magnetic stimulation study comparing different pulse waveforms, current directions and stimulator types. *Clinical Neurophysiology, 112*: 250-258.

Kammer, T. & Nusseck, H-G. (1998). Are recognition deficits following occipital lobe TMS explained by raised detection thresholds? *Neuropsychologia, 36 (11)*: 1161-1166.

Kammer, T., Puls, K., Erb, M. & Grodd, W. (2005a). Transcranial magnetic stimulation in the visual system. II. Characterization of induced phosphenes and scotomas. *Experimental Brain Research, 160*: 129-140.

Kammer, T., Puls, K., Strasburger, H., Hill, N. J. & Wichmann, F. A. (2005b). Transcranial magnetic stimulation in the visual system. I. The psychophysics of visual suppression. *Experimental Brain Research, 160*: 118-128.

Kammer, T., Vorwerg, M. & Herrnberger, B. (2007). Anisotropy in the visual cortex investigated by neuronavigated transcranial magnetic stimulation. *NeuroImage, 36*: 313-321.

Kaplan, E. & Shapley, R. M. (1982). X and Y cells in the lateral geniculate nucleus of macaque monkeys. *Journal of Physiology, 330*: 125-143.

Kastner, S., Demmer, I. & Ziemann, U. (1998). Transient field defects induced by transcranial magnetic stimulation over human occipital pole. *Experimental Brain Research, 118*: 19-26.

Keel, J. C., Smith, M. J. & Wassermann, E. M. (2000). A safety screening questionnaire for transcranial magnetic stimulation. *Clinical Neurophysiology, 112*: 720.

Kelly, D. H. (1961). Visual response to time-dependent stimuli. I. Amplitude sensitivity measurements. *Journal of the Optical Society of America, 51*: 422-429.

Kelly, D. H. (1984). Retinal inhomogeneity. I. Spatiotemporal contrast sensitivity. *Journal of the Optical Society of America, A Optics and image science, 1*: 107-113.

Komssi, S., Kähkönen, S. & Ilmoniemi, R. J. (2004). The effect of stimulus intensity on brain responses evoked by transcranial magnetic stimulation. *Human Brain Mapping, 21*: 154-164.

Kuffler, S. W. (1953). Discharge patterns and functional organization of mammalian retina. *Journal of Neurophysiology, 18*: 37-68.

Kukkonen, H., Rouamo, J., Tiippana, K. & Nasanen, R. (1993). Micherlson contrast, RMS contrast and energy of various spatial stimuli at threshold. *Vision Research, 33*: 1431-1436.

Kulikowski, J. J., Abadi, R. & King-Smith, P. E. (1973). Orientational selectivity of grating and line detectors in human vision. *Vision Research 13 (8)*: 1479-1486.

Lagae, L., Raiguel, S. & Orban, G. A. (1993). Speed and direction selectivity of macaque middle temporal neurons. *Journal of Neurophysiology, 69 (1)*: 19-39.

Lamme, V. A. (2004). Beyond the classical receptive field: contextual modulation of V1 responses. In: L. M. Chalupa & J. S. Werner (Eds.), *The Visual Neurosciences*, Cambridge: MIT Press. pp 720-734.

Lampl, I., Anderson, J. S., Gillespie, D. C. & Ferster, D. (2001). Prediction of orientation selectivity from receptive field architecture in simple cells of cat visual cortex. *Neuron, 30 (1)*: 263-274.

Larsson J. (2001). *Imaging vision: functional mapping of intermediate visual processes in man*. PhD thesis, Karolinska Institutet, Stockholm, Sweden.

Larsson, J., Landy, M. S. & Heeger, D. J. (2006). Orientation-selective adaptation to first- and second-order patterns in human visual cortex. *Journal of Neurophysiology, 95 (2)*: 862-881.

Laycock, R., Crewther, D. P., Fitzgerald, P. B. & Crewther, S. G. (2007). Evidence for fast signals and later processing in human V1/V2 and V5/MT+: A TMS study of motion perception. *Journal of Neurophysiology, 98 (7)*: 1253-1262.

Ledgeway, T. & Hess, R. F. (2002). Failure of direction identification for briefly presented second-order motion stimuli: evidence for weak direction selectivity of the mechanisms encoding motion. *Vision Research, 42 (14)*: 1739-1758.

Ledgeway, T. & Hutchinson, C. V. (2008). Choice reaction times for identifying the direction of first-order motion and different varieties of second-order motion. *Vision Research, 48 (2)*: 208-222.

Ledgeway, T. & Smith, A. T. (1994). Evidence for separate motion-detecting mechanisms for first- and second-order motion in human vision. *Vision Research, 34*: 2727-2740.

Legge, G. E. (1978). Sustained and transient mechanisms in human vision: temporal and spatial properties. *Vision Research, 18 (1)*: 69-81.

Livingstone, M. S. & Hubel, D. (1984). Anatomy and physiology of a color system in the primate visual cortex. *Journal of Neuroscience, 4 (1)*: 309-356.

Livingstone, M. S. & Hubel, D. (1987). Connections between layer 4B of area 17 and the thick cytochrome oxidase stripes of area 18 in the squirrel monkey. *Journal of Neuroscience, 7 (11)*: 3371-3377.

Livingstone, M. S. & Hubel, D. (1988). Segregation of form, color, movement, and depth: Anatomy, physiology, and perception. *Science, 240 (4853)*: 740-749.

Logothetis, N. K. (1999). Vision: a window on consciousness. *Scientific American, 281(5)*: 69-75.

Loshin, D. S. & Jones, R. (1982). Contrast sensitivity as a function of exposure duration in the amblyopic visual system. *American Journal of Optometry and Physiological Optics, 59 (7)*: 561-567.

Lu, Z. L. & Sperling, G. (2001). Sensitive calibration and measurement procedures based on the amplification principle in motion perception. *Vision Research, 41*: 2355-237.

Maccabee, P. J. & Amassian, V. E. (2008). Lessons learned from magnetic stimulation of physical models and peripheral nerve in vitro. In: E. M. Wassermann, C. M. Epstein, U. Ziemann, V. Walsh, T. Paus & S. H. Lisanby (Eds). *The Oxford handbook of Transcranial magnetic stimulation.* New York: Oxford University Press. Pp 47-56.

Maccabee, P. J., Amassian, V. E., Eberle, L. P. & Cracco, R. Q. (1993). Magnetic coil stimulation of straight and bent amphibian and mammalian peripheral nerve in vitro: locus of excitation. *Journal of Physiology, 460*: 201-219.

Maccabee, V. E., Amassian, L. P., Eberle, A. P., Rudell, R. Q., Cracco, K. S., Lai, M. & Somasundarum, M. (1991). Measurement of the electric field induced into inhomogeneous volume conductors by magnetic coils: application to human spinal neurogeometry. *Electroencephalography and Clinical Neurophysiology/Evoked Potentials Section, 81 (3)*: 224-237.

Maeda, F., Keenan, J. P., Tormos, J. M., Topka, H. & Pascual-Leone, A. (2000). Modulation of corticospinal excitability by repetitive transcranial magnetic stimulation. *Clinical Neurophysiology, 111 (5)*: 800-805.

Maffei, L. & Fiorentini, A. (1973). The visual cortex as a spatial frequency analyser. *Vision Research, 13(7)*: 1255-1267.

Majaj, N. J., Carandini, M., Movshon, J. A. (2007). Motion integration by neurons in macaque MT is local, not global. *Journal of Neuroscience, 27 (2)*: 366-370.

Mareschal, I. & Shapley, R. M. (2004). Effects of contrast and size on orientation discrimination. *Vision Research, 44 (1)*: 57-67.

Marr, D. & Hildreth, E. (1980). Theory of edge detection. *Proceedings of the Royal Society of London B Biological Sciences, 207 (1167)*: 187-217.

Marr, D. & Ullman, S. (1981). Directional selectivity and its use in early visual processing. *Proceedings of the Royal Society of London, B211*: 151-180.

Masur, H., Papke, K. & Oberwittler, C. (1993). Suppression of visual perception by transcranial magnetic stimulation – experimental findings in healthy subjects and patients with optic neuritis. *Electroencephalography and Clinical Neurophysiology, 86*: 259-267.

Mather, G. (1989). Temporal properties of apparent motion in subjective figures. *Perception, 17*: 729-736.

Matthews, N., Luber, B., Qian, N. & Lisanby, S. H. (2001). Transcranial magnetic stimulation differentially affects speed and direction judgments. *Experimental Brain Research, 140*: 397-406.

Maunsell, J. H. R, Ghose, G. M., Assad, J. A., McAdams, C. J., Boudreau, C. E. & Noeranger, B. D. (1999). Visual response latencies of magnocellular and parvocellular LGN neurons in macaque monkeys. *Visual Neuroscience, 16*: 1-14.

Maunsell, J. H. R, & Gibson, J. R. (1992). Visual responses latencies in striate cortex of the macaque monkey. *Journal of Neurophysiology, 68 (4)*: 1332-1344.

Maunsell, J. H. R, & Newsome W. T. (1987). Visual processing in monkey extrastriate cortex. *Annual Review of Neuroscience, 10*: 363-401.

Maunsell, J. H. R. & Van Essen, D. C. (1983). The connections of middle temporal visual area (MT) and their relationship to a cortical hierarchy in the macaque monkey. *Journal of Neuroscience, 3 (12)*: 2563-2586.

McAdams, C. J. & Maunsell, J. H. (2000). Attention to both space and feature modulates neuronal responses in macaque area V4. *Journal of Neurophysiology, 83 (3)*: 1751-1755.

McKeefry, D. J., Burton, M. P., Vakrou, C., Barrett, B. T. & Morland, A. B. (2008). Induced deficits in speed perception by transcranial magnetic stimulation of human cortical areas V5/MT+ and V3A. *The Journal of Neuroscience, 28 (27)*: 6848-6857.

McRobbie, D. & Foster, M. A. (1984). Thresholds for biological effects of time-varying magnetic fields. *Clinical Physics and Physiological Measurement, 5 (2)*: 67-78.

Mechelli, A., Friston, K. J., Frackowiak, R. S. & Price, C. J. (2005). Structural covariance in the human cortex. *Journal of Neuroscience, 25 (36)*: 8303-8310.

Mechler, F. & Ringach, D. L. (2002). On the classification of simple and complex cells. *Vision Research, 42*: 1017-1033.

Meissirel, C. & Chalupa, L. M. (1994). Organization of pioneer retinal axons within the optic tract of rhesus monkey. *Proceedings of the National Academy of Science, USA, 26*: 3906-3910.

Merigan, W. H., Byrne, C. E. & Maunsell, J. H. (1991). Does primate motion perception depend on the magnocellular pathway? *Journal of Neuroscience, 11 (11)*: 3422-3429.

Merigan, W. H., Katz, L. M. & Maunsell, J. H. (1991). The effects of parvocellular lateral geniculate lesions on the acuity and contrast sensitivity of macaque monkeys. *Journal of Neuroscience, 11 (4)*: 994-1001.

Merigan, W. H. & Maunsell, J. H. R. (1993). How parallel are the primate visual pathways? *Annual Review of Neuroscience, 16*: 369-402.

Meyer, B. U., Diehl, R., Steinmetz, H., Britton, T. C. & Benecke, R. (1991). Magnetic stimuli applied over motor and visual cortex: influence of coil position and field polarity on motor responses, phosphenes, and eye movements. *Electroencephalography and Clinical Neurophysiology Supplements, 43* :121-134.

Miller, M. B., Fendrich, R., Eliassen, J.C., Demirel, S. & Gazzaniga, M.S. (1996). Transcranial magnetic stimulation: delays in visual suppression due to luminance changes. *Neuroreport, 7 (11)*: 1740-1744.

Moliadze, V., Zhao, Y., Eysel, U. & Funke, K. (2003). Effect of transcranial magnetic stimulation on single-unit activity in the cat primary visual cortex. *Journal of Physiology, 553 (2)*: 665-679.

Morrone, M. C., Tosetti, M., Montanaro, D., Fiorentini, A., Cioni, G. & Burr, D. C. (2000). A cortical area that responds specifically to optic flow, revealed by fMRI. *Nature Neuroscience, 3*: 1322-1328.

Movshon, J. A., Adelson, E. H., Gizzi, M. S. & Newsome, W. T. (1985). The analysis of moving visual patterns. In *Pattern Recognition Mechanisms*, ed. C. Chagas, R. Gattass, C.Gross (Pontificiae Academiae Scientiarum Scripta Varia 54, 117-151). Rome: Vatican Press. (Reprinted in *Experimental Brain Research, Supplementum, 11*: 117-151).

Movshon, J. A. & Newsome, W. T. (1996). Visual response properties of striate cortical neurons projecting to area MT in macaque monkeys. *Journal of Neuroscience, 16 (23)*: 7733-7741.

Movshon, J. A., Thompson, I. D. & Tolhurst, D. J. (1978). Receptive field organization of complex cells in the cat's striate cortex. *Journal of Physiology, 283*: 79-99.

Nagaranjan, S. S. (1993). Effects of induced electric fields on finite neuronal structures: A simulation study. *IEEE Transactions on Biomedical Engineering, 40 (11)*: 1175-1188.

Nagarajan, S. S., Durand, D. M. & Warman, E. N. (1993). Effects of induced electric fields on finite neuronal structures: a simulation study. *IEEE Transactions on Biomedical Engineering, 40 (11)*: 1175-1188.

Nakatani, K., Tamura, T., Yau, K. W. (1991). Light adaptation in retinal rods of the rabbit and two other nonprimate mammals. *The Journal of General Physiology, 97(3)*: 413-425.

Nakayama, K. (1985). Biological image motion processing: A review. *Vision Research, 25 (5)*: 625-660.

Naya, Y., Yoshida, M. & Miyashita, Y. (2001). Backward spreading of memory-retrieval signal in the primate temporal cortex. *Science, 291 (5504)*: 661-664.

Neri, P., Morrone, M. C. & Burr, D. C. (1998). Seeing biological motion. *Nature, 395 (6705)*: 894-896.

Newsome, W. T. & Paré, E. B. (1988). A selective impairment of motion perception following lesions of the middle temporal visual area (MT). *The Journal of Neuroscience, 8 (6)*: 2201-2211.

Niehaus, L., Meyer, B. U. & Weyh, T. (2000). Influence of pulse configuration and direction of coil current on excitatory effects of magnetic motor cortex and nerve stimulation. *Clinical Neurophysiology, 111 (1)*: 75-80.

Nowak, L. G., James, A. C. & Bullier, J. (1997). Corticocortical connections between visual areas 17 and 18a of the rat studied in vitro: Spatial and temporal organisation of functional synaptic responses. *Experimental Brain Research, 117*: 219-241.

Ono, M., Kubik, S. & Abernathy, C. D. (1990). *Atlas of the Cerebral Sulci*. Georg Thieme Verlag: New York.

Orban, G. A., Dupont, P., De Bruyn, B., Vogels, R., Vandenberghe, R. & Mortelmans, L. (1995). A motion area in human visual cortex. *Proceedings of the National Academy of Science USA. 92(4)*: 993-997.

Pantle, A. & Sekuler, R. (1968). Size-detecting mechanisms in human vision. *Science, 162 (858)*: 1146-1148.

Papageorgiou, E., Wermund. T. & Wilhelm, H. (2009). Pupil perimetry demonstrates hemifield pupillary hypokinesia in a patient with a pretectal lesion causing a relative afferent pupil defect but no visual field loss. *Journal of Neuroophthalmology, 29 (1)*: 33-36.

Pascual-Leone, A., Gates, J. R. & Dhuna, A. (1991). Induction of speech arrest and counting errors with rapid-rate transcranial magnetic stimulation. *Neurology, 41 (5)*: 697-702.

Pascual-Leone, A., Grafman, J. & Hallett, M. (1995). Procedural learning and prefrontal cortex. *Annals of the New York Academy of Sciences, 769*: 61-70.

Pascual-Leone, A., Walsh, V. & Rothwell, J. (2000). Transcranial magnetic stimulation in cognitive neuroscience – virtual lesion, chronometry and functional connectivity. *Current Opinion in Neurobiology, 10*: 232-237.

Paus, T., Jech, R., Thompson, C. J., Comeau, R., Peters, T. & Evans, A. C. (1997). Transcranial magnetic stimulation during positron emission tomography: A new method for studying connectivity of the human cerebral cortex. *The Journal of Neuroscience, 17 (9)*: 3178-3184.

Perone, J. A. & Thiele, A. (2001). Speed skills: Measuring the visual speed analyzing properties of primate MT neurons. *Nature Neuroscience, 4 (5)*: 526-532.

Perry, V. H. & Cowey, A. (1984). Retinal ganglion cells that project to the superior colliculus and pretectum in the macaque monkey. *Neuroscience, 12 (4)*: 1125-1137.

Pierrot-Deseilligny, C., Rosa, A., Masmoudi, K., Rivaud, S & Gaymard, B. (1991). Saccade deficits after a unilateral lesion affecting the superior colliculus. *Journal of Neurology Neurosurgery and Psychiatry, 54(12)*: 1106-1109.

Polyak, S. (1957). *The Vertebrate Visual System*. University of Chicago: Chicago.

Priebe, N. J., Cassanello, C. R. & Lisberger, S. G. (2003). The neural representation of speed in macaque area V5/MT. *Journal of Neuroscience, 23 (13)*: 5650-5661.

Rademacher, J., Caviness, V. S., Steinmetz, H. & Galaburda, A. M. (1993) Topographical variation of the human primary cortices: implications for neuroimaging, brain mapping, and neurobiology. *Cerebral Cortex, 3(4)*: 313-329.

Raiguel, S., Van Hulle, M. M., Xiao, D. K., Marcar, V. L., Lagae, L. & Orban, G. A. (1997). Size and shape of receptive fields in the medial superior temporal area (MST) of the macaque. *Neuroreport, 8 (12)*: 2803-2808.

Ramachandran, V. S. & Gregory, R. L. (1978). Does colour provide an input to human motion perception? *Nature, 275 (5675):* 55-56.

Ratliff, F. (1965). *Mach Bands*. Holden-Day: San Francisco.

Rees, G., Friston, K. & Koch, C. (2000). A direct quantitative relationship between the functional properties of human and macaque V5. *Nature Neuroscience, 3 (7)*: 716-723.

Rees, G., Kreiman, G. & Koch, C. (2002). Neural correlates of consciousness in humans. *Nature Review Neuroscience 3(4)*: 261-270.

Reich, D. S., Mechler, F. & Victor, J. D. (2001). Temporal coding of contrast in the primary visual cortex: When, what, and why. *Journal of Neurophysiology, 85 (3)*: 1039-1050.

Reichardt, W. (1961). Autocorrelation, a principle for the evaluation of sensory information by the central nervous system. In: W. A. Rosenblith, (Ed.). *Sensory Communication.* New York: Wiley.

Reid, R. C. & Alonso, J. M. (1996). The processing and encoding of information in the visual cortex. *Current Opinion in Neurobiology, 6 (4)*: 475-480.

Reilly, J. P. (1989). Peripheral nerve stimulation by induced electric currents: exposure to time-varying magnetic fields. *Medical and Biological Engineering and Computing, 27 (2)*: 101-110.

Reilly, J. P. &. Diamant, A. M. (2003). Spatial relationships in electrostimulation: Application to electromagnetic field standards, *IEEE Transactions on Biomedical Engineering*, *50 (6)*: 783-785.

Ridder, W. H. & Tomlinson, A. (1993). Suppression of contrast sensitivity during eyelid blinks. *Vision Research, 33 (13)*: 1795-1802.

Ridding, M. C. & Rothwell, J. C. (2007). Is there a future for therapeutic use of transcranial magnetic stimulation? *Nature Reviews Neuroscience, 8*: 559-567.

Riedel, E., Stephan, T., Marx, E., Deutschländer, A., Brüning, R. & Brandt, T. (2004). Areas MT/V5 and their transcallosal connectivity in cortical dysplasia by fMRI. *Neuroreport, 15 (12)*: 1877-1881.

Robson, J. G. (1966). Spatial and temporal contrast sensitivity function for the visual system. *Journal of the Optical Society of America, 56*: 1141-1142.

Robson, T. (1999). Topics in computerized visual-stimulus generation. In: R. H. S. Carpenter & J. G. Robson (Eds.) *Vision Research: A Practical Guide to Laboratory Methods.* Oxford University Press: Oxford.

Robson, J. G., Tolhurst, D. J., Freeman, R. D. & Ohzawa, I. (1988). Simple cells in the visual cortex of the cat can be narrowly tuned for spatial frequency. *Visual Neuroscience, 1 (4)*: 415-419.

Roth, B. J. & Basser, P. J. (1990). A model of the stimulation of a nerve fiber by electromagnetic induction. *IEEE Transactions on Biomedical Engineering, 37 (6)*: 588-597.

Rudiak, D. & Marg, E. (1994). Finding the depth of magnetic brain stimulation: A re-evaluation. *Electroencephalography and Clinical Neurophysiology, 93*: 358-371.

Ruohonen, J. & Ilmoniemi, R. J. (1999). Modelling of the stimulating field generation in TMS. *Electroencephalography and Clinical Neurophysiology Supplement,* 51: 30-40.

Sack, A. T., Kohler, A., Linden, D. E. J., Goebel, R. & Muckli, L. (2006). The temporal characteristics of motion processing in hMT/V5+: Combining fMRI and neuronavigated TMS. *NeuroImage, 29 (4)*: 1326-1335.

Salvador, R., Silva, S., Basser, P. & Miranda, P. (2008). A simulation study of the mechanisms that govern direct activation of neurons in the motor cortex by transcranial magnetic stimulation. *Brain Stimulation*, *1 (3)*: 251-252.

Sandell, J. H. & Schiller, P. H. (1982). Effect of cooling area 18 on striate cortex cells in the squirrel monkey. *Journal of Neurophysiology, 48 (1)*: 38-48.

Savage, G. L. (1996). Temporal summation for grating patches detected at low light levels. *Optometry and Vision Science, 73 (6)*: 404-412.

Schiller, P. H., Logothetis, N. K. & Charles, E. R. (1990). Role of the color-opponent and broad-band channels in vision. *Visual Neuroscience, 5*: 321-346.

Sclar, G. & Freeman, R. D. (1982). Orientation selectivity in the cat's striate cortex is invariant with stimulus contrast. *Experimental Brain Research, 46 (3)*: 457-461.

Sclar, G., Maunsell, J. H. & Lennie, P. (1990). Coding of image contrast in central visual pathways of the macaque monkey. *Vision Research, 30 (1)*: 1-10.

Schluter, N. D., Rushworth, M. F., Mills, K. R. & Passingham, R. E. (1999). Signal-, set-, and movement-related activity in the human premotor cortex. *Neuropsychologia, 37 (2)*: 233-243.

Schnapf, J. L., Kraft, T. W. & Baylor, D. A. (1987). Spectral sensitivity of human cone photoreceptors. *Nature, 325(6103)*: 439-441.

Schnapf, J. L., Nunn, B. J., Meister, M. & Baylor. D. A. (1990). Visual transduction in cones of the monkey Macaca fascicularis. *Journal of Physiology, 42* : 681-713.

Shapley, R. & Lennie, P. (1985). Spatial frequency analysis in the visual system. *Annual Reviews of Neuroscience, 8*: 547-583.

Shapley R. M., Kaplan, E. & Soodak, R. (1981). Spatial summation and contrast sensitivity of X and Y cells in the lateral geniculate nucleus of the macaque. *Nature, 292(5823)*: 543-545.

Shapley, R. M. & Victor, J. D. (1978). The effect of contrast on the transfer properties of cat retinal ganglion cells. *Journal of Physiology, 285*: 275-298.

Shipley, W. C., Kenney, F. A. & King, M. E. (1945). Beta movement under binocular, monocular, and interocular stimulation. *American Journal of Psychology, 581*: 545-549.

Shipp, S. & Zeki, S. (1989). The organization of connections between areas V5 and V1 in macaque monkey visual cortex. *European Journal of Neuroscience, 1 (4)*: 309-332.

Siebner, H. R., Peller, M., Willoch, F., Minoshima, S., Boecker, H., Auer, C., Drzezga, A., Conrad, B. & Bartenstein, P. (2000). Lasting cortical activation after repetitive TMS of the motor cortex: a glucose metabolic study. *Neurology, 54 (4)*: 956-963.

Sillito, A. M, Kemp, J. A., Milson, J. A. & Berardi, N. (1980). A re-evaluation of the mechanisms underlying simple cell orientation selectivity. *Brain Research, 194 (2)*: 517-520.

Silvanto, J., Lavie, N. & Walsh, V. (2005). Double dissociation of V1 and V5/MT activity in visual awareness. *Cerebral Cortex, 15*: 1736-1741.

Silvanto, J., Muggleton, N. G., Cowey, A. & Walsh, V. (2007). Neural adaptation reveals state-dependent effects of transcranial magnetic stimulation. *European Journal of Neuroscience, 25*: 1874-1881.

Silveira, L. C. & Perry, V. H. (1991). The topography of magnocellular projecting ganglion cells (M-ganglion cells) in the primate retina. *Neuroscience, 40 (1)*: 217-237.

Simmers, A. J., Ledgeway, T., Hess, R. F. & McGraw, P. V. (2003). Deficits to global motion processing in human amblyopia. *Vision Research, 43*: 729-738.

Simmers, A. J., Ledgeway, T., Mansouri, B., Hutchinson, C. V. & Hess, R. F. (2006). The extent of the dorsal extra-striate deficit in amblyopia. *Vision Research, 46*: 2571-2580.

Simoncelli, E.P. & Heeger, D. J. (1998). A model of neuronal responses in visual area MT. *Vision Research, 38 (5)*: 743-761.

Sincich, L. C. & Horton, J. C. (2003). Independent projection streams from macaque striate cortex to the second visual area and middle temporal area. *Journal of Neuroscience, 23 (13)*: 5684-5692.

Sincich, L. C. & Horton, J. C. (2005). The circuitry of V1 and V2: Integration of color, form, and motion. *Annual Review of Neuroscience, 28*: 303- 326.

Sincich, L. C., Park, K. F., Wohlgemuth, M. J. & Horton, J. C. (2004). Bypassing V1: A direct geniculate input to area MT. *Nature Neuroscience, 7 (10)*: 1123-1128.

Skottun, B. C., Bradley, A., Sclar, G., Ohzawa, I. & Freeman, R. D. (1987). The effects of contrast on visual orientation and spatial frequency discrimination: A comparison of single cells and behaviour. *Journal of Neurophysiology, 57 (3)*: 773-786.

Skottun, B. C., De Valois, R. L., Grosof, D. H., Movshon, J. A., Albrecht, D. G. & Bonds, A. B. (1991). Classifying simple and complex cells on the basis o response modulation. *Vision Research, 31*: 1079-1086.

Smith, M. A., Majaj, N. J. & Movshon, J. A. (2005). Dynamics of motion signaling by neurons in macaque area MT. *Nature Neuroscience, 8 (2)*: 220-228.

Smith, A. T., Snowden, R. J. & Milne, A. B. (1994). Is global motion really based on spatial integration of local motion signals? *Vision Research, 34 (18)*: 2425-2230.

Smith, A. T., Wall, M. B., Williams, A. L. & Singh, K. D. (2006). Sensitivity to optic flow in human cortical areas MT and MST. *European Journal of Neuroscience, 23 (2)*: 561-569.

Somers, D. C., Nelson, S. B. & Sur, M. (1995). An emergent model of orientation selectivity in cat visual cortical simple cells. *Journal of Neuroscience, 15*: 5448-5465.

Sommer, M., Alfaro, A., Rummel, M., Speck, S., Lang, N., Tings, T. & Paulus, W. (2006). Half sine, monophasic and biphasic transcranial magnetic stimulation of the human motor cortex. *Clinical Neurophysiology, 117 (4)*: 838-844.

Sommer, M. & Paulus, W. (2008). TMS waveform and current direction. In: E. M. Wassermann, C. M. Epstein, U. Ziemann, V. Walsh, T. Paus & S. H. Lisanby (Eds). *The Oxford handbook of Transcranial magnetic stimulation.* New York: Oxford University Press.

Sompolinsky, H. & Shapley, R. (1997). New perspectives on the mechanisms for orientation selectivity. *Current Opinion in Neurobiology, 7 (4)*: 514-522.

Stensaas, S. S., Eddington, D. K. & Dobelle, W. H. (1974). The topography and variability of the primary visual cortex in man. *Journal of Neurosurgury, 40 (6)*: 747–755.

Stewart, B. R. (1972). Temporal summation under dark adaptation. *Journal of the Optical Society of America, 62*: 449-457.

Stewart, L., Battelli, L., Walsh, V. & Cowey, A. (1999). Motion perception and perceptual learning studied by magnetic stimulation. *Electroencephalography and Clinical Neurophysiology, Supplement, 51*: 334-350.

Stewart, L. M., Walsh, V. & Rothwell, J. C. (2001). Motor and phosphene thresholds: A transcranial magnetic stimulation correlation study. *Neuropsychologia, 39*: 415-419.

Stuart, G., Spruston, N., Sakmann, B. & Häusser, M. (1997). Action potential initiation and backpropagation in neurons of the mammalian CNS. *Trends in Neuroscience, 20 (3)*: 125-131.

Tanaka, K., Hikosaka, K., Saito, H., Yukie, M., Fukada, Y. & Iwai, E. (1986). Analysis of local and wide-field movements in the superior temporal visual areas of the macaque monkey. *Journal of Neuroscience, 6 (1)*: 134-144.

Tanaka, K., Fukada, Y., Saito, H. (1989). Underlying mechanisms of the response specificity of expansion/contraction and rotation cells in the dorsal part of the medial superior temporal area of the macaque monkey. *Journal of Neurophysiology, 62 (3)*: 642-656.

Tanaka, K., Sugita, Y., Moriya, M. & Saito, H. (1993). Analysis of object motion in the ventral part of the medial superior temporal area of the macaque visual cortex. *Journal of Neurophysiology, 69 (1)*: 128-142.

Tasman W. (1973). The retina and optic nerve. *Archives of Ophthalmology, 89(5)*: 422-436.

Tay, G., Chilbert, M., Battocletti, J., Sances, A. Jr., Swiontek, T. & Kurakami, C. (1989). Measurement of magnetically induced current density in saline and in vivo, in: Y. Kim, F. A. Spelman (Eds.), Proceedings of the Annual International Conference of the IEEE Engineering in Medicine and Biology Society 4, IEEE, Seattle (1989), pp. 1167-1168.

Terao, Y. & Ugawa, Y. (2002). Basic mechanisms of TMS. *Journal of Clinical Neurophysiology, 19 (4)*: 322-343.

Theoret, H., Kobayashi, M., Ganis, G., Di Capua, P. & Pascual-Leone, A. (2002). Repetitive transcranial magnetic stimulation of human area MT/V5 disrupts perception and storage of the motion aftereffect. *Neuropsychologia, 40*: 2280-2287.

Thickbroom, G. W., Sammut, R. & Mastaglia, F. L. (1998). Magnetic stimulation mapping of motor cortex: factors contributing to map area. *Electroencephalography and Clinical Neurophysiology, 109 (2)*: 79-84.

Thut, G., Northoff, G., Ives, J. R., Kamitani, Y., Pfennig, A., Kampmann, F., Schomer, D. L., Pascual-Leone, A. (2003). Effects of single-pulse transcranial magnetic stimulation (TMS) on functional brain activity: a combined event-related TMS and evoked potential study. *Clinical Neurophysiology, 114 (11)*: 2071-2080.

Tolhurst, D. J. (1975). Sustained and transient channels in human vision. *Vision Research, 15*: 1151-1155.

Tootell, R. B., Reppas, J. B., Kwong, K. K., Malach, R., Born, R. T., Brady, T. J., Rosen, B. R. & Belliveau, J. W. (1995). Functional analysis of human MT and related visual cortical areas using magnetic resonance imaging. *Journal of Neuroscience, 15*: 3215-3230.

Tootell, R. B., Silverman, M. S., Switkes, E. & De Valois, R. L. (1982). Deoxyglucose analysis of retinotopic organization in primate striate cortex. *Science, 218 (4575)*: 902-904.

Tulunay-Keesey, U. & Jones, R. M. (1976). The effect of micromovements of the eye and exposure duration on contrast sensitivity. *Vision Research, 16 (5)*: 481-488.

Ueno, S., Tashiro, T. & Harada, K. (1998). Localized stimulation of neural tissues in the brain by means of paired configuration of time-varying magnetic fields. *Journal of Applied Physics, 64*: 5862-5864.

Ullman, S. (1979). *The interpretation of visual motion.* Cambridge: MIT Press.

Ungerleider, L. G. & Mishkin, M. (1982). Two Cortical Visual Systems. In: D. J. Ingle, M. Goodale, R. J. W. Mansfield. *Analysis of Visual Behaviour*. pp. 549-586.

Van Essen, D. C. & Gallant, J. L. (1994). Neural mechanisms of form and motion processing in the primate visual system. *Neuron 13(1)*: 1-10.

Van Essen, D. C. & Maunsell, J. H. R. (1983). Hierarchical organization and functional streams in the visual cortex. *Trends in Neuroscience, 6*: 370-375.

Van Essen, D. C., Maunsell, J. H. R. & Bixby, J. L. (1981). The middle temporal visual area in the macaque: myeloarchitecture, connections, functional properties and topographic organization. *Journal of Computational Neurology, 199 (3)*: 293-326.

van Nes, F. L., Koenderink, J. J., Nas, H. & Bouman, M. A. (1967). Spatiotemporal modulation transfer in the human eye. *Journal of the Optical Society of America, 57*: 1082-1088.

Van Santen, J. P. H. & Sperling, G. (1984). A temporal covariance model of motion perception. *Journal of the Optical Society of America A, 1*: 451-473.
Van Santen, J. P. H. & Sperling, G. (1985). Elaborated Reichardt detectors. *Journal of the Optical Society of America A, 2*: 300-321.

VanderWerf, F., Brassinga, P., Retis, D., Aramideh, M., Ongerboer de Visser, B. (2003). Eyelid movements: behavioural studies of blinking in humans under different stimulus conditions. *Journal of Neurophysiology, 89*: 2784-2796.

Vassilev, A. & Manahilov, V. (1986). The effect of grating contrast on the human visually evoked potential. *Acta Physiologica et Pharmacologica Bulgarica, 12 (4)*: 53-57.

Wada, S., Kubota, H., Maita, S., Yamamoto, I., Yamaguchi, M., Andoh, T., Kawakami, T., Okumura, F & Takenaka, T. (1996). Effects of stimulus waveform on magnetic nerve stimulation. *Japanese Journal of Applied Physiology, 35*: 1983-1988.

Wagner, T., Eden, U., Fregni, F., Valero-Cabre, A., Ramos-Estebanez, C., Pronio-Stelluto, V., Grodzinsky, A., Zahn, M. & Pascual-Leone, A. (2008). Transcranial magnetic stimulation and brain atrophy: a computer-based human brain model study. *Experimental Brain research, 186 (4)*: 539-550.

Wagner, T., Gangitano, M., Romero, R., Théoret, H., Kobayashi, M., Anschel, D., Ives, J., Cuffin, N., Schomer, D. & Pascual-Leone, A. (2004). Intracranial measurement of current densities induced by transcranial magnetic stimulation in the human brain. *Neuroscience Letters, 354 (2)*: 9-94.

Wagner, T., Rushmore, J., Eden, U., Valero-Cabre, A. (2009). Biophysical foundations underlying TMS: setting the stage for an effective use of neurostimulation in the cognitive neurosciences. *Cortex, 45 (9)*:1025-1034.

Wall, M. B., Lingnau, A., Ashida, H. & Smith, A. T. (2008). Selective visual responses to expansion and rotation in the human MT complex revealed by functional magnetic resonance imaging adaptation. *European Journal of Neuroscience, 27 (10)*: 2747-2757.

Walsh, V., Ashbridge, E. & Cowey, A. (1998). Cortical plasticity in perceptual learning demonstrated by transcranial magnetic stimulation. *Neuropsychologia, 36 (1)*: 45-48.

Walsh, V. & Cowey, A. (2000). Transcranial magnetic stimulation and cognitive neuroscience. *Nature Neuroscience, 1 (1)*: 73-79.

Walsh, V., Ellison, A., Battelli, L. & Cowey, A. (1998). Task-specific impairments and enhancements induced by magnetic stimulation of human visual area V5. *Proceedings of the Royal Society of London B: Biological Sciences, 265*: 537-543.

Walsh, V. & Rushworth, M. (1998). A primer of magnetic stimulation as a tool for studying neuropsychology. *Neuropsychologia, 37*: 125-135.

Wassermann, E. M. (1998). Risk and safety of repetitive transcranial magnetic stimulation: Report and suggested guidelines from the International Workshop on the Safety of Repetitive Transcranial Magnetic Stimulation, June 5-7, 1996. *Electroencephalography and Clinical Neurophysiology, 108*: 1-16.

Watamaniuk, S. N., Sekuler, R. & Williams, D. W. (1989). Direction perception in complex dynamic displays: the integration of direction information. *Vision Research, 29 (1)*: 47-59.

Watson, A. B. (1979). Probability summation over time. *Vision Research, 19 (5)*: 515-522.

Watson, A. B. & Ahumada, A. J. (1985). Model of human visual-motion sensing. *Journal of the Optical Society of America A, 2*: 322-341.

Watson, J. D. G., Myers, R., Frackowiak, R. S. J., Hajnal, J. V., Woods, R. P., Mazziotta, J. C., Shipp, S. & Zeki, S. M. (1993). Area V5 of the human brain: Evidence from a combined study using positron emission topography and magnetic resonance imaging. *Cerebral Cortex, 3*: 79-84.

Webb, B. S., Ledgeway, T. & McGraw, P. V. (2007). Cortical pooling algorithms for judging global motion direction. *Proceedings of the National Academy of Sciences of the United States of America, 104 (9)*: 3532-3537.

Westheimer, G. (1998). Lines and Gabor functions compared as spatial visual stimuli. *Vision Research, 38 (4)*: 487-491.

Williams, D. & Phillips, G. (1987). Cooperative phenomena in the perception of motion direction. *Journal of the Optical Society of America A, 4 (5)*: 878-885.

Williams, D., Phillips, G. & Sekuler, R. (1986). Hysteresis in the perception of motion direction as evidence for neural cooperativity. *Nature, 324 (6094)*: 253-255.

Williams, D. W. & Sekuler, R. (1984). Coherent global motion percepts from stochastic local motions. *Vision Research, 24 (1)*: 55-62.

Williams, D., Tweten, S. & Sekuler, R. (1991). Using metamers to explore motion perception. *Vision Research, 31 (2)*: 275-286.

Wilson, H. R., Ferrera, V. P. & Yo, C. (1992). A psychophysically motivated model for two-dimensional motion perception. *Visual Neuroscience, 9 (1)*: 79-97.

Xiao, D. K., Raiguel, S., Marcar, V. & Orban, G. A. (1997). The spatial distribution of the antagonistic surround of MT/V5 neurons. *Cerebral Cortex, 7 (7)*: 662-677.

Yazar, F., Mavity-Hudson, J., Ding, Y.,, Oztas, E. & Casagrande, V A. (2004). Layer IIIB-beta of primary visual cortex (V1) and its relationship to the koniocellular (K) pathway in macaque. *Society for Neuroscience Abstract, 34*: 300.17.

Yoshioka, T., Blasdel, J. B., Levitt, J. B. & Lund, J. S. (1996). Relation between patterns of intrinsic lateral connectivity, ocular dominance, and cytochrome-oxidase regions in macaque striate cortex. *Cerebral Cortex, 6*: 297-310.

Young, M. P. (1992). Objective analysis of the topological organization of the primate cortical visual system. *Nature, 358(6382)*: 152-155.

Zeeman, W. P. C. & Roelofs, C. O. (1953). Some aspects of apparent motion. *Acta Psychologica*, *9*: 159-181.

Zeki, S. M. (1969). The secondary visual areas of the monkey. *Brain Research, 13*: 197-226.

Zeki, S. M. (1973). Comparison of the cortical degeneration in the visual regions of the temporal lobe of the monkey following section of the anterior commissure and the splenium. *Journal of Computational Neurology. 148 (2)*: 167-175.

Zeki, S. M. (1974). Functional organization of a visual area in the posterior bank of the superior temporal sulcus of the rhesus monkey. *Journal of Physiology, 236 (3)*: 549-573.

Zeki, S. M. (1980). The representation of colours in the cerebral cortex. *Nature, 284(5755)*: 412- 418.

Zeki, S. M. & Shipp, S. (1988). The functional logic of cortical connections. *Nature (London)*, 335: 311-317.

Zeki, S. M., Watson, J. D. G., Lueck, C. J., Friston, K. J., Kennard, C. & Frackowiak, R. S. J. (1991). A direct demonstration of functional specialization in human visual cortex. *The Journal of Neuroscience, 11 (3)*: 641-649.

Zilles, K., Clarke, S. (1997) Architecture, connectivity and transmitter receptors of human extrastriate visual cortex. Comparison with non-human primates. In: K. S. Rockland, J. H. Kaas & A. Peters (Eds.), *Cerebral cortex Vol. 12*, New York: Plenum Press. pp. 673–742.

Zilles, K., Schleicher, A., Langemann, C., Amunts, K., Morosan, P., Palomero-Gallagher, N., Schormann, T., Mohlberg, H., Buergel, U. & Steinmetz, H. (1997). Quantitative analysis of sulci in the human cerebral cortex: Development, regional heterogeneity, gender difference, asymmetry, intersubject variability and cortical architecture. *Human Brain Mapping, 5 (4)*: 218–221.

Zlatkova, M., Vassilev, A. & Mitov, D. (2000). Temporal characteristics of line orientation identification. *Perception & Psychophysics, 62 (5)*: 1008-1018.